DOKUZ EYLÜL UNIVERSITY

GRADUATE SCHOOL OF NATURAL AND APPLIED SCIENCES

CHEMODYNAMICS OF ORGANOPHOSPHATE FLAME RETARDANTS IN İZMİR AREA

by

Barış YAMAN

March, 2021

IZMIR

CHEMODYNAMICS OF ORGANOPHOSPHATE FLAME RETARDANTS IN İZMİR AREA

A Thesis Submitted to the
Graduate School of Natural and Applied Sciences of Dokuz Eylül University In Partial Fulfillment of the Requirements for the Degree of Doctor of Philosophy in Environmental Engineering Program

by
Barış YAMAN

March, 2021
IZMIR

Ph.D. THESIS EXAMINATION RESULT FORM

We have read the thesis entitled **"CHEMODYNAMICS OF ORGANOPHOSPHATE FLAME RETARDANTS IN İZMİR AREA"** completed by **BARIŞ YAMAN** under supervision of **PROF.DR. MUSTAFA ODABAŞI** and we certify that in our opinion it is fully adequate, in scope and in quality, as a thesis for the degree of Doctor of Philosophy.

Prof.Dr. Mustafa ODABAŞI

Supervisor

Prof.Dr. Aysun SOFUOĞLU	Prof.Dr. Abdurrahman BAYRAM
Thesis Committee Member	Thesis Committee Member
Prof.Dr. Eftade GAGA	Prof.Dr. Perihan Binnur KURT KARAKUŞ
Examining Committee Member	Examining Committee Member

Prof.Dr. Özgür ÖZÇELİK

Director

Graduate School of Natural and Applied Sciences

ACKNOWLEDGEMENTS

I would like to express my gratitude to my advisor Prof.Dr. Mustafa ODABAŞI for his encouragement, suggestions, and guidance in the light of his extensive knowledge in the field, and above all for his amiable altitude throughout this study.

I would like to express my appreciation to Prof.Dr. Aysun SOFUOĞLU, Prof.Dr. Abdurrahman BAYRAM, Prof.Dr. Perihan Binnur KURT KARAKUŞ and Prof.Dr. Eftade GAGA for their valuable support and suggestions throughout the study. Also, I would like to express my appreciation to Dr. Yetkin DUMANOĞLU, Ersan GÜNEL and Önder KADIOĞLU for their support.

I would like to thank to members of the research group; Prof.Dr. Tolga ELBİR, Dr. Melik KARA, Hasan ALTIOK and Gizem TUNA TUYGUN for their help and support during the preparation of this study.

Finally, I am notably thankful to my wife Tuğçe YAMAN and my family for the endless understanding and support during my educational life.

I thank Izmir Metropolitan Municipality for their support in water sampling sites and providing meteo-oceanographic data.

This thesis was supported by Dokuz Eylül University (Project no: 2018.KB.FEN.024).

Barış YAMAN

CHEMODYNAMICS OF ORGANOPHOSPHATE FLAME RETARDANTS IN İZMİR AREA

ABSTRACT

As a result of restrictions on production and use of brominated flame retardants (BFRs) due to their persistence, toxicity and bioaccumulation; organophosphate esters (OPEs) became a more widely used group of alternative additives within a number of applications (i.e. flame retardants and plasticizers) during the production of many consumer goods in global scale. OPEs are reported as stable toward biodegradation and highly resistant, while some OPEs reported as toxic, neurotoxic, and carcinogenic. Although OPEs are being widely investigated in the literature, the number of studies in Turkey is inadequate. In order to investigate their transport, environmental behavior and fate, several physicochemical properties (octanol-air partition coefficient - K_{OA}, Henry's Law constant - H, supercooled liquid vapor pressure - P_L, LDPE-water partition coefficient - $K_{PE\text{-}W}$ and PUF-air partition coefficient - $K_{PUF\text{-}Air}$) for the eleven studied OPEs were experimentally determined. Their distribution between gas and particle-phases in the atmosphere was also investigated. Ambient air, soil and seawater concentrations were measured for summer and winter in thirty eight sampling sites covering industrial, urban, suburban and rural areas in Izmir. Highest OPE levels were observed in industrial sites followed by urban, suburban and rural sites. Ambient air and soil OPE levels were comparable to those reported in the literature while seawater concentrations were slightly higher. Air-soil and air-seawater exchange of OPES were also evaluated using measured OPE levels and experimentally determined physicochemical properties. The exchange directions did not change with season and they were mostly affected by OPE levels detected in the matrices of interest.

Keywords: Organophosphate flame retardants, organophosphate ester (OPE), physicochemical properties, air-seawater exchange, air-soil exchange

ORGANOFOSFATLI ALEV GECİKTİRİCİ BİLEŞİKLERİN İZMİR BÖLGESİNDEKİ KİMYASAL DİNAMİKLERİ

ÖZ

Kalıcılıkları, toksisiteleri ve biyo-birikim potansiyelleri sebebiyle bromlu alev geciktiricilerin (BFR'ler) üretimine ve kullanımına yönelik uygulanan kısıtlamaların sonucunda; organofosfat esterleri (OPE'ler), küresel ölçekte birçok endüstriyel ürünün üretimi sırasında çeşitli uygulamalarla (alev geciktirici ve plastikleştirici) yaygın olarak kullanılan alternatif katkı kimyasalları grubu haline gelmiştir. OPE'lerin birçoğu biyolojik olarak bozunmaya karşı stabil ve oldukça dirençli; bazıları ise toksik, nörotoksik ve kanserojen olarak rapor edilmektedir. OPE'lerin literatürde geniş çapta araştırılmasına rağmen Türkiye'de yürütülen çalışma sayısı halen yetersizdir. Bu bileşiklerin çevresel ortamlardaki taşınım süreçlerinin, davranışlarının ve akıbetlerinin belirlenebilmesi için bazı fizikokimyasal özellikleri (oktanol-hava faz dağılım katsayısı - K_{OA}, Henry Yasası sabiti - H, aşırı soğutulmuş sıvı buhar basıncı - P_L, LDPE-su faz dağılım katsayısı - $K_{PE\text{-}W}$ ve PUF-hava dağılım katsayısı - $K_{PUF\text{-}Air}$) deneysel olarak belirlenmiştir. Atmosferde gaz ve partikül fazlar arasındaki dağılımları da araştırılmıştır. İzmir'de endüstriyel, kentsel, yarı-kentsel ve kırsal alanları kapsayan otuz sekiz örnekleme noktasında yaz ve kış mevsim şartlarını temsil edecek şekilde dış hava, toprak ve deniz suyu OPE konsantrasyonları ölçülmüştür. En yüksek OPE seviyeleri sırasıyla endüstriyel, kentsel, yarı-kentsel ve kırsal alanlarda tespit edilmiştir. Dış hava ve toprak örneklerindeki OPE konsantrasyonları, literatürdeki çalışmalara benzer seviyelerde; deniz suyu konsantrasyonları ise daha yüksek seviyelerde belirlenmiştir. Hava-toprak ve hava-deniz suyu arasındaki taşınım yönleri de ölçülen OPE seviyeleri ve deneysel olarak belirlenen fizikokimyasal özellikler kullanılarak belirlenmiştir. Taşınım yönleri mevsimsel olarak önemli bir değişkenlik göstermezken, ilgili matrislerde tespit edilen OPE seviyelerinin taşınım yönlerini etkileyen birincil faktör olduğu görülmüştür.

Anahtar kelimeler: Organofosforlu alev geciktiriciler, organofosfat esterleri (OPE), fizikokimyasal özellikler, hava-deniz suyu taşınımı, hava-toprak taşınımı

CONTENTS

Page

Ph.D. THESIS EXAMINATION RESULT FORM ii
ACKNOWLEDGEMENTS iii
ABSTRACT iv
ÖZ v
LIST OF FIGURES ix
LIST OF TABLES xii

CHAPTER 1 - INTRODUCTION 1

CHAPTER 2 - LITERATURE REVIEW 5

2.1 Characteristics of OPEs 5
2.2 Applications, Sources and Environmental Occurrence 10
2.3 Environmental Levels 11
2.3.1 Air 11
2.3.2 Water 15
2.3.3 Soil 18
2.4 Sampling and Analytical Methods 21
2.4.1 Sample Collection 21
2.4.2 Sample Preparation 23
2.4.3 Instrumental Analysis 23

CHAPTER 3 - MATERIALS AND METHODS 25

3.1 Laboratory Studies 25
3.1.1 Measurement of Octanol/Air Partition Coefficients (K_{OA}) 25
3.1.2 Measurement of Supercooled Liquid Vapor Pressures (P_L) 26
3.1.3 Measurement of PUF-Air Partition Coefficients ($K_{PUF\text{-}Air}$) 27
3.1.4 Measurement of Henry's Law Constants (H) 28

3.1.5 Measurement of LDPE-Water Partition Coefficients (K_{PEW}) 31
3.1.5.1 Absorption-Desorption Experiment 31
3.1.5.2 Desorption Experiment with Pre-loaded LDPE sheets 32
3.2 Field Studies 34
3.2.1 Study Area 34
3.2.2 Ambient Air Sampling 39
3.2.2.1 Active Air Sampling 39
3.2.2.1.1 Measurement of Total Suspended Particulates (TSP), Elemental Carbon (EC) and Organic Carbon (OC) Contents.. 41
3.2.2.2 Passive Air Sampling 42
3.2.3 Soil Sampling 44
3.2.4 Seawater Sampling 44
3.2.5 Sample Preparation 47
3.2.6 Instrumental Analysis 48
3.2.7 QA/QC 48

CHAPTER 4 - RESULTS AND DISCUSSION 52

4.1 Laboratory Studies 52
4.1.1 Octanol/Air Partition Coefficients 52
4.1.2 Supercooled Liquid Vapor Pressures 58
4.1.3 PUF-Air Partition Coefficients 66
4.1.4 Henry's Law Constants 69
4.1.5 LDPE-Water Partition Coefficients 72
4.2 Field Studies 75
4.2.1 Gas and Particle Phase OPE Concentrations 75
4.2.1.1 Phase Partitioning Modeling 78
4.2.1.1.1 K_{OA} Model. 78
4.2.1.1.2 Soot Model. 78
4.2.1.1.3 The steady-state model 79
4.2.1.1.4 pp-LFER model. 80
4.2.1.2 Gas-phase Fractions 81

4.2.1.3 Performances of the Phase Partitioning Models 81
4.2.2 Spatial and Seasonal Variations of Atmospheric OPE Concentrations ... 89
4.2.3 Spatial and Seasonal Variations of Soil OPE Concentrations 104
4.2.4. Air-Soil Exchange of OPEs 116
4.2.5 Spatial and Seasonal Variations of Seawater OPE Concentrations 120
4.2.6 Air-Water Exchange of OPEs 129
4.2.6.1 Fugacity Fractions 130
4.2.6.2 Air-Seawater Exchange Fluxes 132

CHAPTER 5 - CONCLUSIONS 139

REFERENCES 144

LIST OF FIGURES

Page

Figure 3.1 Schematic illustration and a view of the $K_{PUF\text{-}Air}$ experimental set up 28
Figure 3.2 Schematic layout of Henry's law constant's experimental train 30
Figure 3.3 Study area and sampling points 36
Figure 3.4 Sampling points in **(a)** urban and sub-urban, **(b)** industrial and **(c)** rural sites (in addition to ambient air and soil samples, the seaside sampling points in blue, red and green circles include also seawater passive samples) 38
Figure 3.5 Meteorology stations in urban and suburban sites 39
Figure 3.6 Collection of gas and particulate phase samples 40
Figure 3.7 Sample thermogram for NIOSH 870 42
Figure 3.8 **(a)** Passive air sampler apparatus and **(b)** deployment 43
Figure 3.9 Collection of soil samples 44
Figure 3.10 Seawater passive sampler apparatus before and after deployment 46
Figure 4.1 Relationships between the logarithm of the ratio of the retention times of OPEs to the retention time of the standard reference compounds (fluorene, pyrene and *p,p*'-DDT) at five to eight temperatures and the ln K_{OA} values of the reference compounds at these temperatures (p<0.01) 56
Figure 4.2 Relationship between the directly measured K_{OA} values for OCPs (n=9), PAHs (n=5), and PBDEs (n=5) at 25°C and $K_{OA\text{-}GC}$ values derived from GC retention times 57
Figure 4.3 Comparison of the K_{OA} values determined for OPEs in this study with the values reported in the literature 58
Figure 4.4 Relationships between the logarithm of the ratio of the retention times of OPEs to the retention time of the standard reference compounds (fluorene, pyrene and *p,p*'-DDT) at five to eight temperatures and the ln P_L values of the reference compounds at these temperatures (p<0.01) 61

Figure 4.5 Relationship between the GC determined vapor pressure ($P_{L\text{-}GC}$) and the vapor pressure of supercooled liquid (P_L) derived from literature data at 25°C for five PAHs (fluorene, phenanthrene, fluoranthene, pyrene, and chrysene) and *p,p*'-DDT. The dashed line represents a 1:1 relationship, the solid line is the fit through the data points. 62
Figure 4.6 Comparison of the P_L values determined for OPEs in this study with the values reported in literature 63
Figure 4.7 Relationship of log K_{OA} and log P_L of OPEs with their molecular weights 65
Figure 4.8 Variation of measured log $K_{PUF\text{-}air}$ with log K_{OA} (at 25°C) in the present study and those estimated from relationships reported by previous studies 68
Figure 4.9 Comparison of experimental and literature (Pa m^3/mol) values for OPEs. Dashed diagonal line indicates the 1:1 relationship 71
Figure 4.10 Comparison of experimental K_{PEW} values of OPEs with estimated ones73
Figure 4.11 Relationship between K_{PEW} values of OPEs to K_{OW} 74
Figure 4.12 Compound-specific total (gas + particle phase) OPE compositions (W: winter, S: summer) 76
Figure 4.13 Relationship between measured Σ_{11}OPE concentrations and daily average temperatures for both sampling seasons 77
Figure 4.14 Comparison of the measured and predicted K_P values by four partitioning models. The dashed lines represent a 1:1 relationship 83
Figure 4.15 Relationship between log K_{OA} and measured/modeled gas-phase fractions. Chlorinated OPEs are shown with blue-framed markers 84
Figure 4.16 Relationships between the measured and modeled gas-phase fractions of OPEs 85
Figure 4.17 Ambient air $\sum_{11}$OPE concentrations in winter 95
Figure 4.18 Ambient air $\sum_{11}$OPE concentrations in summer 96
Figure 4.19 Seasonal variations of ambient air OPE concentrations in urban and suburban sites 98
Figure 4.20 Seasonal variations of ambient air OPE concentrations in industrial and rural sites 99

Figure 4.21 Compound-specific compositions in winter 101
Figure 4.22 Compound-specific compositions in summer 102
Figure 4.23 PCA loading plot for air samples..... 104
Figure 4.24 Soil $\sum_{11}$OPE concentrations in winter 109
Figure 4.25 Soil $\sum_{11}$OPE concentrations in winter 110
Figure 4.26 Seasonal variations of soil OPE concentrations in urban and suburban sites..... 111
Figure 4.27 Seasonal variations of soil OPE concentrations in industrial and rural sites..... 112
Figure 4.28 Compound-specific soil compositions in winter 115
Figure 4.29 Compound-specific soil compositions in summer..... 115
Figure 4.30 Air-soil fugacity fractions of OPEs in both seasons..... 119
Figure 4.31 Winter $\sum_{11}$OPE concentrations in seawater..... 125
Figure 4.32 Summer $\sum_{11}$OPE concentrations in seawater 126
Figure 4.33 Seasonal variations of seawater $\sum_{11}$OPE concentrations..... 128
Figure 4.34 Compound-specific compositions in winter (left side) and in summer 129
Figure 4.35 Air-water fugacity fractions of OPEs in both seasons..... 132
Figure 4.36 Air-water fugacity fluxes for individual OPEs..... 137

LIST OF TABLES

Page

Table 2.1 List of the OPEs to be investigated 7

Table 2.2 Atmospheric OPE levels (in pg/m^3) from different locations reported in the literature 14

Table 2.3 Aquatic OPE levels (in ng/L) in different water bodies reported in the literature 17

Table 2.4 Soil OPE levels (in ng/g dw) reported in the literature 20

Table 3.1 Sampling program 37

Table 3.2 Temperature profile of NIOSH 870 41

Table 3.3 Surrogate recovery efficiencies (%) for field samples and laboratory experiments 50

Table 3.4 Instrumental detection limits for OPEs 51

Table 3.5 MDL values for field samples 51

Table 4.1 Uncalibrated ($K_{OA\text{-}GC}$, average±SD, n=3) and calibrated (K_{OA}, average±propagated error) octanol–air partition coefficients for OPEs at 25 °C, energies of phase transfer (ΔU_{OA}, average±propagated error), and regression parameters for Eq. (4.9) 55

Table 4.2 Uncalibrated ($P_{L\text{-}GC}$, average ± SD, n = 3) and calibrated (P_L, average ± propagated error) vapor pressures for OPEs at 25°C, enthalpies of vaporization (ΔH_{vap}, average ± propagated error), and regression parameters for Eq. (4.16) 60

Table 4.3 Regression parameters (A and B) for the equation log $K_{PUF\text{-}air} = A + B/T$ (T is the temperature in Kelvin), enthalpies (kJ/mol), log $K_{PUF\text{-}air}$ ± SD at 25°C 67

Table 4.4 The regression parameters (±standard errors) for the equation ln$H$=A+B/T(K), enthalpies and entropies of phase change, and H values measured at 25°C (average ± SD) for OPEs in deionized water 71

Table 4.5 Experimental K_{PEW} values (L/kg) for OPEs measured in DI water at 19.2°C 73

Table 4.6 Average gas and particle phase OPE concentrations for winter and summer sampling periods 75
Table 4.7 Comparison of overall average OPE concentrations (ng/m^3) obtained in this study with those reported in the literature 77
Table 4.8 Particulate matter characteristics for summer and winter seasons 82
Table 4.9 Activity coefficients of OPEs in octanol and in organic matter in particles 89
Table 4.10 Ambient air OPE concentrations (ng/m^3) in winter 93
Table 4.11 Ambient air OPE concentrations (ng/m^3) in summer 94
Table 4.12 PCA results for OPEs in air samples 104
Table 4.13 Soil OPE concentrations (ng/g) in winter 107
Table 4.14 Soil OPE concentrations (ng/g) in summer 108
Table 4.15 Seawater OPE concentrations (ng/L) in winter 124
Table 4.16 Seawater OPE concentrations (ng/L) in summer 124
Table 4.17 Calculated air-water exchange fluxes (ng/m^2 day) 136

CHAPTER 1
INTRODUCTION

Organic flame retardants (FRs) have been applied for several decades to reduce the flammability of various industrial and commercial products (Kemmlein, Hahn, & Jann, 2003; van der Veen & de Boer, 2012). Brominated flame retardants (BFRs) and organophosphate esters (OPEs) are chemicals used in a wide range of households and consumer products to reduce their flammability in order to meet the fire regulations (Ali et al., 2012; Tajima et al., 2014; Yang, Ding, Huang, Xie, & Liu, 2014). Some BFRs (i.e. polybrominated diphenyl ethers (PBDEs)) have historically been the most widely used, but their use has been restricted/banned globally due to their persistence, bioaccumulation, and toxicity (Andrae, 2007; Fromme et al., 2014; Moller, Xie, Caba, Sturm, & Ebinghaus, 2011; Qiu, Zhu, & Hu, 2010). The restrictions on the production and usage of PBDEs have led to the application of alternative FRs to meet the fire safety regulations for various consumer products. Among those alternatives, OPEs have been associated recently with a variety of applications in a wide range of products (Cequier et al., 2014; Kemmlein et al., 2003; Lai et al., 2015; van der Veen & de Boer, 2012).

OPEs are widely utilized as flame retardants, plasticizers and anti-foaming agents in a variety of industries, including plastics, furniture, textile, electronics, construction, vehicle and petroleum industries (Marklund, Andersson, & Haglund, 2003). In general, the halogenated OPEs are used as flame retardants, while the non-halogenated ones are mostly used as plasticizers (Andresen, Grundmann, & Bester, 2004). As in the case of many additives, organophosphate compounds are just mixed, and not chemically bonded, with the containing materials, therefore they can be easily released into the surrounding environment via volatilization, abrasion and/or leaching during their lifetime, including production, usage, disposal and recycling processes (Rodriguez et al., 2006; Wei et al., 2015). The major commercial products that known to include OPEs are; textile coatings, upholstery, rubber, polyurethane foam, antistatic agents, cellulose, cotton, cutting oils, electronic equipments such as

video display units cables, hydraulic fluids, casting resins, glues, engineering thermoplastics, epoxy resins and phenolic resins (van der Veen & de Boer, 2012).

Because of production and use restrictions placed on BFRs, a high production volume and a high consumption level is expected to increase for OPEs yearly (US-EPA, 2015; Wei et al., 2015). In 1992, the worldwide usage of FRs was estimated at 600,000 tons, of which approximately 17% were OPEs (OECD, 1995; WHO, 1997). By 2001 and 2004, the global consumption volume of OPEs totaled 186,000 tons (Marklund, Andersson, & Haglund, 2005a) and 300,000 tons (of which 70% was consumed as FRs) (Makinen et al., 2009; Moller et al., 2012) respectively. In a more recent research, global OPE use was estimated as 620,000 tons corresponding to 30% of global FR consumption and it was expected to be approximately 680,000 tons by 2015 ("China Market Research Reports," 2016). In Western Europe, the usage of OPEs sharply increased from 58,000 tons in 1998 to 83,000 tons in 2001 and to 85,000 tons in 2005, and up to 91,000 tons in 2006; the OPEs were responsible for 20% of the total consumption of FRs in 2006 (Marklund, Andersson, & Haglund, 2005b; Reemtsma, Quintana, Rodil, Garcia-Lopez, & Rodriguez, 2008). Nevertheless, recent studies indicated that the general production and usage of OPEs can be expected to increase in the future (Moller et al., 2012).

OPEs are known to be relatively stable toward biodegradation, especially halogenated OPEs show a high resistance, while their potential to bioaccumulate and -magnify is limited due to their relatively low log K_{OW} (octanol-water partition coefficient) values (<5 for most OPEs) (Reemtsma et al., 2008). Nevertheless, they have been recently detected in marine coastal biota samples (Kim et al., 2011; Sundkvist, Olofsson, & Haglund, 2010). More studies are available on their occurrence in the aquatic environment mainly focusing on the freshwater environment (Andresen et al., 2007; Kim, Cho, Kim, Vanderford, & Snyder, 2007; Regnery & Puttmann, 2010a) and on indoor air/dust (Carlsson, Nilsson, Becker, & Ostman, 1997; Marklund et al., 2003). Even though the predicted atmospheric half-lives of OPEs are generally below the threshold (2 days) to meet the long-range atmospheric transport (LRAT) criterion of the Stockholm Convention, their

occurrence in snow and precipitation (Marklund, Andersson, & Haglund, 2005c; Regnery & Puttmann, 2009, 2010b), pine needles from the Sierra Nevada, U.S. (Aston, Noda, Seiber, & Reece, 1996), and in volcanic lakes in Italy (Bacaloni et al., 2008) clearly shows their occurrence in the outdoor environment followed by deposition to non-source regions.

As a result of increased scientific interest in OPEs, numerous studies have reported OPEs in indoor air (Bjorklund, Isetun, & Nilsson, 2004; Chung & Ding, 2009; Fromme et al., 2014; Yadav & Devi, 2019), human blood (Greaves, Su, & Letcher, 2016), hair, nail (Liu, Salamova, He, & Hites, 2015) and urine (Cequier, Sakhi, Marce, Becher, & Thomsen, 2015) indoor dust (Fromme et al., 2014; Takeuchi et al., 2014; Tao, Sellstrom, & de Wit, 2019; Yadav & Devi, 2019), river water (Bollmann, Moler, Xie, Ebinghaus, & Einax, 2012; Li, Wang, & Kannan, 2019; Wang et al., 2015; Wolschke, Suhring, Xie, & Ebinghaus, 2015) and sediments (Chung & Ding, 2009; Cristale, Vazquez, Barata, & Lacorte, 2013c; Ren et al., 2019), lakes (McDonough, Puggioni, Helm, Muir, & Lohmann, 2016; Venier, Dove, Romanak, Backus, & Hites, 2014), sea water (Bollmann et al., 2012; Li et al., 2017a), as well as fish and biota (Campone, Piccinelli, Ostman, & Rastrelli, 2010; He, Lu, & Wei, 2019b; Kim et al., 2011; Li et al., 2019; Sundkvist et al., 2010). In addition to monitoring studies, Ma and Hites (2013) carried out a chromatographic analysis optimization study, Teo, McDonald, Coleman, and Khan (2015) researched isotope dilution method for OPEs, Brommer, Jantunen, Bidleman, Harrad, and Diamond (2014) determined vapor pressures of 11 OPEs and Ni, Kumagai, and Yanagisawa (2007) developed a passive flux sampler to investigate OPEs emissions while Abdollahi et al. (2017) compared polyurethane foam (PUF) and sorbent impregnated (SIP) PUF disk passive air samplers for measuring OPEs. Number of studies related to both measurement and understanding of their occurrence and fate in the environment can be found in the literature. However, there is not a comprehensive and large scale investigation focusing on environmental chemodynamics of OPEs and their exchange mechanisms between environmental mediums (air, water and soil). Although levels in water (lake, river, and sea water) and air (ambient and indoor air) were previously measured in the literature, there is

still limited data on the OPE levels in soil and sea water (He et al., 2019a; Hu et al., 2014; Li et al., 2017a; Li et al., 2019). Additionally, there are only a few researches that measured K_{OA} (octanol-air partition coefficient) values of some OPEs as an essential physicochemical parameter, while *H* (Henry's Law Constant) values of OPEs have not been determined experimentally to date (Wang et al., 2017a). Besides, there are only a few studies in Turkey investigating OPEs in soil samples from industrial regions and indoor dust samples (Kurt-Karakus, Jantunen, Topcu, & Tepe, 2014; Kurt-Karakus, Alegria, Birgul, Gungormus, & Jantunen, 2018; Shoeib et al., 2019). Within the scope of the present study; 11 most commonly researched and detected OPEs (triethyl phosphate, tributyl phosphate, tris[2-chloroethyl] phosphate, tris[1-chloro-2-propyl] phosphate, tris[3-chloropropyl] phosphate tris[1,3-dichloro-2-propyl] phosphate, tris[2-butoxyethyl] phosphate, triphenyl phosphate, 2-ethylhexyl diphenyl phosphate, tris[2-ethylhexyl] phosphate, tri[2-isopropylphenyl] phosphate) were investigated to fill the gaps in the literature and in Turkey. The main objectives of the present study are:

i. To experimentally determine physicochemical properties (K_{OA}, *H*, supercooled liquid vapor pressure – P_L, gas-particle partition coefficient – *K*p, LDPE-water partition coefficient - K_{PE-W} and PUF-air partition coefficient $K_{PUF-Air}$) for the OPEs in order to evaluate their transport, environmental behavior and fate.
ii. To investigate gas-particle partitioning of OPEs in the atmosphere,
iii. To determine spatial and seasonal variations of atmospheric OPE concentrations in Izmir region,
iv. To investigate the spatial and seasonal variations of OPE levels in soil and to assess their air-soil exchange patterns.
v. To determine the spatial and seasonal variations of seawater OPE concentrations in order to evaluate their air-seawater exchange.

CHAPTER 2
LITERATURE REVIEW

2.1 Characteristics of OPEs

Phosphorus containing flame retardants (FRs) can be categorized in three main groups including (i) inorganic FRs (red phosphorus and ammonium polyphosphate), (ii) organic compounds with three different structures as organophosphate esters (OPEs), phosphonates and phosphinates and (iii) halogenated OPEs (EFRA, 2007). Halogenated OPEs combine the properties of both the halogen and the phosphorus components. The presence of halogen also increases the lifetime of the flame retardants in the end-product by decreasing its mobility in the polymer (Fisk, Girling, & Wildey, 2003; van der Veen & de Boer, 2012). Within these three groups, two basic types of OPEs can be recognized as reactive and additive OPEs. Reactive OPEs are chemically bonded to a polymer molecule, which makes it more stable against to losses during the lifetime (van der Veen & de Boer, 2012). Additive OPEs are mixed into the polymer and their concentration may decrease during the lifetime of the treated product. Thereby, the flame retardant properties can decrease in time (Fisk et al., 2003). On the other hand, these compounds could also be classified as alkyl-, aryl-, oligo- and chlorinated OPEs according to their chemical structures. The most known chlorinated OPEs tris(1,3 dichloro-2-propyl)phosphate (TDCiPP), tris(1-chloro-2-propyl)phosphate (TCiPP), and tris(2-chloroethyl)phosphate (TCEP) were reported as toxic and carcinogenic while TCEP, triphenyl phosphate (TPhP), and tributyl phosphate (TnBP) were reported to be neurotoxic (EU, 2008; Kim & Kannan, 2018; WHO, 1991a, 1991b, 1998).

There is a great variation in physicochemical properties of OPEs such as water solubility, log K_{OW}, log K_{OA}, H and vapor pressure. Most of these properties in the literature were obtained from commercial standard reference compounds and/or several databases based on approximate calculations and predictive models (ChemSpider, 2011; Sigma-Aldrich, 2016; US-EPA, 2019; Wang et al., 2017a). For example, K_{OA} values of almost all OPEs are estimated to greater than one, and thus

these compounds predominantly partition into organic phases (i.e. soil and biota).Even so log K_{OA} values of some OPEs vary within a wide range from 5.31 (TCEP) to 14.98 (tris[2-ethylhexyl] phosphate - TEHP). Similarly, most of the OPEs have a positive log K_{OW} value, which means they are more lipophilic than hydrophilic. The log K_{OW} values also vary considerably between the different OPE groups. In previous studies, researchers mostly use these estimated values due to lack of experimental values. Table 2.1 summarizes the selected physicochemical properties of 11 OPEs that were investigated in the present study.

Table 2.1 List of the OPEs to be investigated

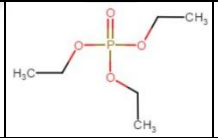
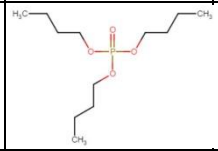
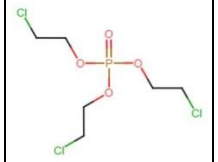
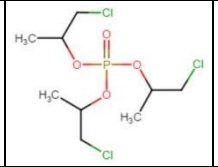
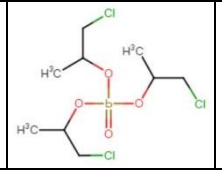
	Compound	Acronym	CAS No.[1]	Molecular Structure[1]	Molecular Weight [1] (g/mole)	log K_{OA}[2]	log K_{OW}[2]	H[2] (atm m^3/mole)	Common Applications
1	triethyl phosphate	TEP	78-40-0		182.15	6.63	0.87	5.83×10^{-7}	PVC, polyester resins (to lower the overall viscosity of the formulations) high-viscosity polyol formulations, polyurethane foam (van der Veen & de Boer, 2012; WHO, 1997)
2	tributyl phosphate	TBP TnBP	126-73-8		266.31	8.24	3.82	3.19×10^{-6}	Antifoam agent, hydraulic fluids, lacquers, extractant for metal complexes, plastic, solvent (Andresen et al., 2004; Sigma-Aldrich, 2016)
3	tris(2-chloroethyl) phosphate	TCEP	115-96-8		285.49	5.31	1.63	2.55×10^{-8}	PVC, cellulose, coatings, polyester resins, textile, polyurethane foam (Andresen et al., 2004; WHO, 2000)
4	tris(1-chloro-2-propyl) phosphate *isomer 1*	TCPP TCiPP1	13674-84-5		327.57	7.60[3]	6.04[3]	5.96×10^{-8}	Polyurethane foam, fabrics (Keller, Raju, Webster, & Stapleton, 2014; OECD, 2011)
5	tris(1-chloro-2-propyl) phosphate *isomer 2*	TCPP TCiPP2	76025-08-6[3]		327.57	7.61[3]	6.06[3]	5.96×10^{-8}	n.s.

Table 2.1 continues

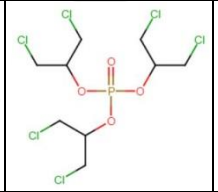
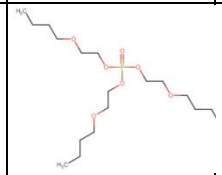
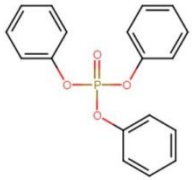
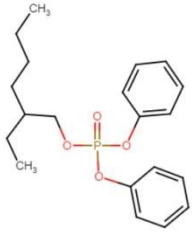
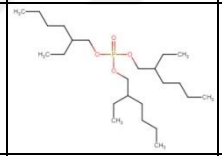
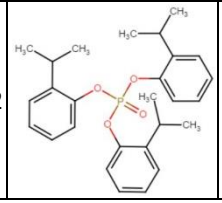
	Compound	Acronym	CAS No.[1]	Molecular Structure[1]	Molecular Weight [1] (g/mole)	log K_{OA}[2]	log K_{OW}[2]	H[2] (atm m^3/mole)	Common Applications
6	tris(1,3-dichloro-2-propyl) phosphate	TDCPP TDCiPP	13674-87-8		430.90	10.62	3.65	2.61×10^{-9}	Plastic, textile, polyurethane foam (Andresen et al., 2004; WHO, 1997)
7	tris(2-butoxyethyl) phosphate	TBEP TBOEP	78-51-3		398.47	13.06	3.00	1.20×10^{-11}	Antifoam agent, floor polish, lacquers, plastic, rubber, solvent (Andresen et al., 2004; WHO, 2000)
8	triphenyl phosphate	TPP TPhP	115-86-6		326.28	8.46	4.70	3.98×10^{-8}	Hydraulic fluids, PVC, electronic equipment such as video display units cables, casting resins, glues, engineering thermoplastics, phenylene-oxide-based resins, phenolic resins (Andresen et al., 2004; Bjorklund et al., 2004; WHO, 1997)
9	2-ethylhexyl diphenyl phosphate	EDP DPEHP EHDPP	1241-94-7		362.40	8.38	6.30	2.48×10^{-7}	Hydraulic fluids, PVC, food packaging (WHO, 1997)

Table 2.1 continues

	Compound	Acronym	CAS No.[1]	Molecular Structure[1]	Molecular Weight [1] (g/mole)	log K_{OA}[2]	log K_{OW}[2]	H[2] (atm m^3/mole)	Common Applications
10	tris(2-ethylhexyl) phosphate	TEHP	78-42-2		434.63	14.98	9.49	9.56×10^{-5}	PVC, cellulose, paints and coatings, rubber, solvent, polyurethane foam (WHO, 2000, 1997)
11	tris(2-isopropylphenyl) phosphate	TPPP T2iPPP	64532-95-2		452.52	13.99	9.07	2.93×10^{-7}	n.s.

(1): TOXNET (2016); (2): US-EPA (2019); (3): Truong, Diamond, Helm, and Jantunen (2017)

n.s.: not specified

2.2 Applications, Sources and Environmental Occurrence

As previously mentioned, OPEs became more and more widely used commercial compounds over the years with number of intended purposes. Halogenated OPEs are frequently used as flame retardants, whereas the non-halogenated OPEs are primarily employed as plasticizers (Andresen et al., 2004). In the gas-phase, halogenated OPEs remove H^+ and OH^- radicals from the flammable gasses, by reaction with the Br and Cl atoms. The removal of the H^+ and OH^- radicals results in a slowdown of the burning process, and reduces the spreading of the fire (EFRA, 2007). The effectiveness of the halogenated OPEs depends on the number of halogen atoms present in the molecule. Another flame retarding mechanism of OPEs occurs in the solid-phase by heating of phosphorus to form a polymer of phosphoric acid. This acid causes a char layer, which shields the material from oxygen, in that way preventing the formation of flammable gasses (Chen, Hu, & Song, 2008; van der Veen & de Boer, 2012). OPEs may also be used as stabilizers for anti-foaming agents and as additives to floor polishes, lubricants, lacquers and hydraulic fluids. For example, the most common chlorinated OPEs (TCEP, TCiPP and TDCiPP) are generally applied in flexible and rigid PUFs, whereas tris(2-butoxyethyl) phosphate – TBOEP is widely used in floor wax and as a plasticizer in vinyl plastics and rubber stoppers (Marklund et al., 2003). TPhP is primarily used in unsaturated polyester resins and in PVC as a plasticizer (Wei et al., 2015). Additionally, TBOEP, TPhP and TnBP are utilized as extreme pressure additives and anti-wear agents in hydraulic fluids, lubricants, transmission fluids and motor oils (Regnery, Puttmann, Merz, & Berthold, 2011). TnBP is also used as an antifoaming agent in concrete, as a wetting agent in casein glue and as a pasting agent in pigment paste (Marklund et al., 2005a).

As in the case of many additives, organophosphate compounds are just mixed, and not chemically bonded, with the containing materials, therefore they can be easily released into the surrounding environment via volatilization, abrasion and/or leaching during their lifetime, including production, use, disposal, and recycling processes. Because of the extremely high OPE concentrations, a wide variety of

consumer products and building materials might act as potential sources of OPEs to the environment (Wei et al., 2015). Previous studies indicated that various building materials, soft foams, paints and wallpapers primarily contained TCEP, whereas insulation and sealant foams were dominated by TCiPP. For example, acoustic ceiling coatings contained the highest level of TCEP (68.0 mg/g), whereas soft PUFs had lower levels of TCEP (19.8 mg/g) (Ingerowski, Friedle, & Thumulla, 2001). Marklund et al. (2005c) measured TPhP levels in turbo oil, engine and accessory oil, and jet engine oil from an airport as 6.10, 8.90 and 1.90 μg/g whereas tris (2,4,6-trimethoxyphenyl) phosphine (TMPP) were detected at 12,000, 6,300 and 6,500 μg/g in the same compartments, respectively. Concerning the PUF samples from different furnishings (e.g., couches, chairs, mattress pads, pillows and insulation foam from a laboratory-grade dust sieve) in the USA, TCiPP and TDCiPP were quantified at 0.5–2.2% and 1–5% (by weight), respectively (Stapleton et al., 2009). Based on the EU risk assessment, approximately 40% of the TCiPP in a finished product was available for release, whereas the total continental European and the total regional emission discharges of TCiPP to the air were estimated at 89.6 and 135 kg/d, respectively (EU, 2008). Additionally, Marklund et al. (2005c) pointed out that traffic is another major source of number of OPEs. In addition to production and usage of OPEs, treatment of e-waste, which has shown to be an important source of PBDEs in the atmosphere, might also be an important source of OPEs (Chen et al., 2009; Muenhor, Harrad, Ali, & Covaci, 2010; Tian et al., 2011). In the literature, industrialized countries (i.e., U.S.A., Japan, China, and Germany) are also referred as "*source regions*" for OPEs, due to such kind of recycling, treatment, and dismantling processes (Moller et al., 2012).

2.3 Environmental Levels

2.3.1 Air

Air, which is an important compartment of the environment, is regarded as a major reservoir for the OPEs released from consumer products, resulting in the ubiquitous detection of OPEs in the atmosphere. Since, most of the consumer

products located in indoor environments, OPEs usually emitted into indoor environments and may eventually reach to the ambient air through ventilation processes (Marklund et al., 2003). Although scientific interests largely focused on investigating OPEs in indoor (Bjorklund et al., 2004; Chung & Ding, 2009; Fromme et al., 2014; Hartmann, Burgi, & Giger, 2004; Takeuchi et al., 2014), several studies on OPEs in ambient air can also be found in the literature (Liu et al., 2016a; Moller et al., 2011; Salamova, Ma, Venier, & Hites, 2014b). For instance, Salamova et al. (2014b) measured particle-phase levels of 12 OPEs in the North American Great Lakes atmosphere. They determined atmospheric ΣOPE concentrations ranging from 120±18 to 2,100±400 pg/m^3 at five urban sites dominated by TCEP, TCiPP, and TDCiPP. In another study, Moller et al. (2011) measured ΣOPE concentrations for 8 compounds from 110 to 1,400 pg/m^3 while TCiPP dominated all samples. They also noted that the highest concentrations were observed in continental air masses showing the high influence of industrialized regions including production sites on atmospheric emissions and concentrations. Wolschke et al. (2016) measured the concentration (gas + particle phase) of total 9 studied OPEs was on average 5 pg/m^3 in the marine atmosphere of the German Coast. In addition to researches in marine and remote air, OPEs were also measured in urbanized, semi-urbanized and rural locations. Shoeib, Ahrens, Jantunen, and Harner (2014) collected ambient air samples from an urban location in Toronto for 15 PBDEs, 11 BFRs, 2 CFRs (chlorinated flame retardants) and 6 OPEs. They determined that ΣOPE mean concentration of 2,643 pg/m^3 was ~70 times higher than ΣBDEs and ~240 times higher than other detected CFRs. In another metropolitan city Bursa, Turkey, Kurt-Karakus et al. (2018) collected OPE samples from 8 sites including urban, sub-urban, industrial, rural and background environments using PUF-PAS (PUF-Passive Air Sampler). They measured total OPE concentrations ranged from 529 to 19,139 pg/m^3 with overall detection frequencies of 100% (TCiPP and TPhP), 88% (TBOEP), 85% (TCEP), 78% (TEHP) and 20% (tri(2-isopropylphenyl) phosphate - T2iPPP). Ohura, Amagai, Senga, and Fusaya (2006) obtained substantially high ΣOPE levels (10,600 - 91,400 pg/m^3) for the outdoor air from Japanese house backyards during the summer and winter, possibly because of intensive usage and the significant release of OPEs from the domestic products in the houses. Although several studies indicated

that indoor consumer products and building materials are substantial sources for atmospheric OPEs in urban sites, several researches showed that traffic may also be another significant source (Green et al., 2008; Marklund et al., 2005c). Another inference from the recent studies is that OPEs may reach to sparsely populated rural areas, remote sites and even arctic regions via LRAT (Moller et al., 2012; Suhring et al., 2016a). Further results from the recent literature were given in Table 2.2.

Table 2.2 Atmospheric OPE levels (in pg/m^3) from different locations reported in the literature

Location	Characteristics	TCiPP	TCEP	TDCiPP	TPhP	TEHP	TnBP	TiBP	TBOEP	T2iPPP	ΣOPE
Tianjin, China[(1)]	Urban	1,080±872	432±396	111±87.9	267±114	113±71.2	74.3±58.5	n.r.	44.2±45.5	n.r.	2,180±1,490
N.E. of Beijing, China[(1)]	Rural	318±304	51.4±40.1	17.2±13.2	49.8±27.7	28.4±12.4	21.4±13.6	n.r.	28.2±20.1	n.r.	531±393
Bursa, Turkey[(2)]	Industrial	256	b.d.l.	b.d.l.	237	112	n.r.	n.r.	n.r.	n.r.	4019
	Urban	220	39	b.d.l.	54	b.d.l.	n.r.	n.r.	n.r.	n.r.	1115
Albany, New York, USA[(3)]	Urban (Airport)	591**	373**	219**	493**	37.7**	259**	261**	n.r.	n.r.	3880
Canadian Arctic Sea[(4)]	Arctic	92±88*	118±120	10±12	22±26	n.a.	747±876	n.r.	n.d.	n.a.	291±591
German Coast[(5)]	Sub-urban (sea side village)	9.8±6.1	3.4±2.1	0.95±0.76	3.2±3.2	11.4±13.1	6.3±10.8	8.6±5.8	n.r.	n.r.	n.r.
Chicago[(6)]	Urban	530±80	180±25	120±46	140±22	41±6	250±53	n.r.	320±36	4.0±1.1	1,500±170
Sturgeon Point[(6)]	Rural	170±54	130±27	28±3	43±10	8.5±2.8	34±7	n.r.	76±13	3.6±0.4	340±85
Eagle Harbor[(6)]	Remote	32±9	5.5±0.9	52±19	55±13	8.7±2.2	180±60	n.r.	68±15	n.r.	170±52
Shimizu, Japan (summer)[(7)]	Industrialized Urban	n.r.	14.3	n.r.	n.r.	n.r.	13.7	n.r.	n.r.	n.r.	n.r.
Shimizu, Japan (winter)[(7)]		n.r.	6.59	n.r.	n.r.	n.r.	9.27	n.r.	n.r.	n.r.	n.r.
Northern Pacific Ocean[(8)]	Arctic	98-269*	159-282*	5-8*	9-2*4	1-12*	6-14*	14-21*	b.d.l.-16*	n.r.	
Indian Ocean[(8)]	Antarctic	37-549*	46-570*	b.d.l.-220*	b.d.l.-74*	4-51*	7-75*	7-96*	b.d.l.-44*	n.r.	230-2900
Mediterranean Sea[(9)]	Remote	n.r.	70-854*	b.d.l.-460*	b.d.l.-80*	56-307*	56-600*	4-650*	n.r.	n.r.	400-5100
Black Sea[(9)]	Remote	n.r.	300-2,417*	b.d.l.-97*	3-40*	36-190*	202-370*	66-190*	n.r.	n.r.	1,700-6,160

(1): Zhang et al. (2019a); (2): Kurt-Karakus et al. (2018); (3): Li et al. (2019); (4): Suhring et al. (2016a); (5):Wolschke et al. (2016); (6):Salamova et al. (2014b); (7):Ohura et al. (2006); (8):Moller et al. (2012); (9): Castro-Jimenez, Berrojalbiz, Pizarro, and Dachs (2014)

n.a.: not applicable; b.d.l.: below detection limit; n.r.: not reported; *:min.-max, **:median

2.3.2 Water

Surface waters (Andresen et al., 2004; Bollmann et al., 2012; Regnery & Puttmann, 2010a), drinking waters (Kim et al., 2007; Li et al., 2014), lakes (Salamova et al., 2014b; Venier et al., 2014), rivers (Wang et al., 2015; Wolschke et al., 2015), waste waters (Bester, 2005; Kim et al., 2007) and even sea waters (Hu et al., 2014; Li et al., 2017a) are aquatic mediums that OPEs were widely investigated. Andresen et al. (2004) measured concentrations of 20–200 ng/L for TCiPP, 13–130 ng/L for TCEP, about 50 ng/L for TDCiPP, 10–200 ng/L for TBOEP, up to 40 ng/L for TPHP in a river, and concentrations of 400 ng/L for TCPP, 130 ng/L for TCEP, about 120 ng/L for TDCiPP and 500 ng/L for TBOEP in effluent of a sewage treatment plant. Bollmann et al. (2012) investigated spatial and seasonal variations of 16 different OPEs in the surface waters and found out TCiPP was the predominant compound in most samples followed by TEP and TiBP (tri-isobutyl phosphate). Five Great Lakes in Canada were investigated for flame retardants and legacy chemicals and ΣOPE concentrations ranged from 7.3±4.5 ng/L (Lake Huron) to 96±43 ng/L (Lake Erie). The most abundant OPE was TBOEP, with the highest concentration of 75±39 ng/L (Venier et al., 2014). In another study; Bacaloni et al. (2008) selected three lakes from urban, sub-urban and rural areas and investigate OPE concentrations during a year. Results indicated that maximum OPE levels were reached in October-November, and concentrations decreased to a minimum value in March-April according to local anthropogenic activities. In China, 40 rivers from a heavily industrialized region under intense anthropogenic influences were investigated for 11 OPEs with their spatial distributions (Wang et al., 2015). Extremely high TCiPP concentration in a river were measured by Cristale, Katsoyiannis, Sweetman, Jones, and Lacorte (2013b) near high populated areas and wastewater discharges as 113-26,050 ng/L with a mean value of 6,040 ng/L. Table 2.3 lists the previously reported aquatic OPE concentrations from several studies. As can be inferred from the table, concentrations are highly variable due to type of the studied locations and also compound species. Urbanized and industrialized regions have higher OPE levels compared to rural areas, while TCiPP and TCEP were the predominant compounds in most cases. Lakes and rivers were the most commonly investigated water bodies,

while there are very limited researches report OPE levels in seawater (Andresen et al., 2007; Hu et al., 2014).

Table 2.3 Aquatic OPE levels (in ng/L) in different water bodies reported in the literature

Matrice	Location	Characteristics	TCiPP	TCEP	TDCiPP	TPhP	TBP	TnBP	TiBP	TBOEP	TEP	ΣOPE
Lake	Erie[1]	urban	12	1.5	4	1.2	n.r.	2.2	n.r.	74.9	n.r.	95
	Huron[1]	urban	2.6	0.28	0.87	0.13	n.r.	0.27	n.r.	5.2	n.r.	7.3
	Michigan[1]	urban	3	0.38	1.1	0.13	n.r.	0.61	n.r.	2.6	n.r.	9.3
	Albano[2]	urban [a]*	6±3	5±2	5±2	7±5	n.r.	42±11	81±12	10±6	26±4	182±45
		urban [b]*	34±19	9±4	60±36	3±2	n.r.	45±26	96±21	53±18	5±4	305±130
	Vico[2]	sub-urban [a]*	12±11	n.q.	7±3	6±3	n.r.	17±8	31±9	75±18	2±1	150±53
		sub-urban [b]*	3±1	4±4	2±3	6±2	n.r.	5±5	3±3	11±9	1±0	35±27
	Martignano[2]	rural [a]*	n.q.	n.d.	4±3	2±1	n.r.	5±3	13±5	23±9	2±2	49±23
		rural [b]*	n.q.	n.d.	2±0	4±3	n.r.	10±3	5±2	8±5	2±1	31±14
River	China[3]	urban+industrial[c]**	5-921	1-268	<LOD-44	<LOD-16	<LOD-81	n.r.	<LOD-218	<LOD-47	n.r.	6-1595
	Ruhr[4]	industrial [d]	130	190	41	<LOD	n.r.	60	50	<LOD	n.r.	471
		industrial [e]	150	81	<LOD	12	n.r.	26	150	130	n.r.	549
	U.K.[5]	urban**	113-26,050	119-316	62-149	6.3-22	n.r.	n.r.	n.r.	n.r.	n.r.	n.r.
Precipitation	Frankfurt[6]	urban**	32-3,562	10-485	<LOD-532	n.r.	n.r.	<LOD-1679	<LOD-	<LOD-505	n.r.	42-8,173
	Bekond[6]	sub-urban**	5-1,214	<LOD-127	<LOD-87	n.r.	n.r.	<LOD-110	<LOD-160	<LOD-205	n.r.	5-1903
	Feldberg[6]	rural**	<LOD-1,154	11-390	<LOD-497	n.r.	n.r.	<LOD-458	<LOD-424	<LOD-242	n.r.	11-3165
Sewage water	n.r.[7]	urban [f]*	0.35±0.02	0.05±0.01	n.r.	0.47±0.05	n.r.	0.36±0.01	0.18±0.02	33.73±3.41	n.r.	35.1±3.52
	n.r.[7]	urban [g]*	0.37±0.01	0.12±0.01	n.r.	0.22±0.02	n.r.	0.18±0.03	0.26±0.02	9.53±0.54	n.r.	10.7±0,63
Seawater	China[8]	urban+industrial***	84.12	134.4	109.3	n.r.	n.r.	n.r.	n.r.	n.r.	n.r.	424.6
	Atlantic and Arctic Ocean[9]	remote***	1.6	0.6	0.004	b.d.l.	n.r.	0.10	0.23	n.r.	n.r.	2.63
	China[10]	sub-urban***	12.9	1.56	0.51	0.36	n.r.	1.51	1.48	0.42	10.3	18.1
	Bohai Bay [11]	sub-urban***	237	182	12.7	1.95	11.4	n.r.	97.2	17.3	1500	2202

(1):Venier et al. (2014); (2):Bacaloni et al. (2008); (3):Wang et al. (2015); (4): Andresen et al. (2004); (5): Cristale et al. (2013b); (6): Regnery and Puttmann (2010b); (7): Rodriguez et al. (2006); (8): Hu et al. (2014); (9): Li et al. (2017a); (10): Lai et al. (2019); (11): Chen et al. (2019) n.r.: not reported; n.q.: not quantified; n.d. not detected; LOD: limit of detection; a: samples collected in June; b: samples collected in January; c: ranges of 40 studied rivers; d: samples collected in July; e: samples collected in September; f: influent water; g: effluent water; *: mean±std. dev.; **:min.-max; ***: median

2.3.3 Soil

Many studies have discussed the occurrence and fate of OPEs in air, water, indoor dust and precipitation. However, a limited number of studies have reported OPE levels in soil (Cui et al., 2017; He, Yang, Yang, Li, & Wei, 2017; Li et al., 2019; Mihajlovic & Fries, 2012; Wang et al., 2019; Zheng et al., 2016). Soil is composed of mainly mineral particles and organic matter (OM) and generally indicated being a primary environmental medium acting as a sink for most hydrophobic organic compounds such as OPEs (van der Veen & de Boer, 2012; Wei et al., 2015). Thus, it is widely put forward that surface soil acts as an urban environmental pollution indicator as it collects number of inputs of pollutants from ranging stationary or dynamic sources such as industrial sites, urban traffic, and building construction materials (Lu, Wang, Lei, Huang, & Zhai, 2009). In a recent study, Wang et al. (2019) was conducted a nationwide survey with 98 soil samples targeting 19 OPEs across China. They measured total OPE concentrations in soils ranging from 4.50 to 430 ng/g dry weight (dw) and pointed out some relationships between OPE levels and population density, economic development and urbanization status of the sampling areas. In another research carried out by Ren et al. (2019), 20 soil samples were collected near an OPE production plant that produces and sells several OPEs including TEP, TCEP, TCiPP, TPhP. They determined that the total OPE concentration with an average of 1.10 ng/g dw dominated by TCEP, TCiPP, TPhP. In Bursa, Turkey, Kurt-Karakus et al. (2018) collected soil samples (n=8) from urban, sub-urban, industrial, rural and background sites and their measured total OPE concentrations ranged from 38 to 468 ng/g dw while alkylated OPEs were dominant at six sites and chlorinated OPEs at two sites. Further results reported in previous studies were given in Table 2.4. Additionally, sediment and sludge as structurally similar matrices to soil, have been more widely investigated mediums in the literature. In sludge samples from sewage treatment plants, considerable and comparable concentrations of the ΣOPEs were observed at 620 - 21,000 ng/g in Sweden, Spain and Germany, dominated by TCiPP, tris (2-butoxyethyl) phosphate (TBOEP), ethylhexyl diphenyl phosphate (EHDPP) and TnBP (Bester, 2005; Cristale & Lacorte, 2013; Marklund et al., 2005b). Additionally, Green et al. (2008) detected

7460 - 17,800 and 22,600 - 33,200 ng/g ΣOPE levels in sediments collected from the pump pit at landfill sites and automobile destruction sites in Norway, respectively. In another research, TnBP and trioctyl phosphate(TTP) concentrations were measured as 170 and 390 ng/g, respectively in sediment samples from a river near an industrial point source (Ricking, Schwarzbauer, & Franke, 2003). Mihajlovic, Miloradov, and Fries (2011) collected soil samples from the university campus in Osnabruck, the average concentrations of TCiPP, TPhP and TCEP varied from 1.23 to 4.96 ng/g.

Table 2.4 Soil OPE levels (in ng/g dw) reported in the literature

Location	Characteristics	TnBP	TCEP	TCiPP	TDCiPP	TEHP	TBOEP	TPhP	EHDPP	TEP	ΣOPE
China[(1)]	industrial	0.29-17.6	0.33-50.6	0.33-400	<0.05-65.7	<0.10-18.1	<0.09-12.7	<0.02-1.70	<0.02-1.11	<0.06-11.3	4.80-417
China[(2)]	urban	n.d.-9.97	0.46-11.8	n.d.-167	n.d.-1.87	n.d.-4.01	n.d.-12.8	n.d.-115	n.d.-1.23	n.d.-13.5	1.70-179
Hengshui, Hebei, China[(3)]	near an OPE production plant	-	0.58	0.53	-	-	-	0.04	-	-	n.r.
Bursa, Turkey[(4)]	urban industrial suburban rural background	-	1.03-2.30	7.11-64.08	-	-	-	1.63-2.67	-	-	37-468
Osnabruck, Germany[(5)]	suburban	-	5.07-23.48	5.66-19.82	-	-	-	-	-	-	n.r.
Hung Yen, Vietnam[(6)]	e-waste site	-	<2-20	<4-300	<2-99	-	-	9.9-4,100	<2-60	-	12-4,900
	open-burning site	-	<2	<4	<2-3.0	-	-	<3-55	<2	-	<4-120
	rice paddy site	-	<2	<4	<2	-	-	<3-8.0	<2	-	<4-11
Guangzhou, China[(7)]	urban (park areas)	2-23	3-8	0.2-3	2-15	1-7	13-67	0.4-4	2-9	4-11	41-150
	urban (paddy and vegetable fields)	2-25	n.d.-47	n.d.-1	n.d.-11	n.d.-15	17-114	1-5	n.d.-22	1-7	63-250

(1): Wang et al. (2019); (2): He et al. (2019a); (3): Ren et al. (2019); (4): Kurt-Karakus et al. (2018); (5): Mihajlovic and Fries (2012); (6): Matsukami et al. (2017); (7):Cui et al. (2017)

n.r.: not reported, n.d.: not detected

2.4 Sampling and Analytical Methods

2.4.1 Sample Collection

Increasing interest on OPEs resulted in a wide range of analytical and experimental methods. In the case of sampling OPEs in the ambient air, researchers mostly used high-volume air samplers (Luo, Bao, Guo, Li, & Zeng, 2016; Luo, Bao, Wu, Li, & Zeng, 2014; Moller et al., 2012; Salamova et al., 2014b; Wolschke et al., 2016; Wu, Venier, & Salamova, 2020). Such kind of active air sampling techniques, could offer information on gas and particle phase distribution in high temporal resolution, however, it is not suitable for massive field monitoring to determine the spatial distribution due to the dependence on power supplies as well as instrumental expenses (Ahrens, Harner, Shoeib, Koblizkova, & Reiner, 2013; Liu et al., 2016a). Nevertheless, passive air samplers (PASs) could provide integrated data for relatively long sampling periods with simplicity and low cost, making it feasible to simultaneous sampling at a large geographical scale (Harner, Farrar, Shoeib, Jones, & Gobas, 2003). In the literature, Ni et al. (2007) developed a new type of passive flux sampler that includes Empore C18FF adsorbent disk. In another study, PUF and SIP-PUF passive air sampling methods were compared separately for the analysis of OPEs in outdoor atmospheric environment (Liu et al., 2016a). While, Abdollahi et al. (2017) characterized sampling rates, uptake ratios and passive sampler medium – air partition coefficients ($K_{PSM\text{-}Air}$) for PUF and SIP-PUF disks for several OPEs.

The conventional, and most common, water sampling technique is the active (snap-shot) sampling, of a defined volume of water at a given time using bailers or pumps (Salamova et al., 2014b; Wolschke et al., 2015). In most of these studies, collected water samples were filtered with glass fiber filters to separate dissolved and particulate phases. However, in such sample collection procedures, target compounds can be sorbed to tubes and sampling containers and also they may be degraded and/or may decay during transport (Bopp, Weiss, & Schirmer, 2005; Powell & Puls, 1997). To overcome these challenges, passive sampling techniques have emerged as an efficient way of sample collection, which leads to integrated, efficient and

relatively inexpensive characterization of aqueous pollutants (Cristale, Katsoyiannis, Chen, Jones, & Lacorte, 2013a). Many types of passive sampling techniques have been developed; the uptake of contaminants is usually achieved by sorption/binding onto a media with specific properties which facilitate this process. Vrana et al. (2005) reviewed passive sampling techniques for monitoring organic pollutants in water and noted that ceramic dosimeter, Chemcatcher, POCIS (Polar Organic Chemical Integrated Sampler), TLC (Thin Layer Chromatography) plate and SPMD (semipermeable membrane devices) are some of the used samplers in the literature. Alvarez et al. (2004) developed a passive in situ sampling device, POCIS, that integratively concentrates trace levels of complex mixtures of hydrophilic organic pollutants, enables the determination of their time weighted average water concentrations of waterborne contaminants. Though, it was also noticed that POCIS provides good performance especially with compounds with log K_{ow}<3 (Alvarez et al., 2007). As a more practical and low-cost passive water sampling technique, low density polyethylene (LDPE) sheets were widely used to investigate several organic pollutants in environmental waters (Khairy & Lohmann, 2014; Khairy, Muir, Teixeira, & Lohmann, 2014; Liu et al., 2016b). Briefly, LPDE sheets containing no additives were cut into specific dimensions and cleaned by soaking in a series of organic solvents (pentane, dichloromethane-DCM, acetone, and hexane). Then, cleaned sheets are loaded with performance reference compounds (PRCs) according to procedure detailed by (Booij, Smedes, & van Weerlee, 2002) to determine the sampling rates of the LPDEs for specific compounds. Although using LPDE sheets as passive samplers showed good performances for most of organic pollutants, there are limited number of studies that investigates OPEs in water using LDPE (Yang et al., 2017). Further descriptions on LDPE passive samplers were given in Section 3.2.3.

In several researches soil samples were usually collected from a depth of 0-20 cm of a selected sampling area after removing surface grass root material and large stones. In most of these studies several sub-samples were collected from the defined sampling area to provide composite samples (Mihajlovic & Fries, 2012; Odabasi et al., 2016; Odabasi et al., 2015).

2.4.2 Sample Preparation

Several sample preparation and extraction procedures can be found in the literature. For example, Salamova et al. (2014b) extracted their OPE samples using Soxhlet extraction for 24 h with 50% (v/v) acetone in hexane, followed by fractionation in silica-gel column with 25 mL of hexane, 25 mL of 50% (v/v) hexane in DCM, and 25 mL of 70% (v/v) acetone in DCM, respectively. In another study, Liu et al. (2016a) used accelerated solvent extraction (ASE) system with hexane/DCM (1/1, v/v) as the extraction solvent at 100 °C and 1500 psi in three static cycles of 10 min. Samples were then transferred to a gel permeation chromatography column (GPC) and cleaned up in an alumina column. All target OPEs were eluted with 80 mL of 1:3 hexane/dichloromethane mixture (v/v). Abdollahi et al. (2017) extracted their PUF and SIP-PUF disks by using a pressurized liquid extraction (PLE) system using petroleum ether/acetone (83/17, v/v; 2 cycles).

OPEs in liquid phases were usually cleaned up and fractionated by using commercial solid phase extraction (SPE) cartridges (i.e., Bond Elute, Oasis HLB) while acetonitrile/methanol, dichloromethane, toluene or methanol were commonly used as elution solvents (Quednow & Puttmann, 2009; Regnery & Puttmann, 2010a; Rodriguez et al., 2006). Though, particulate phase OPEs containing filters were sonicated in general (Bollmann et al., 2012; Regnery & Puttmann, 2010b; Wolschke et al., 2015).

2.4.3 Instrumental Analysis

Chromatographic techniques including gas chromatography (GC) and liquid chromatography (LC) are widely used to analyze OPE compounds. In a recent study, Liu et al. (2016a) quantified their OPE samples using ultrahigh performance liquid chromatography (UHPLC) (Thermo Fisher Scientific Inc., Waltham. MA) coupled with API 5500 triple-quadrupole mass spectrometer (TQ-MS) (AB SCIEX Inc. Framingham, MA) and an Acquity UPLC BEH C8 analyte column (2.1 mm i.d. x 100 mm length, 1.7 μm, Waters) was selected for analyte separation. However, GC

systems have been more commonly used as chromatographic separation instruments in related studies (Lai et al., 2015; Ni et al., 2007; Wang et al., 2015). For instance, Wang et al. (2015) analyzed their OPE samples using a GC (Agilent 6890) coupled to a mass selective detector (MSD) (Agilent 5975) (GC-MS) equipped with a programmed temperature vaporizer (PTV) injector. The GC separation was performed with an HP-5MS column (30m x 0.25mm i.d.; 0.25 μm film thickness, J&W Scientific). Although, MSDs mostly coupled with GC systems (Abdollahi et al., 2017; Suhring et al., 2016a; Wang et al., 2015); some other detectors like flame photometric detector (FPD) (Ni et al., 2007), nitrogen-phosphorous detector (NPD) (Rodriguez et al., 2006), have also been used in previous studies. To analyze OPEs by GC-MS, it is important to understand the mass spectra of these compounds using various ionization modes. Ma and Hites (2013) prepared a systematic overview of the electron impact (EI), electron capture negative ionization (ECNI) and positive chemical ionization (PCI) mass spectra of OPEs. EI provides the best sensitivity for the quantitative measurement of these compounds, but PCI and ECNI both have considerable qualitative selectivity.

CHAPTER 3
MATERIALS AND METHODS

3.1 Laboratory Studies

3.1.1 Measurement of Octanol/Air Partition Coefficients (K_{OA})

K_{OA} values for 11 interested OPEs and four of their deuterated derivatives, triethyl phosphate-D15 (TEP-d15), tris(2-chloroethyl) phosphate-D12 (TCEP-d12), tris(1,3-dichloro-2-propyl) phosphate-D15 (TDCiPP-d15), and triphenyl phosphate-D15 (TPHP-d15), were determined as a function of temperature using the gas chromatographic retention time (RT) method for the first time in the literature. The only requirements for this method are knowledge of the temperature-dependent K_{OA} of a standard reference compound and directly measured K_{OA} values for a sufficient number of calibration compounds (Wania, Lei, & Harner, 2002).

Two OPE solutions (at 2 μg/mL) were used. The first solution contained seven OPEs (TEP, TEP-d15, TnBP, TCEP, TCEP-d12, tris[1-chloro-2-propyl] phosphate isomer 1-TCiPP1, tris[1-chloro-2-propyl] phosphate isomer 2-TCiPP2) and the second solution contained eight OPEs (TDCiPP, TDCiPP-d15, TBOEP, TPHP, TPHP-d15, EHDPP, TEHP, and T2iPPP). Reference compounds (fluorene, pyrene, and *p,p*'-DDT) were also added to these solutions. These solutions were run within three different chromatographic temperature ranges with 5-10 °C intervals in triplicate: 100 to 120 °C (TEP, TEP-d15), 145 to 180 °C (TnBP, TCEP, TCEP-d12, TCiPP1, TCiPP2), 210–250 °C (TDCiPP, TDCiPP-d15, TBOEP, TPHP, TPHP-d15, EHDPP, TEHP, T2iPPP). The MSD was run in full scan mode and OPEs were identified using spectral library search.

Isothermal RTs of 19 additional compounds that have directly measured K_{OA} values with the generator column method (i.e., organochlorine pesticides- OCPs, polycyclic aromatic hydrocarbons-PAHs, and PBDEs) were also determined. The included compounds were α-hexachlorocyclohexane, endosulfan I, aldrin, dieldrin,

α-chlordane, γ-chlordane, *trans*-nonachlor, *cis*-nonachlor, heptachlor, *p,p*'-dichlorodiphenyltrichloroethane (*p,p*'-DDT), fluorene, phenanthrene, fluoranthene, pyrene, 2,4,4'-tribromodiphenyl ether (PBDE-28), 2,2',4,4'-tetrabromodiphenyl ether (PBDE-47), 2,2',4,4',5-pentabromodiphenyl ether (PBDE-99), 2,2',4,4',6-pentabromodiphenyl ether (PBDE-100), 2,2',4,4'5,6'-hexabromodiphenyl ether (PBDE-154). These compounds were used as calibration compounds. Isothermal RTs were measured at eight different temperatures (between 180–250 °C for OCPs, 145–180 °C for PAHs, and 220–255 °C for PBDEs) in triplicate. *p,p*'-DDT (for OCPs and PBDEs) and phenanthrene (for PAHs) were utilized as the reference compounds

A GC (Agilent 6890N) equipped with a mass selective detector (Agilent 5973N MSD) and a capillary column with a non-polar stationary phase (HP5-ms, 30 m, 0.25mm, 0.25 mm) was used to determine the isothermal retention times of OPEs (Yaman, Dumanoglu, & Odabasi, 2020). Fluorene, pyrene, and *p,p*'-DDT were used as reference compounds for OPEs. Isothermal retention times of 19 additional nonpolar compounds having directly measured K_{OA} values (i.e., OCPs, PAHs, and PBDEs) were also determined. *p,p*'-DDT (for OCPs and PBDEs) and phenanthrene (for PAHs) were used as the reference compounds (Odabasi, Cetin, & Sofuoglu, 2006).

3.1.2 Measurement of Supercooled Liquid Vapor Pressures (P_L)

Isothermal retention times obtained from GC-MS runs detailed in the previous section (3.3.1) were also used to determine temperature dependent P_L values of 11 OPEs by means of the approach utilized by Lei, Chankalal, Chan, and Wania (2002) and Wong, Lei, Alaee, and Wania (2001). Similar to K_{OA} determinations, fluorene, pyrene, and *p,p*'-DDT were used as reference compounds for calculation of P_L values. A further calibration based upon a 18-point calibration curve which derived from literature values was also applied to initially calculated P_Ls. Details of these calculations are presented in Section 4.1.2.

3.1.3 Measurement of PUF-Air Partition Coefficients ($K_{PUF\text{-}Air}$)

$K_{PUF\text{-}Air}$ values for the studied OPEs were determined within a laboratory scale experimental set-up. Detailed diagram of the experimental set-up was given in Figure 3.1. A water jacketed glass generator column adapted from Francisco, Harner, and Eng (2017) was used to measure $K_{PUF\text{-}Air}$ constants for the OPEs. Two PUF disks were cut into a diameter of 75 mm, pre-cleaned and spiked with an OPE mixture were placed on top of each other into the column (Figure 3.1). To obtain 10 μg of each OPE per PUF pair, 1 ml of spike solution was diluted in 10 ml hexane and spiked onto PUF disks using Pasteur pipettes providing homogenous distribution on PUF disks. The excess hexane was then evaporated under a gentle stream of chromatographic grade N_2 gas. Prior to spiking OPEs, PUF disks were pre-cleaned in a Soxhlet extraction column using acetone:hexane (50:50, v:v) mixture for 24 hours.

During the experiment, a gentle stream of ultra-pure nitrogen gas was passed through the column while the water jacket was set to a certain temperature using a circulating water bath. OPEs in the outlet gas were trapped with a sorbent (XAD-2) filled tube which was replaced with the new one in every 24 h. Two sorbent traps, one for backup, were installed in the first day of each temperature. Measurements were replicated at 15, 25, 35, 45 and 50°C, respectively and 3 days for each temperature. The flow rates were measured and set to approximately 12 L/hr using a rotameter connected to the sorbent tube (Francisco et al., 2017). At the end of the experimental program, sorbent tube samples and also the PUF pairs for each temperature set were extracted and prepared for instrumental analysis. Sorbent-trapped gas-phase samples were sonicated in 20 ml acetone:hexane (50:50, v:v), while PUF phase OPEs were extracted for 12 hours in Soxhlet column using acetone:hexane (50:50, v:v) mixture as the extraction solvent. Prior to extraction, all samples were spiked with OPE surrogate standards.

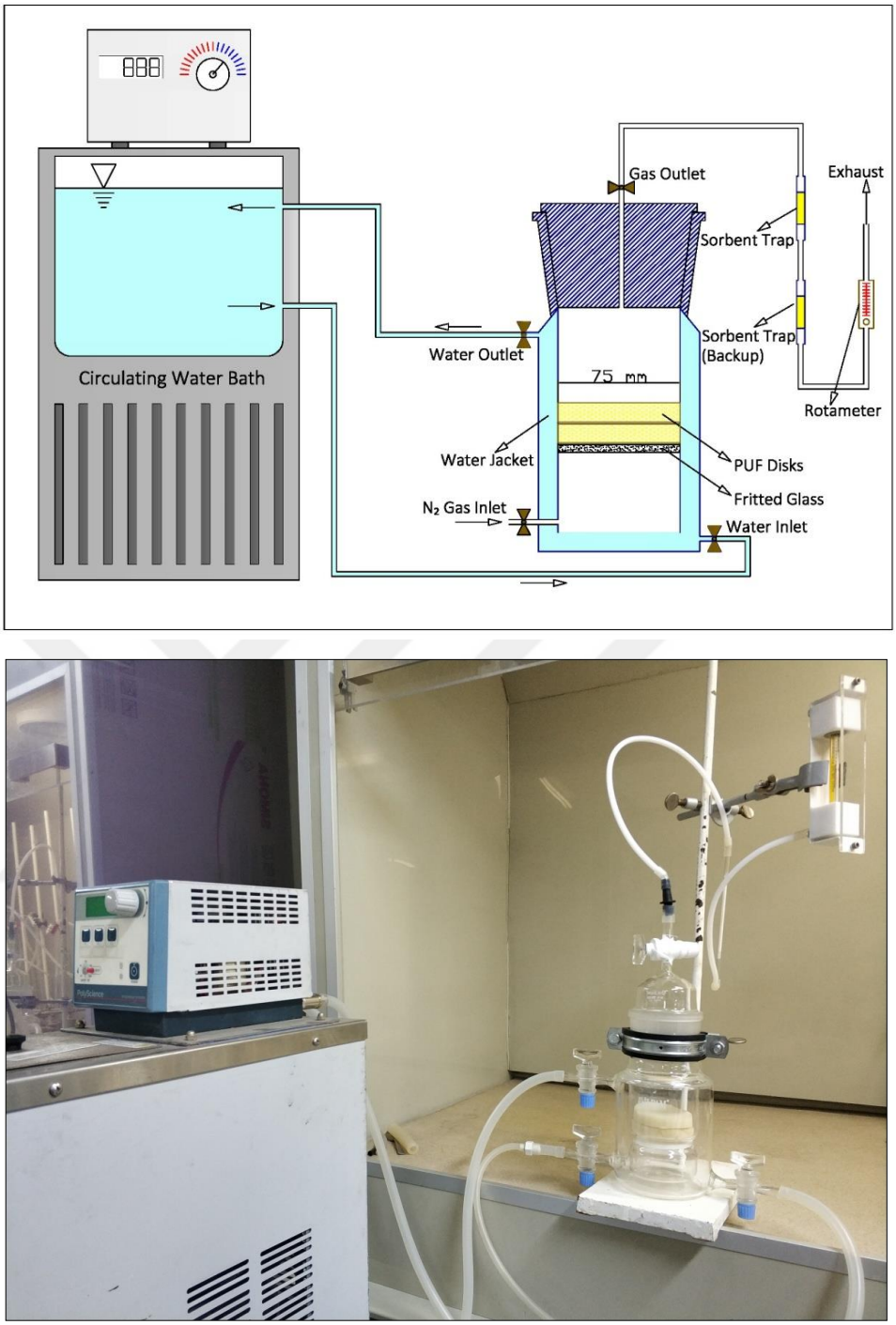


Figure 3.1 Schematic illustration and a view of the $K_{PUF\text{-}Air}$ experimental set up (Personal archive, 2021)

3.1.4 Measurement of Henry's Law Constants (H)

Henry's Law constants (*H*) for OPEs were measured at various temperatures by using the gas-stripping technique that was previously applied by Bamford, Poster,

and Baker (2000) for polychlorinated biphenyls (PCBs), Cetin and Odabasi (2005) for PBDEs and Cetin, Ozer, Sofuoglu, and Odabasi (2006) for organochlorine pesticides (OCPs).

The gas-stripping apparatus (Figure 3.2) consist of a water-jacketed glass reactor (height=75 cm, diameter=5 cm) filled with 1 L deionized water at a depth of 50 cm (Odabasi & Adali, 2016). The water depth was selected based on previous studies indicating that the equilibrium between gas and water-phases is achieved at less than 50 cm of water depth (Bamford et al., 2000; Cetin & Odabasi, 2005; Cetin et al., 2006). Preliminary calculations concerning instrumental detection limits and durations of experiments are necessary owing to different water solubility characteristics of OPEs to obtain detectable gas-phase and aqueous concentrations. The OPE solutions (having concentrations of 10 μg/mL for each 11 OPEs) were prepared in acetone and 0.5 mL was spiked into the 1 L water in the reactor, resulting in 5 μg/mL aqueous concentrations. These initial aqueous concentrations corresponded to a range of 4.48×10^{-5}% (TEP)-7.5% (EHDPP) of their solubilities. Then, compressed chromatographic grade N_2 gas (200 mL/min) was passed through a 40-μm fritted glass diffuser from the bottom of the reactor (Odabasi & Adali, 2016). Pure N_2 was passed through an impinger filled with deionized water to saturate it with water vapor before introduced into the reactor. Flow rates of N_2 were measured using a flow meter and the temperature was controlled by a constant-temperature circulated water bath (Odabasi & Adali, 2016).

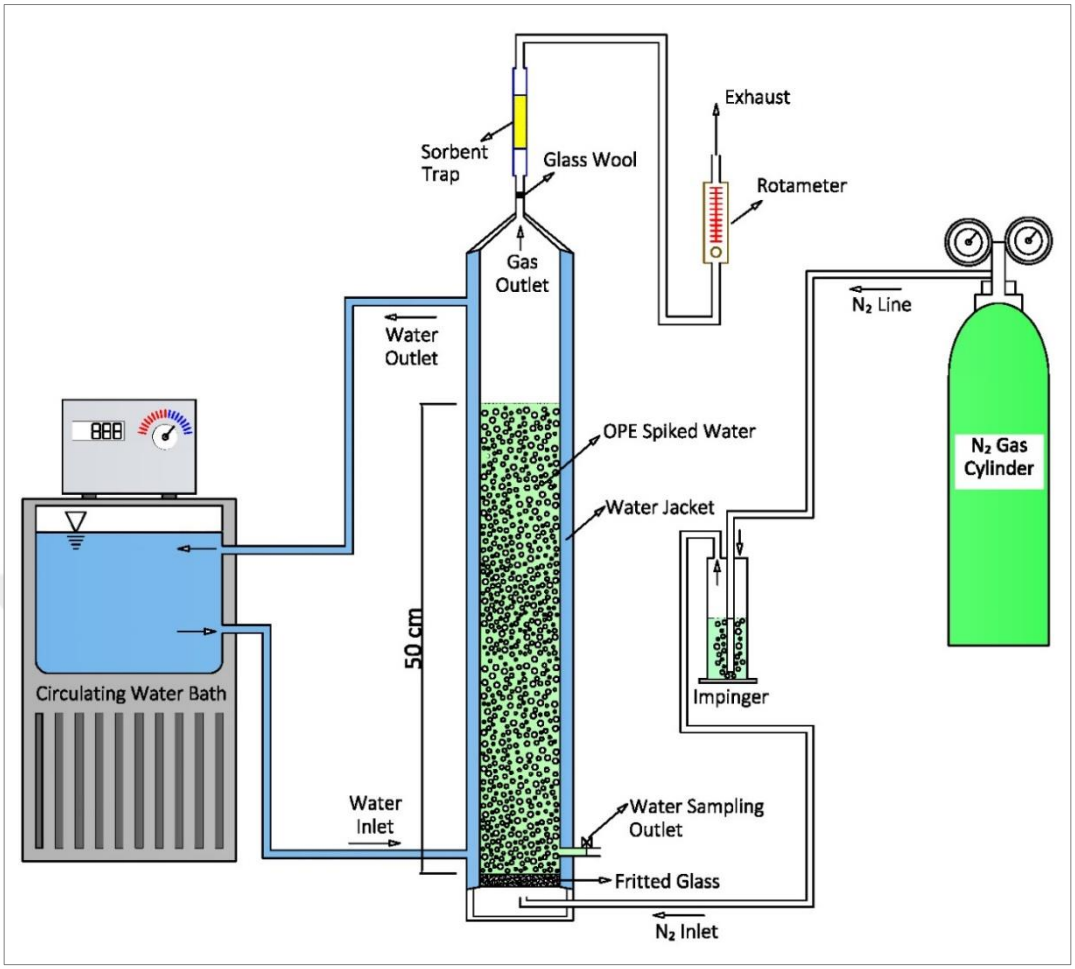


Figure 3.2 Schematic layout of Henry's law constant's experimental train

A 5-cm section of the tube exiting the inner chamber was plugged with pre-baked silanized glass wool to prevent the escape of the water droplets that may be produced during the bubbling process. Vapor phase OPEs was captured by an XAD-2 resin filled glass column. Two sorbent traps, one for backup, were installed in the first day of each temperature. Water samples (10 mL) were drawn through a valve located at the base of the reactor at the start and end of each certain experimental period (Odabasi & Adali, 2016). Above mentioned procedure was applied at five different temperatures including 15, 20, 25, 30 and 35°C and replicated three times for each temperature (Odabasi & Adali, 2016). At the end of the experiment, gas-phase OPE samples were collected with XAD-2 sorbent tube and extracted into hexane in an ultrasonic bath. Water-phase OPEs were extracted by adding XAD-2 resin inside the water sample and XAD-2 was separated from water by filtering through a glass-wool plugged funnel. Then, XAD-2-sorbed OPEs were extracted by soaking in

acetone:hexane (1:1) mixture for 24 h and sonicated for 10 minutes. Prior to extraction, all samples were spiked with OPE surrogate standards.

3.1.5 Measurement of LDPE-Water Partition Coefficients (K_{PEW})

LDPE, as one of most commonly used polymer with a wide range of product applications (i.e. food and drink packaging, containers, electronic devices etc.), was employed as the polymer-based sampling material in this study (Lohmann, 2012). Thin sheet formed (~50 μm thickness) and produced for food storage bags were used in the present study. In order to get successful passive sampler applications for measuring freely-dissolved organic pollutants in water, it is crucial to obtain accurate polymer-water partition coefficients. The sorption efficiency of LDPE in water is directly proportional to K_{PEW} (LDPE-water partitioning coefficient). In order to determine experimental K_{PEW} values for investigated OPEs, a laboratory study was conducted. The experiment was designed to investigate both adsorption and desorption patterns of OPEs on LDPE by following the procedure defined as "single dose design" in the Guidelines prepared by Booij, Smedes, & Allan (2017). In single dose design, a certain amount of the compound in interest is spiked into LDPE (desorption experiment) or water (absorption experiment). Before using LDPE sheets either in laboratory experiments or in field samplings, they have to be cleaned to remove additional contaminants and manufacturing residuals that may cause contamination in further analytical steps. As defined by Booij et al. (2017), cut LDPE sheets in a desired size were soaked for 48 h in each DCM, acetone-hexane (50/50 v/v), methanol and deionized (DI) water, and sonicated for 10 min, respectively. All the LDPE sheets employed in the present study were cleaned according to same procedure.

3.1.5.1 Absorption-Desorption Experiment

In absorption-desorption experiments, six 1 L exposure bottles were filled with DI water to investigate absorption and desorption of OPEs in water-LDPE system. Pre-cleaned 1 g LDPE sheets (15 x 16 cm) were also placed into the bottles. LDPE

masses, water volume and initial OPE concentrations in the exposure vials were determined as suggested by Booij et al. (2017). It was assumed that, when equilibrium occurred, all OPE masses in exposure bottles will be either absorbed by LDPEs or remain in the aqueous phase, and they will not be adsorbed on the walls of the bottle. OPE solutions were prepared in acetone and spiked into water in bottles. Since they have low estimated K_{PEW} values, the first five OPEs (TEP, TnBP, TCEP, TCiPP1, TCiPP2) were spiked to obtain 10,000 ng mass per bottle to achieve detectable amounts in LDPE phase. The next four more hydrophobic OPEs (TDCiPP, TBOEP, TPHP, and EHDPP) were spiked in 1,000 ng. The rest two OPEs (TEHP, T2iPPP) were excluded from the experimental procedure since they have very low solubilities and high estimated K_{PEW} values that do not allow them to be detected in aqueous phase, in accordance with the preliminary calculations and experiments. The estimated equilibrium times for absorption process ranged from several minutes (TEP) to 0.26 days (EHDPP) for 1 g LDPE (Booij et al., 2017). Although all the OPEs can easily reach to equilibrium state during absorption process, there might be significant errors in estimated equilibrium times arising from assumed initial values (i.e. K_{PEW}s, D_p – diffusion coefficient of LDPE, k_w – mass transfer coefficient of water boundary layer) employed in calculations. In order to ensure that the equilibrium is completed, absorption process was extended to 30 days as suggested by Burgess et al. (2015). Hence, the amber exposure bottles were shaken for 1 month on a shaker. At the end of the 30-days absorption period, 3 of the 6 bottles were separated for the extraction of OPEs in LDPE and aqueous phases. OPE-absorbed LDPE sheets in the remaining 3 bottles were taken into desorption process for 30 more days by transferring them in amber bottles filled with 1 L fresh DI water. Finally, 6 water and 6 LDPE samples from both absorption and desorption experiments were extracted and analyzed for OPEs.

3.1.5.2 Desorption Experiment with Pre-loaded LDPE sheets

Booij et al. (2017) have suggested that experiments should be designed to obtain detectable amounts (typically >10xMDL) in both water and LDPE phases in order to reduce the uncertainty in measured K_{PEW} values. For most of the OPEs, amounts

found in LDPE and aqueous phase samples pairs were <10xMDL except for TEP and TCEP in absorption experiments. Therefore, a different approach, OPE spiked (loaded) sheets were employed in the second set of experiments. Loading an organic compound into LDPE in water phase is primarily controlled by K_{PEW} of the compound in interest. In accordance with the early results of absorption-desorption experiment, equilibrium time of a compound in a water-LDPE system, may reach up to months to years (for highly hydrophobic compounds, K_{PEW}>6) depending on estimated K_{PEW} values. Therefore, addition of a water miscible organic solvent (i.e. methanol) can help to increase the absorbed amounts at relatively shorter periods by swelling the LDPE to some extent, even though the LDPE–water/solvent partition coefficients are lower compared to LDPE–water (Booij et al., 2002). Booij et al. (2002) investigated the uptake performances of several PCBs and PAHs by incubating LDPE sheets in solutions having different methanol/water volume ratios (100/0, 80/20, and 50/50). They put forward that the solution 80/20 (MeOH/water) showed best uptake performances. The concentrations in LDPE sheets did not changed after 8 h of incubation and the equilibrium time typically completed within 7 days. They also determined K_{MS} (LDPE – methanol/water partitioning coefficient) values for PAHs (acenaphthene-D10, phenanthrene-D10, chrysene-D12) and PCBs (PCB-4, PCB-29, PCB-155 and PCB-204) which were strictly correlated (r^2=0.91) with K_{OW}s. In the present study, this relationship was used to estimate K_{MS} values for OPEs and thus to calculate initial solution concentrations and expected OPE amounts loaded into LDPE sheets. Hence, the initial spiking concentrations of OPEs (2 to 10 µg/mL of each compound) in the loading solutions were also adjusted to below their solubilities and to obtain detectable amounts (typically >10xMDL) in both water and LDPE phases using estimated K_{PEW}s as specified by Booij et al. (2017). Although Booij et al. (2002) reported best uptake results for 80/20 solution for several PAHs and PCBs, preliminary experiments carried out within the present study showed that MeOH/Water (20/80) solvent system was more efficient to load OPEs into LDPE sheets, rather than (80/20) and (50/50). Thereby, 5 identical OPE loading solutions (20/80) were prepared for 5 replicates in 40 mL amber vials, then the calculated amount of 11 OPEs were spiked into these solutions. Pre-cleaned LDPE sheets were

placed into these vials and loading was achieved by shaking these vials on a shaker table for one week.

After loading procedure, OPE-loaded LDPE sheets were taken out from vials and rinsed with ultra-pure water to remove residual MeOH. To desorb loaded OPEs from LDPE sheets, they were transferred to amber bottles containing 1 L ultra-pure water. The required water volume (1 L) and LDPE amount (1 g) using in both desorption and adsorption experiments were determined using estimated K_{PEW}s according to phase ratios (mK_{PEW}/V_W), where, m (g) is the LDPE mass and V_W (L) is the water volume (Booij et al., 2017). The predicted equilibrium times ranged between a few minutes for TEP (with the highest solubility of $1.12x10^7$ µg/L and the lowest estimated log K_{PEW} of 0.47) and 0.86 day for TEHP (with the lowest solubility of 0.015 µg/L and the highest estimated log K_{PEW} of 9.89). Although all the OPEs can easily reach to equilibrium state, desorption process was carried out for 30 days on a shaker table as in the absorption experiment.

Water-phase OPE compounds of K_{PEW} experiments were extracted by adding XAD-2 resin to each of one-liter water samples and soaking overnight. Then, water was separated from XAD-2 by filtering through pre-baked glass wool using a funnel. Finally, XAD-2-sorbed OPEs and also LDPE sheets were extracted by soaking in acetone:hexane (1:1) mixture for 24 h and sonicating for 10 minutes. The obtained C_W and C_{LDPE} values were used to determine experimental K_{PEW} values according to procedure detailed in Section 4.1.5.

3.2 Field Studies

3.2.1 Study Area

Within the scope of the thesis, Izmir, Turkey was assigned as the study area. Izmir is a metropolitan city, with a population of 4.11 million people, and it is the center of a highly industrialized area by the Aegean Sea shoreline of Turkey. Izmir is densely populated over two narrow flat basins between three series of mountains aligned

perpendicular to the seashore (Demircioglu, Sofuoglu, & Odabasi, 2008; Odabasi, Cetin, Demircioglu, & Sofuoglu, 2008). Environmental chemodynamics of 11 selected OPEs (see Table 2.1) were investigated in Izmir covering four types of regions as; industrial, urban, sub-urban and rural, under different levels of anthropogenic influences. Aliaga, Izmir is also a coastal town located ~45 km north of Izmir city center was chosen as the study region with 14 sampling points representing heavy industrial activities. According to the literature, number of environmental pollution monitoring, inventorying and modeling studies widely focused on this region since it contains a number of significant air pollutant sources including five scrap iron–steel processing plants with electric arc furnaces (EAFs), several steel rolling mills, large petroleum refineries, a petrochemical complex, a natural gas-fired power plant, a fertilizer plant, ship breaking yards, coal storage and packing, scrap storage and classification sites, large slag and scrap piles, heavy traffic, very intense transportation activities including ferrous scrap trucks and busy ports used for transportation (Aydin, Kara, Dumanoglu, Odabasi, & Elbir, 2014; Dumanoglu et al., 2014; Kara et al., 2014). Urban sites were selected in Izmir city center covering 14 sampling points and representing intense population and traffic influences; while Dokuz Eylul University Tinaztepe Campus in Buca, Izmir was also assigned as sub-urban area including 5 sampling sites with sparse traffic and much lower anthropogenic activities. Additionally, 5 rural sampling points were assigned in forested region of Kozak/Bergama/Izmir with relatively high altitudes (~500-600 m) and away from possible sources. Study area and the sampling sites (n=38) was illustrated in Figure 3.3. In order to determine gas-particulate phase partitioning behavior of OPEs, two sets of (14 days each) active air sampling was also conducted under winter and summer season conditions in the city center of Izmir.

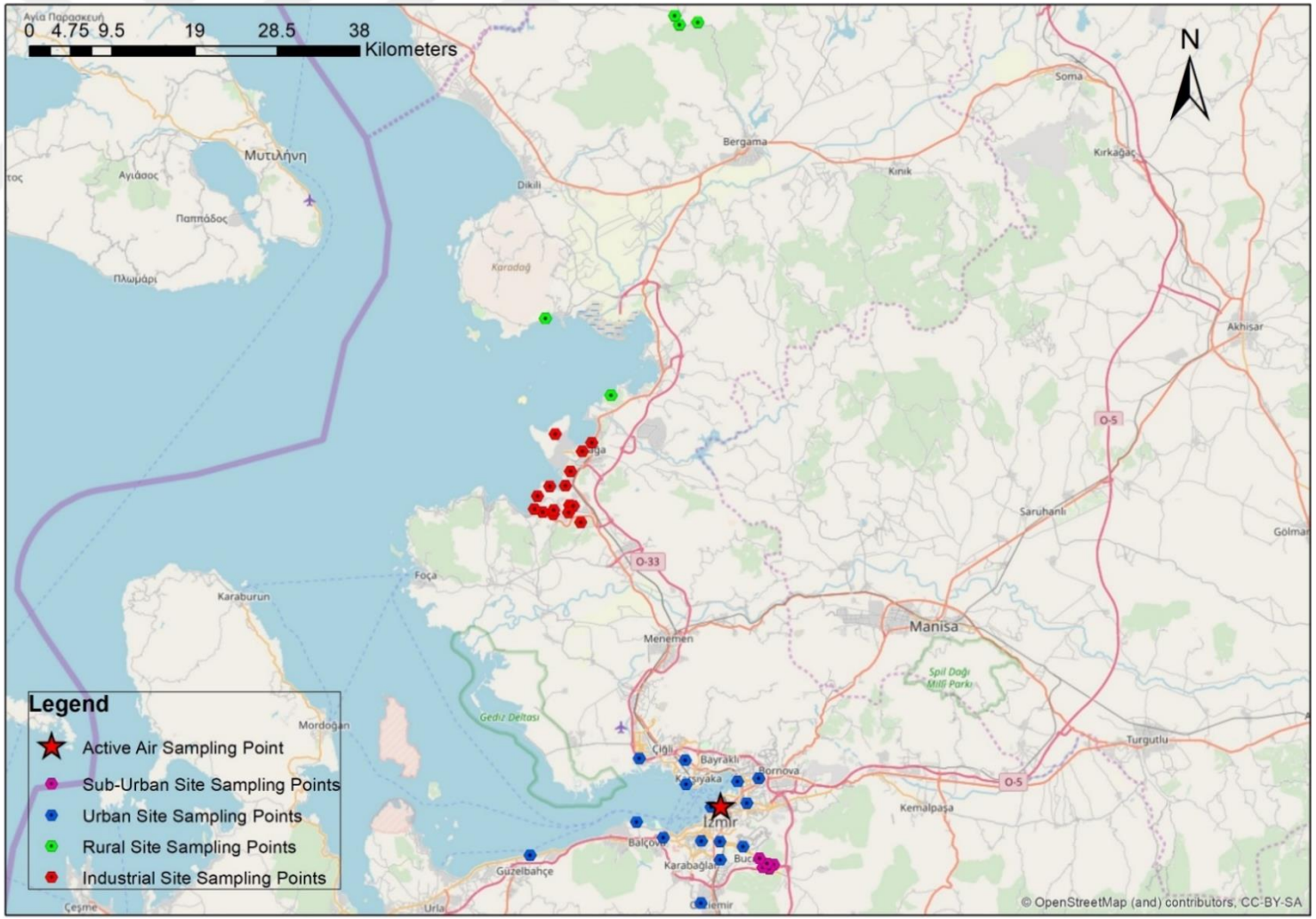


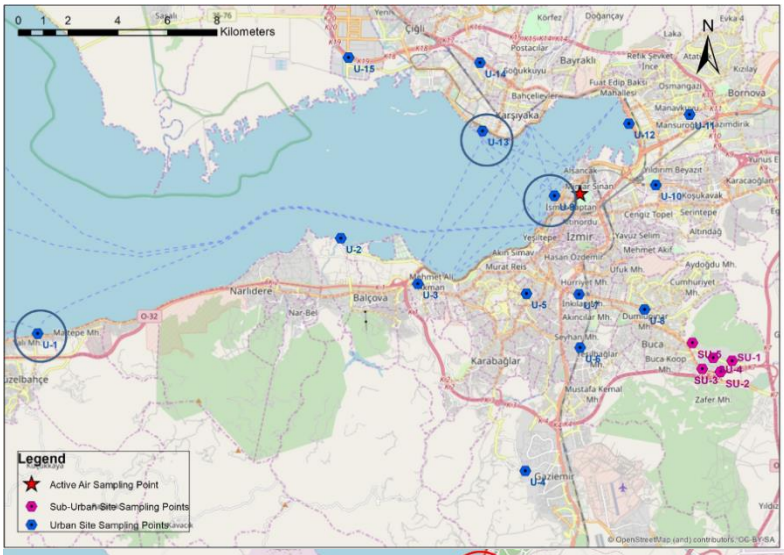
Figure 3.3 Study area and sampling points

Sample collection was carried out within two campaigns representing winter (January-March 2019) and summer (August-October 2019) conditions. During each campaign, 38 ambient air, 38 soil and 7 seawater samples were collected from industrial, urban, suburban and rural sampling sites detailed above. A detailed illustration of the sampling sites were given in Figure 3.4 and the sampling program was tabulated in Table 3.1. Site-specific meteorological data those used to calculate OPE concentrations for each sampling point were obtained from General Directorate of State Meteorology. The nearest meteorological station within 5 km was chosen to represent each sampling point. In Figure 3.5, meteorological stations in urban and suburban sampling sites and 5-km circles for each station were depicted.

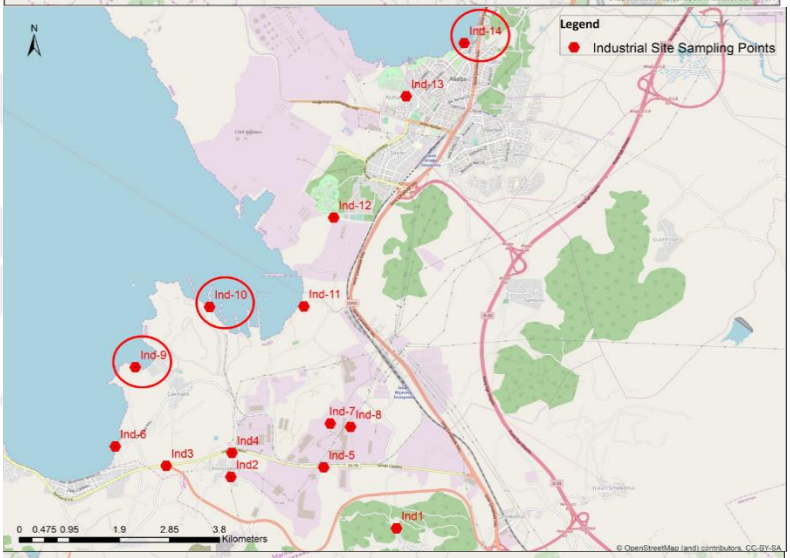
Table 3.1 Sampling program

Sample Type	**Sampling Site**				**Total # of Samples**	**Season**
	Urban	**Industrial**	**Suburban**	**Rural**		
Ambient Air	14	14	5	5	38	Winter 2019
	14	14	5	5	38	Summer 2019
Soil	14	14	5	5	38	Winter 2019
	14	14	5	5	38	Summer 2019
Seawater	3	3	-	1	7	Winter 2019
	3	3	-	1	7	Summer 2019
Active Air Sampling	14	-	-	-	14	Winter 2017
	14	-	-	-	14	Summer 2017

(a)



(b)



(c)

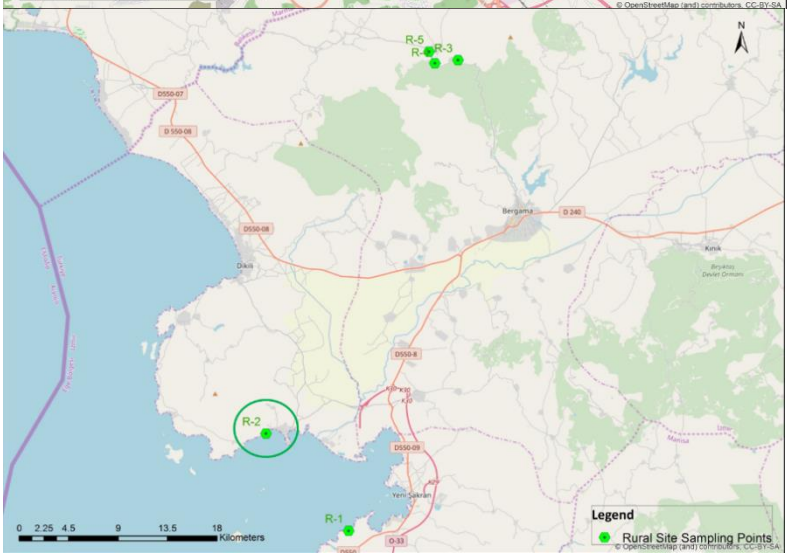


Figure 3.4 Sampling points in **(a)** urban and sub-urban, **(b)** industrial and **(c)** rural sites (in addition to ambient air and soil samples, the seaside sampling points in blue, red and green circles include also seawater passive samples)

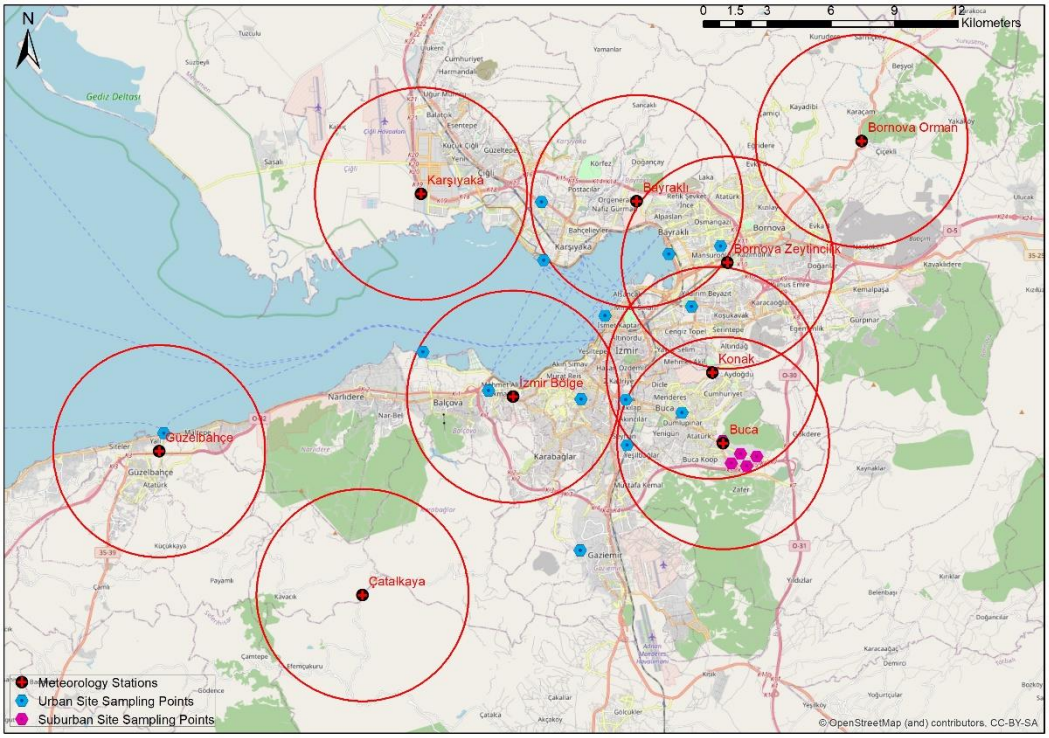


Figure 3.5 Meteorology stations in urban and suburban sites

3.2.2 Ambient Air Sampling

3.2.2.1 Active Air Sampling

For massive field monitoring studies of organic pollutants, passive air sampling techniques (using passive samplers such as PUFs) are more suitable since they do not need power supplies as well as they have lower expenses. Hence, PAS consisted of PUF disks were primarily used to monitor OPEs in the study region comprising 38 sampling sites in industrial, urban, sub-urban and rural areas. Although the common knowledge is PUF samplers are primarily target gas-phase pollutants, it has been revealed in recent years that significant amounts of particles are collected by these samplers (Harner, Mitrovic, Ahrens, & Schuster, 2014; Harner et al., 2013; Markovic, Prokop, Staebler, Liggio, & Harner, 2015). Therefore, understanding of gas and particle phase partitioning behaviors and determining phase fractions are crucial to demonstrate their fate in the environment.

In order to investigate gas and particle phase partitioning of OPEs, an active air sampling was carried out in Izmir city center within two campaigns representing winter (in February of 2017) and summer (in July and August of 2017) conditions. Samples were collected for 14 days for each campaign. A view of the sampling site was given in Figure 3.6. Particulate and gas phase OPE samples were taken simultaneously using a modified high-volume sampler model GPS-11 (Thermo-Andersen Inc.). Particles were collected on 10.5 cm diameter glass fiber filters and the gas-phase compounds were collected in a modified cartridge containing XAD-2 resin placed between layers of PUF (Yaman et al., 2020). Sample preparation and extraction procedure for gas and particle phase OPE samples were detailed in Section 3.2.5. Concurrently, particle samples were collected on quartz filters using another high volume sampler to determine total suspended particulate matter (TSP) and its OM content (Yaman et al., 2020). The overall average sampling time and sampling volume were 23.8 h and 321.4±23.7 m^3, respectively.



Figure 3.6 Collection of gas and particulate phase samples (Personal archive, 2021)

3.2.2.1.1 Measurement of Total Suspended Particulates (TSP), Elemental Carbon (EC) and Organic Carbon (OC) Contents. As pointed out in the previous section, one of the two high volume air samplers was employed to collect TSP in the active air sampling site. TSP mass was obtained by subtracting the initial weight from the final weight of the quartz filters. For determination of carbonaceous species in the quartz filters, Sunset EC-OC thermal analyzer was used. Firstly, sample collected quartz filters were weighed. A standardized size (1x1.5 cm) punch is cut from that filter and placed in the oven. Temperature profile of NIOSH 870 method was shown in Table 3.2. Sample thermogram of NIOSH 870 is shown in Figure 3.7. For carbonates determination, one punch of sample was kept in a petri dish containing 30% HCl acid fume for 3 hours.

Table 3.2 Temperature profile of NIOSH 870

Mobile phase	**Time (s)**	**Temperature (^{o}C)**
Helium	10	1
Helium	80	310
Helium	80	475
Helium	80	615
Helium	110	870
Helium	45	550
Oxygen	45	550
Oxygen	45	625
Oxygen	45	700
Oxygen	45	775
Oxygen	45	850
Oxygen	110	870
Calibration gasCH_4	120	1
Offline	1	0

Sucrose solution was used to calculate the relative error of the analysis in every ten samples. A punch (1.5 cm^2) was cut from a clean quartz filter and 10 µL of the standard (containing 35.04 µg sucrose) was pipetted onto 1.5 cm^2 filter. The

arithmetic mean of relative error of applied sucrose standards (n=4) was determined as 1.4%. MDLs of OC and EC determined using the amounts found in six filter blanks and the average air sampling volume were 0.44 and 0.02 µg/m^3, respectively.

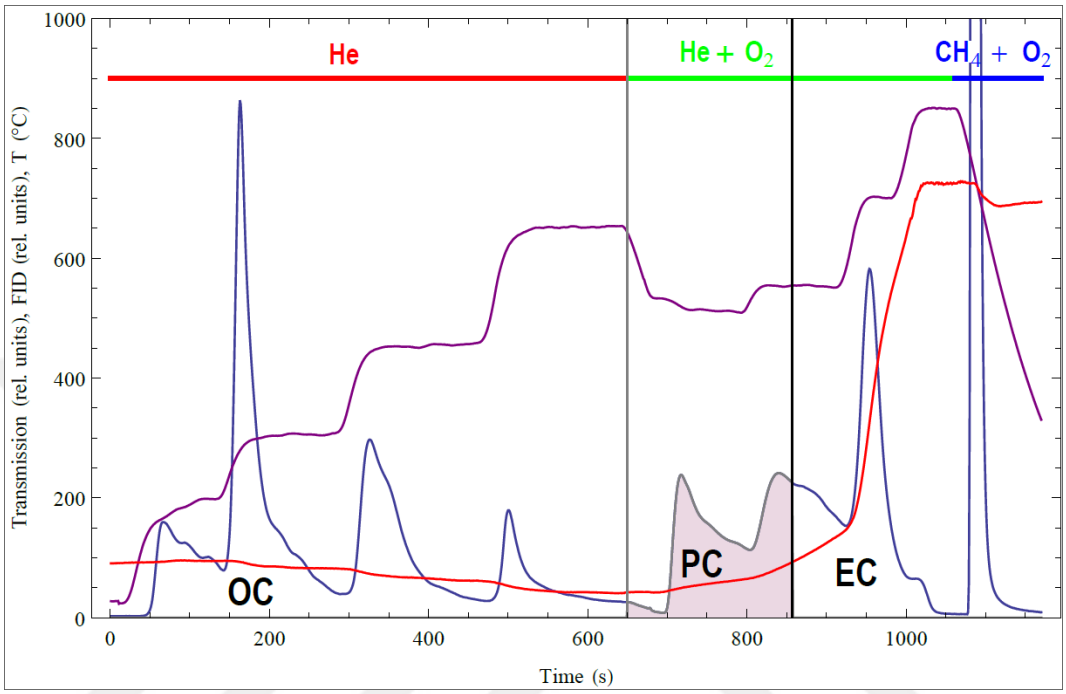


Figure 3.7 Sample thermogram for NIOSH 870

3.2.2.2 Passive Air Sampling

PAS with depuration compounds (DCs) (^{13}C-PCB 3, ^{13}C-PCB 9, ^{13}C-PCB 15, PCB 30, PCB 107, and PCB 198) spiked PUF disks (14 cm diameter, 1.35 cm thick, 365 cm^2 surface area, 0.0213 g/cm^3 density, 4.40 g mass, 207 cm^3 volume) were used to collect ambient air samples (Dumanoglu, Gaga, Gungormus, Sofuoglu, & Odabasi, 2017). PUF disks were placed inside a stainless steel chamber consisted of two stainless steel bowls that protects the foam disk from precipitation, coarse particle deposition, and ultraviolet radiation, and minimizes the effects of wind speed on the uptake rate (Figure 3.8). Prior to deployment of samplers, PUF disks were pre-cleaned in acetone-hexane (50/50 v/v) mixture using soxhlet extraction for 24 h, then DCs (^{13}C–PCB 3, ^{13}C–PCB 9, ^{13}C–PCB 15, PCB 30, PCB 107, and PCB 198), 17.5–20 ng per sample (dissolved in 10 mL hexane) were homogeneously spiked into pre-cleaned PUF disks to determine the compound-specific sampling rates. Then, hexane

were evaporated using an N_2 stream and samplers were stored in their containers (pre-cleaned glass jars) in a freezer (Dumanoglu et al., 2017).

PASs were deployed in 38 sampling sites including 14 sites in urban area (Izmir City Center), 14 in industrial area (Izmir, Aliaga), 5 in sub-urban area (Izmir, Buca, DEU Tinaztepe Campus) and 5 in rural area (Izmir, Bergama, Kozak). During two sampling seasons, a total of 76 air samples were collected.

(a)



(b)



Figure 3.8 **(a)** Passive air sampler apparatus and **(b)** deployment (Personal archive, 2021)

3.2.3 Soil Sampling

Soil samples were collected from a depth of 0 to 5 cm, after removing surface grass root material and large stones (Figure 3.9). The samples were transferred directly into a glass container, which were immediately closed and stored in freezer. To overcome soil inhomogeneities, three subsamples were taken and mixed for each sampling site.

Five grams of each soil samples were weighed for extraction and analysis of OPEs, while 10 grams were weighed to determine OM and moisture content. In order to measure moisture content, 10 g soil samples were dried at 105°C and reweighed at every 24 h until the constant weight observed. Differences between the first and last (approximately after 5 days) weights were utilized as moisture contents. Then, dried soil samples were kept in a muffle furnace at 450°C for 12 h and the OM contents were evaluated using the loss of ignition.



Figure 3.9 Collection of soil samples (Personal archive, 2021)

3.2.4 Seawater Sampling

Seawater passive samplers (SPSs) were deployed in 7 coastal sites out of the 38 passive sampling points. Three SPSs were placed in Izmir Bay (U-1, U-9, U-13) and Aliaga (Ind-9, Ind-10, Ind-14), while one SPS were placed in north of Aliaga (Candarli) (R-2) as a rural sampling site (Figure 3.4).

SPSs were consisted of 25 x 36 cm (corresponding to an average mass of ~3.74 g) cut LDPE sheet as the seawater OPE sampling material. An aluminum frame and a galvanic metal cage that used to keep LDPE sheet in planar position and protect it from marine organisms and other physical effects. SPS apparatus was shown in Figure 3.10. Before they deployed in sea, LPDE sheets were cleaned to remove any contaminants by soaking for 48 h in a series of solvents or solvent mixtures like DCM, acetone-hexane (50/50 v/v), methanol and deionized (DI) water, and sonicated for 10 min, respectively (Burgess et al., 2015). After they are cleaned, LDPE sheets were loaded with PRCs according to method defined by Booij et al. (2002). Booij et al. (2002), investigated uptake performances of several PCBs and PAHs by incubating LDPE sheets in solutions having different methanol/water volume ratios (100/0, 80/20, and 50/50). They suggested that the solution 80/20 (MeOH/water) showed best uptake performances. Accordingly, ten pieces (three for field blanks and initial loaded amount determination) of PRC loading solutions including ^{13}C labeled PCB mixtures (^{13}C-PCB 3, ^{13}C-PCB 9, ^{13}C-PCB 15, PCB 30, PCB 107, and PCB 198) were prepared in 1 ml methanol and they were spiked into methanol/DI water (80/20 v/v) mixtures (75 ml) in individual glass tube containers. Pre-cleaned LDPE sheets were also placed in these containers without folding to provide whole surface contact with the solution. Then, the containers were shaken for 7 days in a shaker plate to facilitate the uptake of PRCs by LDPE sheets until equilibrium. Then, PRC loaded LDPE sheets were kept in DI water for one day to remove the MeOH. Pre-cleaned and PRC loaded LDPE sheets were stored in their containers in a freezer, until deployment. PRCs were used to determine sampling rates and uptake performances of LDPE sheets.

SPSs were fastened to an anchored rope and suspended in near surface (~0.50 m depth) water, also to determine air-water exchange directions. SPSs were deployed simultaneously as possible as at the same locations (within a few ten meters) to PASs. To avoid SPSs drifted or broken away due to environmental conditions, they were mostly deployed to commercial ports and meteo-oceanographic observation stations of the Izmir municipality. However, a few of SPSs had to be deployed in

public places. The deployment duration for SPS and PAS was held on approximately 60 days for both summer and winter campaigns.



Figure 3.10 Seawater passive sampler apparatus before and after deployment (Personal archive, 2021)

At the end of the sampling period, SPS were collected, LDPE sheets were separated from the apparatus and directly placed in amber glass bottles filled with seawater. The samples were immediately transported to laboratory and prepared for instrumental analysis as detailed in Section 3.2.5.

3.2.5 Sample Preparation

PUFs and LDPE passive samples were collected after approximately 60 days of deployment and immediately transferred to laboratory. Prior to extraction, all samples were spiked with OPE surrogate standards (Falay et al., 2013). Passive air sampling PUFs were Soxhlet extracted for 12 hours with a mixture of 1:1 acetone:hexane. LDPE sheets from seawater samples were extracted by soaking in 1:1 acetone:hexane overnight, then they were sonicated for 15 mins (Falay et al., 2013). Before they soaked into extraction solvent, LDPE sheets were gently wiped with pre-cleaned laboratory tissues to remove any accumulated biofilms and surface growths (Burgess et al., 2015). Five grams of soil samples were soaked in 40 mL of 1:1 acetone:hexane mixture overnight. Then, they were sonicated for 15 mins (Kaya et al., 2012). In active air sampling, gas phase OPEs collected with sorbent cartridges were Soxhlet extracted for 12 h with acetone:hexane (1:1) while, particulate phase OPEs on glass fiber filters were extracted by soaking in acetone:hexane (1:1) overnight and sonicating for 10 minutes.

All the extract volumes were reduced and transferred into hexane using a rotary evaporator and a high purity N_2 stream. After concentrating to 2 mL, samples were cleaned up on a commercial SPE column (Agilent Bond Elute SI) (Cetin, 2014). The column was pre–washed with 20 mL acetone. Then, the sample in 2 mL hexane was added to the column and OPEs were eluted within two particular fractions as 30 mL hexane and 30 mL acetone, respectively. The fractions were then combined and final extracts were solvent exchanged into hexane and concentrated to 1 mL under a gentle stream of N_2 (Cetin & Odabasi, 2008).

Prior to sampling for TSP, baked and cooled quartz filters were weighed using a micro balance capable of weighing 0.1 mg. After sampling, they were reweighed. Prior to weighing before and after sampling, all filters were conditioned overnight in a clean room having a constant temperature and humidity (Cetin & Odabasi, 2008). TSP was obtained by subtracting the initial weight from the final weight (Cetin & Odabasi, 2008).

3.2.6 Instrumental Analysis

All samples from field (active and passive air sampling, seawater sampling, and soil sampling) and laboratory studies (PUF-Air Partition Coefficients, Henry's Law Constants, and LDPE-Water Partition Coefficients) were analyzed for 11 OPE compounds using an Agilent 6890N GC-MS (Agilent 5973 inert MSD) at electron impact ionization and selected ion monitoring mode (SIM). An HP5-MS-UI capillary column (30 m, 0.25 mm, 0.25 μm) was utilized for the analysis and helium as the carrier gas. The initial oven temperature was held at 50 °C for 1 min and raised to 200 °C at 25 °C/min, 200–300 °C at 8 °C/min, and held for 3 min. The injector, ion source, and quadrupole temperatures were 250, 230, and 150 °C, respectively. High purity helium was used as the carrier gas at constant flow mode (1.5 mL/min). The MSD was run in selected ion-monitoring (SIM) mode. Compounds were identified based on their retention times, target and qualifiers ions. Quantification of compounds was based on internal standard calibration procedure (Bozlaker, Muezzinoglu, & Odabasi, 2008a; Cetin, Yatkin, Bayram, & Odabasi, 2007; Odabasi et al., 2009).

3.2.7 QA/QC

All samples were spiked with surrogate standards (recovery standards) prior to extraction to determine analytical recovery efficiencies. The overall analytical recoveries ranged between 55.3±10.5 (TEP-d15) and 99.8±23.1% (TDCiPP-d15) in active air samples, 55.5±10.7 (TEP-d15) and 111.5±21.0% (TPHP-d15) in ambient air samples, 51.8±12.8 (TEP-d15) and 110.9±17.3% (TPHP-d15) in soil samples,

51.0±4.96 (TEP-d15) and 110.3±19.4% (TDCiPP-d15) in seawater samples. Further recovery efficiencies including also laboratory experiments ($K_{PUF-Air}$, H, K_{PEW}) were presented in Table 3.3. The averaged sampling rates for both air and seawater samples were determined as 3.94 m^3/day and 14.4 L/day using the loss of spiked DC or PRC amounts. Blank samples were prepared representing both for field (air, seawater, soil sampling) and laboratory studies ($K_{PUF-Air}$, H, K_{PEW} experiments) and they were tested in every step of studies to detect any contamination from laboratory and field apparatus and sample preparation. The definition of method detection limit that used (MDL) was: MDL=Mean blank value+3SD. Instrumental detection limits (IDL) were determined from linear extrapolation from the lowest standard in calibration curve using the area of a peak having a signal/noise ratio of 3 (Odabasi et al., 2006). Instrumental detection limits were individually determined during the GC-MS analysis for both active air samples and the other field samples (PUF, soil and seawater), and given in Table 3.4. Instrumental detection limit was used for the compounds that are not detected in blanks. MDLs in terms of concentrations in different sample types (air, soil, and seawater) derived using MDL masses and average sample volumes or amounts. They ranged from 0.009 (TCEP) to 0.130 (TCiPP1) ng/m^3 in particle phase active air samples, from 0.012 (TDCiPP) to 0.220 (TCiPP1) in gas phase active air samples, 0.00074 (T2iPPP) to 0.29 (TCiPP1) ng/m^3 in ambient air samples, from 0.026 (T2iPPP) to 5.32 ng/g (TCiPP1) in soil samples, and from 0.0011 (T2iPPP) to 0.056 (TCiPP1) ng/L in seawater samples (Table 3.5). Five levels of calibration standards were used to calibrate the GC/MS system (Cetin et al., 2007). System performance was verified by the analysis of the mid-point calibration standard for every 12 hours during the analysis period (Karaca & Tasdemir, 2013). The GC-MS system was recalibrated if the deviation from initial calibration was >10%.

Table 3.3 Surrogate recovery efficiencies (%) for field samples and laboratory experiments

		TEP-d15	TCEP-d12	TDCiPP-d15	TPHP-d15
			Active Air Sampling		
Particle Phase	AVG	55.3	81.4	92.8	84.5
	SD	10.5	18.3	14.9	11.6
Gas Phase	AVG	76.2	89.0	99.8	98.2
	SD	21.7	25.3	23.1	12.8
			Passive Air Sampling		
PUF Samples	AVG	55.5	59.2	88.0	111
	SD	10.7	21.5	25.3	21.0
			Soil Sampling		
Soil Samples	AVG	51.8	70.0	107	111
	SD	12.8	22.2	19.6	17.3
			Seawater Sampling		
Seawater Samples	AVG	51.0	97.5	110	102
	SD	4.96	19.2	19.4	16.9
			K_{PEW} experiments		
LDPE-phase	AVG	53.2	74.8	100.7	104.1
	SD	6.1	29.9	19.2	18.5
Aqueous-phase	AVG	77.4	122.5	128.1	112.6
	SD	11.3	11.6	13.7	11.4
			***H* experiments**		
Gas-phase	AVG	89.0	88.5	96.0	110.9
	SD	16.5	21.2	16.6	13.3
Aqueous-phase	AVG	78.2	77.0	103.4	113.8
	SD	18.9	20.7	21.3	12.9
			$K_{PUF\text{-}Air}$ experiments		
Gas-phase	AVG	110.5	90.5	87.9	86.1
	SD	15.3	10.0	8.4	9.4
PUF	AVG	59.3	80.9	108.4	96.8
	SD	7.2	19.9	19.3	8.8

Table 3.4 Instrumental detection limits for OPEs

Compound	Instrumental Detection Limits	
	Active Air Sampling (pg/μL)	PUF, Soil and Seawater (pg/μL)
TEP	5	1.55
TnBP	5	1.36
TCEP	3	2.33
TCiPP1	5	3.42
TCiPP2	2.5	2.15
TDCiPP	4	2.95
TBOEP	5	3.37
TPHP	2.5	1.94
EHDPP	3	1.54
TEHP	5	2.91
T2iPPP	4.5	2.47

Table 3.5 MDL values for field samples

Compound	Active Air Sampling		PAS	Soil	Seawater
	Particle (ng/m^3)	Gas (ng/m^3)	PUF (ng/m^3)	(ng/g)	(ng/L)
TEP	0.015	0.015	0.015	0.31	0.0016
TnBP	0.015	0.015	0.0073	0.27	0.0014
TCEP	0.009	0.015	0.0017	0.28	0.0021
TCiPP1	0.130	0.220	0.29	5.32	0.056
TCiPP2	0.046	0.051	0.024	1.92	0.022
TDCiPP	0.011	0.012	0.011	0.27	0.0030
TBOEP	0.015	0.015	0.013	0.30	0.0034
TPHP	0.015	0.015	0.0026	0.079	0.0050
EHDPP	0.025	0.025	0.0072	0.29	0.011
TEHP	0.015	0.015	0.0051	0.20	0.0029
T2iPPP	0.014	0.014	0.00074	0.026	0.0011

CHAPTER 4
RESULTS AND DISCUSSION

4.1 Laboratory Studies

4.1.1 Octanol/Air Partition Coefficients

As detailed in Section 3.3.1. temperature dependent K_{OA} values for 11 interested OPEs were measured using their chromatographic retention times. The retention time of a chemical on a GC column (t_R) is related to stationary phase-gas phase partition coefficient (K_{SG}). The following was proposed for a chemical *i* and a reference chemical eluted on a gas chromatographic column (Wania et al., 2002):

$$K_{SGi}/K_{SGref} = t_{Ri}/t_{Rref} \quad (4.1)$$

For a suitable stationary phase, the partitioning of a chemical between stationary and gas phases could be related to the octanol-air partitioning. This is based on the presumption that the ratio of the activity coefficients of chemical *i* and of the reference chemical in octanol (ξ_{OCTi}/ξ_{OCTref}) is the same as the ratio of activity coefficients of these chemicals in the GC-column stationary phase (ξ_{Si}/ξ_{Sref}). The following could be written considering the equilibrium partition coefficients:

$$K_{OAi}/K_{OAref} = K_{SGi}/K_{SGref} \quad (4.2)$$

K_{OA} values of a chemical *i* and of a reference chemical could be associated to their retention times (t_{Ri} and t_{Rref}) on the same gas chromatographic column via Eqs. (4.1) and (4.2):

$$K_{OAi}/K_{OAref} = t_{Ri}/t_{Rref} \quad (4.3)$$

Eqs. (4.4) and (4.5) were derived by Wania et al. (2002) via Eq. (3) and the Van't Hoff equation expressing the effect of temperature on K_{OA}:

$$\ln K_{OAi} = \left(\Delta U_{OAi}/\Delta U_{OAref}\right) \ln K_{OAref} + C \quad (4.4)$$

$$\ln\left(t_{Ri}/t_{Rref}\right) = \left[\left(\Delta U_{OAi}/\Delta U_{OAref}\right) - 1\right] \ln K_{OAref} + C = S \ln K_{OAref} + C \quad (4.5)$$

where ΔU_{OA} (kJ/mol) is the internal energy for octanol-air phase transfer and C is the integration constant. This is based on the assumption that the phase transfer energies are not dependent on temperature, within the range of environmental and GC run temperatures (Odabasi et al., 2006).

Regression of ln (t_{Ri}/t_{Rref}) vs. ln K_{OAref} results in a straight line having a slope of S=[($\Delta U_{OAi}/\Delta U_{OAref}$)-1] and an intercept of C (Eq. (4.5)). (t_{Ri}/t_{Rref}) is the relative retention time (RRT) at the temperature where the reference chemical has its temperature-adjusted octanol-air partition coefficient (K_{OAref}) (Odabasi et al., 2006). The K_{OAi} of chemical i at a reference temperature was calculated utilizing Eq. (4.4) where K_{OAref} is the K_{OA} of the reference chemical at that temperature. ($\Delta U_{OAi}/\Delta U_{OAref}$) = S+1 and C were acquired from the slope and intercept of Eq. (4.5), respectively (Odabasi et al., 2006).

Fluorene, pyrene, *p,p*'-DDT were employed as the reference compounds to estimate the K_{OAi} for OPEs in the present study. By means of the generator column method, Harner and Bidleman (1998a) determined temperature (T, K) dependent K_{OA} values for fluorene and pyrene, and Shoeib and Harner (2002b) measured K_{OA} values for *p,p*'-DDT. The following equations were found for these reference compounds:

$$\log K_{OA} = -4.56 + 3985(T,K)^{-1}, \quad r^2 = 0.990; \quad \text{(pyrene)} \quad (4.6)$$

$$log\, K_{OA} = -7.74 + 4332(T,K)^{-1}, \quad r^2 = 0.995; \quad \text{(fluorene)} \quad (4.7)$$

$$\log K_{OA} = -5.63 + 4603(T,K)^{-1}, \quad r^2 = 0.995; \quad (p,p'\text{-DDT}) \quad (4.8)$$

K_{OAref} values in Eqs. (4.4) and (4.5) at the temperatures of isothermal GC-RT runs were calculated via Eqs. (4.6)-(4.8).

The relation of ln (t_R/t_{Rref}) to ln K_{OAref} is presented in Figure 4.1 where t_R and t_{Rref} are the retention times of target and reference compounds, respectively and K_{OAref} is the octanol-air partition coefficient of the reference compound. These correlations were substantially linear for all OPEs with very high r^2values (>0.99) and p<0.01. Determined log $K_{OA\text{-}GC}$ and log K_{OA} values of OPEs at 25°C were listed in Table 4.1 along with the A and B values of the temperature regressions::

$$\log K_{OA} = A + B/(T, K) \tag{4.9}$$

The internal energies of octanol-air transfer (ΔU_{OA}) are also given in Table 4.1. The $K_{OA\text{-}GC}$ values calculated from triplicate runs had small relative standard deviations (0.4–3.3%) indicating high reproducibility.

There was a high correlation between the experimental log K_{OA} values (at 25°C) of PAHs (Harner & Bidleman, 1998a), OCPs (Shoeib & Harner, 2002b), and PBDEs (Harner & Shoeib, 2002) measured by the generator-column technique vs. $K_{OA\text{-}GC}$ (Figure 4.2):

$$\log K_{OA} = 0.991 \pm 0.0029 \log K_{OA-GC} + 0.162 \pm 0.264 \quad (r^2=0.986,\ p<0.01,\ n=19) \tag{4.10}$$

Table 4.1 Uncalibrated ($K_{OA\text{-}GC}$, average±SD, n=3) and calibrated (K_{OA}, average±propagated error) octanol–air partition coefficients for OPEs at 25 °C, energies of phase transfer (ΔU_{OA}, average±propagated error), and regression parameters for Eq. (4.9)

OPEs	**Reference Compound**	**log $K_{OA\text{-}GC}$**	**log K_{OA}**	***B***	***A***	**ΔU_{OA} (kJ mol^{-1})**
TEP	fluorene	5.09±0.006	5.21±0.30	3392	-6.18	65.0±2.7
TnBP	fluorene	7.35±0.003	7.44±0.30	4739	-8.46	90.7±3.8
TCEP	fluorene	7.83±0.003	7.91±0.35	5001	-8.87	95.8±4.0
TCiPP1	fluorene	7.96±0.003	8.05±0.35	5071	-8.96	97.1±4.1
TCiPP2	fluorene	8.02±0.004	8.11±0.35	5103	-9.01	97.7±4.1
TDCiPP	pyrene	10.00±0.011	10.07±0.39	4674	-5.62	89.5±5.3
TBOEP	pyrene	10.67±0.002	10.73±0.41	5103	-6.39	97.7±5.8
TPHP	pyrene	10.25±0.006	10.32±0.4	4804	-5.80	92.0±5.5
EHDPP	pyrene	10.50±0.002	10.56±0.40	4961	-6.09	95.0±5.6
TEHP	*p*,*p*'-DDT	10.83±0.002	10.89±0.41	5211	-6.60	99.8±5.1
T2iPPP	*p*,*p*'-DDT	11.73±0.002	11.78±0.43	5605	-7.02	107.3±5.5
TEP-d15	fluorene	5.04±0.003	5.15±0.30	3343	-6.07	64.0±2.8
TCEP-d12	fluorene	7.77±0.005	7.86±0.35	4969	-8.82	95.1±4.0
TDCiPP-d15	pyrene	9.94±0.006	10.01±0.39	4641	-5.57	88.9±5.3
TPHP-d15	pyrene	10.21±0.009	10.28±0.40	4782	-5.77	91.6±5.4

$K_{OA\text{-}GC}$ values were adjusted for the methodical departures from those directly measured by generator column technique using this calibration equation (Eq. (4.10)) (Table 4.1). Adjustment resulted in slight differences and K_{OA} values were 1.05-1.26 times higher than $K_{OA\text{-}GC}$ values. Errors specified for log K_{OA} values in Table 4.1 were estimated by error propagation employing the standard error of the slope and intercept of the Eq. (4.10) and the standard deviations of the log $K_{OA\text{-}GC}$ values. The propagated errors (3.65–5.83%) are mainly contributed by the uncertainty of the constants in the calibration equation instead of the uncertainty in determined $K_{OA\text{-}GC}$ values.

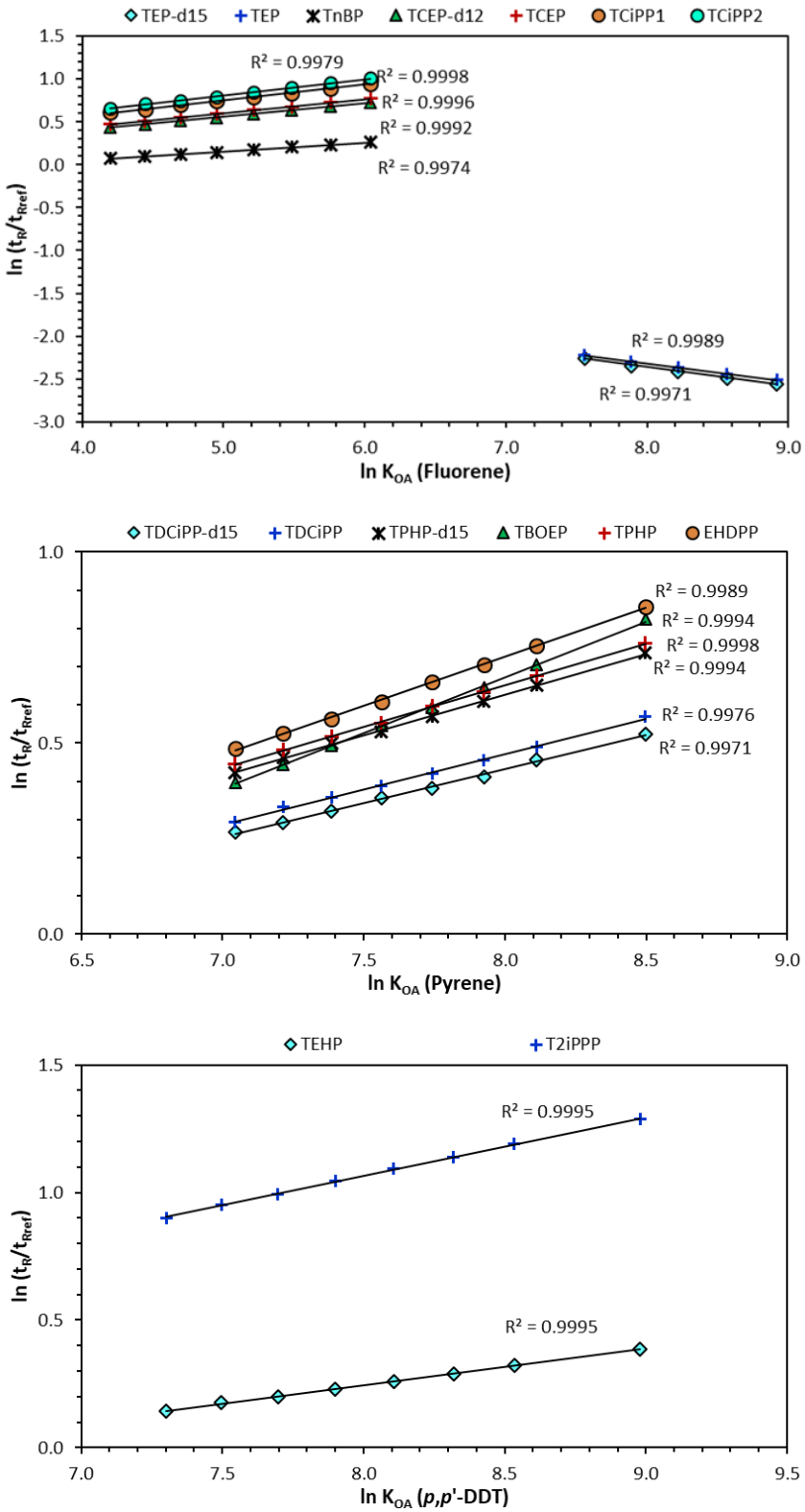


Figure 4.1 Relationships between the logarithm of the ratio of the retention times of OPEs to the retention time of the standard reference compounds (fluorene, pyrene and *p*,*p*'-DDT) at five to eight temperatures and the ln K_{OA} values of the reference compounds at these temperatures (p<0.01)

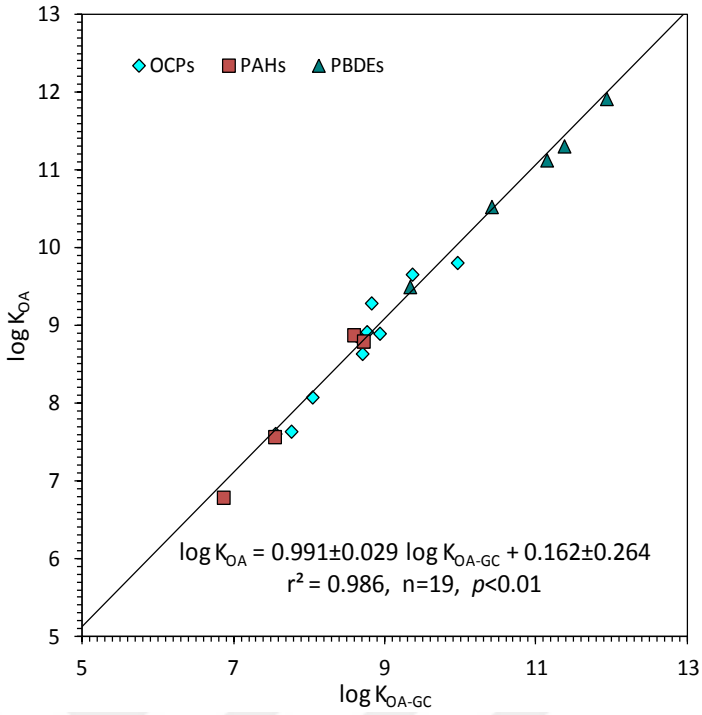


Figure 4.2 Relationship between the directly measured K_{OA} values for OCPs (n=9), PAHs (n=5), and PBDEs (n=5) at 25°C and $K_{OA\text{-}GC}$ values derived from GC retention times

log K_{OA} values for OPEs were compared to those determined by GC-RT method (Wang et al., 2017a; Okeme et al., 2020), estimated by EPI Suite software (US-EPA, 2019) and estimated values compiled by Suhring, Wolschke, Diamond, Jantunen, and Scheringer (2016b) (Figure 4.3). The agreement was generally good. However, for log K_{OA} > 11 literature values were higher than ones determined in the present study. Differences between the estimated and measured K_{OA} values have also been indicated previously (Harner & Bidleman, 1998a; Harner & Mackay, 1995; Odabasi & Cetin, 2012; Odabasi et al., 2006; Shoeib & Harner, 2002b) (Figure 4.3).

ΔU_{OA} values ranged between 65.0 (triethyl phosphate) and 107.3 kJ/mol (tri(2-isopropylphenyl) phosphate) (Table 4.1). Recently Wang et al. (2017a) have reported a similar range between 69.7 (tributyl phosphate) and 113.1 kJ/mol (tris(2-ethylhexyl) phosphate). ΔU_{OA} values for OPEs obtained in the present study were also in the ranges reported for different compound groups like PBDEs (74.5-105 kJ/mol) (Harner & Shoeib, 2002), PCBs (72.6-89.9 kJ/mol) (Harner & Bidleman,

1996; Harner & Mackay, 1995; Komp & McLachlan, 1997), and OCPs (61.9-105.0 kJ/mol) (Shoeib & Harner, 2002b).

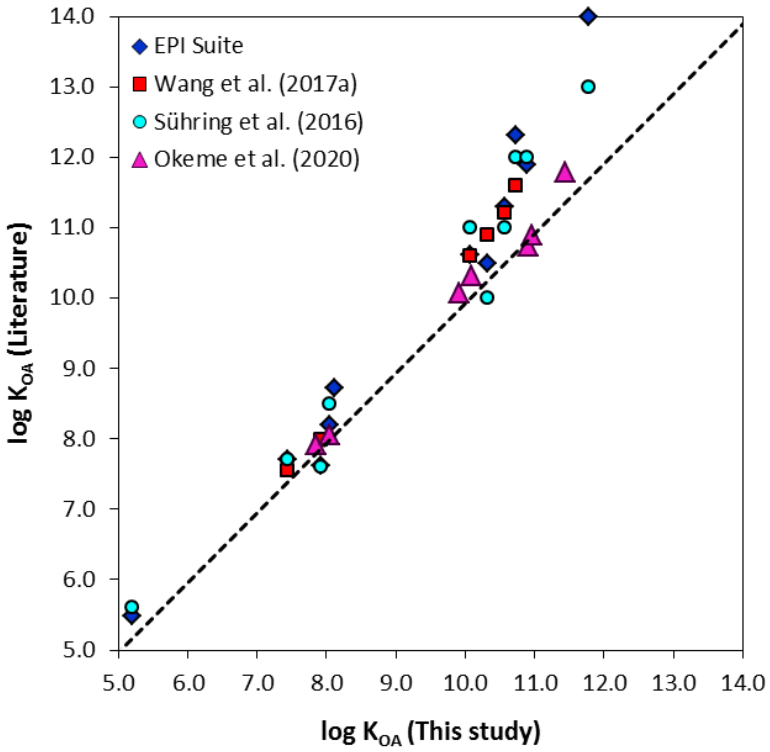


Figure 4.3 Comparison of the K_{OA} values determined for OPEs in this study with the values reported in the literature

4.1.2 Supercooled Liquid Vapor Pressures

P_L values were calculated from the GC-RTs by means of the approach utilized by Lei et al. (2002) and Wong et al. (2001). For each OPE, a vapor pressure ($P_{L\text{-}GC}$) at 25°C was determined using Eq. (4.11):

$$\ln P_{L-GC} = \left(\Delta H_{vap}/\Delta H_{vap-ref}\right) \ln P_{L-ref} + C \qquad (4.11)$$

where, $P_{L\text{-}ref}$ (Pa) and $\Delta H_{vap\text{-}ref}$ (kJ/mol) are the liquid phase vapor pressure at 25°C and the enthalpy of vaporization of a reference chemical. It was assumed that the enthalpies of vaporization are not variable in the temperature interval of interest (between 25°C and temperatures of GC-RT determinations). The term ($\Delta H_{vap}/\Delta H_{vap\text{-}ref}$) and the constant C in Eq. (4.11) were taken from the linear

regression of ln ($t_R/t_{R\text{-}ref}$) at each temperature versus ln $P_{L\text{-}ref}$ (Lei et al., 2002; Wong et al., 2001):

$$\ln\left(t_R/t_{R-ref}\right) = \left[1 - \left(\Delta H_{vap}/\Delta H_{vap-ref}\right)\right] \ln P_{L-ref} - C \qquad (4.12)$$

Eq. (4.12) presumes that the infinite dilution activity coefficients in the GC column stationary phase are equal for the compound of interest and the reference chemical. Since this is an estimate, P_{GC} may not be always equal to P_L. Therefore, method calibration with related compounds having well established vapor pressures is suggested (Lei et al., 2002; Wong et al., 2001).

Fluorene, pyrene and *p*,*p*'-DDT were employed as the reference chemicals. Ma, Lei, Xiao, Wania, and Wang (2010) reviewed and listed the physico-chemical properties of 15 polycyclic aromatic hydrocarbons (PAHs) commonly analyzed and detected in the environment. By correlating the temperature dependent P_L values reported by Ma et al. (2010), the following relationship was derived for fluorene:

$$\log P_L(\text{Pa}) = 11.09 - 3{,}385(T, \text{K})^{-1}, \quad R^2 = 0.998 \text{ (fluorene)} \qquad (4.13)$$

Lei et al. (2002) reviewed a number of determined values of solid-phase vapor pressures (P_S) for pyrene as a function of temperature. P_L was determined by converting the P_S by means of the melting point temperature and entropy of fusion, and it was related to 1/*T* (K):

$$\log P_L(\text{Pa}) = 11.70 - 4{,}164(T, \text{K})^{-1}, \quad R^2 = 0.999 \text{ (pyrene)} \qquad (4.14)$$

Bidleman, Leone, and Falconers (2003) converted the solid-phase vapor pressures of *p*,*p*'-DDT from five studies to liquid-phase vapor pressures using the experimental entropy of fusion values from four studies and melting point temperature, and related them to 1/*T* (K):

$$\log P_L(\text{Pa}) = 12.38 - 4{,}665\ (T, \text{K})^{-1}, \quad R^2 = 0.997\ (p, p' - \text{DDT}) \qquad (4.15)$$

The relation of ln (t_R/t_{Rref}) to ln P_{Lref} is depicted in Figure 4.4 where t_R and t_{Rref} are the retention times of target and reference compounds, respectively and P_{Lref} is the supercooled liquid vapor pressure of the reference compound. These correlations were very linear for all OPEs with high r^2values (>0.99) and p<0.01. $P_{L\text{-}GC}$ and P_L values of OPEs (at 25°C) were given in Table 4.2 along with the intercepts (b_L) and slopes (m_L) of the temperature correlations:

$$\log P_L(\text{Pa}) = m_L(T, \text{K})^{-1} + b_L \qquad (4.16)$$

Table 4.2. Uncalibrated ($P_{L\text{-}GC}$, average ± SD, n = 3) and calibrated (P_L, average ± propagated error) vapor pressures for OPEs at 25°C, enthalpies of vaporization (ΔH_{vap}, average ± propagated error), and regression parameters for Eq. (4.16)

OPEs	**Reference Compound**	**log $P_{L\text{-}GC}$ (Pa)**	**log P_L (Pa)**	**m_L**	**b_L**	**ΔH_{vap} (kJ mol^{-1})**
TEP	fluorene	1.43 ± 0.0060	1.59 ± 0.013	-2,651	10.49	-50.7 ± 0.14
TnBP	fluorene	-0.82 ± 0.0026	-0.81 ± 0.0034	-4,105	12.97	-78.6 ± 0.051
TCEP	fluorene	-1.30 ± 0.0037	-1.32 ± 0.0032	-4,388	13.41	-84.0 ± 0.062
TCiPP1	fluorene	-1.44 ± 0.0033	-1.47 ± 0.0044	-4,464	13.51	-85.5 ± 0.077
TCiPP2	fluorene	-1.50 ± 0.0036	-1.53 ± 0.044	-4,498	13.56	-86.1 ± 0.077
TDCiPP	pyrene	-3.46 ± 0.012	-3.63 ± 0.013	-5,240	13.95	-100.3 ± 0.18
TBOEP	pyrene	-4.13 ± 0.0014	-4.35 ± 0.0009	-5,703	14.79	-109.2 ± 0.019
TPHP	pyrene	-3.71 ± 0.0056	-3.91 ± 0.0068	-5,380	14.15	-103.0 ± 0.096
EHDPP	pyrene	-3.96 ± 0.0019	-4.16 ± 0.026	-5,550	14.47	-106.3 ± 0.019
TEHP	*p*,*p*'-DDT	-4.28 ± 0.0043	-4.52 ± 0.0016	-5,694	14.59	-109.0 ± 0.033
T2iPPP	*p*,*p*'-DDT	-5.19 ± 0.0022	-5.49 ± 0.0034	-6,120	15.05	-117.2 ± 0.048
TEP-d15	fluorene	1.49 ± 0.0037	1.66 ± 0.0026	-2,598	10.38	-49.7 ± 0.12
TCEP-d12	fluorene	-1.24 ± 0.0051	-1.26 ± 0.0041	-4,354	13.35	-83.4 ± 0.088
TDCiPP-d15	pyrene	-3.40 ± 0.0061	-3.57 ± 0.0069	-5,203	13.89	-99.6 ± 0.098
TPHP-d15	pyrene	-3.67 ± 0.0098	-3.86 ± 0.0098	-5,356	14.11	-102.6 ± 0.15

Enthalpy of vaporization (ΔH_{vap}) values are also presented in Table 4.2. Relative standard deviations for P_{GC} values calculated from triplicate runs were small (0.4–2.9%).

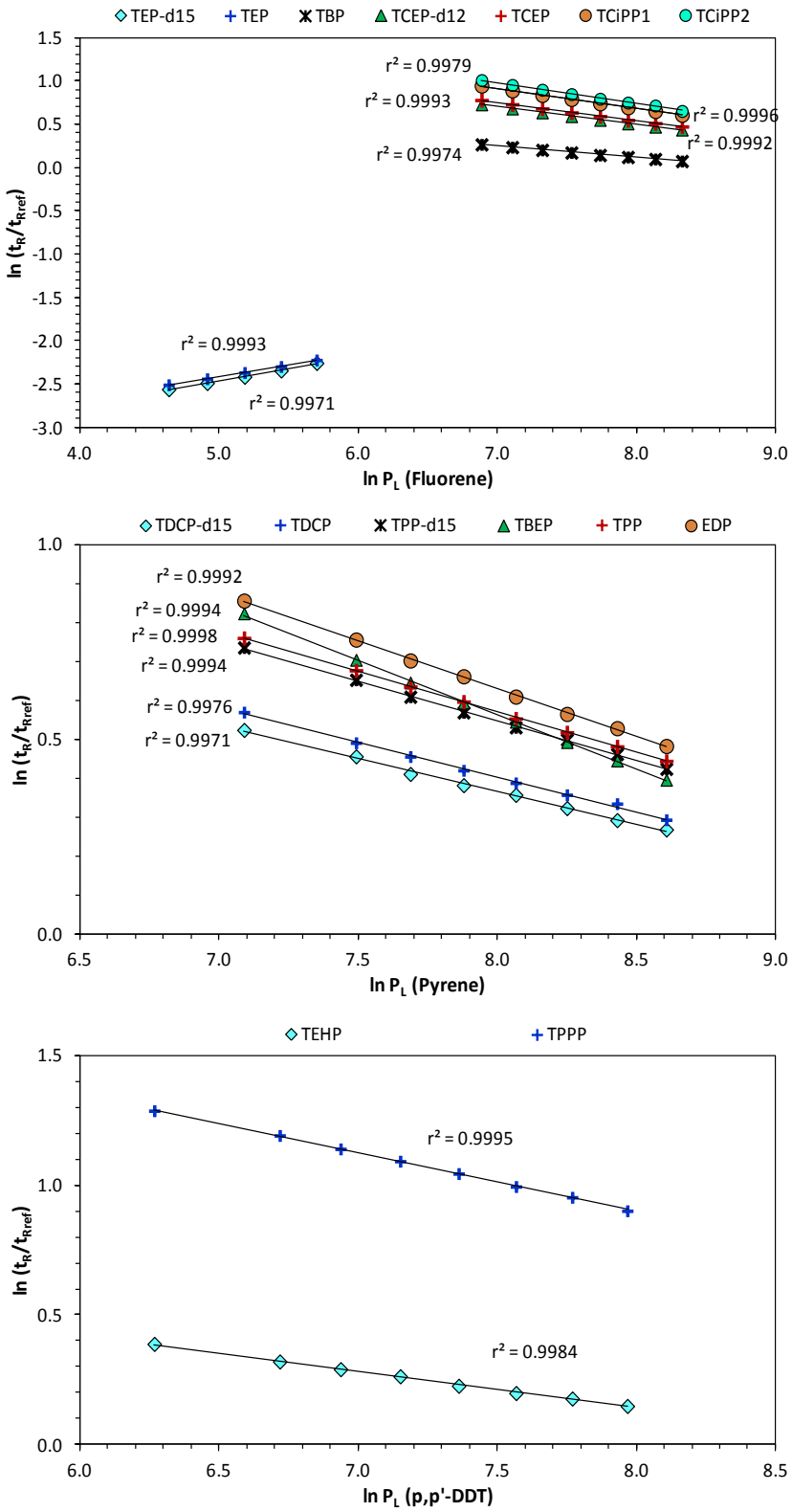


Figure 4.4 Relationships between the logarithm of the ratio of the retention times of OPEs to the retention time of the standard reference compounds (fluorene, pyrene and *p*,*p*'-DDT) at five to eight temperatures and the ln P_L values of the reference compounds at these temperatures (p<0.01)

Five PAHs (fluorene, phenanthrene, fluoranthene, pyrene, and chrysene) and *p,p*'-DDT having experimentally determined vapor pressures (at 25°C) were used as the calibration chemicals (Bidleman et al., 2003; Lei et al., 2002; Ma et al., 2010). The following equation was derived by linear regression of $P_{\text{L-GC}}$ values for calibration chemicals and literature P_{L} (Figure 4.5):

$$\log P_L(\text{Pa}) = 1.070 \pm 0.031 \log P_{\text{GC}}(\text{Pa}) + 0.068 \pm 0.056$$
$$r^2=0.987,\ p<0.01,\ n=18 \qquad (4.17)$$

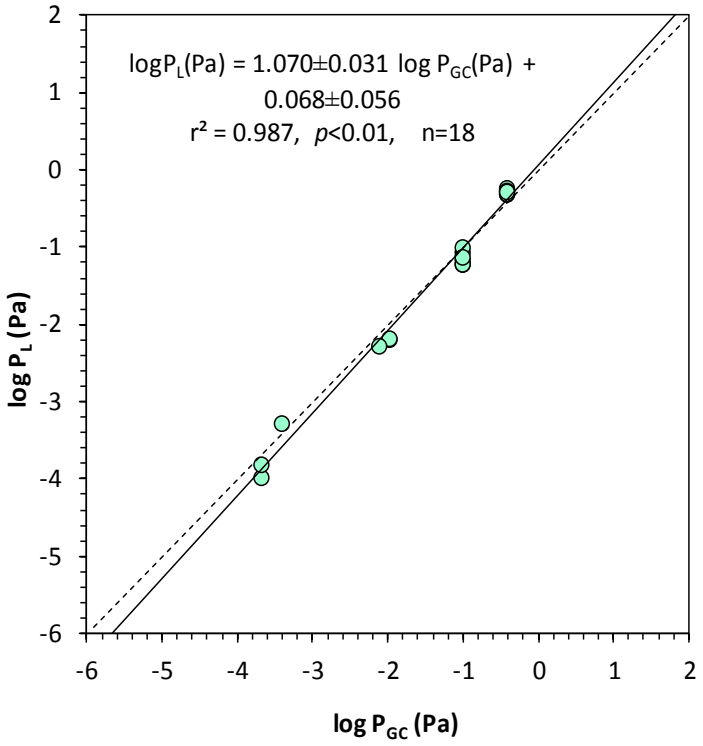


Figure 4.5 Relationship between the GC determined vapor pressure ($P_{\text{L-GC}}$) and the vapor pressure of supercooled liquid (P_{L}) derived from literature data at 25°C for five PAHs (fluorene, phenanthrene, fluoranthene, pyrene, and chrysene) and *p,p*'-DDT (Lei et al., 2002). The dashed line represents a 1:1 relationship, the solid line is the fit through the data points.

$P_{\text{L-GC}}$ values were corrected for the methodical departures from directly measured P_{L} values using this calibration equation (Eq. (4.17)) (Table 4.2). P_{L} values were slightly different than $P_{\text{L-GC}}$ values (1.02-1.10 times higher). Errors specified for log P_{L} values in Table 4.2 were estimated by error propagation utilizing the standard

error of the slope and intercept of the Eq. (4.17) and the standard deviations of the log $P_{L\text{-}GC}$ values. The propagated errors (3.10–7.53%) are mainly contributed by the uncertainty of the coefficients in Eq. (4.17) instead of the uncertainty in determined $P_{L\text{-}GC}$ values.

As researchers' interest in OPEs has increased recently, the number of studies on these compounds has also increased. However, there are only a few studies reporting experimental P_L values for OPEs. P_L values determined in the present study were compared to those reported by three recent studies (Brommer et al., 2014; Suhring et al., 2016b; Wang et al., 2017b) (Figure 4.6). The agreement with the values reported by two experimental studies (Brommer et al., 2014; Wang et al., 2017b) was good as shown by high r^2, slope close to 1 (p<0.01). However, P_L values reported by Wang et al. (2017b) were slightly lower while those compiled by Suhring et al. (2016b) showed some scatter.

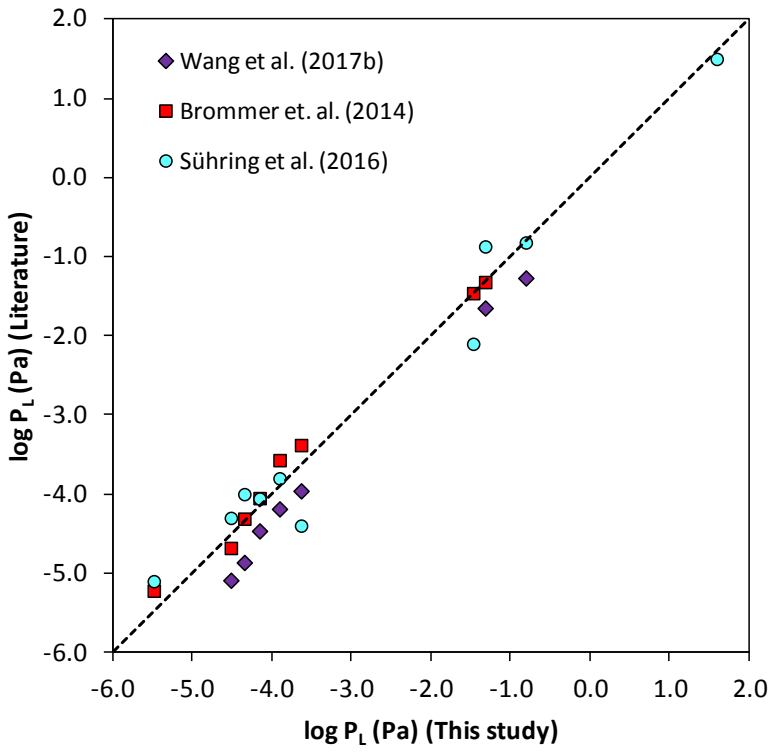


Figure 4.6 Comparison of the P_L values determined for OPEs in this study with the values reported in literature (Brommer et al., 2014; Suhring et al., 2016b; Wang et al., 2017b).

ΔH_{vap} values ranged between 50.7 (triethyl phosphate) and 117.1 kJ/mol (tri(2-isopropylphenyl) phosphate) (Table 4.2). Recently Wang et al. (2017b) have reported a similar range for OPEs between 74.1 (tributyl phosphate) and 111.4 kJ/mol (tris(2-ethylhexyl) phosphate).

log K_{OA} values of OPEs increased linearly with increasing molecular weights (MW) and the overall correlation was good (r^2=0.835, p<0.01). Correlations were substantially higher for sub-groups with r^2 values of 0.986, 0.979, and 0.958 (p<0.01) for alkyl- (TEP, TEP-d15, TnBP, TEHP, and TBOEP), aryl- (TPHP, TPHP-d15, EHDPP, and T2iPPP), and chlorinated-OPEs (TCEP, TCEP-d12, TCiPP2, TCiPP1, TDCiPP, and TDCiPP-d15), respectively (Figure 4.7). For similar MWs, aryl-OPEs had higher log K_{OA} values than alkyl- and chlorinated-OPEs. log P_L values of OPEs decreased linearly with increasing MW with similar r^2 values observed for log K_{OA} and MW correlations (Figure 4.7).

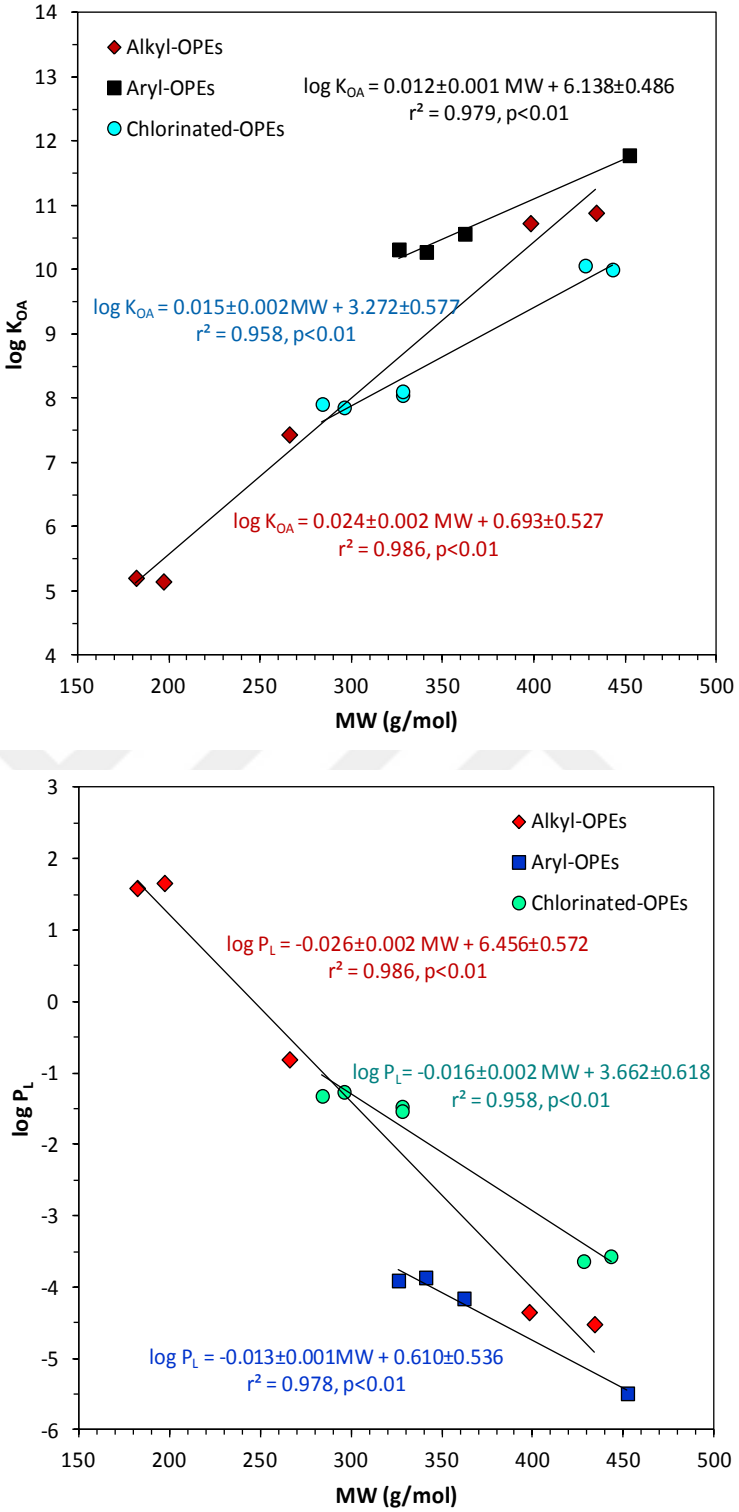


Figure 4.7 Relationship of log K_{OA} and log P_L of OPEs with their molecular weights

4.1.3 PUF-Air Partition Coefficients

A total of 20 gas-phase samples (3 sorbent traps and a backup trap for each 5 temperatures) and 5 PUF pairs were extracted and analyzed for 11 OPEs. Seven of 11 included OPEs were above MDL in gas-phase samples, allowing the determination of temperature dependent $K_{PUF\text{-}Air}$ values. However, the remaining four OPEs (TPHP, EHDPP, TEHP and T2iPPP) were below MDL, thus their $K_{PUF\text{-}Air}$ values could not be measured. OPE amounts in backup traps were below MDLs indicating that breakthrough was not a problem. $K_{PUF\text{-}Air}$ values (dimensionless) were calculated as C_{PUF}/C_{Air}, where C_{PUF} and C_{Air} are the OPE concentrations in the PUF disks and outlet air stream of the generator column (ng/mL), respectively. The air concentration (C_{Air}, ng/mL) was calculated by dividing the analyte mass collected in the trap (m_{Air}, ng/sample) by the total air volume sampled (~288,000 mL). The two PUF disks combined had a volume of 95 mL. The OPE concentration in PUFs (C_{PUF}, ng/mL) was calculated by dividing the mass on PUF (m_{PUF}, ng/sample) by the PUF volume (V_{PUF}, mL). Mass of OPEs in the PUF measured after the collection of three daily gas-phase samples (m_{PUF3}). Therefore, for each temperature set, the mass of OPE on the PUF disks at days 0, 1, 2, and 3 was adjusted by adding the amount collected in the previous gas-phase sample ($m_{PUF2} = m_{PUF3} + m_{Air3}$, $m_{PUF1} = m_{PUF3} + m_{Air3} + m_{Air2}$, $m_{PUF0} = m_{PUF3} + m_{Air3} + m_{Air2} + m_{Air2}$; $C_{PUF1} = [(m_{PUF0} + m_{PUF1})/2)]/V_{PUF}$, $C_{PUF2} = [(m_{PUF1} + m_{PUF2})/2)]/V_{PUF}$, $C_{PUF3} = [(m_{PUF2} + m_{PUF3})/2)]/V_{PUF}$; $K_{PUF\text{-}Air1} = C_{PUF1}/C_{Air1}$, $K_{PUF\text{-}Air2} = C_{PUF2}/C_{Air2}$, $K_{PUF\text{-}Air3} = C_{PUF3}/C_{Air3}$). For the most volatile OPE TEP, by the end of the experiment, OPE amounts in the PUF disk decreased by 2.3, 8.2, 21.7, 42.2, and 55% at temperatures 15, 25, 35, 45, and 50°C, respectively. For less volatile OPEs, the decrease was minimal (up to 7% for TnBP at 50°C) and the resulting adjustment to C_{PUF} was negligible (<1.0%). log $K_{PUF\text{-}Air}$ values at 25°C and also regression parameters for TEP, TnBP, TCEP, TCiPP1, TCiPP2, TDCiPP and TBOEP were given in Table 4.3.

Table 4.3 Regression parameters (*A* and *B*) for the equation log $K_{PUF\text{-}air} = A + B/T$ (T is the temperature in Kelvin), enthalpies (kJ/mol), log $K_{PUF\text{-}air}$ ± SD at 25°C

OPE	A	B	r^2	$\Delta H_{PUF\text{-}air}$ (kj/mol)	log $K_{PUF\text{-}air}$ (25°C)
TEP	-7.68	3,809	0.993	72.9	5.04±0.11
TnBP	-8.88	4,536	0.991	86.9	6.26±0.05
TCEP	-3.53	3,147	0.972	60.3	6.91±0.08
TCiPP 1	-7.46	4,170	0.982	79.8	6.50±0.03
TCiPP 2	-6.76	3,987	0.989	76.3	6.59±0.03
TDCiPP	-5.79	3,918	0.979	75.0	7.43±0.06
TBOEP	-3.21	3,352	0.997	64.2	8.08±0.01

Relationships between measured log $K_{PUF\text{-}Air}$ and log K_{OA} were compared in Figure 4.8 with the results those reported in previous studies. Tromp et al. (2019), Saini, Clarke, and Harner (2019a), Francisco et al. (2017) and Shoeib and Harner (2002a) derived the following equations for the relationships between log K_{OA} values and log $K_{PUF\text{-}Air}$, respectively:

$$\log K_{PUF-Air} = 0.940 \log K_{OA} - 1.105; \quad \text{for PAHs, PCBs, OCPs, OPEs} \qquad (4.18)$$

$$\log K_{PUF-Air} = 0.6087 \log K_{OA} + 2.3821; \quad \text{for OPEs} \qquad (4.19)$$

$$\log K_{PUF-Air} = 0.6574 \log K_{OA} + 1.2946; \quad \text{for PAHs, alkyl-PAHs, OCPs} \qquad (4.20)$$

$$\log K_{PUF-Air} = 0.6366 \log K_{OA} - 3.1774; \quad \text{for PCBs} \qquad (4.21)$$

The lines in Figure 4.8 were drawn according to Equations 4.18, 4.19, 4.20 and 4.21. Shoeib and Harner (2002a), derived their equation (Eq. 4.21) being log $K_{PUF\text{-}Air}$ in (m^3/g), and it was made dimensionless by multiplying it with density of PUF (g/m^3). As can be inferred from Figure 4.8 the variation of log K_{OA} with log $K_{PUF\text{-}Air}$ were in the ranges those reported in the literature. The relationship between log K_{OA} and log $K_{PUF\text{-}Air}$ for OPEs derived in the present study was;

$$\log K_{PUF-Air} = 0.5194 \log K_{OA} + 2.4192; \; r^2=0.96 \qquad (4.22)$$

The measured 7 $K_{PUF\text{-}Air}$ values were used to calculate compound-specific sampling rates for PUF ambient air passive samplers within the present study. $K_{PUF\text{-}Air}$ values for four OPEs that could not be measured were determined according to Equation (4.22) using experimentally determined K_{OA} values.

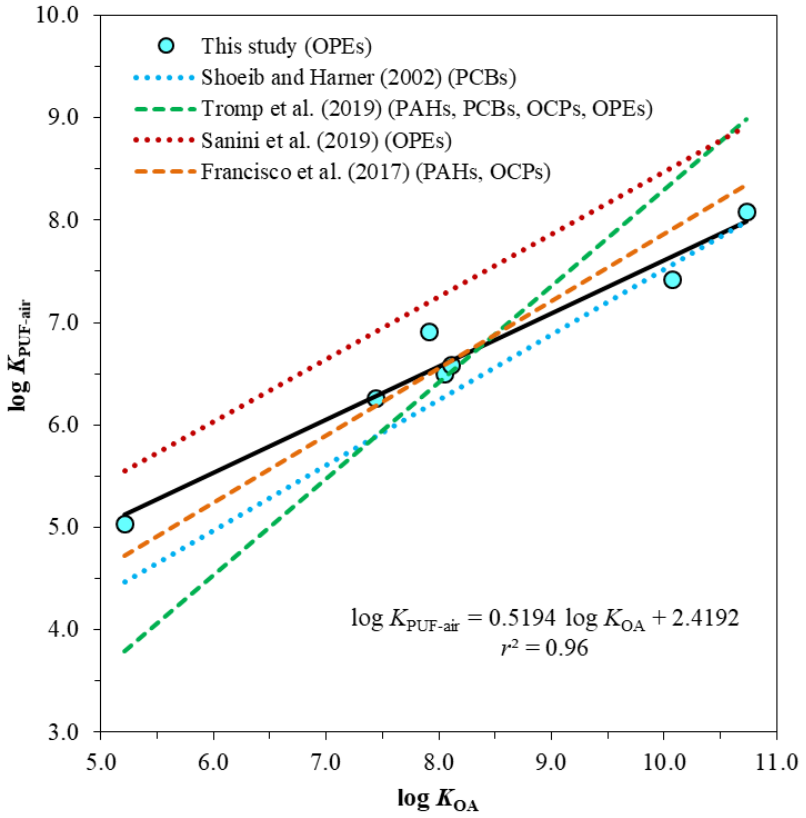


Figure 4.8 Variation of measured log $K_{PUF\text{-}air}$ with log K_{OA} (at 25°C) in the present study and those estimated from relationships reported by previous studies

There are two experimental $K_{PUF\text{-}Air}$ values for TEP previously measured by Tromp et al. (2019) and Saini et al. (2019a). Tromp et al. (2019) reported their log $K_{PUF\text{-}Air}$ values at 20.7°C as 5.32±1.32 for TEP while Saini et al. (2019a) reported a value of 6.01 adjusted to same temperature. log $K_{PUF\text{-}Air}$ of TEP was 5.28 (at 20.7°C) in the present study, which is in very good agreement with the value reported by Tromp et al. (2019). It is important to get accurate $K_{PUF\text{-}Air}$ values especially for OPEs having lower K_{OA} values (i.e. TEP and TnBP) compared to those having high K_{OA}. Because volatile OPEs can easily reach equilibrium (within hours to a few

days) during the long deployment periods, while the remaining OPEs stay in linear uptake phase (Shoeib & Harner, 2002a).

4.1.4 Henry's Law Constants

H is defined as (Bamford et al., 2000; Cetin & Odabasi, 2005; Cetin et al., 2006):

$$H = P_g / C_w \tag{4.23}$$

where, P_g is the partial pressure in gas-phase (Pa) and C_w is the aqueous concentration (mol/m^3).

Dimensionless Henry's law constant (H') can be calculated by converting the partial pressure to molar concentration by the use of ideal gas law [$p = (nRT)/V$] (mol/m^3):

$$H' = H / R\,T \tag{4.24}$$

where, R is the ideal gas constant (8.314 Pa m^3/mol K) and T is the absolute temperature (K).

The H could be expressed as a function of temperature using the following equation (Bamford et al., 1999):

$$\ln H = \frac{-\Delta H_H}{R\,T} + \frac{\Delta S_H}{R} \tag{4.25}$$

where, ΔH_H (J/mol) and ΔS_H (J/mol K) are the enthalpy and entropy of the phase change from the aqueous phase to the gas phase, respectively.

ΔH_H and ΔS_H can be obtained from the slope and intercept of ln H vs. 1/T plot, respectively when directly measured H values at different temperatures are available.

The following equation was used to calculate the experimental H' values:

$$H' = C_g / \left[\left(C_{w(n)} + C_{W(n+1)} \right) / 2 \right] \quad (4.26)$$

where, C_g (ng/L) is the gas-phase OPE concentration, and $C_{w(n)}$ and $C_{w(n+1)}$ are the aqueous OPE concentrations (ng/L) measured at the start and at the end of gas-phase sampling interval, respectively.

Three *H* values were determined according to Eq. (4.26) representing each respective experiment conducted at certain temperatures (15, 20, 25, 30 and 35 °C) using the OPE concentrations measured in water (*n*=4) and gas-phase (*n*=3) samples for individual experimental period (24 h). OPE amounts in backup traps were below MDLs indicating that breakthrough was not a problem for the gas-phase sampling. The determined *H* values (*n*=3) were averaged and then ln (*H*) were regressed against the 1/*T*(K). The regression parameters and standard deviations for the equation ln *H*=*A*+*B*/*T*(K) were given in Table 4.4. Enthalpies and entropies of phase change, and also *H* values measured at 25°C (average ± SD) for OPEs were also tabulated. In deionized water, *H* values (at 25°C) were ranged between 12.012 ± 3.039 (TnBP) and 0.021 ± 0.003 Pa m^3/mol (TEP). Except TnBP, all the OPEs have *H* values <1 Pa m^3/mol. Based on a literature search, there is no studies reporting experimental *H* values for interested OPEs. Therefore, experimental *H* values obtained within the present study were compared with; (i) the values from The Estimation Programs Interface (EPI) Suite TM (v1.43), (ii) the values derived from K_{OW}/K_{OA} equation (employing experimental K_{OA} values), and (iii) the values calculated with pp-LFER estimation procedure (Ulrich et al., 2017). Comparisons between experimental and estimated *H* values were illustrated in Figure 4.9. The distribution is significantly scattered, and in general, estimated values were lower than the experimental ones. However, *H* values derived from K_{OW}/K_{OA} equation showed the best agreement with experimental values.

ΔH_H values ranged between 16.8 (TEP) and 125.7 (T2iPPP) kJ/mol in the present study. Although there is no previous study reporting ΔH_H values for OPEs, measured

values fall within the ranges reported for other organic compound groups (Bamford et al., 2000; Cetin & Odabasi, 2005; Cetin et al., 2006).

Table 4.4 The regression parameters (±standard errors) for the equation ln$H$=A+B/T(K), enthalpies and entropies of phase change, and H values measured at 25°C (average ± SD) for OPEs in deionized water

	r^2	A	B	ΔS_H (kj/mol K)	ΔH_H (kj/mol)	H (Pa m^3/mol)
TEP	0.98	2.92±0.49	-2,025±147	0.02	16.84	0.021±0.003
TnBP	0.97	21.29±1.83	-5,631±545	0.18	46.82	12.012±3.039
TCEP	0.99	10.13±0.69	-3,571±204	0.08	29.69	0.162±0.023
TCiPP1	0.97	13.81±1.61	-4,999±481	0.11	41.56	0.053±0.013
TCiPP2	0.99	7.44±0.67	-3,137±201	0.06	26.08	0.046±0.013
TDCiPP	0.98	25.80±2.25	-8,057±671	0.21	66.99	0.328±0.072
TBOEP	0.99	24.14±1.04	-7,564±309	0.20	62.88	0.269±0.086
TPHP	0.99	45.09±2.21	-13,899±659	0.37	115.56	0.258±0.063
EHDPP	0.99	47.17±2.13	-14,485±633	0.39	120.43	0.217±NA
TEHP	0.98	43.48±3.73	-13,858±1,111	0.36	115.22	0.060±0.014
T2iPPP	0.99	48.41±3.07	-15,122±915	0.40	125.72	0.115±0.030

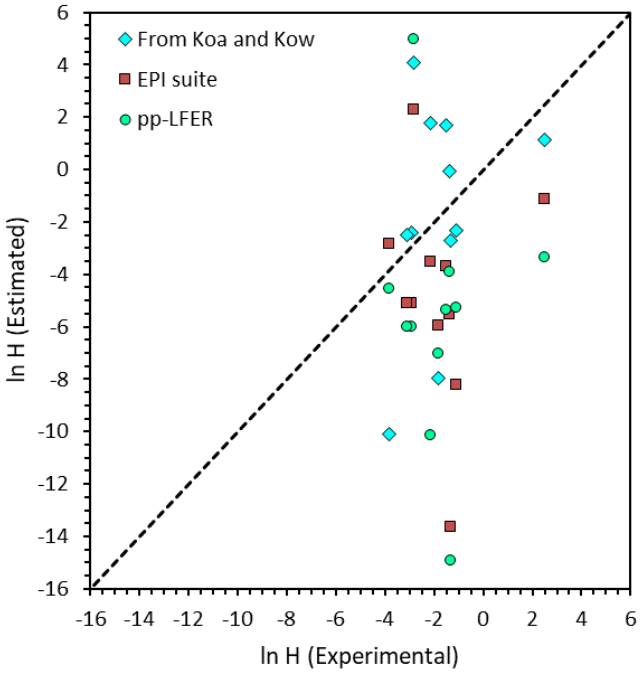


Figure 4.9 Comparison of experimental and literature (Pa m^3/mol) values for OPEs. Dashed diagonal line indicates the 1:1 relationship

4.1.5 LDPE-Water Partition Coefficients

The availability of accurate K_{PEW} is crucial for successful application of sea water passive samplers used in this study. The obtained water- and LDPE-phase OPE concentrations from the K_{PEW} experiment detailed in Section 3.1.5, were used to determine values for 11 OPEs. At the equilibrium, Lohmann (2012) expressed the partitioning constant between LDPE and water, K_{PEW} (L/kg) as:

$$K_{PEW} = C_{LDPE}/C_W \tag{4.27}$$

where, C_W (ng/L) and C_{LDPE} (ng/kg) are the OPE concentrations in water and LDPE. Table 4.5 summarizes the experimentally determined log K_{PEW} values for 11 OPE compounds. LDPE and aqueous sample pairs meeting the condition sample amount>10xMDL were used to calculate log K_{PEW} values. As a result, K_{PEW} values for TEP and TCEP were derived from absorption experiments while the values for the remaining OPES were calculated based on desorption experiments. It should be noted that K_{PEW} values were measured in DI and at an average temperature of 19.2°C.

Lohmann (2012) denoted that solubility (S), in kg/L, as another physicochemical parameter that could be employed to predict K_{PEW} of a certain organic compound according to:

$$\begin{aligned} \log K_{PEW} &= -1.06 \log S - 1.60 \\ r^2 &= 0.91, SE = 0.37, n = 100 \end{aligned} \tag{4.28}$$

The required S values for Eq. (4.28) were obtained from The Estimation Programs Interface (EPI) Suite TM (v1.43). The experimental K_{PEW} values were compared with the predicted ones according to Equation 4.28 and also with K_{OW} values obtained from EPI Suite (v1.43) as indicated in Figures 4.10 and 4.11, respectively. Estimated and measured log K_{PEW} values correlated well (r^2=0.86, p<0.01). However, slope of the regression line was 1.86, indicating estimated values were

substantially higher than the experimental ones. log K_{PEW} values correlated well with the log K_{OW} values (r^2=0.85, p<0.01). log K_{PEW} values also correlated well with the log S values (log K_{PEW}= -0.487 log S + 0.265, r^2=0.86, p<0.01). These good correlations suggest that these relationships could be used to estimate the log K_{PEW} values for OPEs.

Table 4.5 Experimental K_{PEW} values (L/kg) for OPEs measured in DI water at 19.2°C

	log K_{PEW}	
	Average	SD
TEP	0.83	0.18
TnBP	2.39	0.15
TCEP	1.43	0.23
TCiPP1	3.48	0.08
TCiPP2	3.17	0.07
TDCiPP	2.78	0.06
TBOEP	2.59	0.14
TPHP	2.70	0.54
EHDPP	4.21	0.07
TEHP	5.43	0.17
T2iPPP	5.48	0.09

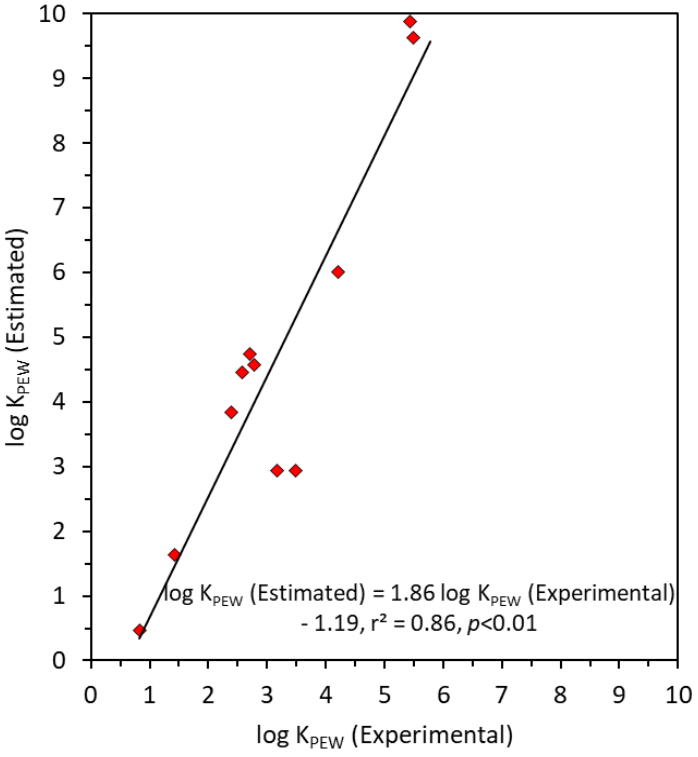


Figure 4.10 Comparison of experimental K_{PEW} values of OPEs with estimated ones

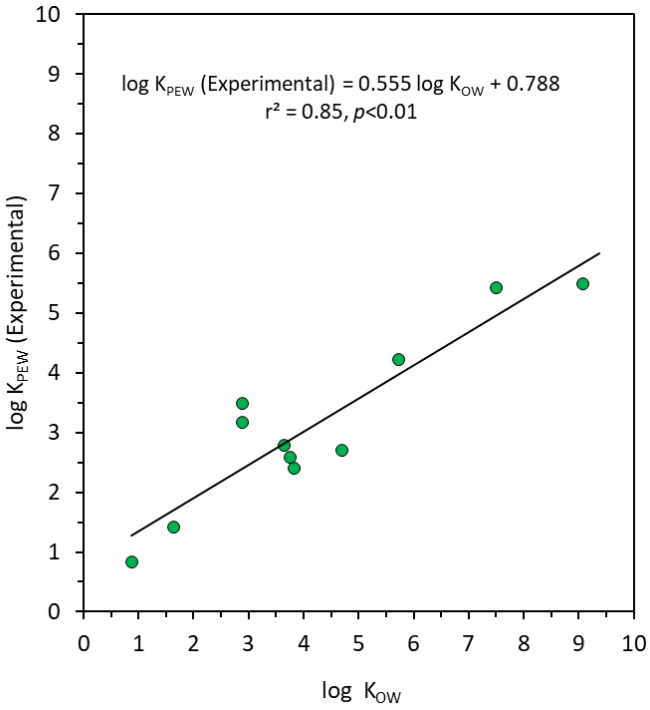


Figure 4.11 Relationship between K_{PEW} values of OPEs to K_{OW}

According to literature, K_{PEW} values for OPEs have not been experimentally measured to date. Lohmann (2012) comprehensively reviewed K_{PEW}s for diverse groups of organics including PAHs, PCBs and various other organic compounds (OCPs, PBDEs and PCDD/Fs). They derived several relationships between K_{PEW}s and some other physicochemical properties (i.e. K_{HDW} (hexadecane-water partitioning coefficient), K_{OW} and S) of these compounds. Although, Eq. (4.28) derived by Lohmann (2012) represents a large number of compounds (excluding OPEs) with a relatively good correlation, they reported a significant standard error (0.37). Moreover, seawater concentrations determined using predicted K_{PEW} values ($C_{SW\text{-}pred}$) differed from those derived using experimental K_{PEW} values ($C_{SW\text{-}exp}$) with a factor ($C_{SW\text{-}pred}/C_{SW\text{-}exp}$) ranging from 0.011 (TPHP) to 6.18 (TCiPP1). Therefore, it is crucial to use experimental K_{PEW} values to determine the aqueous OPE concentrations accurately.

4.2 Field Studies

4.2.1 Gas and Particle Phase OPE Concentrations

Gas and particle phase OPE samples representing both summer and winter conditions were collected from the urban sampling site (Izmir City Center) and they were analyzed for 11 OPEs. Average concentrations are given in Table 4.6. Total (gas+particle) Σ_{11}OPE concentrations ranged between 1.79-8.90 ng/m^3 (4.43±1.70 ng/m^3). OPE congener based composition profiles were demonstrated in Figure 4.12. Although there were sample by sample variations, OPE profiles during the sampling periods were similar. According to compound-specific concentrations, TCiPP1, and TnBP were the most abundant OPEs followed by TEP in all samples while TEHP and T2iPPP were the least abundant ones. These three OPEs comprise more than %50 of total OPE concentrations in most samples. In terms of OPE groups, Σ_{11}OPEs were dominated by chlorinated-OPEs (TCEP, TCiPP1, TCiPP2, TDCiPP). The average contribution of chlorinated-OPEs to Σ_{11}OPEs was 52.1±7.7%. Similar high contributions of chlorinated-OPEs were also reported by recent studies (Moller et al., 2012; Rauert et al., 2016; Shoeib et al., 2014).

Table 4.6 Average gas and particle phase OPE concentrations for winter and summer sampling periods

OPE	**Average Concentrations (ng/m^3)**			
	Particle phase		**Gas phase**	
	Winter	**Summer**	**Winter**	**Summer**
TEP	n.d.	0.028±0.0074	0.37±0.19	0.63±0.22
TnBP	0.086±0.067	0.047±0.021	0.44±0.28	0.57±0.19
TCEP	0.085±0.027	0.046±0.015	0.067±0.042	0.37±0.25
TCiPP1	0.68±0.26	0.29±0.13	0.55±0.53	1.46±0.77
TCiPP2	0.21±0.08	0.090±0.040	0.13±0.12	0.48±0.29
TDCiPP	0.063±0.036	0.11±0.039	0.030±0.0091	0.085±0.062
TBOEP	0.16±0.13	0.086±0.038	0.015±0.018	0.093±0.056
TPHP	0.36±0.18	0.057±0.028	0.053±0.034	0.14±0.048
EHDPP	0.28±0.25	0.27±0.17	0.11±0.096	0.14±0.088
TEHP	n.d.	0.097±0.11	n.d.	0.029±0.010
T2iPPP	0.0070±0.0027	0.014±0.012	n.d.	0.0035±0.0015
Σ_{11}OPE	1.95±0.77	1.15±0.36	1.77±0.84	4.00±1.77

n.d.: *not detected.*

Seasonal gas and particle phase Σ_{11}OPE variations were illustrated in Figure 4.13. Average Σ_{11}OPE gas-phase concentrations were 1.77 ± 0.84 and 4.00 ± 1.77 ng/m^3, while particle-phase concentrations were 1.95 ± 0.77 and 1.15 ± 0.36 ng/m^3 for winter and summer seasons, respectively. Σ_{11}OPE concentrations generally increased in summer. Except the three highly non-volatile OPEs (EHDPP, TEHP, and TPHP) gas phase concentrations of remaining OPEs positively and strongly correlated with temperature (r^2=0.32-0.62, p<0.01). This could be attributed to enhanced volatilization of OPEs from their sources or environmental surfaces like soil, water, and vegetation at elevated temperatures. From Figure 4.13, it can be also inferred that OPEs shifted to the gas phase during summer since higher temperatures favor their partitioning to the gas-phase.

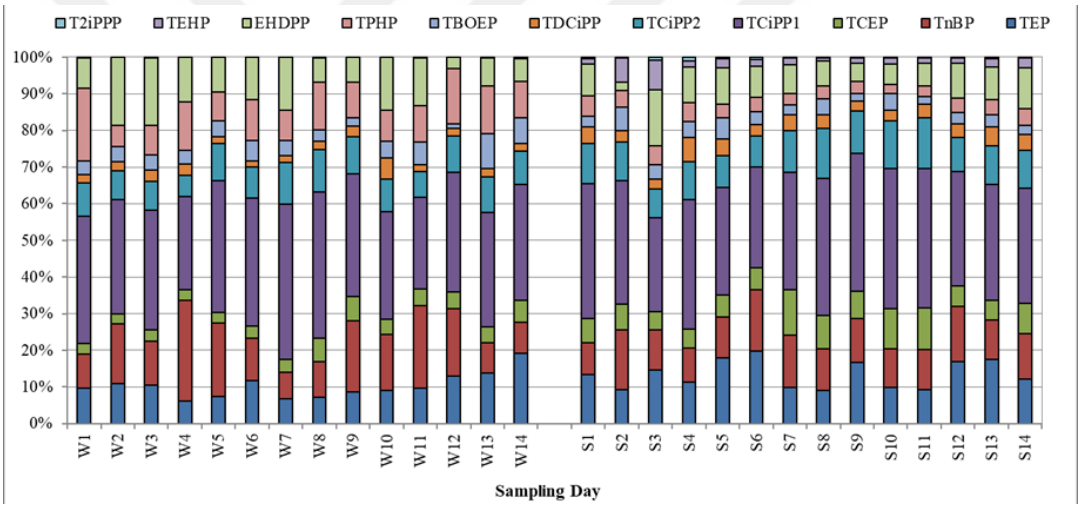


Figure 4.12 Compound-specific total (gas + particle phase) OPE compositions (W: winter, S: summer)

A number of studies that investigates OPEs in ambient air can be found in the literature. However, atmospheric OPE levels reported by the most researchers, usually show considerable variations, probably due to different site characteristics, sampling techniques and number of compounds included. For instance, Salamova et al. (2014b) measured particle phase levels of 12 OPEs in the North American Great Lakes atmosphere. They determined Σ_{12}OPE that atmospheric concentrations ranged from 0.12±0.018 to 2.1±0.4 ng/m^3 at five urban sites, and dominated by TCEP, TCiPP1, and TDCiPP. Average concentration of Σ_9OPEs (gas + particle phase) measured by Wolschke et al. (2016) was 0.005 ng/m^3 in the marine atmosphere of

the German Coast. The only previous study on atmospheric OPE levels in Turkey was carried out in a highly industrialized area using passive samplers (Kurt-Karakus et al., 2018). They have reported a range of 0.53-19.14 ng/m^3 for Σ_6OPEs. Further comparisons on compound basis were presented in Table 4.7.

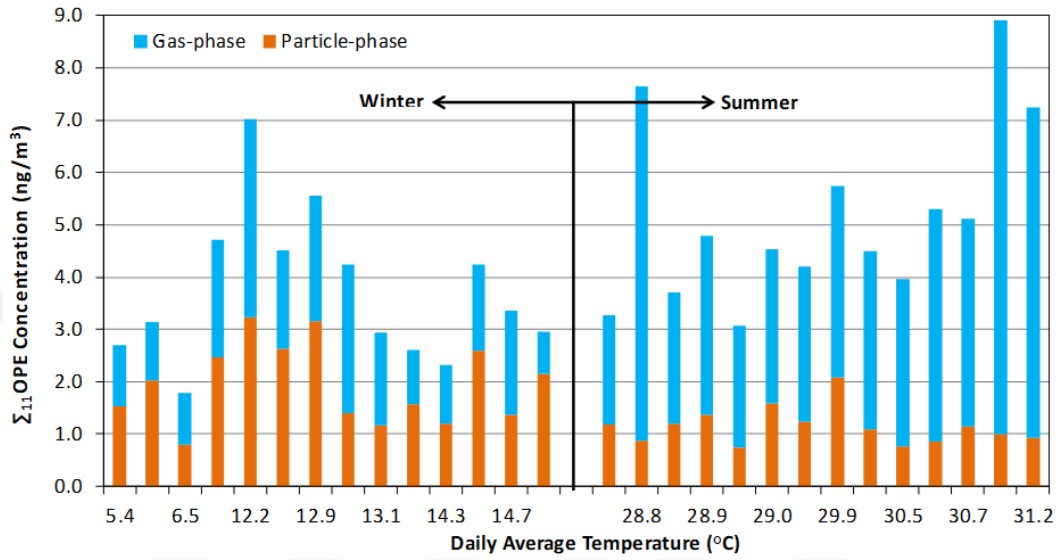


Figure 4.13 Relationship between measured Σ_{11}OPE concentrations and daily average temperatures for both sampling seasons

Table 4.7 Comparison of overall average OPE concentrations (ng/m^3) obtained in this study with those reported in the literature

OPE	Phase	Lai et al. (2015)	Salamova, Hermanson, and Hites (2014a)	Moller et al. (2011)	Kurt-Karakus et al. (2018) [a]	Wu et al. (2020)	This study
TnBP	particle	0.0027	0.17	0.032	n.r.	n.d. - 0.56	0.066
	gas	n.r.	n.r.	n.d.		n.d. - 0.22	0.50
TCEP	particle	0.046	0.019	0.036	0.090±0.031	n.d. - 0.84	0.065
	gas	n.r.	n.r.	0.032		n.d. - 0.42	0.22
TCiPP1	particle	0.025	0.062	0.29	n.r.	n.d. - 0.66	0.49
	gas	n.r.	n.r.	0.078		n.d. – 0.25	1.00
TPHP	particle	0.0081	0.020	0.022	0.16±0.067	n.d. - 0.13	0.21
	gas	n.r.	n.r.	0.028		n.d. - 0.063	0.10
TBOEP	particle	n.r.	0.10	0.031	7.10±4.65	n.d. - 0.24	0.12
	gas	n.r.	n.r.	0.030		n.d. - 0.025	0.054
TEHP	particle	0.0051	0.012	0.0082	0.097±0.11	n.d. - 0.17	0.097
	gas	n.r.	n.r.	0.0040		n.d. - 0.013	0.0035
Av. Temp. (°C)		n.r.	-7.5	9.2	n.r.	21.6	20.6

n.r.: *not reported;* n.d.: *not detected;* [a] *total (gas+particle phase) concentrations*

4.2.1.1 Phase Partitioning Modeling

Experimentally obtained gas and particle phase OPE concentrations were also compared with the values those derived by four widely used partitioning models. Generally, performances of partitioning models are compared to experimental results in the basis of gas-particle partition coefficients, K_p ($m^3/\mu g$). Distribution of organic chemicals between the gas and particle phases in air is explained employing the K_p (Harner & Bidleman, 1998b):

$$K_p = (C_P/C_{TSP})/C_g \quad (4.29)$$

4.2.1.1.1 K_{OA} Model. Based on the assumption that the main partitioning mechanism is absorption, K_{OA} could be used to predict K_p (Harner & Bidleman, 1998b):

$$K_p = (f_{OM} MW_{OCT} \xi_{OCT}) K_{OA}/(\rho_{OCT} MW_{OM} \xi_{OM} 10^{12}) \quad (4.30)$$

where, f_{OM} is the OM fraction of TSP, MW_{OCT} and MW_{OM} are the average molecular weights of octanol and the OM (g/mol), ρ_{OCT} is the octanol density (0.820 kg/L), ξ_{OCT} is the activity coefficient of the sorbed chemical in octanol, ξ_{OM} is the activity coefficient of the chemical in the OM. Assuming that ξ_{OCT}/ξ_{OM} and $MW_{OCT}/MW_{OM} = 1$, Eq. (4.30) could be simplified to:

$$logK_p = logK_{OA} + logf_{OM} - 11.91 \quad (4.31)$$

4.2.1.1.2 Soot Model. It was suggested that besides the absorption into OM, adsorption to soot carbon in atmospheric particles could also be a significant sorption mechanism. The soot model for the particle-gas partitioning accounting for soot carbon adsorption in addition to OM absorption was developed by Dachs and Eisenreich (2000):

$$K_p = f_{OM}\frac{\xi_{OCT}}{\xi_{OM}}\frac{MW_{OCT}}{MW_{OM}\rho_{OCT}10^{12}}K_{OA} + f_{EC}\frac{a_{EC}}{a_{AC}10^{12}}K_{SA} \quad (4.32)$$

where, f_{EC} is the elemental carbon (EC) fraction in the particulate matter, a_{EC} and a_{AC} are the specific surface areas of EC and activated carbon, respectively; K_{SA} is the soot–air partition coefficient. In this model, EC and octanol represent the soot carbon in partitioning by adsorption, and OM in partitioning by absorption, respectively.

The model suggested by van Noort (2003), could be utilized to calculate the K_{SA} depending on liquid vapor pressure (P_L, P_a) and specific surface area of elemental carbon (a_{EC}, m^2/g):

$$\log K_{SA} = -0.85 \log P_L + 8.94 - \log(998/a_{EC}) \quad (4.33)$$

The a_{EC} value of 62.7 m^2/g was obtained from a previous study (Jonker & Koelmans, 2002). It was assumed that $a_{EC}/a_{AC}=1$, $f_{OM}=1.6f_{TOC}$, where f_{TOC} is the total organic carbon fraction (Dachs & Eisenreich, 2000; Ribes, Van Drooge, Dachs, Gustafsson, & Grimalt, 2003).

4.2.1.1.3 The steady-state model. The Li−Ma−Yang equation, widely used in recent studies, was also applied to particle-gas partitioning in the present study. Within this model Li, Ma, and Yang (2015), calculated the partition coefficient under steady state, K_{PS}, by accounting the wet and dry deposition of particles while exploring the particle-gas partition of PBDEs:

$$\log K_{PS} = \log K_P + \log \alpha \quad (4.34)$$

where, $\log K_P$ is the equilibrium component, expressed by Eq. (4.31), and $\log \alpha$ is the non-equilibrium component, that could be determined using Eq. (4.35):

$$\log \alpha = -(1 + 4.18 \text{ x } 10^{-11} f_{OM} \text{ x } K_{OA}) \quad (4.35)$$

Thus, there are two predicted partition coefficients: K_{PS}, when the particle-gas partitioning is in steady state but not in equilibrium, and K_P, when the particle-gas partitioning is both in steady state and in equilibrium. Eq. (4.34) shows that the equilibrium is just a particular case of the steady state when log α=0, or when the removal of the particles by wet and dry deposition could be disregarded.

4.2.1.1.4 pp-LFER model. A poly-parameter linear free energy relationship (pp-LFER) by Arp, Schwarzenbach, and Goss (2008) was also used to estimate K_p:

$$\log K_p\ (m^3/g) = sS_i + aA_i + bB_i + lL_i + vV_i + c \qquad (4.36)$$

where S_i, A_i, B_i, L_i, and V_i are the compound specific Abraham descriptors for the polarizability/ dipolarizability, electron acceptor (=H-bond donor) capability, electron donor (H-bond-acceptor) capability, logarithm of the hexadecane/air partition coefficient and McGowan volume, respectively.

Corresponding to the Abraham descriptors are the sorbent (i.e., particle) specific descriptors *s*, *a*, *b*, *l*, and *v*, along with the fitting constant, *c*. Equation (4.36) describes the absorption of nonpolar and polar semi-volatile organics to the water-insoluble OM in TSP. It was suggested that the pp-LFERs for Berlin Winter and Duebendorf Fall aerosols could represent sorption to terrestrial aerosols (Arp et al., 2008). Sorbent specific descriptors in Eq. (4.36) (*s*, *a*, *b*, *l*, *v*, and *c*.) for these pp-LFERs at 15 °C and 50% RH for Berlin and Duebendorf are 1.38, 3.21, 0.42, 0.63, 0.98, -7.24 and 1.19, 3.37, 0.03, 0.66, 0.73, -7.08, respectively (Arp et al., 2008). Compound specific Abraham descriptors (S_i, A_i, B_i, L_i, and V_i) were obtained from the UFZ-LSER database (Ulrich et al., 2017). pp-LFERs for Berlin Winter and Duebendorf Fall aerosols estimate the K_p at 15 °C. Arp et al. (2008) suggested that following relationship could be used to estimate enthalpy of particle-gas partitioning, ΔH_{ip}:

$$\Delta H_{ip} = (-0.97 \pm 0.13)\ \Delta H_{ivap} \qquad (4.37)$$

where ΔH_{ivap} is the enthalpy of vaporization. Enthalpies of vaporization determined in the present study were used to estimate ΔH_{ip} values for OPEs and to adjust their K_p values at specific sampling temperatures.

4.2.1.2 Gas-phase Fractions

In the present study f_g values for OPEs were calculated using absorption, soot, steady-state, and pp-LFERs models for winter and summer seasons. Site-specific meteorological data were obtained from General Directorate of State Meteorology. Gas-phase fractions (f_g) of OPEs were estimated as:

$$f_g = 1 - \left[\left(K_p\, C_{TSP}\right)/\left(1 + K_p\, C_{TSP}\right)\right] \quad (4.38)$$

The experimental and modeled K_P values for studied OPEs were determined utilizing Eqs. (4.29), (4.31), (4.32), (4.34), and (4.36) while gas-phase fractions were determined with Eq. (4.38). Temperature dependent K_{OA} and P_L values determined, TSP, OM, and EC contents measured in the present study were used in the calculations.

4.2.1.3 Performances of the Phase Partitioning Models

OPEs showed a wide range of phase-distribution. Some OPEs were mainly in gas (TEP) or particle-phases (T2iPPP) while others were distributed between two-phases. Similar distributions were reported recently by Wolschke et al. (2016) and Wu et al. (2020). TSP values varied between 23.6 and 191 μg/m^3 while EC and OC ranged from 0.05 to 4.22 and 5.75 to 37.1 μg/m^3 with the averages of 1.67 and 11.7 μg/m^3, respectively (Table 4.8). Fourteen-day averaged ambient air temperatures were 11.7°C for winter and 29.6°C for summer. Modeled K_P values were estimated using these parameters and temperature adjusted K_{OA} and P_L values using Eq. (4.31) for partitioning by absorption and Eq. (4.32) for partitioning by both absorption and adsorption, Eq. (4.34) for steady-state partitioning, and Eq. (4.36) for poly-parameter linear free energy relationships. Figure 4.14 compares the modeled K_P values to the experimental ones.

Table 4.8 Particulate matter characteristics for summer and winter seasons

Sample ID	Sampling Volume (m^3)	OC Conc. ($\mu g/m^3$)	EC Conc. ($\mu g/m^3$)	TC Conc. ($\mu g/m^3$)	TSP ($\mu g/m^3$)	f_{OM} (%)	f_{EC} (%)
S-1	360	14.9	1.95	16.8	191	12.4	1.02
S-2	337	7.11	1.25	8.36	40.6	28.0	3.08
S-3	350	5.75	1.10	6.85	53.1	17.3	2.07
S-4	368	8.19	1.91	10.1	121	10.8	1.58
S-5	336	9.69	0.74	10.4	38.7	40.1	1.90
S-6	343	6.61	0.05	7.22	147	7.19	0.03
S-7	365	7.12	0.88	8.00	23.6	48.4	3.74
S-8	340	8.44	1.29	9.73	72.9	18.5	1.76
S-9	343	8.38	1.22	9.59	103	13.0	1.18
S-10	353	8.74	1.42	10.2	109	12.8	1.30
S-11	324	7.96	1.16	9.12	56.8	22.4	2.04
S-12	329	7.94	1.02	8.95	91.5	13.9	1.11
S-13	364	6.29	0.84	7.13	77.0	13.1	1.09
S-14	372	7.89	1.07	8.95	61.5	20.5	1.74
Mean	**349**	**8.21**	**1.13**	**9.39**	**84.8**	**19.9**	**1.69**
Median	**346**	**7.95**	**1.13**	**9.04**	**75.0**	**15.6**	**1.66**
Std. Dev.	**14.6**	**2.10**	**0.46**	**2.34**	**44.6**	**11.3**	**0.88**
W-1	344	8.67	1.42	10.1	62.9	22.1	2.25
W-2	354	6.49	0.83	7.32	50.0	20.8	1.66
W-3	359	8.60	1.34	9.95	64.1	21.5	2.10
W-4	300	37.1	2.58	39.7	157	37.8	1.64
W-5	352	15.6	2.38	18.0	68.7	36.4	3.46
W-6	352	12.6	1.92	14.6	70.2	28.8	2.73
W-7	330	30.2	2.86	33.1	131	36.9	2.19
W-8	355	23.9	4.22	28.1	115	33.3	3.68
W-9	354	12.0	1.93	13.9	64.8	29.6	2.99
W-10	366	8.23	1.55	9.78	54.9	24.0	2.82
W-11	345	11.8	2.36	14.1	82.9	22.7	2.85
W-12	342	8.14	1.99	10.1	110	11.9	1.82
W-13	357	15.0	3.31	18.3	101	23.8	3.28
W-14	350	14.3	2.39	16.6	96.6	23.6	2.48
Mean	**347**	**15.2**	**2.22**	**17.4**	**87.7**	**26.6**	**2.57**
Median	**352**	**12.3**	**2.17**	**14.3**	**76.5**	**23.9**	**2.60**
Std. Dev.	**16.1**	**9.08**	**0.87**	**9.66**	**31.7**	**7.45**	**0.66**

S: summer, W: winter

Slopes of modeled vs. experimental K_P correlations ranged between 1.69±0.07 (steady-state) and 2.02±0.10 (pp-LFER Berlin winter). K_{OA}-, soot-based and steady-state model indicated slightly better correlations (r^2=0.65, p<0.01) compared to pp-LFER models (r^2=0.57-0.58, p<0.01). In general, all four models similarly underestimated the majority of the K_P values except for the compounds having log K_{OA} values of higher than 10. Performances of all models decreased for compounds having higher volatilities such as TEP, TnBP, and TCEP. Similarly, discrepancies between modeled and experimental values were observed in a recent study by Okeme, Rodgers, Jantunen, and Miriam (2018).

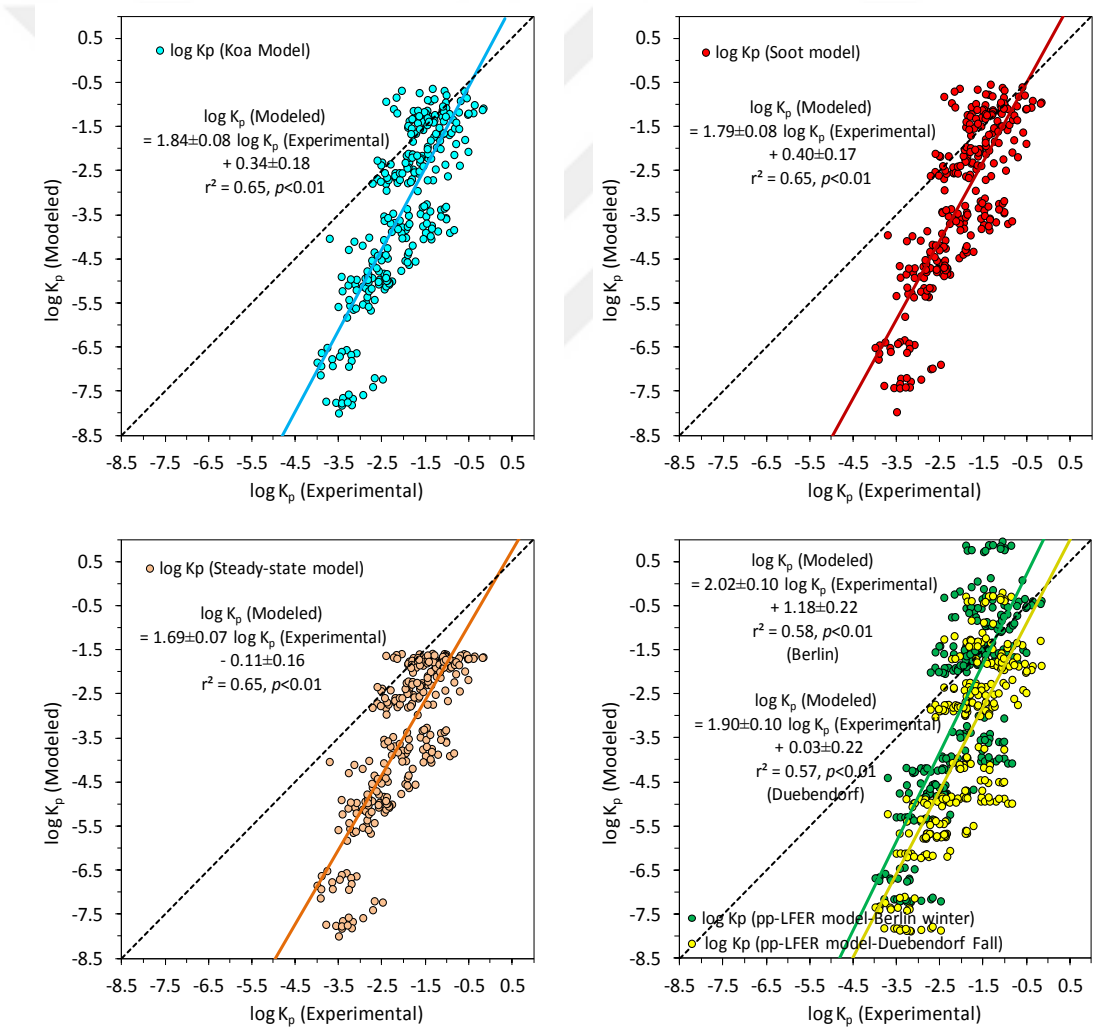


Figure 4.14 Comparison of the measured and predicted K_P values by four partitioning models. The dashed lines represent a 1:1 relationship

Figure 4.15 shows the relationship between f_g and log K_{OA} for winter and summer seasons. Generally, all models captured the observed wide range of phase-partitioning for OPEs. However, majority of models overestimated experimental f_g values, especially for compounds having lower log K_{OA}. Although most of the modeled vs. experimental f_g correlations were significant (p<0.01) with slopes close to 1.0 (except m=0.70±0.12 for the steady state model), their intercepts were >0.2 indicating that models overestimated experimental f_g values (Figure 4.16). Ratios of measured/modeled gas-phase fractions ranged from 0.35 (TCiPP2) to 2.78 (EHDPP) for soot and from 0.35 (TCiPP2) to 2.09 (TPHP) for K_{OA} model, while they ranged between 0.33 (TPHP) and 0.98 (TEP) for steady-state model. Similar K_{OA}-based model performances were reported by Suhring et al. (2016b).

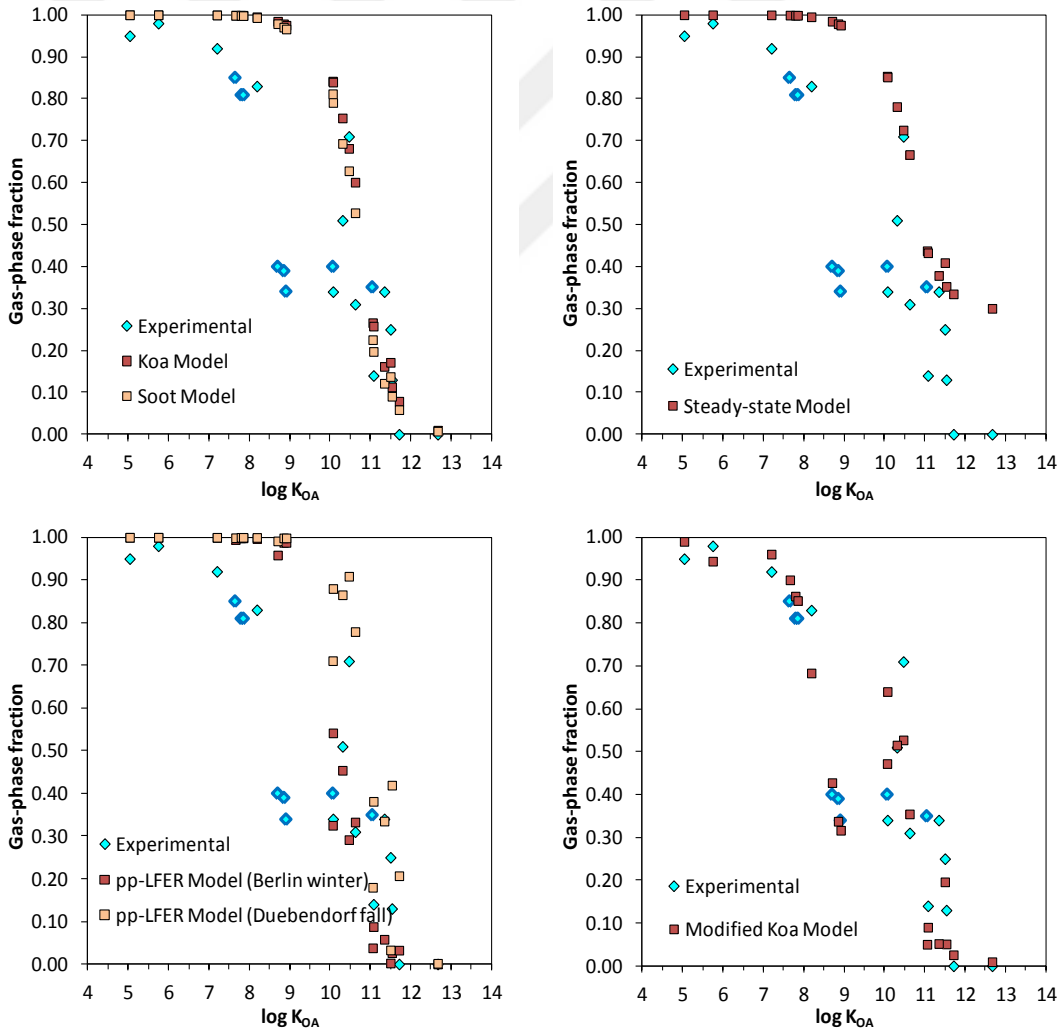


Figure 4.15 Relationship between log K_{OA} and measured/modeled gas-phase fractions. Chlorinated OPEs are shown with blue-framed markers

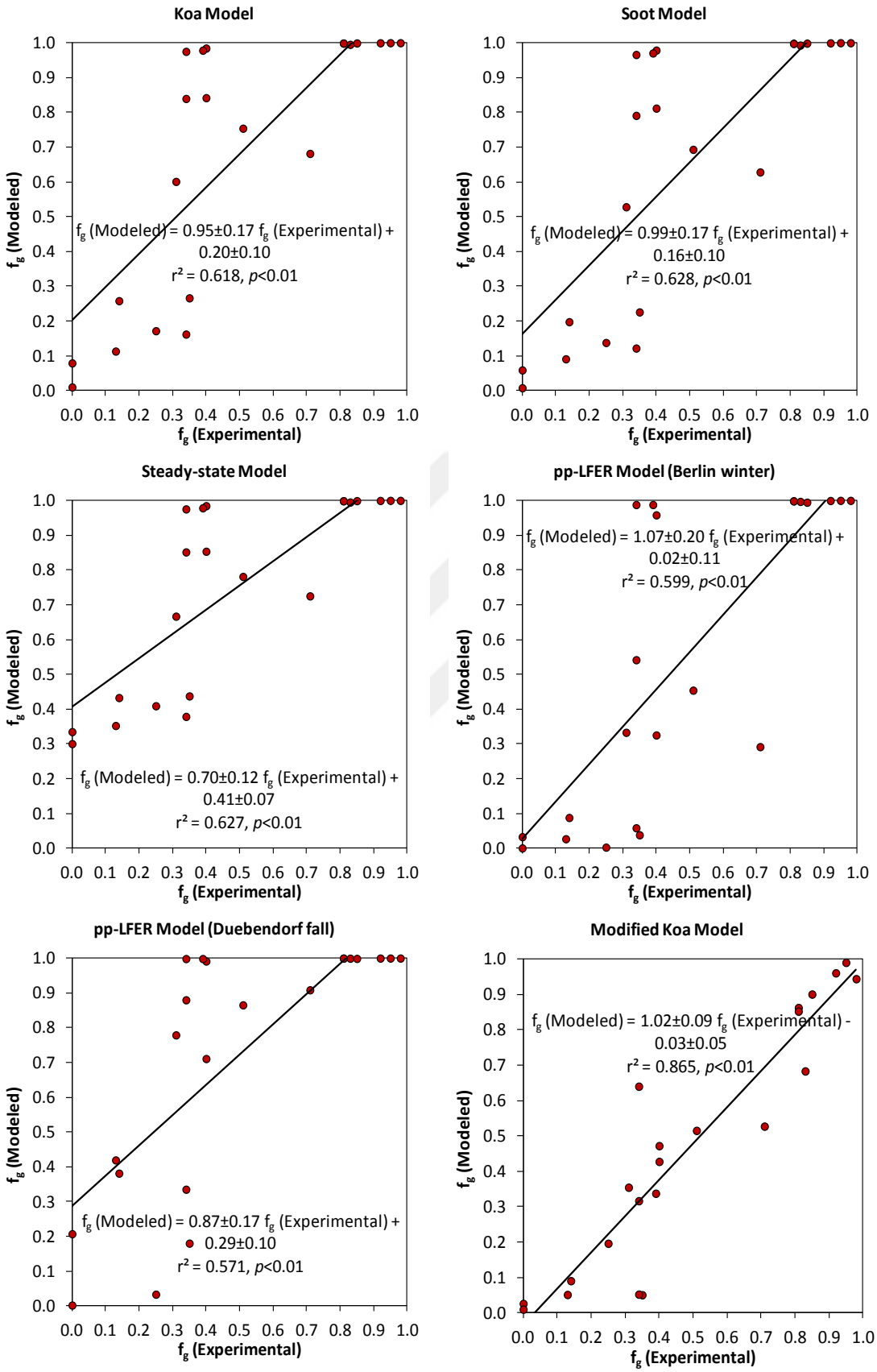


Figure 4.16 Relationships between the measured and modeled gas-phase fractions of OPEs

Ranges of ratios for pp-LFER models were 0.34 (TCiPP1)-5.86 (EHDPP) (Berlin winter) and 0.31 (TBOEP)-7.58 (T2iPPP) (Duebendorf fall). Arp et al. (2008) showed that pp-LFER models used in the present study, give better estimates for various organic compounds (PAHs, PCBs, OCPs, and *n*-alkanes) compared to K_{OA} model. However, pp-LFER models did not perform better than the others for OPEs in the present study. Similarly, Rodgers, Truong, Jantunen, Helm, and Diamond (2018) have reported that pp-LFER models overestimated f_g values for OPEs, especially for TCEP and TCiPP.

Steady-state model predicted f_g values in winter as 0.30, 0.33 and 0.38 for three compounds with the highest K_{OA} values, T2iPPP, TEHP and EHDPP, while the other two models predicted noticeably lower f_g values for these compounds, respectively. The difference can also be noticed in summer samples in a slight manner. Li et al. (2017b), implied in their study that, there are threshold log K_{OA} values (11.4 and 12.5) those affect the partitioning behavior of the compounds. Li et al. (2017b) have suggested that compounds having log K_{OA}>11.4 can be characterized as the non-equilibrium class, while the maximum partitioning occurs only for log K_{OA}>12.5. However, non-equilibrium was not observed for any of the OPEs in the present study within the log K_{OA} range of 11-12.7. Non-equilibrium seems to be a special case for PBDE-209 which has a very high log K_{OA} value of 14.98 (Cetin & Odabasi, 2008; Li et al., 2015; Li et al., 2017b).

In a recent study, f_p (particle-phase fraction) values estimated using K_{OA}-model have a positive relationship with log K_{OA} and for compounds having log $K_{OA}\geq$10.53 such as TCPs (tri-cresyl phosphate *m*, *o* and *p*) and TEHP were estimated to have particle fractions greater than 50% (Okeme et al., 2018). As in the present study, modeled f_g values were overestimated for relatively more volatile compounds while the discrepancy being the highest for TCEP and TCiPP1.

The largest overestimation for modeled gas-phase fractions was for the chlorinated OPEs (TCEP, TCiPP1, TCiPP2, and TDCiPP) (Figure 4.15). Sampling artifacts like gas-phase sorption on glass fiber filters (GFFs) may cause

overestimation of measured particle-phase fractions (and underestimation of the gas-phase fraction) and may contribute to apparent overestimation of modeled gas-phase fractions. Using a poly-parameter linear free energy relationship (pp-LFER) model, Okeme et al. (2018) estimated that 74-100% gas-phase sorption on GFFs is possible for OPEs like TCiPP1, TDCiPP, TPHP, TBOEP but not for TCEP. It was suggested that sorption on GFFs may substantially alter the observed gas-phase fractions especially for relatively volatile OPEs. However, the sorption on GFFs does not have a pronounced effect for the measured gas-phase fractions of non-volatile OPEs as they mainly exist in particle phase (Okeme et al., 2018). Thus, relatively high overestimation for modeled gas-phase fractions for most of the chlorinated OPEs observed in the present study may have been contributed by the sorption of gas phase on GFFs (Figure 4.15). However, lower gas-phase fractions for TCEP than the modeled ones remain unexplained since its sorption on GFF was estimated to be low (Okeme et al., 2018).

It was also suggested that adsorption of water vapor in air results in a water film covering the glass fiber filter surface used for particle sampling. Gas-phase OPEs may be sorbed by this water film, resulting in the overestimation of particle-phase concentrations (Okeme et al., 2018). The effect of relative humidity (RH) on the partitioning of OPEs was investigated in the present study. Particle-phase fractions generally increased with RH. However, correlations between RH and particle-phase fractions were weak (r^2=0.12-0.45) and insignificant (p>0.05), especially for TCEP, TCiPP1, TCiPP2, and TDCiPP which their particle-phase fractions were underestimated by the partitioning models. These results indicate that discrepancy between modeled and observed particle-phase fractions could not be attributed to sorption of hydrophilic OPEs in the water film covering the glass fiber filter. A recent study have also reached to the same conclusion although negative correlations were reported between RH and particle-phase fractions (Wu et al., 2020).

In addition to possible sampling artifacts, there are also some other factors affecting the discrepancy between the modeled and experimental f_g values. Arp et al. (2008) argued that the thermodynamic simplifications behind the traditionally used

single parameter (K_{OA}) models prevent them from being used for a diverse set of polar and non-polar compounds. It was suggested that the diverse specific interactions of polar compounds with OM and octanol could be somewhat different. Two basic assumptions of K_{OA} based models are ξ_{OCT}/ξ_{OM} and MW_{OCT}/MW_{OM} = 1 (Equations 4.30 and 4.31). A recent study by Yazdani, Dillner, and Takahama (2020) indicated that average MW of atmospheric OM range between 200 (rural) and 240 (urban) g/mol. Octanol has a MW of 130.23 g/mol, therefore MW_{OCT}/MW_{OM} could be ~0.54 in an urban atmosphere. Also, ξ_{OCT}/ξ_{OM} may not be equal to unity as suggested by Arp et al. (2008). ξ_{OM} is not known, however, ξ_{OCT} could be estimated from Shoeib and Harner (2002b):

$$K_{OA} = R\,T/\,\xi_{OCT}\,V_{OCT}\,P_L \qquad (4.39)$$

where R is the universal gas constant (8.314 Pa m^3/mol K), T is the temperature (K), ξ_{OCT} is the activity coefficient in octanol, V_{OCT} is the molar volume of octanol ($1.58x10^{-4}$ m^3/mol), and P_L is the supercooled liquid vapor pressure (Pa). Average activity coefficients of OPEs in octanol calculated using Eq. (4.39) ranged between 2.28±0.49 (TEP) and 8.33±0.83 (T2iPPP) at sampling temperatures of the present study (Table 4.8). Using these ξ_{OCT}, experimental f_{OM} and K_p values, and assuming an average MW of 240 g/mol for OM, ξ_{OM} values for OPEs were estimated from Eq. (4.30). They ranged between $2.67x10^{-4}$±2.85 $x10^{-4}$ (TEP) and 4.78±2.39 (T2iPPP). ξ_{OCT}/ξ_{OM} varied between 2 (T2iPPP) and 8527 (TEP) indicating that the assumption of ξ_{OCT}/ξ_{OM} = 1 is not valid, especially for volatile OPEs (Table 4.9).

f_g values were also estimated with the modified K_{OA} model using the average activity coefficients in octanol and OM calculated in the present study. Experimental and estimated f_g values agreed very well with a slope close to unity and an intercept near zero (r^2=0.865, p<0.01) (Figures 4.15 and 4.16). However, there was still some scatter between the experimental and estimated f_g values. This could be attributed to the use of average values of ξ_{OM}. However, ξ_{OM} vary among the sampling events as indicated by the large standard deviations of average values. MW_{OM} may not also be constant (240 g/mol) (Yazdani et al., 2020). This may further contribute to the

discrepancy between measured and modeled f_g values. However, MW_{OM} could not be measured easily for modeling purposes.

Table 4.9 Activity coefficients of OPEs in octanol and in organic matter in particles

	ξ_{OCT} (at 25°C)	ξ_{OCT} (at Sampling temperatures)			ξ_{OM}		
		Average	SD	RSD (%)	Average	SD	RSD (%)
TEP	2.47	2.28	0.49	21	$2.67x10^{-4}$	$2.85 x10^{-4}$	107
TnBP	3.64	3.38	0.64	19	$1.34x10^{-2}$	$1.04 x10^{-2}$	77
TCEP	3.95	3.67	0.67	18	$1.55 x10^{-2}$	$1.08 x10^{-2}$	70
TCiPP1	4.11	3.82	0.69	18	$1.52 x10^{-2}$	$1.38 x10^{-2}$	91
TCiPP2	4.16	3.87	0.70	18	$1.61 x10^{-2}$	$1.24 x10^{-2}$	77
TDCiPP	5.79	6.14	0.69	11	0.28	0.23	81
TBOEP	6.52	6.97	0.85	12	1.71	1.22	72
TPHP	6.03	6.41	0.74	12	1.03	0.34	33
EHDPP	6.12	6.53	0.77	12	1.06	0.96	91
TEHP	6.66	6.99	0.64	9	1.23	0.89	72
T2iPPP	7.90	8.33	0.83	10	4.78	2.39	50

4.2.2 Spatial and Seasonal Variations of Atmospheric OPE Concentrations

Ambient air samples representing winter and summer season conditions collected from industrial (Aliaga, *n*=14), urban (Izmir City Center, *n*=14), suburban (DEU Tinaztepe Campus, *n*=5) and rural (Bergama, *n*=5) sites were analyzed for 11 interested OPEs. Ambient air OPE concentrations C_{air} (ng/m^3) were calculated according to:

$$C_{air} = \frac{m}{V_{air}} \tag{4.40}$$

where, *m* (ng) is the OPE mass detected in PUF sampler and V_{air} (m^3) is effective air volume that sampled by PUF. In order to calculate effective air volume Shoeib and Harner (2002a) derived the following equations:

$$V_{air} = (K'_{PSM-A})\ x\ (V_{PSM})\ x\ \left[1 - exp\left(-\frac{k_A}{K'_{PSM-A}}\ x\ \frac{t}{D_{film}}\right)\right] \quad (4.41)$$

$$K'_{PSM-A} = K_{PSM-A}\ x\ \rho_{PSM} \quad (4.42)$$

where V_{PSM} is the volume (cm^3) of the PUF disk (209.5 cm^3), ρ_{PSM} is the density (g/cm^3) of the disk (0.021 g/cm^3), t is the exposure time (day), k_A is the air–side mass transfer coefficient (MTC) (cm/d), and D_{film} (m) is the effective film thickness (0.0057 m) (Pozo et al., 2004). $K_{PSM–A}$ is the passive sampling medium (PSM)–air partition coefficient which was substituted as experimental $K_{PUF\text{-}Air}$ values for 7 OPEs (TEP, TnBP, TCEP, TCiPP1, TCiPP2, TDCiPP, TBOEP) measured within this study (Section 4.1.3). For the rest 4 OPEs (TPHP, EHDPP, TEHP, T2iPPP) those could not be determined experimentally, $K_{PUF\text{-}Air}$ values determined according to Eq. (4.22) which was derived by regressing log K_{OA} values with experimental $K_{PUF\text{-}Air}$ (Figure 4.8).

k_A in Eq. (4.41) was calculated using the recovery of depuration compounds initially spiked into the PUF disks:

$$k_A = \ln\left(\frac{C_t}{C_0}\right) D_{film} K_{PSM-A} \left(\frac{1}{t}\right) \quad (4.43)$$

where, C_t and C_o (mass/cm^3) are the concentrations in the disk at the end and beginning of the sampling, respectively. Sampling rate (R, m^3/day) is calculated by Shoeib and Harner (2002a):

$$R = k_A A_{PSM} \quad (4.44)$$

where, A_{PSM} is the planar surface area (m^2) of the PUF disk. The calculated R values for winter and summer samples were 4.74 ± 1.30 and 3.13 ± 0.40 m^3/day.

Winter and summer ambient air OPE concentrations were given in Tables 4.10 and 4.11, respectively. In winter samples, total Σ_{11}OPE concentrations ranged from

0.24 to 5.41 ng/m^3 in urban site, 3.09 to 38.8 ng/m^3 in industrial site, 1.63 to 3.47 ng/m^3 in suburban site and from 1.45 to 3.88 ng/m^3 in rural site, while in summer samples ranged from 5.98 to 22.4 ng/m^3 in urban site, 6.15 to 158 ng/m^3 in industrial site, 5.60 to 8.11 ng/m^3 suburban site and from 1.36 to 3.60 ng/m^3 in rural site. Increased OPE levels during summer could be due to enhanced volatilization from their sources or terrestrial surfaces at higher temperatures. Industrial site samples contained higher levels of OPEs as can be seen in Figures 4.17 and 4.18. A remarkable increase was seen in Aliaga, sampling points Ind-5, 7, 8, 10 and 11 those nearby the iron-steel production plants and commercial ports. These plants use variety of scraps as raw material mostly originated from industrial products such as automotive, white goods, electronics and mechanics which have common OPE applications. Therefore, storage, transfer, handling, and use in iron-steel production of these scraps may have caused the elevated ambient air OPE levels in the industrial region. In urban sites, concentrations were also higher compared to suburban and rural sites. In a recent study conducted by Zhou, Hiltscher, Gruber, and Puttmann (2017) ambient air and indoor OPE concentrations were measured simultaneously in an urban site and clearly revealed that emissions from household products and materials used in indoors are a major source of OPEs to the ambient air (Saito, Onuki, & Seto, 2007; Sjodin et al., 2001) also suggested that the indoor is a considerable source for OPEs, from which the OPEs were released to the ambient air through ventilation. Nevertheless, heavy traffic in urban sites was also addressed as another OPE source by Marklund et al. (2005c).

In a recent study, Li et al. (2019) measured ambient air concentrations for 20 OPE compounds in an urban area (near Albany International Airport, Albany, NY, USA) and reported $\sum_{20}$OPE concentrations ranged between 1.32 and 20.7 ng/m^3 which is quite similar to results (ranged from 0.24 to 5.41 ng/m^3 in winter and from 5.98 to 22.4 ng/m^3 in summer) in the present study. Additionally, studies conducted in Beijing, China (1.50-5.64 ng/m^3) (Liu et al., 2016a), Rhine, Germany (mean: 5.13 ng/m^3) (Zhou et al., 2017) and Bursa, Turkey (4.51-19.1 ng/m^3) (Kurt-Karakus et al., 2018) also reported OPE concentrations within the ranges those measured in this study. However, studies reported relatively lower concentrations such as 2.29 ng/m^3

(Toronto, Canada) (Shoeib et al., 2014), 1.50 ng/m^3 (Chicago, Illinois, USA), 2.10 ng/m^3 (Cleveland, Ohio, USA) (Salamova et al., 2014b) can be also found in the literature. Atmospheric OPE levels in urban sites measured in the present study were higher than reported in another urban site, Tianjin (for $\sum_8$OPE max. 2.18±1.49 ng/m^3) (Zhang et al., 2019a), and slightly lower than reported by Ohura et al. (2006) (10.6 – 91.4 ng/m^3) in ambient air samples from house backyards.

It should be also noted researchers generally focus on well-known OPEs such as TCiPP, TCEP, TDCiPP and TnBP, whereas the targeted OPEs widely vary in both quantitative and qualitative manners within the studies which may affect the comparability of total OPE concentrations. Additionally, atmospheric concentrations reported in the literature were measured using different sampling techniques and various of analytical methods that may also explain the discrepancies. Another explanation for different values in the literature that some of the studies report only gas phase OPEs whereas the others report total (gas+particle) concentrations.

Table 4.10 Ambient air OPE concentrations (ng/m^3) in winter

Samp. Point	TEP	TnBP	TCEP	TCiPP1	TCiPP2	TDCiPP	TBOEP	TPHP	EHDPP	TEHP	T2iPPP	Σ_{11}OPE
Urban Sites												
U-1	0.15	0.17	0.084	1.41	0.47	0.066	0.32	0.088	0.34	0.039	0.0040	**3.13**
U-2	0.062	0.15	0.11	1.46	0.49	0.090	0.12	0.10	0.30	0.013	0.0047	**2.89**
U-3	0.10	0.43	0.10	1.75	0.54	0.15	0.28	0.15	1.68	0.16	0.0046	**5.37**
U-4	0.55	0.23	0.13	1.54	0.53	0.28	0.28	0.10	0.50	0.20	0.0075	**4.35**
U-5	0.43	0.61	0.086	1.52	0.52	0.083	0.12	0.13	0.34	0.010	0.0049	**3.86**
U-6	0.10	0.23	0.11	1.49	0.53	0.23	0.14	0.056	0.20	0.026	0.0037	**3.11**
U-7	0.13	0.41	0.092	0.90	0.30	0.13	0.32	0.078	0.35	0.11	0.0038	**2.81**
U-8	0.12	0.41	0.10	1.57	0.55	0.14	0.19	0.089	0.39	0.066	0.0051	**3.61**
U-9	0.17	0.26	0.16	1.84	0.53	0.12	0.33	0.11	1.79	0.11	0.0053	**5.41**
U-10	0.065	0.047	0.0034	n.d.	0.023	0.012	0.030	0.0053	0.014	0.044	0.0017	**0.24**
U-11	0.10	0.17	0.094	1.61	0.46	0.13	0.34	0.094	1.99	0.078	0.0061	**5.07**
U-12	0.13	0.21	0.078	1.84	0.71	0.10	0.21	0.093	0.41	0.089	0.0039	**3.86**
U-13	0.13	0.38	0.11	1.43	0.47	0.12	0.33	0.090	0.62	0.092	0.0050	**3.78**
U-14	0.52	0.23	0.071	1.72	0.65	0.10	0.13	0.14	0.25	0.13	0.0075	**3.96**
Avg.	**0.20**	**0.28**	**0.095**	**1.54**	**0.48**	**0.12**	**0.22**	**0.094**	**0.65**	**0.083**	**0.0048**	**3.68**
Industrial Sites												
Ind-1	0.11	0.12	0.11	2.30	0.75	0.16	0.46	0.14	2.28	0.094	0.0084	**6.53**
Ind-2	0.24	0.22	0.10	2.17	0.80	0.21	0.32	0.09	0.24	0.073	0.0045	**4.47**
Ind-3	0.27	0.24	0.11	2.80	1.10	0.22	0.44	0.09	0.29	0.10	0.0050	**5.66**
Ind-4	0.51	0.15	0.13	3.12	1.17	0.22	0.30	0.11	0.35	0.13	0.0075	**6.20**
Ind-5	7.23	0.68	0.70	18.5	6.48	0.77	1.50	0.85	0.53	1.56	0.041	**38.8**
Ind-6	0.45	0.36	0.07	2.19	0.77	0.21	0.28	0.10	0.36	0.13	0.0055	**4.93**
Ind-7	3.47	0.46	0.66	15.0	5.44	0.34	1.18	0.48	4.35	0.53	0.019	**31.9**
Ind-8	1.41	0.99	0.41	9.06	3.57	0.28	0.65	0.36	0.41	1.10	0.016	**18.3**
Ind-9	0.29	0.17	0.04	2.20	0.78	0.14	0.32	0.09	0.24	0.10	0.0076	**4.38**
Ind-10	4.40	0.52	0.45	10.9	4.13	0.37	0.92	0.35	0.36	0.58	0.018	**23.0**
Ind-11	0.16	0.22	0.13	2.37	0.81	0.22	0.27	0.14	0.55	0.14	0.010	**5.02**
Ind-12	0.18	0.32	0.12	1.95	0.72	0.12	0.46	0.15	0.32	0.84	0.0052	**5.19**
Ind-13	0.88	0.22	0.47	3.21	1.27	0.14	0.32	0.10	0.67	0.07	0.0079	**7.37**
Ind-14	0.09	0.16	0.078	1.20	0.43	0.19	0.21	0.10	0.39	0.24	0.0067	**3.09**
Avg.	**1.41**	**0.35**	**0.26**	**5.50**	**2.01**	**0.26**	**0.55**	**0.23**	**0.81**	**0.41**	**0.012**	**11.8**
Suburban Sites												
SU-1	0.12	0.17	0.12	1.17	0.43	0.24	0.20	0.18	0.77	0.074	0.0075	**3.47**
SU-2	0.081	0.19	0.11	0.86	0.32	0.14	0.091	0.049	0.33	0.042	0.0038	**2.23**
SU-3	0.084	0.12	0.094	0.59	0.23	0.058	0.076	0.043	0.29	0.034	0.0044	**1.63**
SU-4	0.069	0.10	0.10	0.77	0.28	0.23	0.076	0.049	0.33	0.11	0.0052	**2.12**
SU-5	0.10	0.091	0.088	1.02	0.35	0.22	0.17	0.12	0.49	0.10	0.0040	**2.74**
Avg.	**0.090**	**0.13**	**0.10**	**0.88**	**0.32**	**0.18**	**0.12**	**0.088**	**0.44**	**0.072**	**0.0050**	**2.44**
Rural Sites												
R-1	0.027	0.057	0.020	0.74	0.25	0.055	0.050	0.044	0.17	0.026	0.0015	**1.45**
R-2	0.039	0.076	0.015	0.79	0.29	0.065	0.078	0.047	0.16	0.024	0.0040	**1.59**
R-3	0.043	0.12	0.084	1.31	0.52	0.24	0.089	0.073	0.52	0.048	0.0053	**3.05**
R-4	0.12	0.22	0.090	1.69	0.54	0.26	0.15	0.094	0.55	0.15	0.0090	**3.88**
R-5	0.026	0.077	0.030	0.90	0.26	0.12	0.047	0.032	0.28	0.042	0.0025	**1.82**
Avg.	**0.050**	**0.11**	**0.048**	**1.09**	**0.37**	**0.15**	**0.083**	**0.058**	**0.34**	**0.058**	**0.0044**	**2.37**

n.d.: not detected

Table 4.11 Ambient air OPE concentrations (ng/m^3) in summer

Samp. Point	TEP	TnBP	TCEP	TCiPP1	TCiPP2	TDCiPP	TBOEP	TPHP	EHDPP	TEHP	T2iPPP	Σ_{11}OPE
Urban Sites												
U-1	0.18	0.15	1.75	13.0	4.78	0.67	0.18	0.56	0.27	0.25	0.006	**21.8**
U-2	0.60	0.25	0.29	2.64	0.83	0.13	0.33	0.32	0.35	0.22	0.012	**5.98**
U-3	1.14	0.82	0.50	4.71	1.61	0.46	0.97	0.58	0.84	1.00	0.029	**12.7**
U-4	1.08	0.45	0.41	3.09	0.95	0.22	0.29	0.40	0.42	0.18	0.011	**7.51**
U-5	1.46	1.42	1.04	11.1	3.68	0.76	0.69	0.64	0.73	0.82	0.011	**22.4**
U-6	3.06	1.11	0.47	6.84	2.39	0.15	0.79	0.86	1.00	0.62	0.041	**17.3**
U-7	1.26	1.19	0.32	3.02	0.93	0.30	0.40	0.30	0.37	0.13	0.019	**8.24**
U-8	0.78	0.74	0.39	7.14	2.39	0.49	0.60	0.52	0.77	0.55	0.029	**14.4**
U-9	1.11	0.42	0.33	2.73	0.84	0.26	0.62	0.54	0.69	0.29	0.0083	**7.83**
U-10	2.07	0.76	0.36	3.80	1.15	0.19	0.49	0.38	0.48	0.57	0.0070	**10.3**
U-11	0.57	0.50	0.41	5.83	2.07	0.70	0.38	0.26	0.67	0.22	0.0077	**11.6**
U-12	0.84	0.65	0.49	6.62	1.95	0.31	1.22	0.66	0.96	0.34	0.025	**14.1**
U-13	1.05	0.51	0.54	8.74	2.94	0.54	0.40	0.52	0.90	0.21	0.0052	**16.4**
U-14	1.00	0.67	0.51	12.0	4.00	0.31	0.57	0.56	0.67	1.00	0.0084	**21.3**
Avg.	**1.16**	**0.69**	**0.56**	**6.52**	**2.18**	**0.39**	**0.57**	**0.51**	**0.65**	**0.46**	**0.016**	**13.7**
Industrial Sites												
Ind-1	3.18	0.49	0.68	10.8	4.09	0.26	1.01	2.78	0.66	0.56	0.040	**24.6**
Ind-2	5.98	0.23	0.43	14.4	5.24	0.42	0.67	0.53	0.51	0.17	0.018	**28.6**
Ind-3	4.57	0.26	0.28	10.2	3.55	0.34	0.45	0.29	0.39	0.26	0.016	**20.6**
Ind-4	6.85	0.41	0.28	6.82	2.34	0.18	0.58	0.35	0.39	0.35	0.017	**18.6**
Ind-5	23.1	0.49	1.32	49.6	16.3	1.10	1.31	1.88	0.77	1.39	0.048	**97.3**
Ind-6	2.21	0.49	0.32	7.39	2.30	0.36	0.98	0.71	0.88	0.34	0.13	**16.1**
Ind-7	7.14	0.83	0.40	15.0	5.34	0.46	1.02	0.87	0.29	0.86	0.025	**32.2**
Ind-8	15.1	1.26	0.61	61.2	20.7	0.52	0.86	1.18	0.34	5.21	0.040	**107**
Ind-9	7.64	0.36	0.50	9.36	2.31	0.30	1.33	0.67	0.81	0.76	0.033	**24.1**
Ind-10	41.3	1.03	2.19	75.5	24.3	1.87	6.34	2.52	1.50	1.82	0.070	**158**
Ind-11	0.60	0.34	0.18	3.97	1.34	0.24	0.39	0.19	0.41	0.36	0.020	**8.04**
Ind-12	0.37	0.31	0.20	2.39	0.94	0.15	0.36	0.23	0.34	0.83	0.0080	**6.15**
Ind-13	0.44	0.39	0.28	2.70	0.81	0.11	0.37	0.41	0.41	0.52	0.02	**6.48**
Ind-14	0.48	0.44	0.32	2.87	0.73	0.094	0.38	0.52	0.45	0.35	0.027	**6.67**
Avg.	**8.52**	**0.66**	**0.58**	**38.7**	**12.7**	**0.46**	**1.16**	**0.94**	**0.60**	**0.97**	**0.037**	**39.6**
Suburban Sites												
SU-1	0.61	0.27	0.27	2.50	0.79	0.18	0.16	0.22	0.47	0.14	0.0058	**5.60**
SU-2	0.47	0.37	0.34	3.08	0.93	0.10	0.27	0.25	0.87	0.093	0.010	**6.77**
SU-3	0.44	0.37	0.41	4.54	1.13	0.21	0.15	0.24	0.53	0.089	0.0069	**8.11**
SU-4	1.02	0.23	0.32	3.16	0.83	0.13	0.14	0.21	0.46	0.073	0.011	**6.58**
SU-5	0.35	0.25	0.24	3.01	0.92	0.14	0.17	0.22	0.45	0.078	0.0030	**5.83**
Avg.	**0.58**	**0.30**	**0.31**	**3.26**	**0.92**	**0.15**	**0.18**	**0.23**	**0.56**	**0.094**	**0.0075**	**6.58**
Rural Sites												
R-1	0.19	0.13	0.14	1.04	0.35	0.10	0.094	0.10	0.20	0.093	0.0095	**2.46**
R-2	0.21	0.087	0.14	1.91	0.62	0.17	0.082	0.14	0.20	0.047	0.0024	**3.60**
R-3	0.059	0.065	0.084	0.54	0.22	0.10	0.029	0.05	0.17	0.035	0.012	**1.36**
R-4	0.10	0.095	0.22	1.12	0.37	0.11	0.048	0.09	0.18	0.026	0.0053	**2.36**
R-5	0.087	0.054	0.13	1.36	0.50	0.16	0.077	0.10	0.20	0.034	0.0080	**2.70**
Avg.	**0.13**	**0.086**	**0.14**	**1.20**	**0.41**	**0.12**	**0.066**	**0.10**	**0.19**	**0.047**	**0.0074**	**2.50**

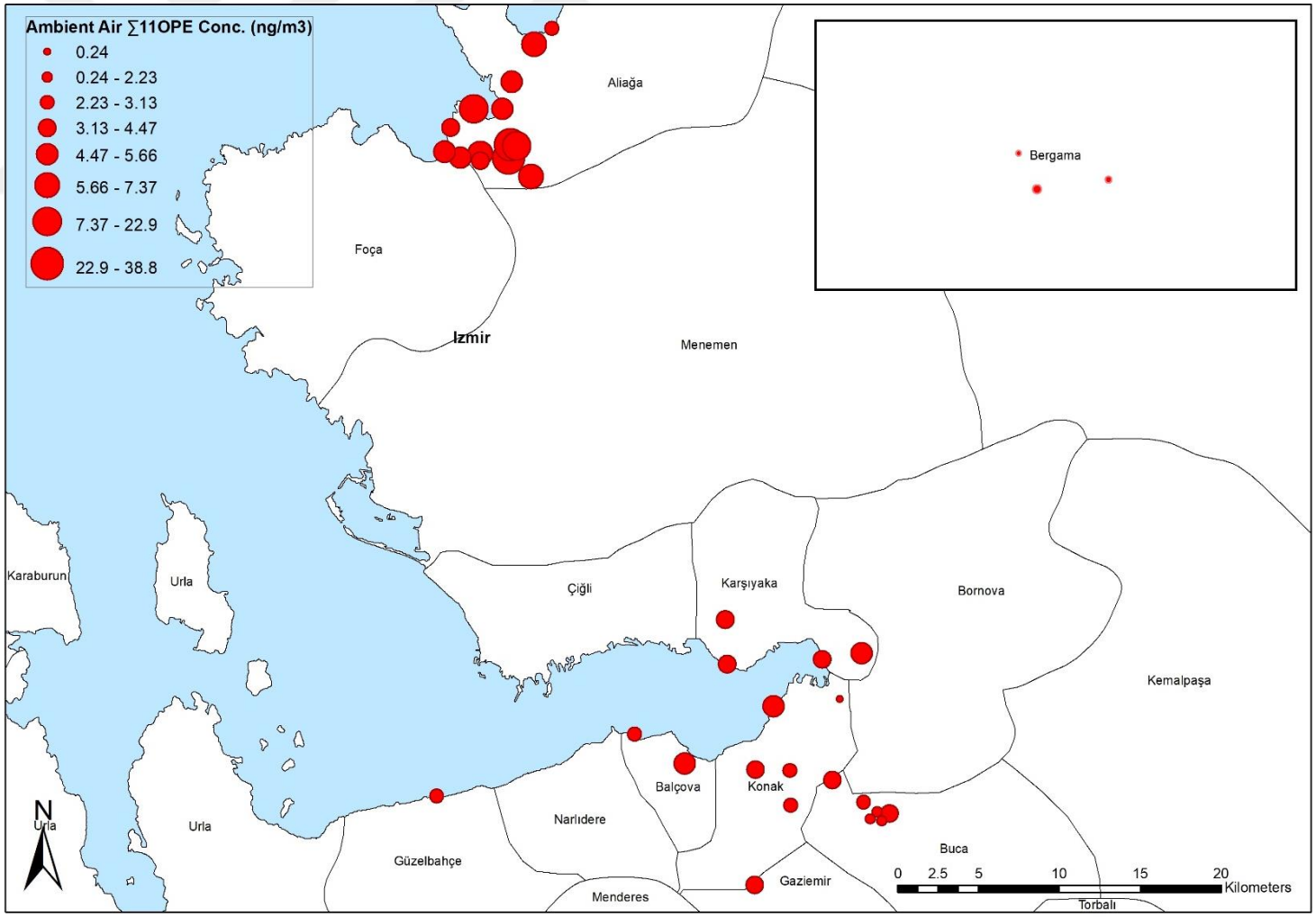


Figure 4.17 Ambient air $\sum_{11}$OPE concentrations in winter

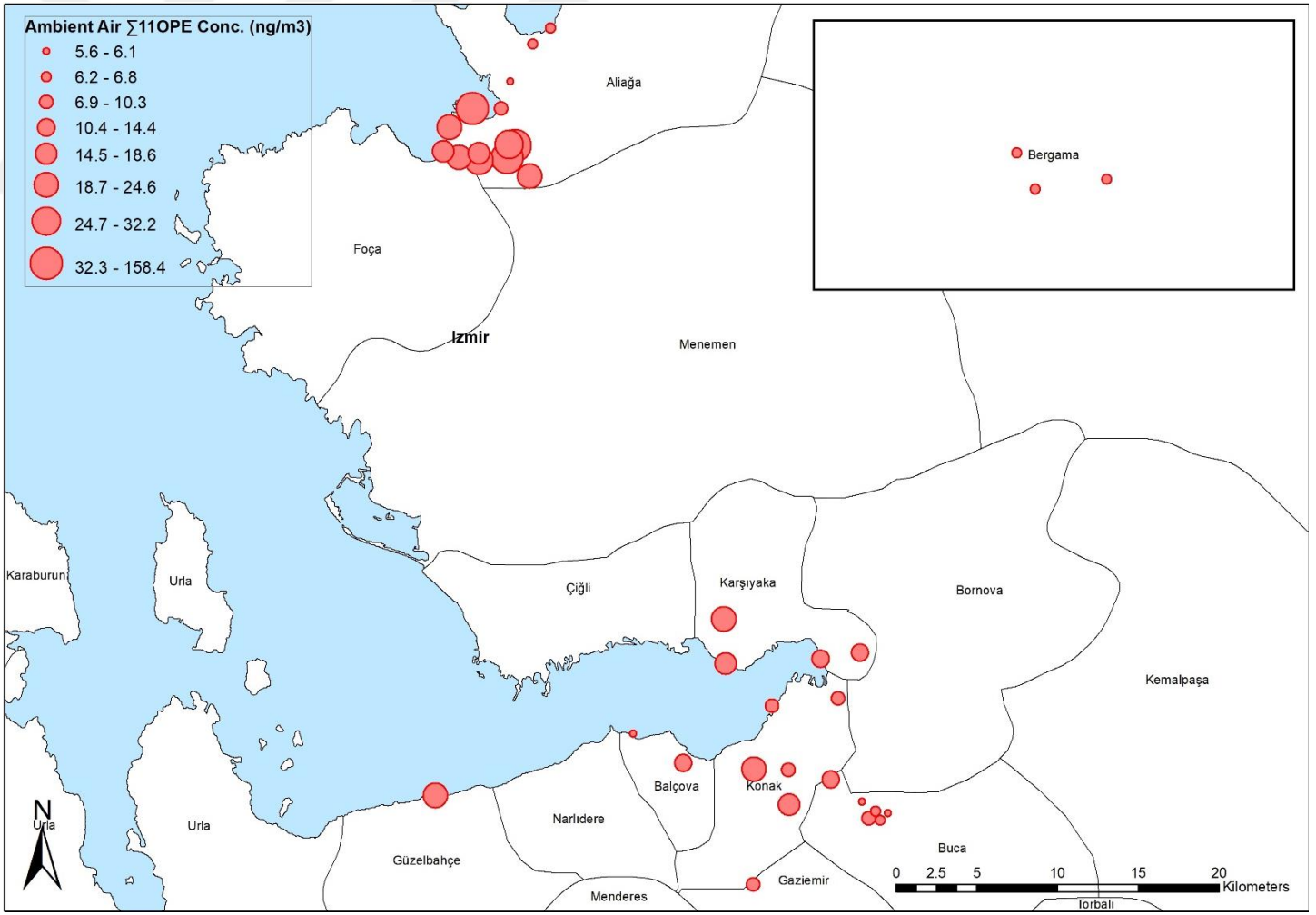


Figure 4.18 Ambient air $\sum_{11}$OPE concentrations in summer

On the basis of seasonal patterns, as the most prominent inference, Σ_{11}OPE concentrations in summer were substantially higher than those measured in winter in most of the sampling sites. The most of the organic pollutants are prone to evaporate and shift to gas phase due to increase in ambient temperatures. The map in Figure 4.19 illustrates the comparison between summer and winter OPE concentrations for the urban sites. Increased evaporation from OPE containing household and office products such as electronic, furniture, white goods, and textiles and intense ventilation of indoor air during summer may cause the observed increase in OPE concentrations in urban sites. Additionally, hydraulic fluids, engine oils and interior trims of vehicles in use and also small and medium sized workshops are thought to be other urban sources (Li et al., 2018; Marklund et al., 2005c; Reemtsma et al., 2008). Industrial site seasonal comparisons were also depicted in Figure 4.20 showing a significant increase of Σ_{11}OPE concentrations in summer, similar to urban sites. In consistence with the present study, Wu et al. (2020) reported that total atmospheric OPE concentrations in summer samples (at 16.2 and 21.6°C) were up to 5 times higher than in winter (at -3.9 and -2.5°C). Average summer/winter ratio of for 38 sampling points was calculated as 4.20 (±6.58) in the present study. Although similar seasonal patterns were pointed out in most studies (Ohura et al., 2006; Saini et al., 2019b; Salamova, Peverly, Venier, & Hites, 2016), some researchers did not report any temperature dependencies (Shoeib et al., 2014). As detailed in Section 4.2.1, in the active sampling site located in Izmir City Centre, a strong positive correlation (r^2=0.32-0.62, p<0.01) was observed between gas phase concentrations and ambient air temperatures except the three highly non-volatile OPEs (EHDPP, TEHP, and TPHP).

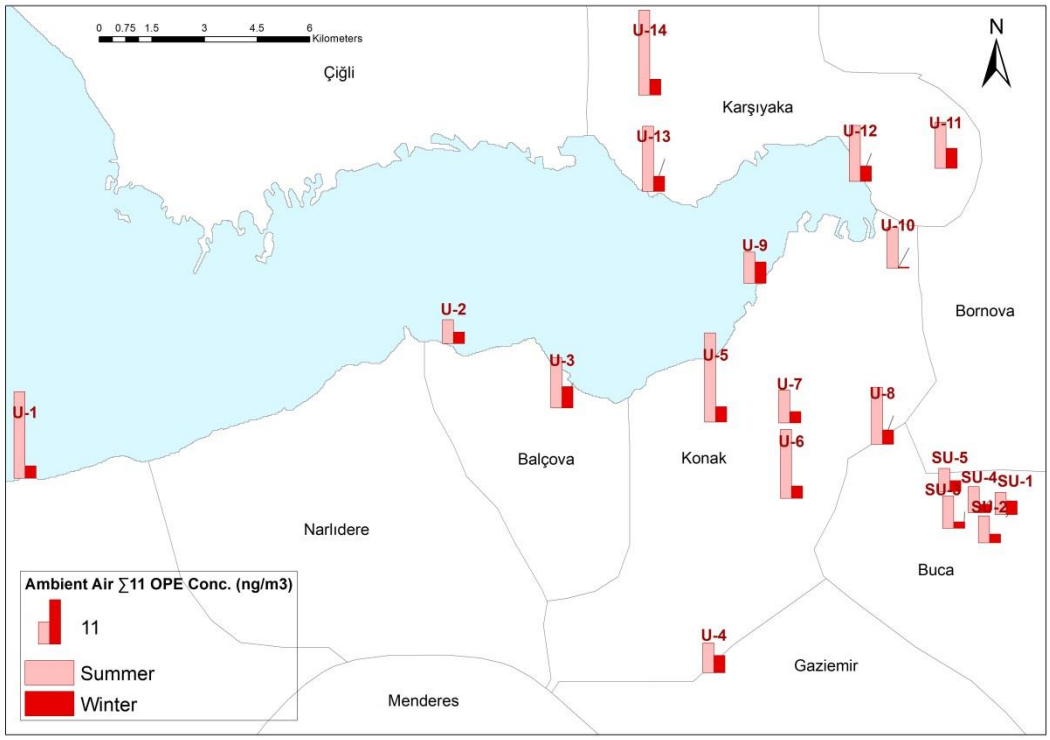


Figure 4.19 Seasonal variations of ambient air OPE concentrations in urban and suburban sites

In the basis of compound-specific contributions, TCiPP1 and TCiPP2 were the most abundant OPEs in all sampling sites and in both seasons. According to averaged concentrations of each four regions (urban, suburban, rural, and industrial), TCiPP1 had contributions more than 36% and 48% for winter and summer seasons, respectively. TCiPP2 was also not less than 9% in any of the sampling sites in both seasons. Another frequently detected chlorinated OPE, TCEP, did not contribute more than 10% any of the sampling sites, whereas contributions of TDCiPP were within the range of 0.49 to 10.9%. On the other hand, T2iPPP was the lowest contributing OPE in all samples. TEP was prominent in Aliaga samples in both seasons, suggesting that this compound may be specifically originated from industrial activities in the region. Additionally, EHDPP was prominent in winter samples. Further details on compound-specific contributions were illustrated for winter and summer seasons in Figures 4.21 and 4.22, respectively.

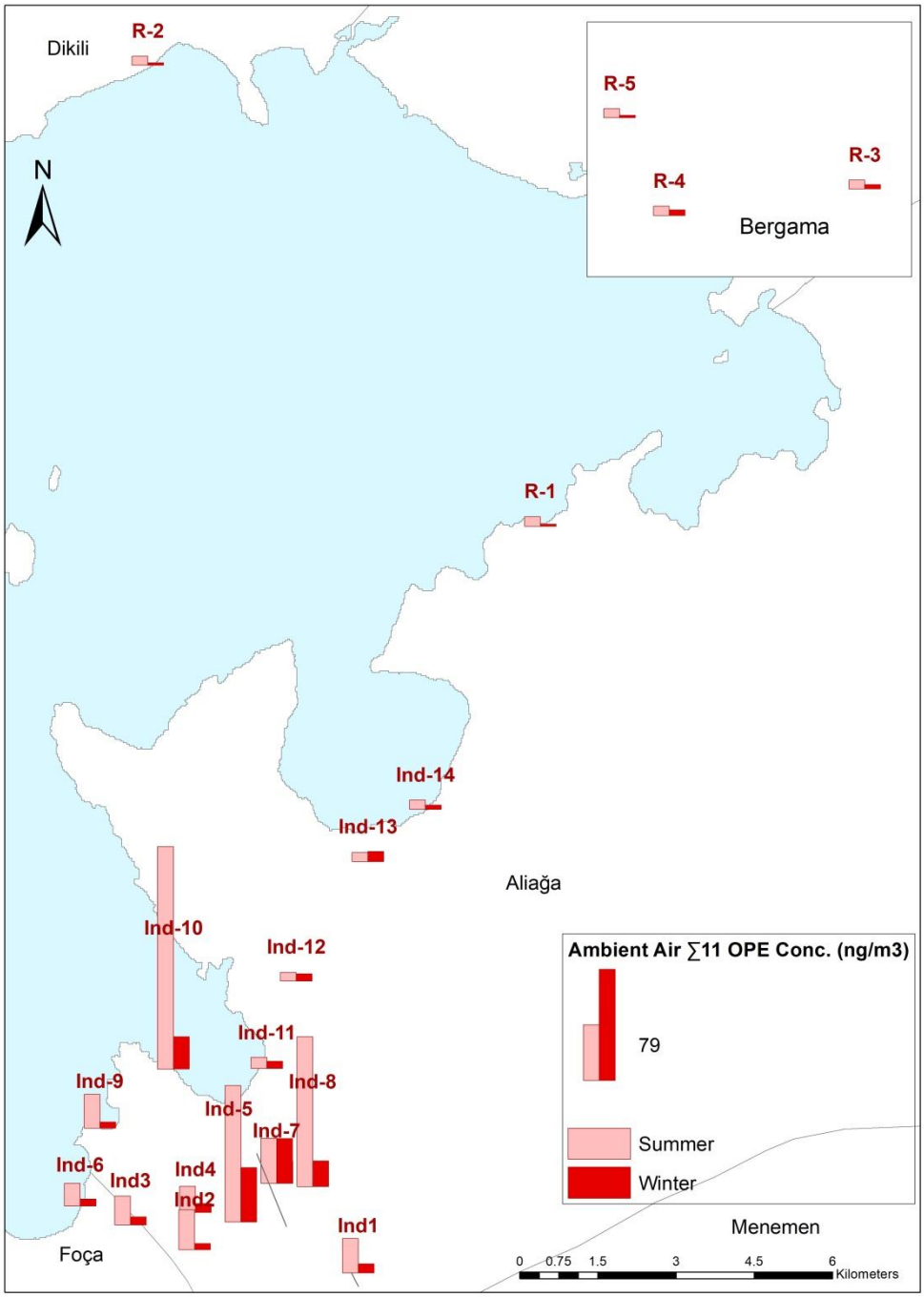


Figure 4.20 Seasonal variations of ambient air OPE concentrations in industrial and rural sites

TCiPP (sum of isomers TCiPP1 and TCiPP2), TBOEP, TCEP and TPhP were reported as the most predominant OPEs in ambient air samples (Kurt-Karakus et al., 2018; Li et al., 2019; Zhang et al., 2019a). For instance, TCiPP, which was measured as 8.70 ng/m^3 (mean of summer season in urban site) in the present study, was also reported by Li et al. (2019) and Zhou et al. (2017) at increased levels of MDL-

6.15 ng/m^3 and 2.66±3.37 ng/m^3, respectively. This compound was also noticed as the most abundant OPE by Liu et al. (2016a) contributing to 78±9% of total OPE concentrations, while the abundance of TCiPP1+TCiPP2 was calculated more than %64 (overall) in the present work. In another study, Zhang et al. (2019a) measured TCEP concentration with a mean of 0.45±0.48 ng/m^3 in Beijing, China which is quite similar to TCEP level of 0.56±0.39 ng/m^3 (mean of summer season in urban site) observed in the present study. Although TCEP had been used as the primary FR additive in many industrial applications until early 1990s, it has been replaced by TCiPP during the last three decades (Suhring et al., 2016a), especially in EU, because of its potential toxic and carcinogenic effects. Low TCEP and high TCiPP levels detected in the present study were mostly in agreement with the literature data. The most common usage of TCiPP is as additive during the production of PUF used for building roof insulation and applications in acrylic resins, adhesives, and acoustic coatings. Therefore, TCiPP detected as the predominant FR chemical in urban areas by most of the researchers (Wang et al., 2020; Wong, de Wit, & Newton, 2018; Zhou et al., 2017). The other chlorinated OPE, TDCiPP, were also measured in the comparable ranges with previous reports (Wang et al., 2020; Zhang et al., 2019a). As an aryl-OPE, TPhP is an important plasticizer being used in PUFs, PVC/ABS plastics and nail polish. TPhP was detected as another prominent OPE in most studies and it was measured as 0.36 ng/m^3, slightly higher than those reported as 0.16 ng/m^3 (annual average) and 0.15±0.11 ng/m^3 by Zhang et al. (2019a) and Kurt-Karakus et al. (2018), while it was lower than 0.49 ng/m^3 (median of n=24) measured by Li et al. (2019). However, its 76-sample-averaged contribution to Σ_{11}OPE concentrations was only 3.13% in the present study. The other aryl-OPE, EHDPP, having similar production purposes with TPhP, detected at higher concentrations ranging between 0.0014 and 4.35 ng/m^3 with a median of 0.41 ng/m^3. Although EHDPP concentrations were relatively higher in industrial sampling sites in winter, contributions to total OPEs were higher in urban, suburban and rural sites, especially in winter. The highest EHDPP concentration, 4.35 ng/m^3 was seen in Ind-7 sampling site located near a coal storage facility, where PUF sampler collected significant amount of particulate matter. EHDPP is a strongly particulate-bonded compound and it has a modeled gas phase concentration of 0.015 ng/m^3, in this sampling site. The

last aryl-OPE, T2iPPP was detected in relatively low levels and did not contribute more than 0.88% in any of the samples. T2iPPP was also reported with the lowest detection frequency by Kurt-Karakus et al. (2018). Alky-OPEs are mostly used as plasticizers in polymers, rubbers, plastics and vinyl-resins (Bjorklund et al., 2004; Saito et al., 2007). TEP was predominant alkyl-OPE with the determined ambient air concentrations ranging between 0.026 and 41.3 ng/m^3. TEP seemed to be related with industrial activities, as it has overall averaged concentrations of 4.95±8.81 ng/m^3 in industrial samples, whereas 0.68±0.70 ng/m^3 in urban site samples. However, Zhou et al. (2017) did not detect this compound in ambient air samples, while Li et al. (2019) reported comparable levels (<MDL-0.54 ng/m^3) with the present study in an urban site. Since TEP is highly volatile, a dramatic increase was observed in summer concentrations while the average value of summer/winter ratios of concentrations measured in 38 sampling points was 8.93. The abundances of the rest three alkyl-OPEs were decreased as follows; TBOEP>TnBP>TEHP, while the same order was also reported by Li et al. (2019).

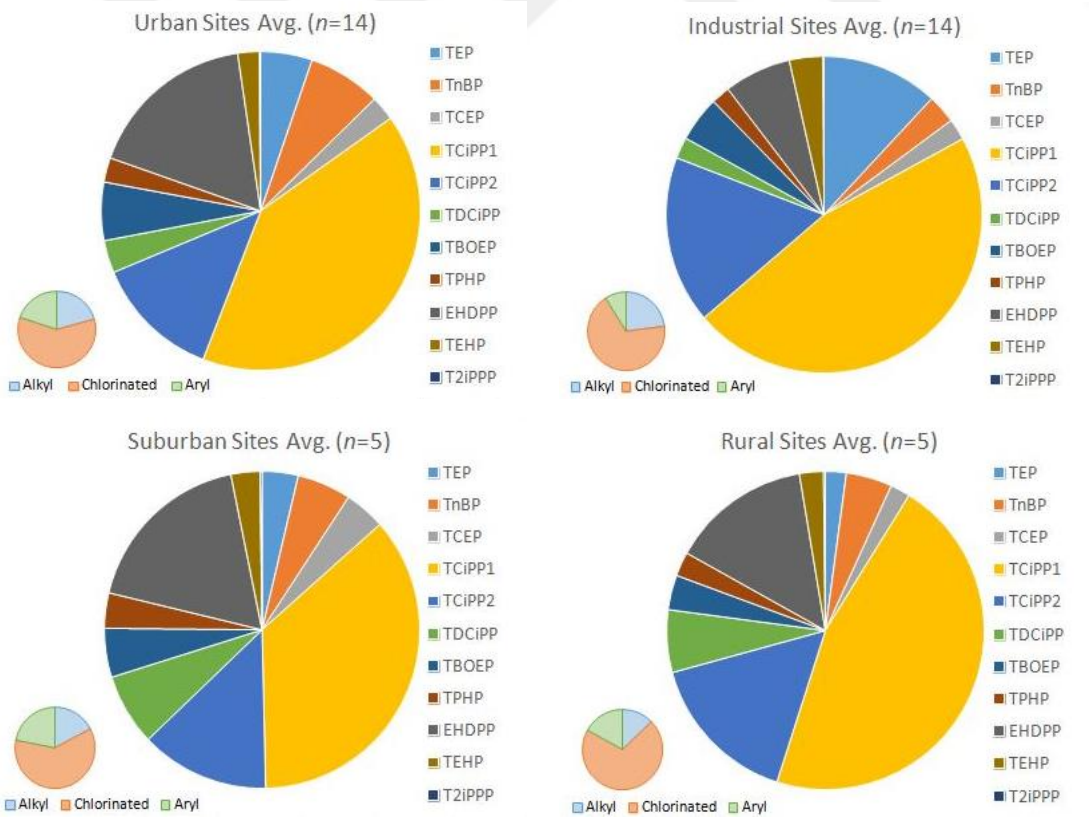


Figure 4.21 Compound-specific compositions in winter

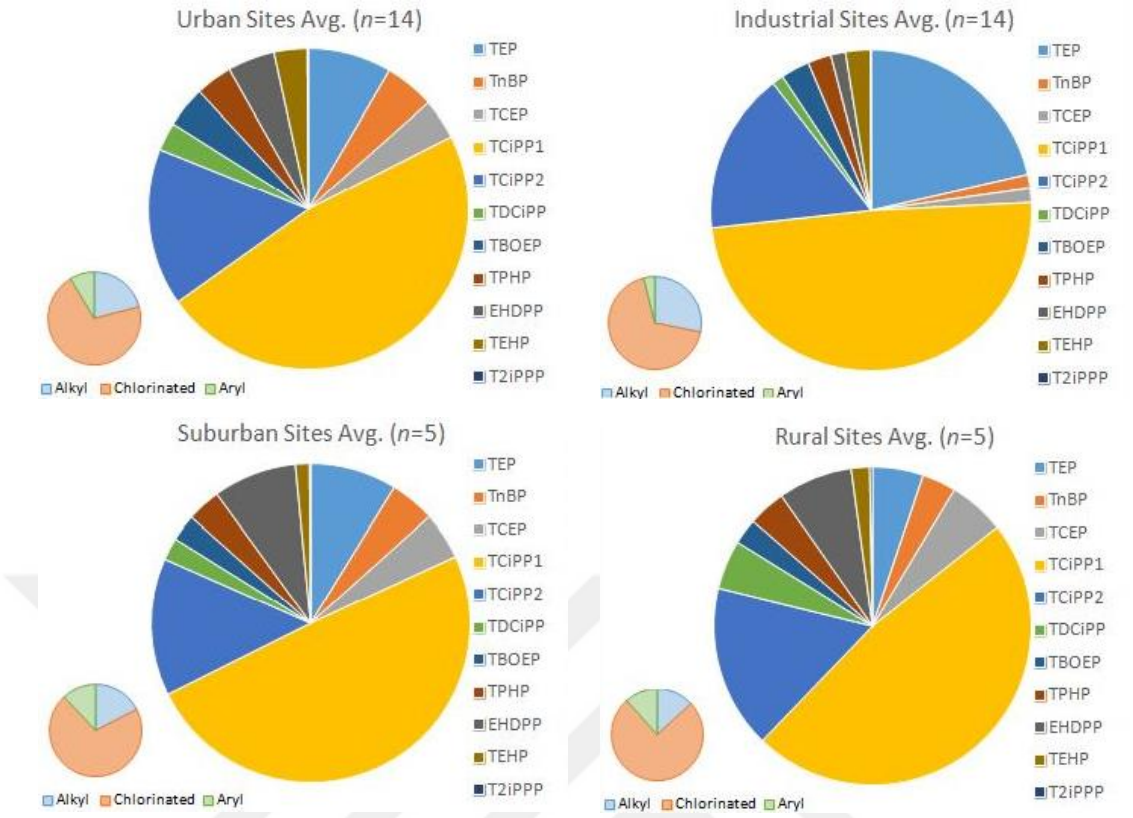


Figure 4.22 Compound-specific compositions in summer

Since they have large production volumes, wide fields of usage and include halogen atoms, chlorinated OPEs are one of the most abundant OPE congeners measured in significant amounts in environmental samples. In most studies alkyl and aryl-OPEs were detected in lower levels compared to chlorinated OPEs. Additionally, Niu, Zhang, Li, He, and Zhang (2019) noted that aryl-OPEs were more prone to degradation in the environment which may also reduce their environmental levels. Generally, compound-specific patterns evaluated in the present study were notably comparable with the related studies. According to current knowledge, OPEs are not produced in Turkey (Civan, 2016; NIP, 2014). Observed similarities on measured levels and detected OPE congeners probably caused by imported finished consumer goods, raw materials, and ferrous scraps from foreign countries.

In order to investigate possible sources of OPEs in ambient air, a Principal Component Analysis (PCA) was applied. Three principal components (PC1, PC2, and PC3) were obtained from PCA using eigenvalues >1.0 and applying Varimax

rotation. These components were accounted 85.2% of the total variances. PC1 accounted 53.1% of total variances and dominated by 8 of the 11 investigated OPEs. PCA loadings were depicted in Figure 4.23 and also tabulated in Table 4.11. The four chlorinated OPEs and TEP, TBOEP, TPhP, and T2iPPP were associated with PC1. Especially, chlorinated OPEs TCEP, TCiPP1 and TCiPP2 have similar loadings probably due to their co-application and/or replacement of TCEP by TCiPP. These findings were quite similar with those reported by Wang et al. (2020) in ambient air samples from Dalian, China. They also evaluated that nine of the 10 covered OPEs were gathered together in PCA loading plot whereas TEHP was seemed to have a different source, as in the present study. Additionally, Zhou et al. (2017) illustrated that TCEP, TEP and TDCiPP might be emitted from the same sources in indoor air as these compounds generally used in renovated building materials (i.e. acoustic ceilings and insulation hard foams). Similarly, TCEP, TEP and TDCiPP also loaded in the same component (PC1) in the present study, whereas atmospheric levels of these compounds, especially TEP, were higher in industrial sites where the residential buildings rarely located, rather than urban sites. PCA loading plots, shared by Zhou et al. (2017) indicating that OPEs originated from more variable sources in indoor air. It should be noted that, indoor air, as a more conservative and small-sized medium that includes the primary sources and thus, might be more indicative to evaluate OPE sources. PC2 was primarily associated with TnBP and TEHP with the loadings of 0.84 and 0.83, respectively. Although the field of usages of TEHP (in PVC, PUF, rubber and polymers) and TnBP (as anti-foaming agent in hydraulic fluids, glues and motor oils) are different, they might be emitted from the same sources, which contain these materials together such as motor vehicles. Therefore, PC2 might be regarded as traffic sources. The last component, PC3 was only loaded by EHDPP with a rate of 0.96, which is also a plasticizer with a wide field of usage, especially in food packaging. Considering the high contributions of EHDPP to total OPE concentrations in non-industrial sites, PC3 may be related to urban sources rather than the industrial activities.

Table 4.12 PCA results for OPEs in air samples

	Principal Component		
	PC1	**PC2**	**PC3**
TEP	0.92		
TnBP		0.84	
TCEP	0.83		
TCiPP1	0.84		
TCiPP2	0.83		
TDCiPP	0.89		
TBOEP	0.87		
TPHP	0.76		
EHDPP			0.96
TEHP		0.83	
T2iPPP	0.72		
% Variance	53.1	22.3	9.9
% Cumulative	53.1	75.3	85.2

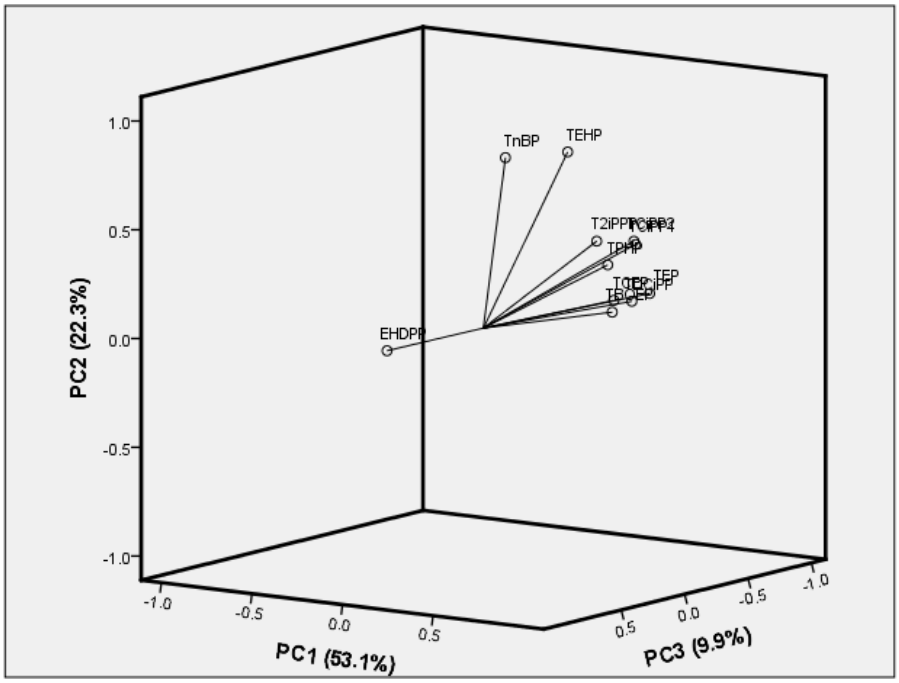


Figure 4.23 PCA loading plot for air samples

4.2.3 Spatial and Seasonal Variations of Soil OPE Concentrations

Collected soil samples from four sampling regions and for two seasons were extracted and analyzed for 11 OPE compounds. Determined concentrations were tabulated in Table 4.13 and 4.14 while spatial variations of these concentrations were

illustrated in Figures 4.24 and 4.25. In winter samples, $\sum_{11}$OPE concentrations averaged for 14 urban, 14 industrial, 5 suburban, and 5 rural sampling sites were 103, 766, 45.5, and 73.6 ng/g, respectively. Average concentrations in summer at these sampling sites were 119, 608, 40.6, and 22.4 ng/g, respectively. Similar to ambient air samples, soil samples collected in the industrial region had significantly higher OPEs levels compared to other sampling sites. Especially, Ind-5, 7, 8 and 10 sampling sites with elevated atmospheric OPEs, also had higher soil concentrations. This may indicate that certain industrial activities in the region (such as scrap processing steel plants) may be important OPE sources. Additionally, high sample concentrations were measured during winter and summer in urban sites (U-5 ,6, 10, 12) that were located in densely populated areas with heavy traffic. The ratio of average industrial/urban soil concentrations ranged from 2.99 (TDCiPP) to 30.6 (TEP) in winter, and from 2.07 (EHDPP) to 10.9 (TCEP) in summer samples. Summer/winter ratios of $\sum_{11}$OPE concentrations also ranged between 0.22 (U-7) and 3.03 (U-6) in urban sites and between 0.23 (Ind-11) and 4.27 (Ind-1) in industrial sites.

The number of studies soil levels of OPEs are still scarce. Reported soil OPE concentrations in such studies also vary with the characteristics of the sampling sites and possible local sources in the studied regions. For instance, Li et al. (2019) analyzed 24 soil samples collected from an urban site for 20 OPE species and determined $\sum_{20}$OPE concentrations ranged between 1.16 and 73.1 ng/g, comprising mainly by chlorinated OPEs (Cl-OPEs, <MDL-54.5 ng/g), aryl-OPEs (0.78-32.7 ng/g), and alkyl-OPEs (0.07-6.57 ng/g). In the present study, 28 urban-site soil samples (winter and summer) contained higher OPEs ranging from 22.9 to 515 ng/g comprising 15.4-482 ng/g of Cl-OPEs, 3.56-26.7 ng/g of alkyl-OPEs and 0.79-19.3 ng/g of aryl-OPEs. Higher global production rates (i.e. TCiPP:40,000 tons/year) (van der Veen & de Boer, 2012) and more persistent properties of Cl-OPEs (Cristale et al., 2017; Liang & Liu, 2016; Regnery & Puttmann, 2010a; Su, Letcher, & Yu, 2016) than aryl- and alkyl-OPEs explain high concentrations of these compounds found in soils. Wang et al. (2019) determined OPE levels in 98 soil samples (mostly urban and industrial) within a nationwide survey and also reported similar results

from 4.50 to 430 ng/g, while Cl-OPEs dominated the compositions, ranging between 1.15 and 420 ng/g. In another study, Kurt-Karakus et al. (2018) analyzed OPE contents of soil samples from eight different (including urban, rural, industrial, background areas) sampling sites and measured total OPE concentrations ranging between 37 and 468 ng/g. They also put forward that alkyl-OPEs were dominated five of the eight sampling sites, while Cl-OPEs were prominent in two sites. However, Cl-OPEs dominated all sampling sites and contributed more than 73% in the present study. Although the OPE amounts in non-industrial site soil samples in the present study were mostly comparable with the literature, industrial soil samples showed relatively much higher OPE levels than previous studies. The overall range of soil OPE concentrations of the present study was as wide as 16.3 ng/g (a rural sampling site in summer) - 3,328 ng/g (an industrial sampling site in winter). A wider range (25-27,900 ng/g) for $\sum_8$OPE was also reported by Yadav, Devi, Li, and Zhang (2018). Nevertheless, there are a few studies reporting very high OPE concentrations in soil from e-waste processing site (Matsukami et al., 2017) and unexpectedly low concentrations even in soil samples close to an OPE production plant site (Ren et al., 2019).

Table 4.13 Soil OPE concentrations (ng/g) in winter

Samp. Point	TEP	TnBP	TCEP	TCiPP1	TCiPP2	TDCiPP	TBOEP	TPHP	EHDPP	TEHP	T2iPPP	Σ_{11}OPE
Urban Sites												
U-1	0.7	2.1	0.7	29.5	9.5	2.5	1.1	0.6	5.4	1.1	0.2	**53.4**
U-2	1.0	2.2	1.2	54.3	14.1	3.1	3.5	0.6	10.2	1.5	0.2	**92.0**
U-3	0.4	0.9	0.7	63.8	16.5	6.5	5.1	0.4	6.4	0.9	0.2	**102**
U-4	0.81	3.60	1.31	16.0	5.75	1.18	1.96	0.45	5.29	0.80	0.14	**37.3**
U-5	4.4	5.4	3.4	63.5	21.9	6.6	6.1	1.7	15.5	2.8	0.4	**132**
U-6	2.87	5.43	2.93	94.3	32.6	7.71	7.34	3.41	9.91	3.34	0.30	**170**
U-7	1.1	4.4	1.9	106	35.1	3.8	8.8	0.6	3.2	6.8	0.2	**172**
U-8	2.5	5.9	2.6	46.7	14.3	3.0	11.4	3.0	15.4	5.0	0.8	**110**
U-9	0.79	1.14	0.73	26.5	9.56	1.13	4.57	0.31	0.38	0.62	0.10	**45.8**
U-10	2.6	3.6	0.8	89.6	26.6	4.1	10.1	1.6	10.5	4.0	0.3	**154**
U-11	1.2	2.3	0.4	10.0	3.5	1.4	2.6	0.9	7.6	1.6	0.2	**31.7**
U-12	1.7	2.4	1.5	88.3	23.2	6.9	6.8	1.1	9.2	2.0	0.2	**143**
U-13	0.9	2.9	1.2	51.6	14.0	1.9	3.2	0.8	10.7	1.7	0.3	**89.1**
U-14	1.5	3.2	2.2	71.1	22.0	2.6	3.4	1.0	3.7	2.0	0.3	**113**
Avg.	**1.6**	**3.2**	**1.5**	**58.0**	**17.8**	**3.7**	**5.4**	**1.2**	**8.1**	**2.4**	**0.3**	**103**
Industrial Sites												
Ind-1	2.64	7.26	3.04	59.8	13.8	3.04	9.93	1.41	12.5	3.83	0.32	**118**
Ind-2	19.6	15.3	7.85	179	70.2	3.99	14.3	4.84	17.6	11.3	0.45	**344**
Ind-3	1.67	5.23	1.06	17.5	6.27	1.51	7.18	1.32	9.12	5.33	0.70	**56.9**
Ind-4	9.15	6.18	2.95	76.9	29.4	2.89	6.78	1.87	12.0	3.00	0.40	**152**
Ind-5	196	36.8	87.1	1,869	686	62.9	124	92.0	49.1	122	2.97	**3,328**
Ind-6	4.82	12.3	6.38	64.2	26.6	3.19	11.7	1.94	17.7	6.71	0.37	**156**
Ind-7	205	81.2	67.6	1,385	504	24.7	189	16.2	22.0	40.7	1.25	**2,536**
Ind-8	12.8	28.6	10.9	216	91.8	4.00	28.6	21.6	10.3	15.9	0.53	**441**
Ind-9	9.11	8.70	4.67	80.9	24.9	2.74	9.18	2.11	6.20	2.62	0.46	**152**
Ind-10	186	8.31	121	1,556	566	19.5	29.6	37.5	10.0	15.1	2.20	**2,551**
Ind-11	21.3	11.5	15.8	273	118	17.5	17.8	3.30	17.9	14.7	0.48	**512**
Ind-12	2.61	25.8	4.44	41.7	15.2	4.65	10.2	3.08	18.6	16.4	0.65	**143**
Ind-13	12.8	38.4	4.53	56.7	23.9	2.60	14.8	2.10	13.0	6.43	0.69	**176**
Ind-14	1.84	7.50	2.49	20.6	6.23	2.49	5.20	1.80	10.1	3.01	0.34	**61.7**
Avg.	**49.0**	**20.9**	**24.3**	**421**	**156**	**11.1**	**34.2**	**13.6**	**16.1**	**19.0**	**0.84**	**766**
Suburban Sites												
SU-1	1.16	2.80	0.97	13.4	4.82	1.46	2.49	0.54	7.07	0.89	0.15	**35.8**
SU-2	1.03	1.36	1.04	7.77	2.52	0.82	3.76	0.77	7.32	1.42	0.21	**28.0**
SU-3	0.75	2.25	2.40	13.6	4.98	1.32	2.36	0.94	6.41	1.39	0.20	**36.6**
SU-4	0.83	1.23	1.17	21.4	6.00	1.45	1.60	0.83	9.87	1.96	0.15	**46.5**
SU-5	1.03	2.30	1.23	44.9	15.2	3.75	3.04	0.59	7.11	0.97	0.11	**80.3**
Avg.	**0.96**	**1.99**	**1.36**	**20.23**	**6.71**	**1.76**	**2.65**	**0.73**	**7.55**	**1.33**	**0.17**	**45.4**
Rural Sites												
R-1	0.79	1.16	1.10	30.8	7.11	1.10	1.10	0.33	7.03	1.29	n.d.	**51.8**
R-2	3.13	2.00	30.68	85.2	31.4	4.00	2.84	1.12	12.8	2.51	n.d.	**175**
R-3	0.46	0.96	0.46	31.4	6.26	1.21	1.02	0.46	7.56	1.38	n.d.	**51.1**
R-4	0.67	0.79	0.67	22.5	5.70	0.94	0.82	0.44	6.87	0.56	n.d.	**40.0**
R-5	0.89	2.21	1.21	26.0	7.60	1.28	1.33	0.43	7.74	0.82	n.d.	**49.5**
Avg.	**1.19**	**1.43**	**6.82**	**39.17**	**11.62**	**1.71**	**1.42**	**0.56**	**8.40**	**1.31**	**0.00**	**73.6**

n.d.: not detected

Table 4.14 Soil OPE concentrations (ng/g) in summer

Samp. Point	TEP	TnBP	TCEP	TCiPP1	TCiPP2	TDCiPP	TBOEP	TPHP	EHDPP	TEHP	T2iPPP	Σ_{11}OPE
Urban Sites												
U-1	0.51	2.14	0.52	50.5	19.3	1.11	2.61	0.52	1.06	1.24	0.17	**79.7**
U-2	0.65	1.15	2.06	10.9	2.79	1.15	1.07	0.39	1.21	1.34	0.18	**22.9**
U-3	2.23	2.30	1.43	22.9	8.60	1.42	1.66	1.21	1.32	0.56	0.11	**43.7**
U-4	3.19	1.63	2.36	29.3	9.86	0.83	0.69	0.79	1.17	2.31	0.17	**52.3**
U-5	2.63	1.70	1.54	48.4	15.1	1.08	3.06	1.14	1.36	1.45	0.19	**77.7**
U-6	5.24	10.1	3.26	338	133	7.90	9.79	4.71	1.75	1.54	0.35	**516**
U-7	3.51	2.43	1.54	17.0	6.10	1.52	3.07	1.34	0.58	1.31	0.23	**38.6**
U-8	1.37	1.96	1.53	31.6	8.24	1.61	2.23	1.21	1.73	1.38	0.26	**53.1**
U-9	0.60	2.02	1.85	14.4	3.11	0.92	5.41	0.64	1.15	1.10	0.48	**31.7**
U-10	8.52	1.79	3.26	149	58.6	1.49	5.02	2.10	2.46	3.06	0.27	**236**
U-11	10.9	3.67	1.72	47.5	15.1	3.23	2.50	1.96	1.97	1.25	0.18	**89.9**
U-12	4.73	6.74	5.80	116	50.4	4.81	4.52	1.69	1.39	3.74	0.34	**200**
U-13	0.67	1.05	1.77	15.8	4.63	1.02	1.32	0.50	1.10	0.53	0.19	**28.6**
U-14	11.1	4.71	3.83	119	42.8	1.99	4.73	3.00	2.59	2.58	0.20	**196**
Avg.	**3.98**	**3.10**	**2.32**	**72.2**	**27.0**	**2.15**	**3.41**	**1.51**	**1.49**	**1.67**	**0.24**	**119**
Industrial Sites												
Ind-1	25.1	4.77	9.24	325	120	2.05	4.70	7.24	0.81	2.29	0.35	**501**
Ind-2	20.8	5.33	29.1	335	132	2.62	5.69	6.54	1.40	1.52	0.25	**540**
Ind-3	14.1	4.84	6.87	99.4	40.8	1.04	2.48	3.06	1.04	1.70	0.87	**176**
Ind-4	6.55	2.76	3.15	94.5	29.6	0.92	3.18	1.94	1.61	1.47	0.14	**146**
Ind-5	78.4	16.9	59.8	791	269	6.54	19.7	52.3	3.14	31.7	1.86	**1,331**
Ind-6	10.5	3.10	21.0	123	46.7	1.08	5.08	1.37	1.07	1.72	0.25	**215**
Ind-7	149	114	84.4	1,036	359	9.94	56.8	23.7	12.4	14.8	0.57	**1,861**
Ind-8	31.1	11.0	12.6	348	126	4.03	10.9	12.3	2.09	38.5	0.40	**597**
Ind-9	17.6	8.67	8.95	85.8	30.4	1.77	6.91	2.03	1.84	2.98	0.23	**167**
Ind-10	91.7	7.10	90.7	1,727	581	63.8	14.3	42.4	3.60	3.39	0.81	**2,626**
Ind-11	6.90	4.63	6.83	65.9	21.1	1.48	4.20	3.38	2.25	2.35	0.33	**119**
Ind-12	3.13	13.8	16.3	44.3	16.3	1.19	10.1	7.82	8.83	2.43	0.20	**124**
Ind-13	3.99	2.53	3.43	27.5	11.5	1.04	1.63	0.60	1.04	1.16	0.48	**55.0**
Ind-14	1.55	3.09	2.13	25.9	6.42	2.16	4.55	1.38	1.89	1.30	0.28	**50.7**
Avg.	**32.9**	**14.5**	**25.3**	**366**	**128**	**7.12**	**10.7**	**11.9**	**3.08**	**7.66**	**0.50**	**607**
Suburban Sites												
SU-1	0.52	1.42	1.31	15.2	3.61	0.93	2.43	1.02	1.79	0.97	0.16	**29.3**
SU-2	3.28	1.17	2.16	60.6	22.2	1.19	1.00	1.27	1.49	1.22	0.15	**95.7**
SU-3	0.69	0.92	1.51	16.9	4.13	0.69	1.21	0.88	1.27	0.65	0.13	**29.0**
SU-4	0.60	0.84	1.24	16.3	3.72	1.03	1.53	0.16	0.64	0.72	0.10	**26.9**
SU-5	0.67	1.03	0.85	13.7	2.82	0.74	0.76	0.36	0.71	0.52	0.11	**22.3**
Avg.	**1.15**	**1.08**	**1.41**	**24.5**	**7.30**	**0.92**	**1.39**	**0.74**	**1.18**	**0.82**	**0.13**	**40.6**
Rural Sites												
R-1	0.70	0.82	1.75	15.2	3.59	0.62	0.60	0.68	1.07	0.40	0.052	**25.5**
R-2	1.73	1.20	1.71	19.8	6.80	0.86	1.08	0.46	1.07	1.01	0.20	**35.9**
R-3	0.43	0.89	1.05	7.43	2.08	0.54	1.74	0.49	0.91	0.85	0.14	**16.5**
R-4	0.46	0.62	0.81	9.35	1.97	0.80	1.13	0.57	1.09	0.99	0.13	**17.9**
R-5	0.66	0.66	0.60	8.56	2.26	0.77	0.60	0.55	0.76	0.70	0.14	**16.3**
Avg.	**0.79**	**0.84**	**1.18**	**12.1**	**3.34**	**0.72**	**1.03**	**0.55**	**0.98**	**0.79**	**0.13**	**22.4**

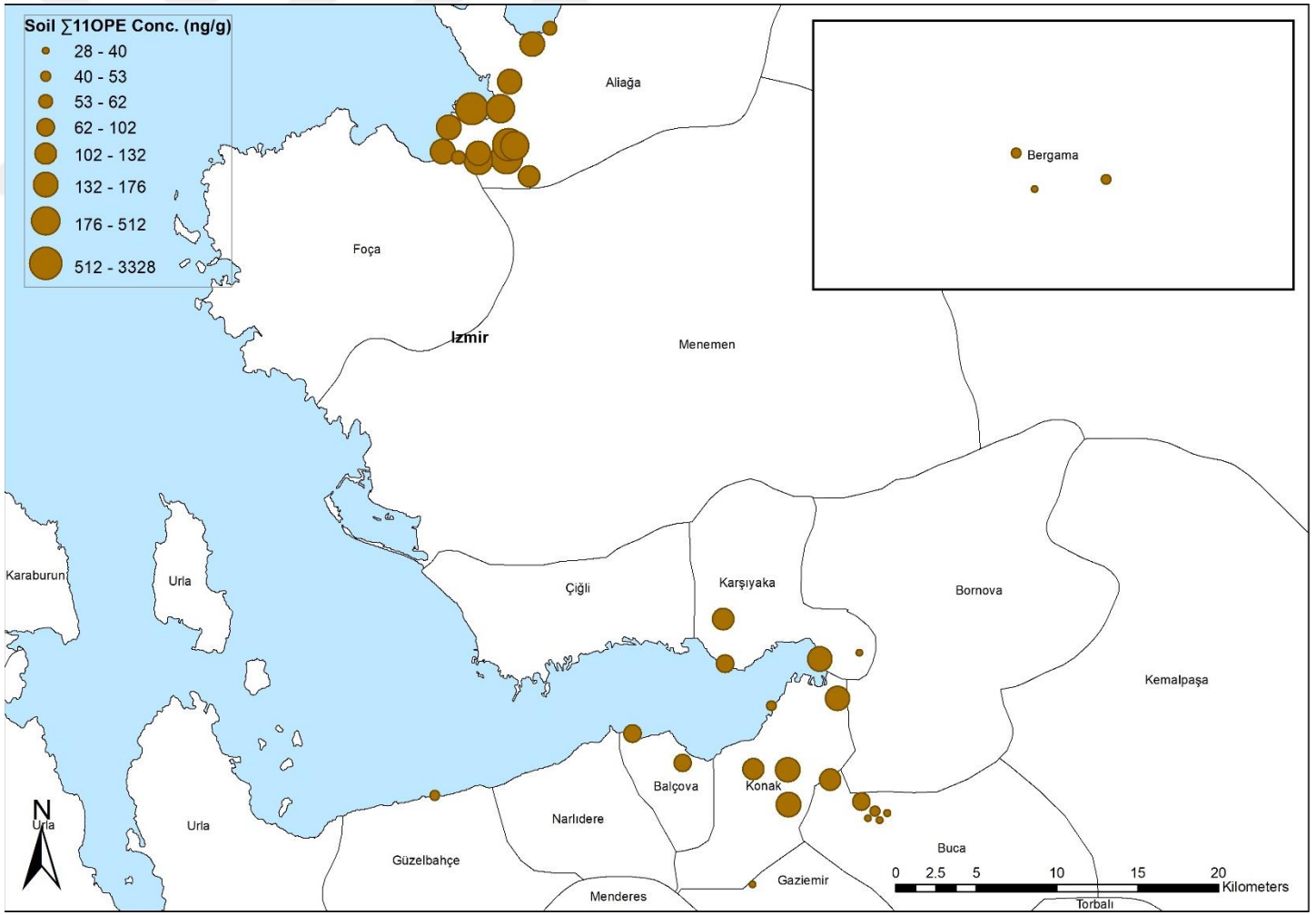


Figure 4.24 Soil $\sum_{11}$OPE concentrations in winter

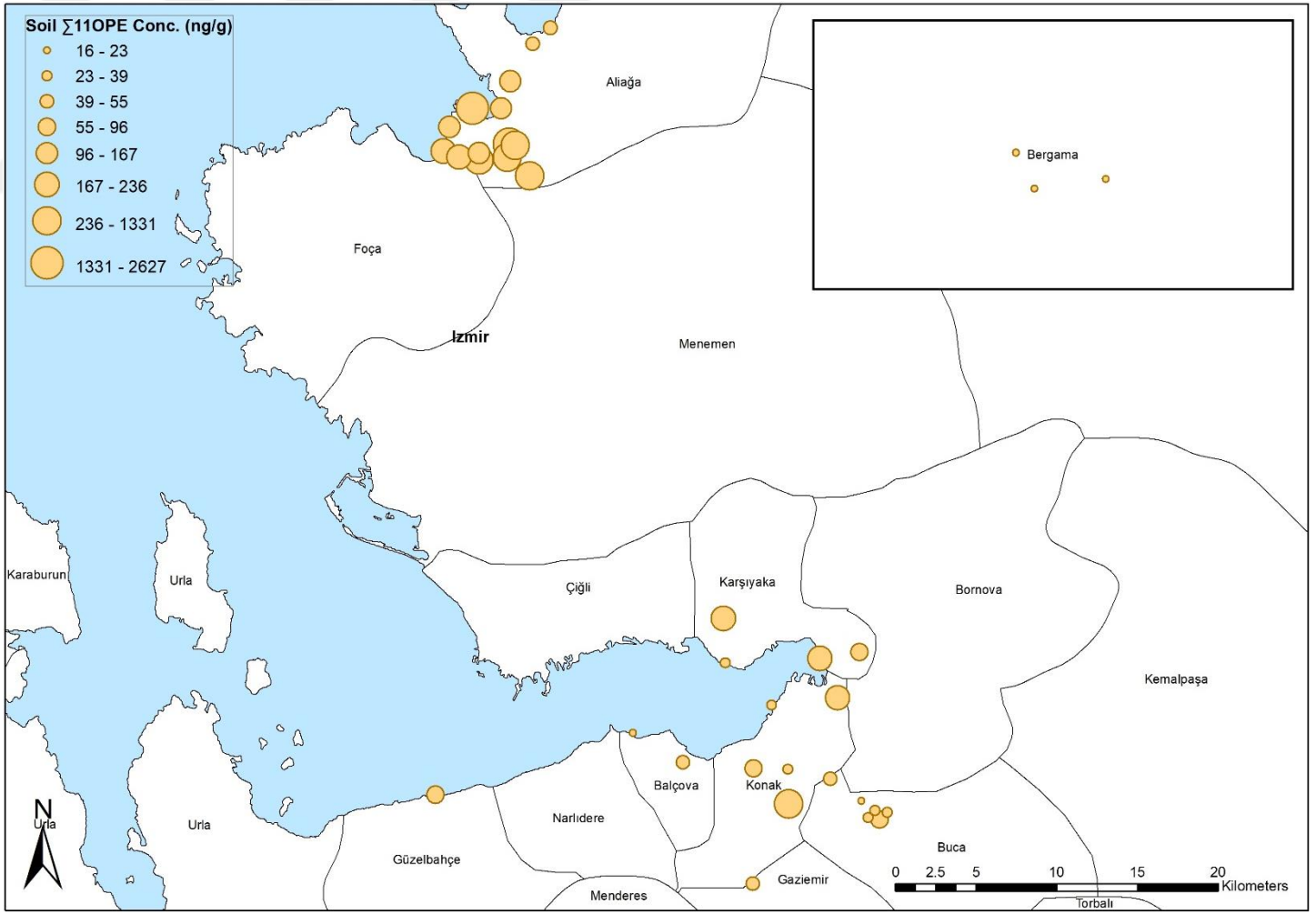


Figure 4.25 Soil $\sum_{11}$OPE concentrations in winter

According to seasonal variations, in 23 out of the 38 sampling sites $\sum_{11}$OPE concentrations were higher in winter (winter/summer>1). Under limited anthropogenic influences, nine of the 10 sampling sites in suburban and rural areas had higher concentrations in winter probably due to effect of wet deposition arising from precipitation in winter. Accordingly, higher levels observed in 14 of the 28 urban and industrial sites in summer might be explained by site-specific OPE sources such as traffic and industrial activities and elevated ambient air levels. The average (*n*=38) winter/summer ratios of 11 OPEs decreased as follows: EHDPP (7.39) > TDCiPP (2.58) > TEHP (2.47) > TBOEP (2.41) > TnBP (2.12) > TCiPP2 (1.81) > TCiPP1 (1.69) > T2iPPP (1.51) > TCEP (1.33) > TPHP (1.14) > TEP (1.13). In consistence with the inference that OPEs tend to evaporate due to the increasing temperature in the ambient air samples resulting in higher concentrations in summer atmospheric samples, soil samples were thus measured at lower concentrations probably due to the tendency to shift to gas phase in the summer. The seasonal distribution profiles were depicted in Figures 4.26 and 4.27.

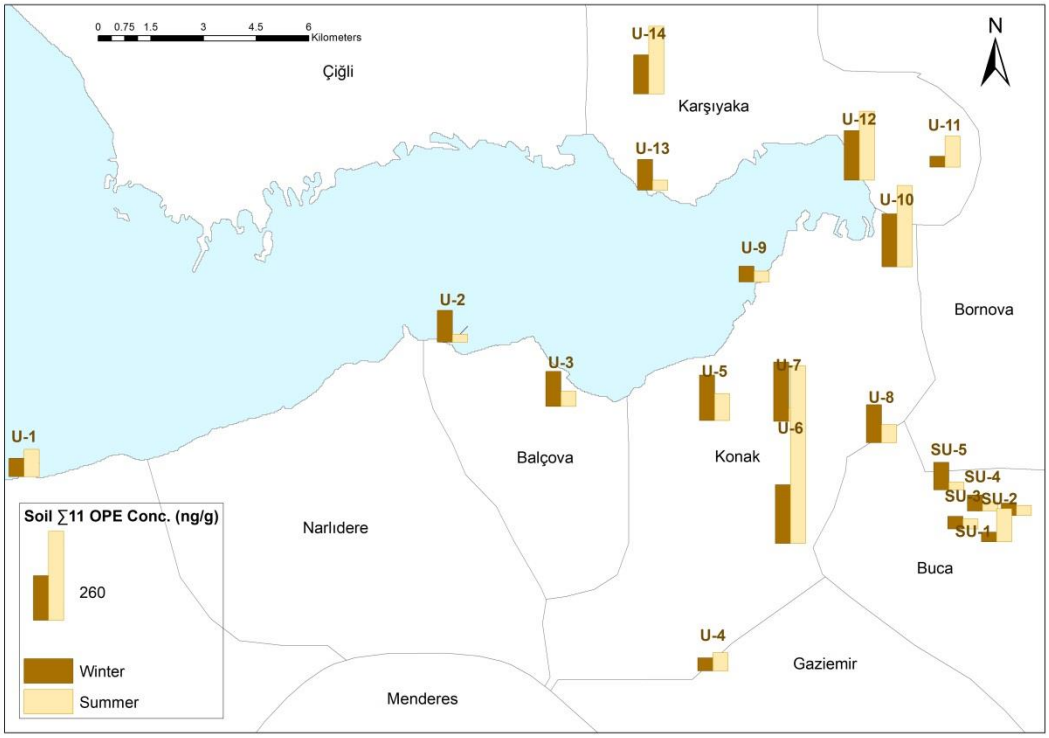


Figure 4.26 Seasonal variations of soil OPE concentrations in urban and suburban sites

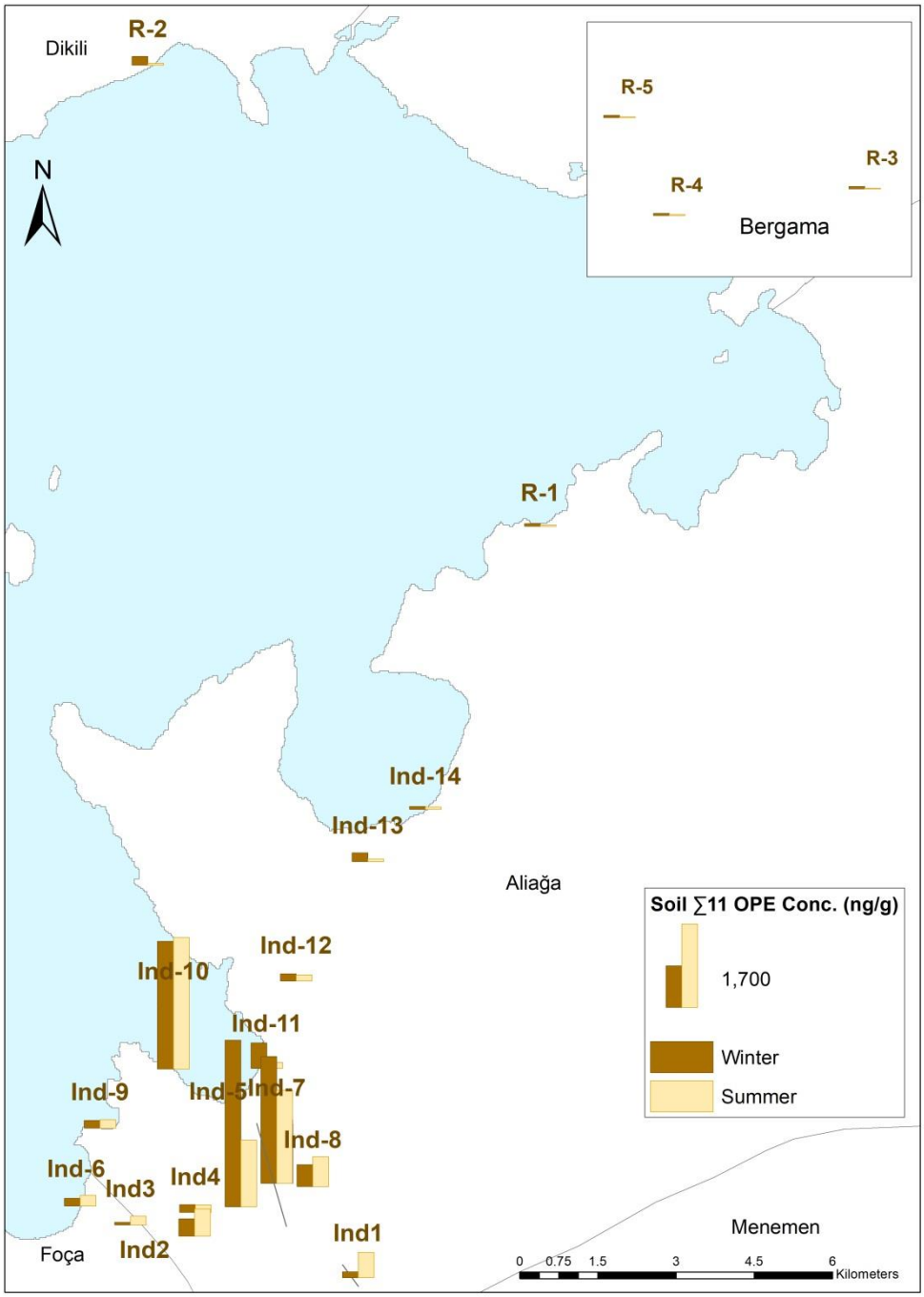


Figure 4.27 Seasonal variations of soil OPE concentrations in industrial and rural sites

As it were in ambient air samples, TCiPP1 and TCiPP2 also dominated soil samples in all four sampling regions and in both seasons. The sum of these two compounds correspond to 69 and 84% of total OPEs in rural and urban sites in summer, while 60 and 75% in suburban and industrial sites in winter samples, respectively. In all sampling sites and both seasons TCiPP1 and TCiPP2 were

contributed to total OPE concentrations not less than 45 and 15%, respectively. In a recent study conducted in China, Dalian, TCiPP was also detected as the most abundant OPE congener in urban, suburban and rural samples, followed by TDCiPP, TNBP, and TCEP, respectively (Wang et al., 2020). Many studies can be found in the literature evaluated TCiPP as the most prominent OPE in soil samples (Kurt-Karakus et al., 2018; Sun & Zhu, 2021; Wang et al., 2019). The median TCiPP concentration (64.5 ng/g) in urban soil was slightly higher than reported by Lu et al. (2014) (15.5–16.7 ng/g) and Kurt-Karakus et al. (2018) (17.1 ng/g). Although Yadav et al. (2018) reported higher median TCiPP concentration (165 ng/g) in soils of four major cities in Nepal, the predominant OPE in that study was tris(methyl phenyl) phosphate (TMPP) which was not covered in the present study. Following TCiPP, TDCiPP and TCEP were the other chlorinated OPEs with the abundances 0.41-6.35% and 0.52-17.5%, respectively. The median values (n=76) for TCEP (2.15 ng/g) and TDCiPP (1.69 ng/g), was quite comparable with 3.07 ng/g and 1.36 ng/g (n=98) reported by Wang et al. (2019). On the other hand, Yadav et al. (2018) measured TCEP concentrations in urban soils of metropolitan cities in Nepal with a median value of 21.2 ng/g. This concentration is more comparable with industrial TCEP levels in the present study, rather than the urban levels. Yadav et al. (2018) also emphasized that, development stage of a country may directly affects TCEP levels, due to lack of regulations and imported consumer goods (i.e., PUF, rubber, textile coatings, interior trims of vehicles) containing TCEP. It should also be noted that the use of TCEP in baby products is restricted in many developed countries including the USA because of its carcinogenic impact (Wu et al., 2016). In terms of alkyl-OPEs, TEP and TBOEP had the highest proportions. In the present study, TEP was detected in significant levels especially in industrial soils in both summer (mean: 48.9±79.8 ng/g) and winter (mean: 32.9±43.3 ng/g) samples. The number of studies that reported TEP concentrations in soil were quite sparse. In one of these studies, Sun and Zhu (2021) measured TEP in industrial (n=6) and urban (n=9) soil samples with means of 17.2 and 0.165 ng/g, respectively. Considering non-industrial TEP levels (i.e. urban mean in winter: 1.60 ng/g) were also significantly lower than industrial levels in the present study. This compound might be mostly originated from industrial activities, as also inferred from ambient air

results (Section 4.2.2). TBOEP is commonly added with a ratio of 0.5-8.0% by mass to floor polish/waxes and is used as a plasticizer in rubber and plastics (Cequier et al., 2014). This OPE was detected with the mean concentrations of 3.41 and 10.7 ng/g in summer, 5.42 and 34.2 ng/g in winter soils of urban and industrial sites, respectively, whereas it was generally measured in much lower levels in the literature (Wang et al., 2020; Wang et al., 2019). However, consistent with the present study Sun and Zhu (2021) reported mean TBOEP concentrations of 73.5 and 18.8 ng/g for industrial and urban sites, respectively. The rest alkyl-OPEs TnBP and TEHP were also measured in industrial soils with the average concentrations of 20.9 and 19.0 ng/g in winter, 14.5 and 7.66 ng/g in summer; while they were detected in urban soils as 3.25 and 2.44 ng/g in winter, and 3.10 and 1.67 ng/g in summer, respectively. Sun and Zhu (2021) denoted that commercial TBOEP formulations may contain the other alkyl-OPEs as impurities since they were strongly correlated with each other. Similar correlations ($0.54< r^2 <0.70$, $p<0.01$) between TBOEP and other alkyl-OPEs (TEP, TnBP, and TEHP) were also observed in the present study. Due to their relatively low production volumes and shorter environmental half-lives, aryl-OPEs are found to be at relatively lower levels among the other OPE congeners in most studies (He et al., 2019a; Wang et al., 2019). In the present study, sum of three aryl-OPEs (TPHP, EHDPP and T2iPPP) contributed 12.0 ± 7.14% and 4.81 ± 2.97% of winter and summer soils. High contributions in winter may be explained by reduced degradation rates under low temperature and limited UV radiation. EHDPP dominated the aryl-OPEs and showed similar seasonality as in atmospheric samples, and thus was prominent in winter soils. The mean ratio of winter/summer EHDPP concentrations was 7.39 ± 4.24 through 38 sampling sites. EHDPP is mainly associated with particle-phase with its high K_{OA} and therefore, dry and wet deposition in winter might have caused the increased soil EHDPP levels in winter. However, the other aryl-OPEs, TPHP and T2iPPP, did not show such seasonal patterns. T2iPPP has the lowest contribution in all samples. Proportions of each OPE species in total OPE concentrations were given in Figure 4.28 and 4.29 for winter and summer, respectively.

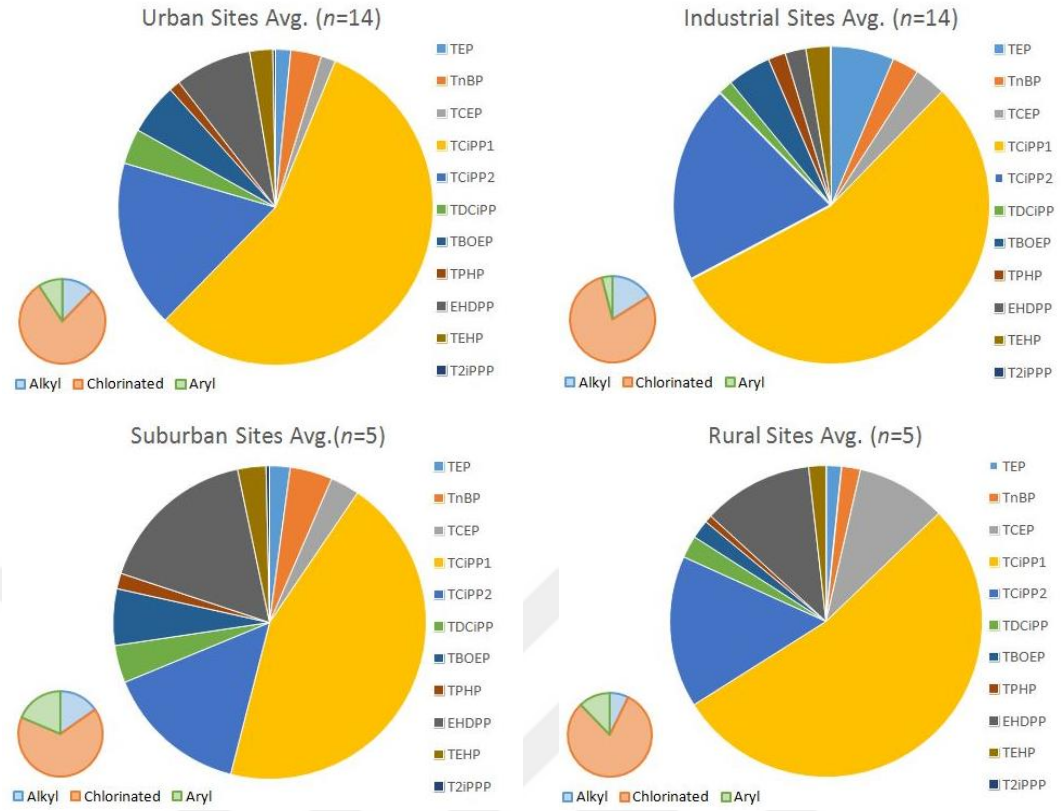


Figure 4.28 Compound-specific soil compositions in winter

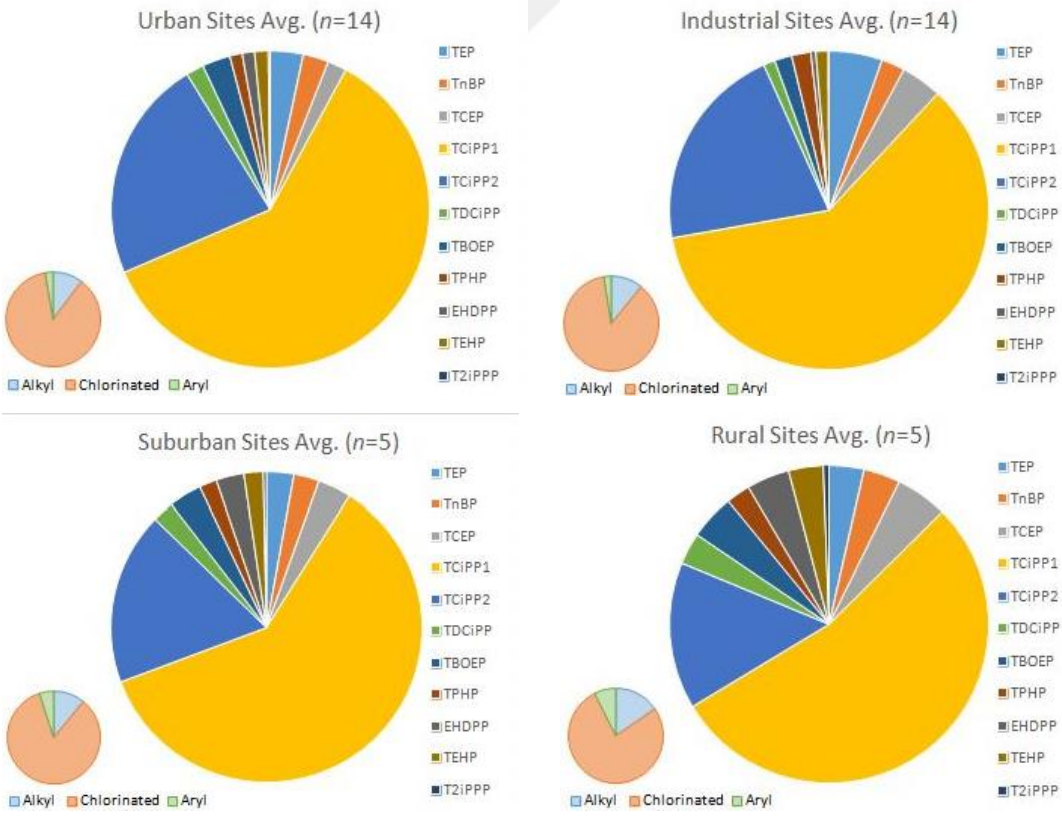


Figure 4.29 Compound-specific soil compositions in summer

4.2.4 Air-Soil Exchange of OPEs

As an important environmental transport mechanism, air-soil exchange behaviors of the studied OPEs were evaluated using fugacity fractions. Fugacity is a quantity of chemical potential of a pollutant in a specific compartment that drives its transfer between media (Meijer et al., 2001). The soil fugacity fraction $[f_S/(f_S+f_A)]>0.5$ implies net contaminant volatilization from soil, values <0.5 indicate net gas-phase deposition from air while in case of equilibrium, $f_S/(f_S+f_A)$ value is ~0.5 (Harner, Green, & Jones, 2000). Therefore the soil fugacity (f_S) can be calculated as;

$$fs = \frac{C_s . \rho_s}{K_{SA}} \tag{4.45}$$

where, C_S is the soil concentration (ng/kg, dry weight), ρ_s is the soil solid density (kg/m^3), and K_{SA} (dimensionless) is the soil-air partition coefficient.

K_{SA} depends on temperature, physicochemical properties of pollutant, and soil properties (i.e., humidity, organic carbon content) (Meijer et al., 2003). Hippelein and McLachlan (1998) derived a linear relationship that correlates K_{SA} to K_{OA} and the organic carbon fraction of the soil:

$$\begin{gathered} K_{SA}= (0{,}411) \text{ x } (\rho s) \text{ x } (\phi_{OC}) \text{ x } (K_{OA}) \\ \phi oc = \frac{OC}{100} \quad \text{and} \quad \text{OM}= (1{,}5) \text{ x } (\text{OC}) \end{gathered} \tag{4.46}$$

where, Φ_{OC} is the fraction of organic carbon on a dry soil basis, OC is organic carbon (%) and OM is organic matter (%). OM was measured for 76 soil samples collected (4.27 ± 3.62%) in the present study. In the calculation of K_{SA}, it was assumed that the OM fraction is 1.5 times of OC and solid soil density, ρs, is 2,0 ± 0,1 g/cm^3 and soil fugacity capacity results fully from the organic carbon fraction (Bidleman & Leone, 2004; Meijer et al., 2001; Odabasi & Cetin, 2012).

Gas-phase concentrations (C_g) of atmospheric OPEs were employed as air fugacities (f_A) in air-soil fugacity fraction calculations. Atmospheric concentration of an organic pollutant measured using a PUF sampler is defined as C_t (ng/m^3). Although PUF samplers are primarily target gas phase pollutants, it has been revealed in recent years that significant amounts of particles are collected by these samplers (Harner et al., 2014; Harner et al., 2013; Markovic et al., 2015). Since C_g is required in order to determine air-soil exchange, OPE concentrations in the gas phase were calculated according to modified K_{OA} model derived in the present study (Section 4.2.1). Distribution of organic compounds between gas and particulate phases depends on K_P (m^3/μg) (Harner & Bidleman, 1998b):

$$K_p = \left(C_p / C_{TSP}\right) / C_g \tag{4.29}$$

where, C_p and C_g are particle and gas phase concentrations (ng/m^3) and C_{TSP} is total atmospheric particulate matter concentration (μg/m^3), respectively.

K_p was calculated using modified K_{OA} model and organic matter fractions of the particles by assuming absorption is the primary exchange mechanism between gas and particle phases (Harner & Bidleman, 1998b).

$$K_p = (f_{OM} MW_{OCT} \xi_{OCT}) K_{OA} / (\rho_{OCT} MW_{OM} \xi_{OM} 10^{12}) \tag{4.30}$$

where, f_{OM} is the OM fraction (assumed as 50%) of TSP, MW_{OCT} (130.23 g/mol) and MW_{OM} (assumed 240 g/mol for urban and industrial sites and 200 g/mol for suburban and rural sites) are the average molecular weights of octanol and the OM (Yazdani et al., 2020), ρ_{OCT} is the octanol density (0.820 kg/L), ξ_{OCT} and ξ_{OM} values were utilized as calculated in Section 4.2.1.3 Temperature depended K_{OA} values for studied OPEs were also calculated using regression parameters (*A* and *B*) those experimentally determined (see Section 4.1.1) in the present study.

Therefore, OPE concentrations in gas phase were calculated according to:

$$C_g = C_t/(C_{TSP}K_P + 1) \quad (4.47)$$

where, C_t (ng/m^3) is total (gas + particle phase) ambient air concentration measured using the PUF sampler. C_{TSP} (in urban sites: 85 μg/m^3, in industrial sites: 95 μg/m^3, in suburban and rural sites: 50 μg/m^3) were also employed as reported previously for the study area (Bozlaker et al., 2008a; Cetin & Odabasi, 2008).

A propagated error analysis was used to estimate the uncertainties of the determined fugacity fractions. The uncertainty of K_{SA} was estimated as 25%. The overall uncertainties of C_gs were determined as 26% by averaging the additional errors originated from modified K_{OA} model while it was assumed that C_s values had uncertainties of 15% (Bozlaker et al., 2008a; Bozlaker, Odabasi, & Muezzinoglu, 2008b). After propagating the errors of all the variables ($K_{SA,}$ $C_{g,}$ C_s) in both soil (f_S) and air (f_A) fugacities, the equilibrium interval of the fugacity fraction [$f_S/(f_S+f_A)$] was calculated as 0.403-0.597 (0.5±0.097).

The transfer directions for the studied 11 OPEs between air and soil were illustrated for both seasons in Figure 4.30. The first five compounds (TEP, TnBP, TCEP, TCiPP1 and TCiPP2) having lower molecular weights and relatively lower K_{OA} values (log K_{OA}<10) tended to evaporate from the soil to the atmosphere both in summer and winter. Especially TEP, having a log K_{OA}<6, thus a low K_{SA}, strictly evaporated to air in all samples. The last five OPEs (TBOEP, TPHP, EHDPP, TEHP, T2iPPP) with higher molecular weights and log K_{OA}>10 were prone to deposit from air to soil in both seasons, while the air-soil exchange direction for TDCiPP was mostly to the atmosphere in winter. Wang et al. (2020) also reported deposition tendencies for TBOEP, TPHP, EHDPP and TEHP, and volatilization for TCEP and TnBP. However, TCiPP (sum of TCiPP1 and 2) indicated a deposition tendency as opposed to the present study. In another study, Han et al. (2020) determined mainly deposition patterns from air to soil for TCEP, TCiPP, TPHP and TEHP, whereas

Yadav et al. (2018) reported net volatilization from soil for TnBP, TCEP, TCiPP, TDCiPP, TPHP, EHDPP, TEHP and TMPP.

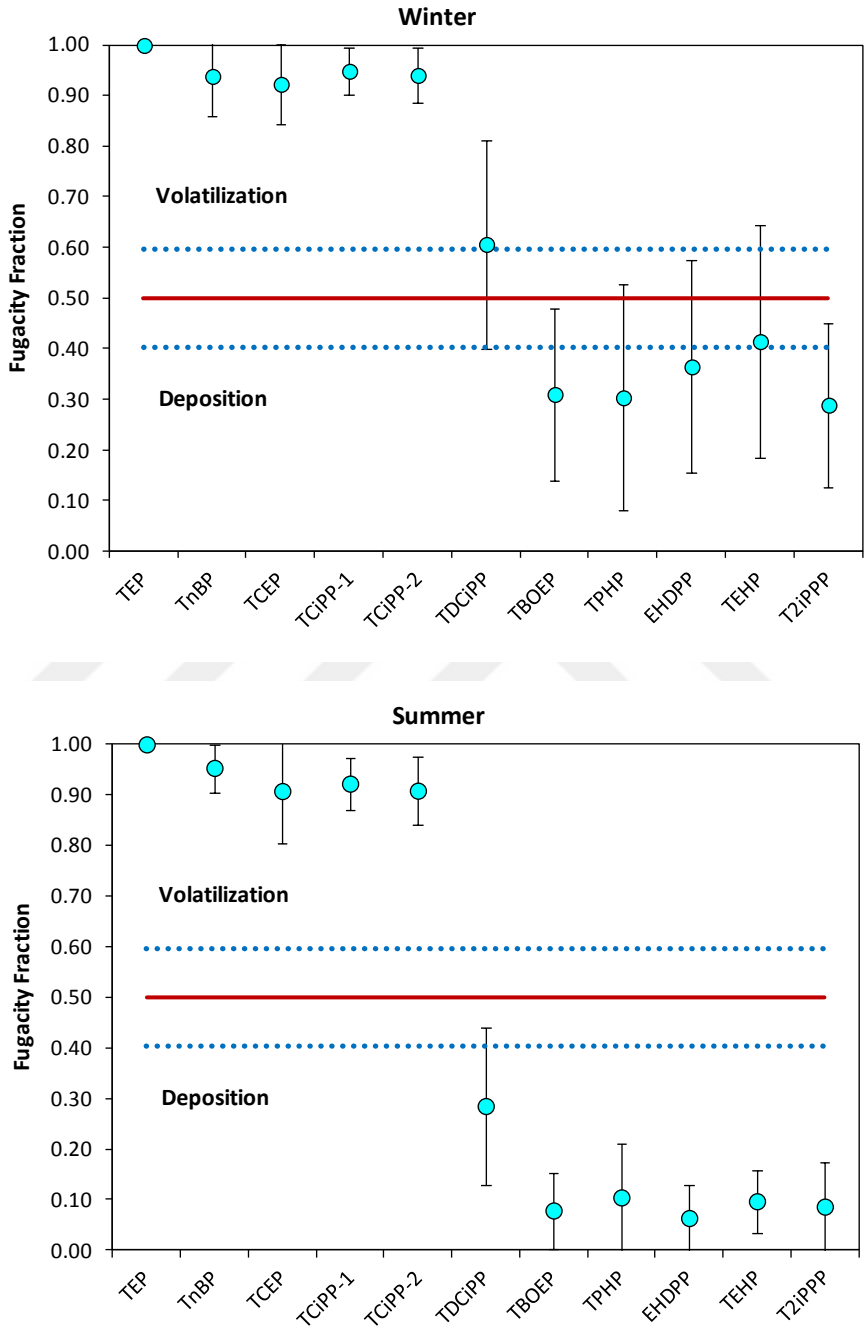


Figure 4.30 Air-soil fugacity fractions of OPEs in both seasons

In general, due to the lower ambient temperatures in winter K_{OA} and K_{SA} values increase, and as a result, fugacity fractions decrease with exchange tendencies

shifting to deposition. However, the air-soil exchange patterns of the present study are somewhat unusual with increased fugacity fractions in winter. This might be attributed to considerably higher ambient air OPE concentrations observed in summer than in winter, while soil concentrations were also slightly higher in winter. OM content of a particular soil sample is one of the key parameter that affects the partitioning behavior between air and soil (Eq. 4.46). OM content of 37 out of 38 soil samples ranged from 0.95 to 7.74% in winter and from 1.10 and 10.0% in summer, while sampling site Ind-7 (located near a coal screening and storing facility) had a substantially higher OM content of 21.9 and 24.9% in winter and summer samples (probably originated from coal dust from a nearby coal processing plant), respectively. Although Ind-7 had one of the highest soil OPE concentrations followed by Ind-5 and -10 (Tables 4.11 and 4.12), it had significantly lower soil fugacities compared to Ind-5 and -10. Air-soil exchange might also be influenced by some other soil characteristics such as moisture content (Bidleman & Leone, 2004). However, moisture content is not taken into account the fugacity fraction calculation used in the present study. Thus, it could be concluded that the air/soil levels and soil properties control air-soil exchange of OPEs rather than the effect of temperature on their physicochemical properties.

4.2.5 Spatial and Seasonal Variations of Seawater OPE Concentrations

Seawater concentrations of OPEs collected using LDPE samplers were calculated according to (Khairy et al., 2014):

$$C_w = \frac{C_{LDPE}}{K_{PEW}\left(1 - e^{-\frac{R_S t}{K_{PEW} m_{LDPE}}}\right)} \tag{4.48}$$

where, C_W (ng/L) and C_{LDPE} (ng/kg) OPE concentrations in sea water and LPDE sheets, respectively, R_S is the sampling rate (L/day), t is deployment time (day) and m_{LDPE} is the mass of LDPE sheet (kg). The required sampling rates (R_S) were also calculated by:

$$E(\%) = 100\left(1 - e^{\left(\frac{-R_S t}{m_{LDPE} K_{PEW}}\right)}\right) \quad (4.49)$$

where E(%) is the equilibrium percentage, t is the deployment time (day), m_{LDPE} is the mass of LDPE sheet. Eq. (4.49) could also be written in the form of:

$$E(\%) = 100(1 - \exp(-R_s \times A) \quad (4.50)$$

where the term A is $t/m\ K_{\mathrm{PEW}}$.

E(%) was determined using the initial (C_0, ng/kg) and final (C_t, ng/kg) concentrations of PRCs loaded to LDPEs as:

$$E(\%) = 100((C_0 - C_t)/C_0) \quad (4.51)$$

C_0 values were determined from the analysis of PRC loaded but unused blank LDPE sheets (average of 3 sheets for each sampling program). C_t was determined by analysis of PRCs in LDPE sheets used for sampling. E(%) values for PRCs were calculated using Eq. (4.51). Then, R_S was calculated through Eq. (4.50) using non-linear regression analysis (IBM SPSS Statistic 24) by assigning E(%) as the dependent variable. K_{PEW} values for PRCs in term A were taken from Lohmann (2012); Smedes, Geertsma, van der Zande, & Booij (2009). R_S values were ranged from 15.0 to 24.8 and from 26.0 to 32.4 L/day in summer and winter samples, respectively. Finally, determined R_S values and measured experimental K_{PEW}s (Section 4.1.5) were used to calculate seawater OPE concentrations according to Eq. (4.48). In a study from the literature, Khairy et al. (2014) calculated R_S values ranged from 15.0 to 80.0 L/day, while Liu et al. (2016b) determined wider range from 19 to 184 L/day for PCBs in lake water. The differences on R_S values among different studies might be due to different PRCs utilized, water body characteristics (i.e. lake or sea water, temperature, salinity, turbulence), and sampler geometry or LDPE masses used in the samplers.

Since they were measured under certain experimental conditions (in DI water at 19.2°C), K_{PEW} values were corrected for site-specific seawater temperatures and also salinities. Additionally, K_{PEW} values of PRCs adopted from Smedes et al. (2009) were also corrected for both parameters. Lohmann (2012) reviewed the effect of environmental parameters on K_{PEW}s and expressed the following equation for water temperature:

$$K_{PEW}(T) = K_{PEW}(298)e^{(\Delta H_{PEW}/R)\left\{\frac{1}{298}-\frac{1}{T}\right\}} \quad (4.52)$$

where K_{PEW}(T) and K_{PEW}(298) are K_{PEW} values at temperature T (K) and 298 K, respectively, ΔH_{PEW} is the enthalpy of polyethylene-water partitioning (kJ/mol), and R is the universal gas constant (8.3143 J/mol/K). ΔH_{PEW} values were taken as -10 and -25 kJ/mol for PRCs (PCBs) and OPEs, respectively, as suggested in the literature (Booij, Hofmans, Fischer, & Van Weerlee, 2003; Lohmann, 2012).

Temperature-adjusted K_{PEW}s were further corrected for site-specific molar salt concentrations according to equation derived by (Lohmann, 2012);

$$\log K_{PEW} = \log K_{PEW0} + K_s I \quad (4.53)$$

where, K_{PEW0} is the freshwater K_{PEW} value, K_s is the Setschenow constant (L/mol), and I is the ionic strength of the salts present in water. It was assumed that all the salt content in seawater consisted of NaCl. Setschenow constants were also determined using compound specific K_{OW} values according to following relationship derived by Ni & Yalkowsky (2003).

$$K_S = 0.040 \log K_{OW} + 0.114 \quad (4.54)$$

Sampling site-specific seawater temperatures and molar salt concentrations representing the deployment periods were obtained from the nearest meteo-oceanographic observation stations of Izmir Metropolitan Municipality. Finally,

adjusted K_{PEW}s were used to determine seawater OPE concentrations in 7 sampling sites for winter and summer seasons.

Measured seawater concentrations in urban, industrial and suburban sites were given for winter and summer seasons in Tables 4.15 and 4.16, respectively. Site-specific distributions of $\sum_{11}$OPEs were also given in Figures 4.31 and 4.32. The average of $\sum_{11}$OPE concentrations in urban (n=3) and industrial sites (n=3) were 210 and 365 ng/L in winter, respectively. In summer samples, the average of $\sum_{11}$OPE concentrations were substantially higher, as 500 and 1,331 ng/L in urban and industrial sites, respectively. As it were in ambient air and soil samples, industrial site seawater samples also had considerably higher levels of OPEs compared to both urban and suburban sites. Especially, sampling points Ind-9 and 10 those located near commercial ports of iron-steel manufacturing plants, had extremely high OPE concentrations, similar to soil and air samples. Although the number of studies reporting OPE concentrations in seawater are still scarce, there are comparable values reported in the literature for various water bodies. In a study from Canada, ∑OPE concentrations in an urban lake water were reported as 96±43 ng/L (Venier et al., 2014). Additionally, Ren et al. (2019) measured extremely increased $\sum_{4}$OPE concentrations in the water samples collected from effluent water of an OPE manufacturing plant with a median of 20,000 ng/L. Niu et al. (2019) also investigated 11 OPE congeners in river water samples influenced from different levels of anthropogenic activities and reported that $\sum_{11}$OPEs ranged from 23.98 to 825 ng/L, and the mean value was 229 ng/L. As one of the rare OPE seawater reports, Hu et al. (2014) collected 11 seawater samples (1 L each) from 3 coastal cities and investigated seawater levels of 4 major OPEs and determined total concentrations ranged from 91.9 to 1,392 ng/L. As in the present study, they also collected seawater samples close to coastline and thus may explain the relatively high OPE levels due to possible municipal and industrial effluents nearby urban and industrial sites. In another study, Zhong et al. (2017) reported lower total seawater concentrations for 7 OPEs ranging between 8.12 and 98.0 ng/L. Although the reported values in the literature differ within a wide range, measured concentrations in the present study were mostly comparable with these values.

Table 4.15 Seawater OPE concentrations (ng/L) in winter

Samp. Point	TEP	TnBP	TCEP	TCiPP1	TCiPP2	TDCiPP	TBOEP	TPHP	EHDPP	TEHP	T2iPPP	Σ_{11}OPE
Urban Sites												
U-1	107	13.8	36.9	2.59	4.08	7.95	10.1	3.81	1.49	0.022	0.0019	**187**
U-9	138	11.3	8.35	0.82	2.41	3.08	6.31	2.63	0.32	0.013	0.0033	**173**
U-13	217	13.4	15.6	0.97	2.63	5.48	10.9	2.61	0.28	0.0088	0.0032	**268**
Avg.	**154**	**13**	**20.3**	**1.46**	**3.0**	**5.50**	**9.1**	**3.02**	**0.70**	**0.015**	**0.0028**	**210**
Industrial Sites												
Ind-9	152	18.0	25.4	5.45	6.62	11.2	37.9	6.21	1.79	0.064	0.0045	**264**
Ind-10	386	37.2	71.0	1.95	5.09	8.28	46.2	3.96	0.78	0.023	0.0070	**560**
Ind-14	179	20.7	15.2	3.58	13.6	8.57	24.2	3.73	0.52	0.019	0.0040	**269**
Avg.	**239**	**25**	**37.2**	**3.66**	**8.4**	**9.3**	**36.1**	**4.6**	**1.03**	**0.036**	**0.0052**	**364**
Suburban Site												
R-2	80.5	5.70	7.40	1.55	1.98	4.34	6.92	2.81	0.34	0.0046	0.0018	**112**

Table 4.16 Seawater OPE concentrations (ng/L) in summer

Samp. Point	TEP	TnBP	TCEP	TCiPP1	TCiPP2	TDCiPP	TBOEP	TPHP	EHDPP	TEHP	T2iPPP	Σ_{11}OPE
Urban Sites												
U-1	130	22.3	316	29.6	16.6	18.6	28.1	14.9	1.90	0.023	0.0039	**578**
U-9	127	18.5	244	21.7	10.3	16.6	15.0	10.8	1.59	0.023	0.0079	**466**
U-13	126	30.7	235	15.0	8.68	12.2	19.8	7.55	1.30	0.021	0.0092	**456**
Avg.	**128**	**24**	**265**	**22.1**	**11.8**	**15.8**	**21.0**	**11.1**	**1.59**	**0.022**	**0.0070**	**500**
Industrial Sites												
Ind-9	832	54.6	580	20.8	11.7	16.3	166	11.9	2.77	0.11	0.012	**1,697**
Ind-10	792	66.4	533	7.20	4.49	7.49	144	9.95	1.04	0.087	0.0073	**1,565**
Ind-14	153	50.0	428	24.5	15.3	18.7	27.3	12.5	2.38	0.12	0.0091	**732**
Avg.	**593**	**57**	**513**	**17.5**	**10.5**	**14.2**	**112**	**11.5**	**2.06**	**0.10**	**0.0095**	**1,331**
Suburban Site												
R-2	85.3	17.8	200	18.6	9.74	14.6	10.1	7.46	1.52	0.011	0.0028	**365**

Season-specific variations $\sum_{11}$OPE compounds in seawater samples were evaluated and depicted in Figure 4.33. Similar to ambient air samples, seawater samples also showed remarkable increase in summer season. Elevated ambient air OPE concentrations may have resulted in increase in seawater concentrations during summer. This observation will be further discussed in Section 4.2.6, air-water exchange. In a recent study, Shi et al. (2016) also evaluated that surface water OPE levels were significantly higher in summer compared to winter. They pointed out that increased water OPE levels were mostly originated from wet deposition process resulted from precipitation primarily occurs in summer in the region where has a semi-humid climate. In the present study, precipitation primarily occurs in winter in Izmir, and thus no precipitation was observed during summer sampling period. Elevated seawater concentrations in summer might be attributed to other mechanisms (i.e. dry gas-deposition and elevated air OPE levels) rather than precipitation. On the

other hand, Regnery and Puttmann (2010a) demonstrated there was no significant seasonal patterns for the OPE levels in an urban lake.

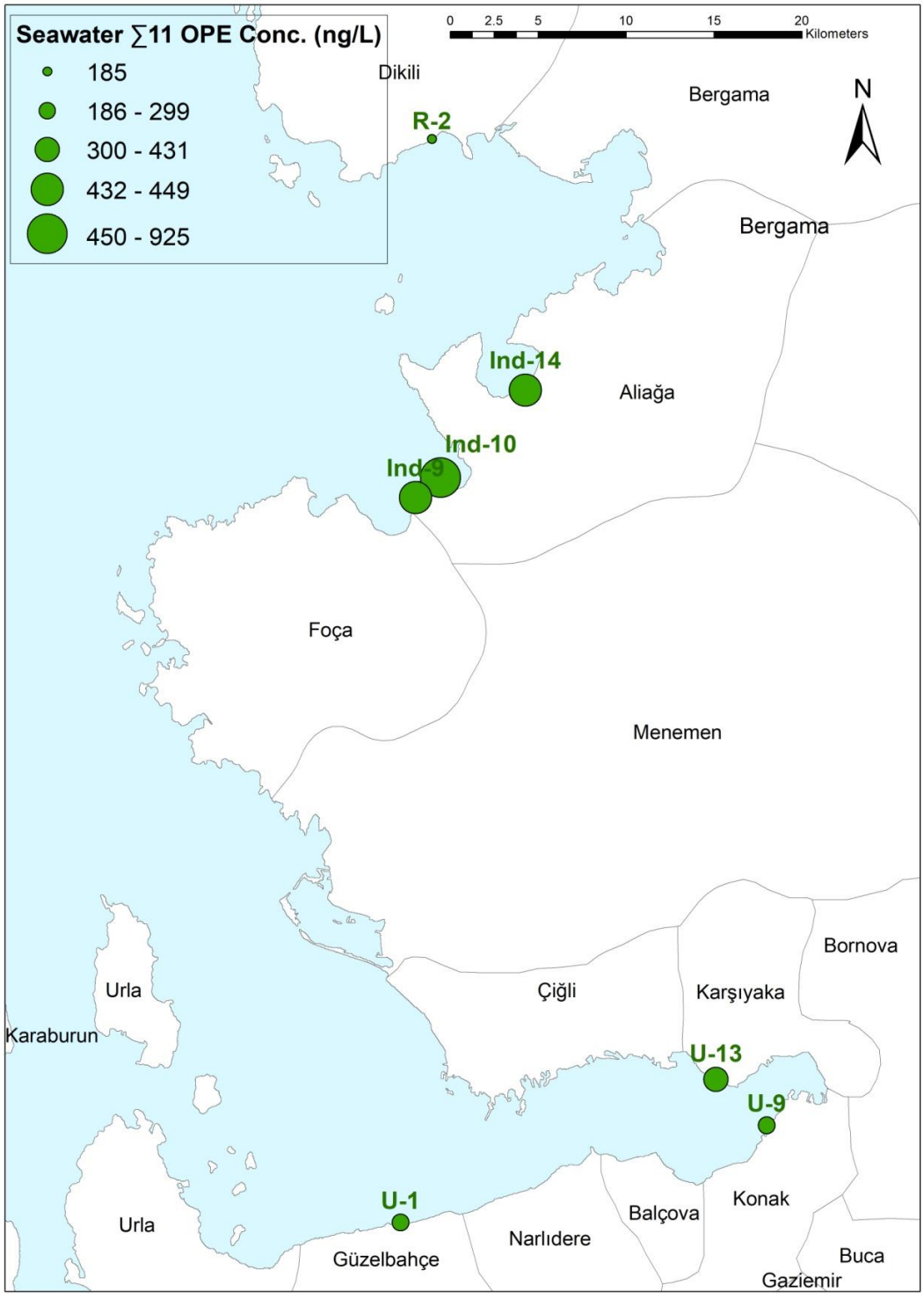


Figure 4.31 Winter $\sum_{11}$OPE concentrations in seawater

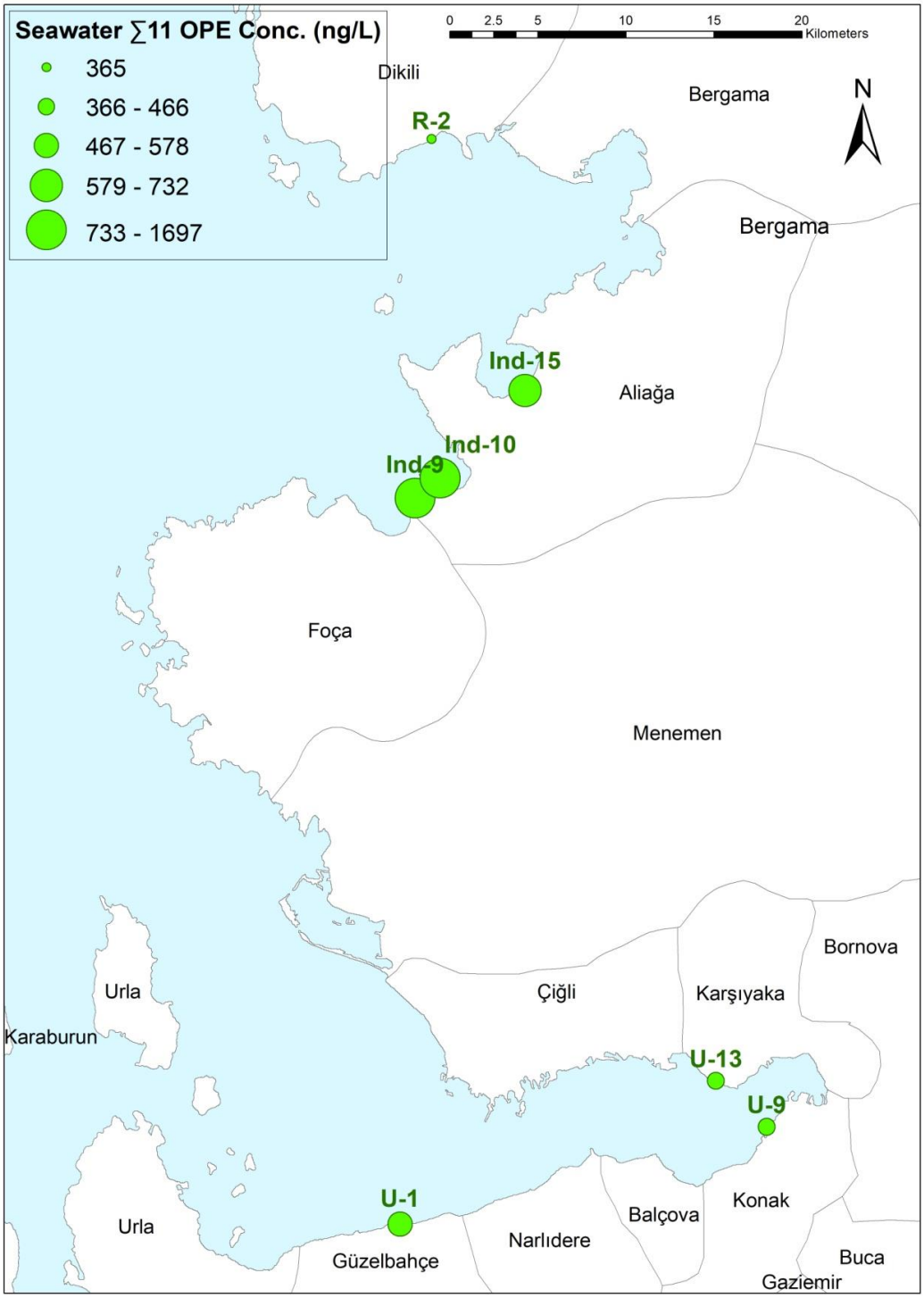


Figure 4.32 Summer $\sum_{11}$OPE concentrations in seawater

Contributions of each OPE species to total OPE concentrations were given in Figure 4.34 for winter and summer. The compound-specific compositions of seawater samples showed quite different patterns compared to ambient air and soil samples. TEP and TCEP were the most prominent OPEs in seawater samples

followed by TnBP, while soil and ambient air samples mostly dominated by TCiPP1 and TCiPP2. These three compounds comprises more than 73% of total OPE concentrations in all sampling sites and in both seasons. TBOEP was another abundant OPE especially in industrial seawater samples. TEP, having the lowest Henry's law constant that indicates its tendency to partition to aqueous-phase, showed a considerable contribution to total OPE concentrations. TCEP also dominated the summer samples and ranged between 200 and 580 ng/L. According to similar studies in the literature TCEP is one of the most abundant OPE detected in water bodies (Hu et al., 2014; Shi et al., 2016; Zhang et al., 2019b; Zhong et al., 2017). For instance, it was reported with an average concentration of 219 ng/L and with a range from 67.5 to 865 ng/L in urban surface waters (rivers and lakes) (Hu et al., 2014; Zhang et al., 2019b). Whereas TCiPP (sum of 1 and 2) was also addressed as another abundant OPE in water samples in most studies, the sum of the contributions of TCiPP1 and TCiPP2 were not higher than 7.98% in any of seawater samples. The other chlorinated OPE, TDCiPP, had also lower contribution in contrast with the literature. Chlorinated OPEs in the present study were mainly contributed by TCEP. Since they are more persistent in the environment and having high production and consumption volumes for primarily flame retarding purposes, chlorinated OPEs, dominated total OPE concentrations in most researches (Niu et al., 2019; Zhang et al., 2019b; Zhong et al., 2017). Although chlorinated OPEs were prominent in ambient air and soil samples collected within the present study, seawater samples mainly consisted of alkyl-OPEs (TEP, TnBP, TBOEP, and TEHP) as illustrated in Figure 4.34. Especially TEP was the most abundant alkyl-OPE detected in 14 seawater samples with contributions between 21 and 81% and concentrations from 80.5 to 832 ng/L. High levels of TEP in industrial seawater samples, even in summer, can be explained by its substantially higher atmospheric levels and high water-solubility of this compound. TEP have not been covered much commonly in previous studies probably due to its high volatility resulting in some analytical/recovery difficulties. However, it was measured in significant amounts (108-258 ng/L) in seawater samples collected by Hu et al. (2014) and (124-212 ng/L) in river samples collected by Wolschke et al. (2015). It should also be noted that, compound-specific compositions did not vary significantly among the sampling sites

in winter, while compositions in industrial sites were somewhat different compared to urban and suburban sites in summer. Three of the 11 covered OPEs, TPHP, EHDPP and T2iPPP, were aryl-OPEs in the present study. TPHP, widely determined as the prominent aryl-OPE in related studies, was also dominated aryl-OPE concentrations of seawater samples in the present study. Additionally, aryl-OPEs had the lowest levels accounting for less than 4% in all sampling sites (Niu et al., 2019; Shi et al., 2016).

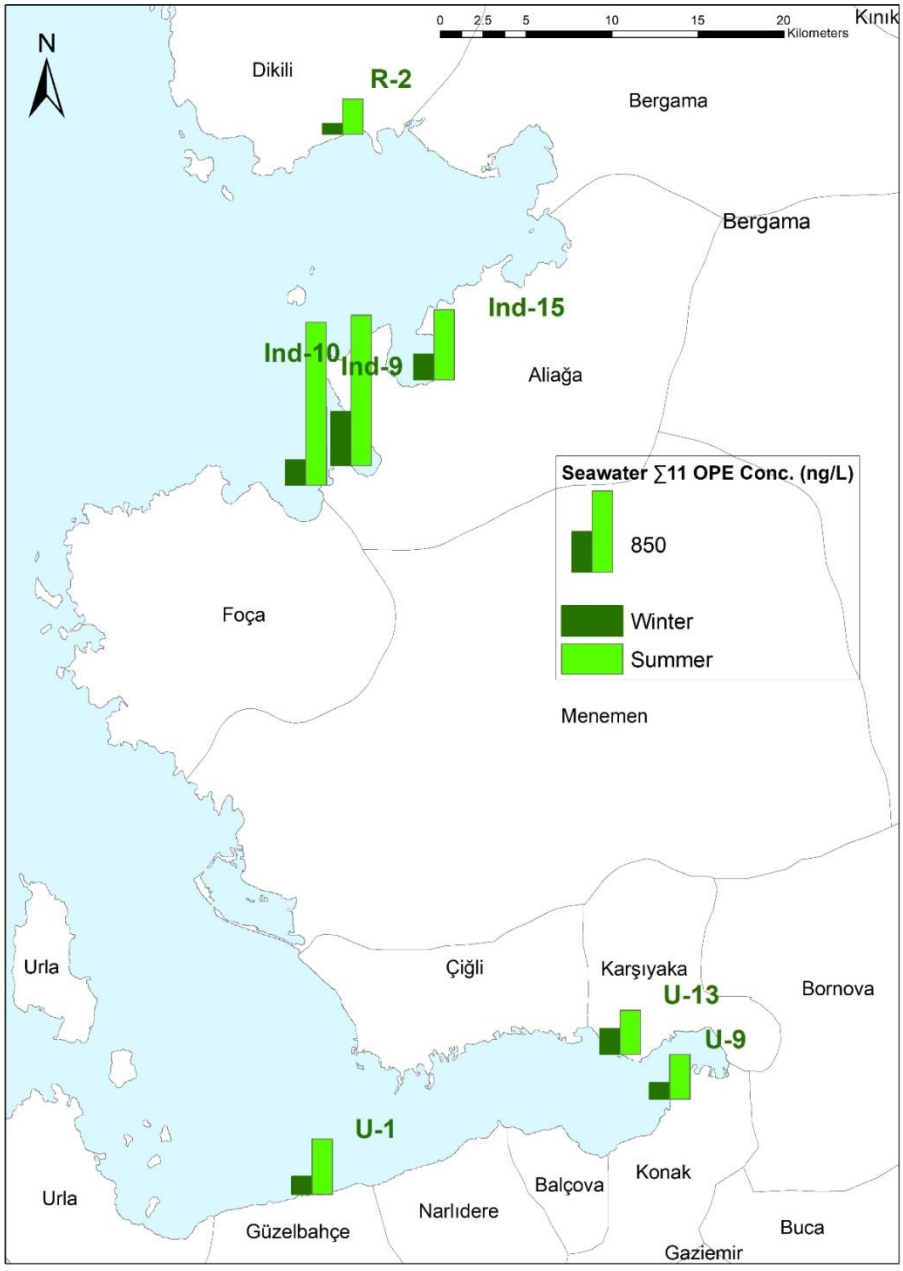


Figure 4.33 Seasonal variations of seawater $\sum_{11}$OPE concentrations

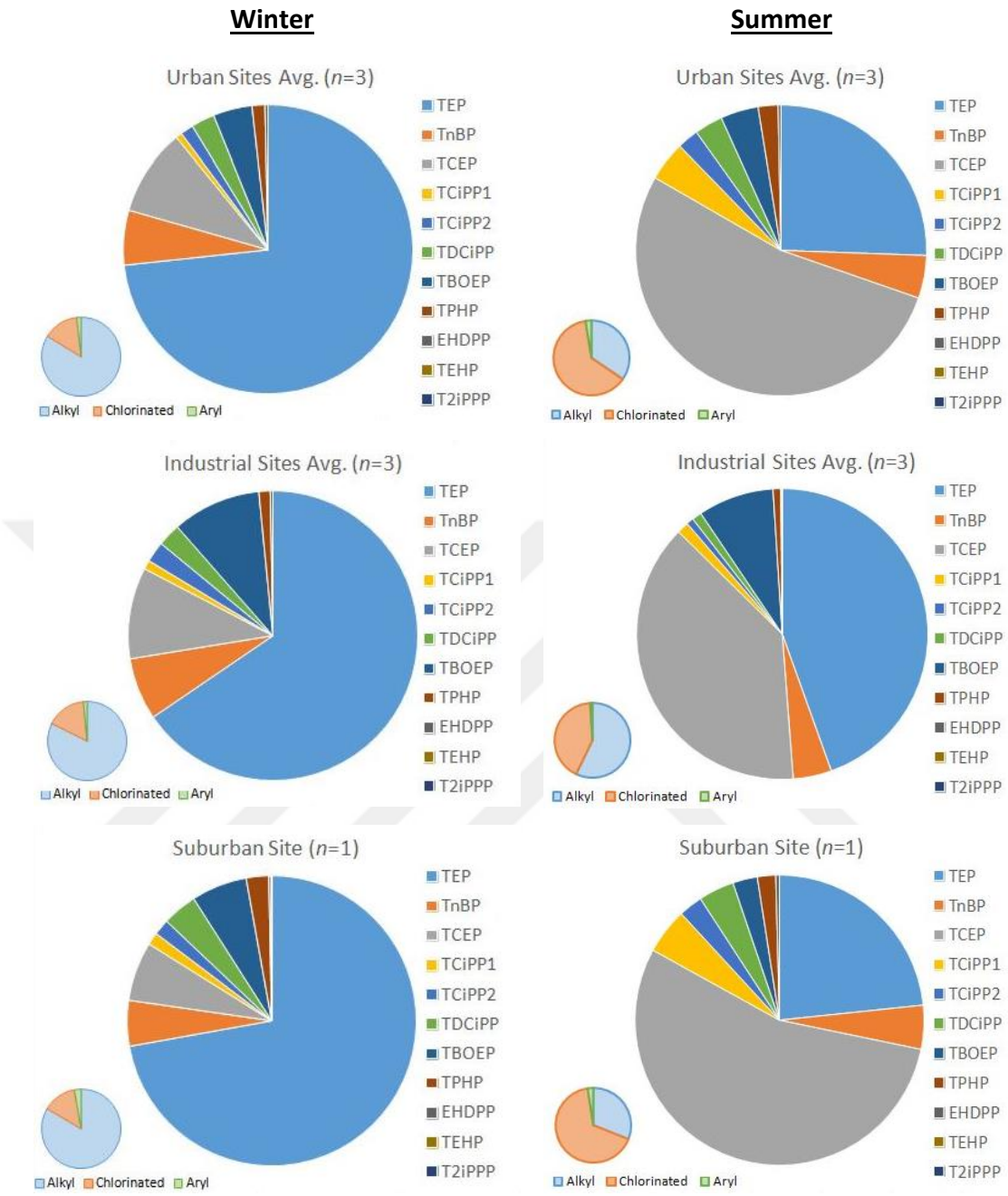


Figure 4.34 Compound-specific compositions in winter (left side) and in summer

4.2.6 Air-Water Exchange of OPEs

Air-water exchange is an important environmental mechanism to investigate whether organic compounds are prone to volatilize from or deposit into water bodies like lakes, river, surface waters or seas. The exchange direction (volatilization or deposition) of the organics between air and water is associated with determination of

fugacity. Additionally, exchange amount of the mass flow of a certain organic compound, from a defined area, through a specific direction is implied as "exchange flux".

4.2.6.1 Fugacity Fractions

The equilibrium status of several organic compounds between air-water interfaces can be determined using fugacity fractions calculated from simultaneously measured aqueous (C_w) and atmospheric levels (C_g), and dimensionless Henrys law constants (H').

$$ff = f_W/(f_W + f_A) = H'C_w/(H'C_w + C_g) \quad (4.55)$$

If the fugacity fraction [$f_W/(f_W+f_A)$] of a certain organic compound is greater than 0.5 it refers the net volatilization from water phase, while compounds having fugacity fraction of less than 0.5 they prone to deposit from gas phase. In equilibrium state, $f_W/(f_W+f_A)$ value converges to 0.5.

Error propagation was applied to quantify the uncertainties of the determined fugacity fractions and fluxes. The equilibrium ranges were also specified by these uncertainties. Errors related to measured/estimated values of H', K_g (gas-phase overall mass transfer coefficient), C_g and C_w were taken into account. The averaged uncertainties of C_gs were determined as 26% as defined in Section 4.2.4 while it was assumed that C_w values had uncertainties of 10% (Bamford, Ko, & Baker, 2002; Cetin & Odabasi, 2007). In order to determine salting-out coefficients (K_s, L/mol) for OPEs, the equation (K_s=0.04 log K_{OW}+0.114) derived by Ni & Yalkowsky (2003) was used. K_s values for 11 OPEs were ranged between 0.149 (TEP) and 0.414 (TEHP). Henry's law constant in salt water (H^*) was determined according to: log (H^*/H)=K_s C_s, where C_s is the molar salt concentration obtained from the nearest meteo-oceanographic observation stations of Izmir Metropolitan Municipality. Experimental H values measured in deionized water had average uncertainties of 6.8%. An additional uncertainty from K_s correction increases the overall uncertainty

to 10.8% for *H**. After propagating all the additional errors discussed above the equilibrium state for OPEs can be expressed as $f_W/(f_W+f_A) = 0.50 \pm 0.074$ which corresponds to 0.426-0.574 equilibrium interval. The average fugacity fractions (n=7) and their standard deviations were given in Figure 4.33. The most of the OPEs (90.9% of all data) were not in the equilibrium interval. Meanwhile, 27.9% of these non-equilibrium OPEs deposited, while the remaining 63.0% tended to volatilize. Relatively high aqueous OPE levels detected in the present study is the major factor increasing the water phase fugacities ($f_W=C_W H'$) and also fugacity fractions. However, for TnBP, the volatilization process was primarily driven by its high *H* value of 12.01 Pa m^3/mol. In a recent study, Liu et al. (2016b) investigated air-water exchange of a number of PCBs with relatively high *H* values ranging from 8.51 (PCB180) to 65.9 (PCB187) Pa m^3/mol and they determined that most of the PCBs were prone to evaporate from water to air. The average seawater temperatures in the present study were 12.5 and 25.5°C in winter and summer, respectively. Although water temperature is an effective parameter on *H'* values, variation of temperature is not sufficient to reverse the exchange direction especially for OPEs with $f_W/(f_W+f_A)\approx1$ and ≈0 while the OPEs close to equilibrium interval were more sensitive to temperature changes. In winter, relatively low seawater OPE levels and also low *H'* values arising from low water temperatures reduce seawater fugacity fractions. However, *ff* values and thus the volatilization tendencies in winter were still slightly higher than in summer for most OPEs (Figure 4.35). Because the increase in gas-phase atmospheric OPEs in summer has a more determinative effect on fugacity fractions in the present study. In general, TCiPP1, TCiPP2 and TEHP primarily tended to deposit from atmosphere to seawater while the rest of the aqueous OPEs acted as a source to the atmosphere. EHDPP and T2iPPP were in the equilibrium between air and water phases, especially in winter.

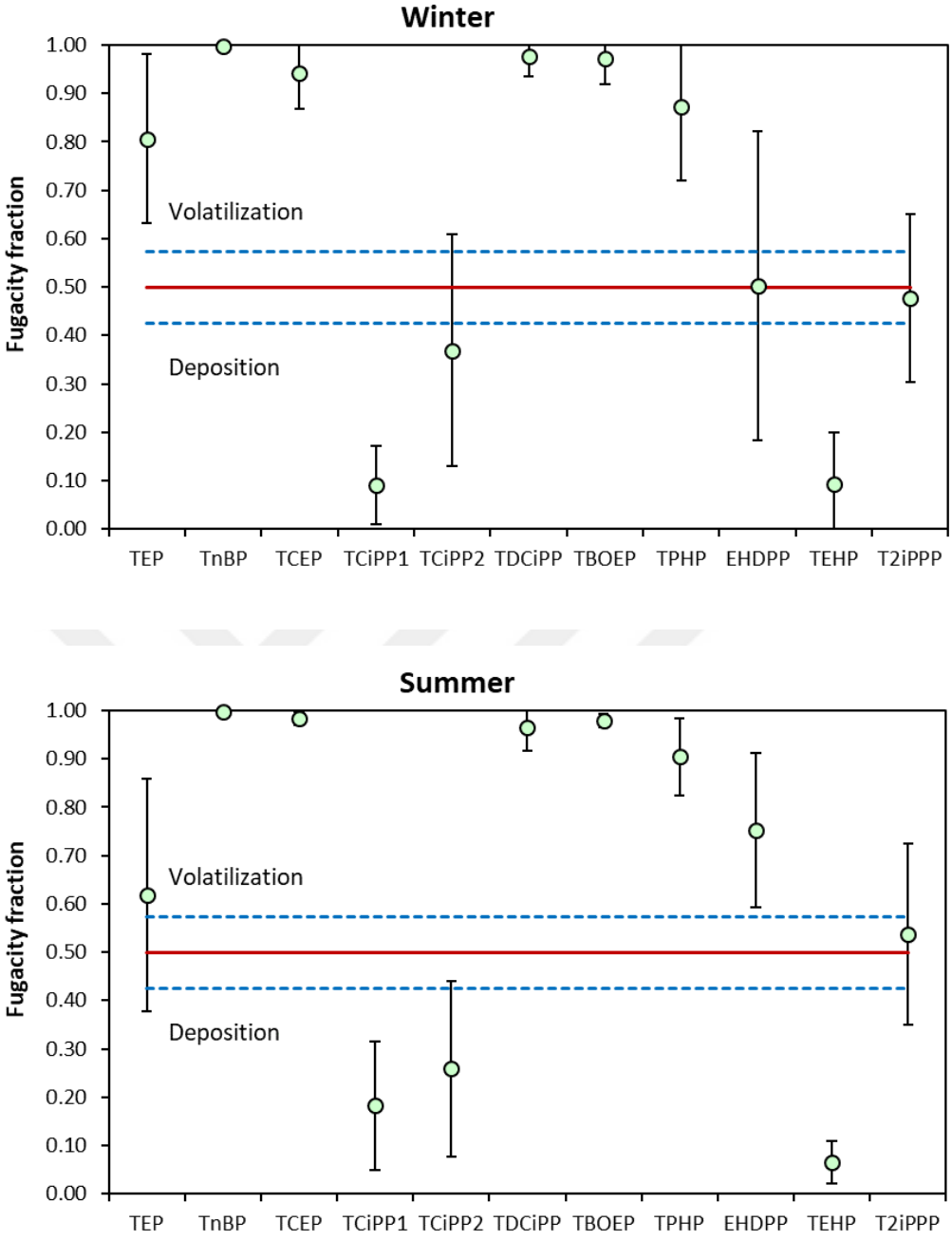


Figure 4.35 Air-water fugacity fractions of OPEs in both seasons

4.2.6.2 Air-Seawater Exchange Fluxes

The exchange flux of a certain organic compound between air and water phases can be determined according to compound-specific Henry's Law constants, the divergence of concentrations in air and water phases, and the overall mass transfer

coefficient (Schwarzenbach, Gschwend, & Imboden, 2003). The fugacity difference of a compound in the atmosphere and surface water can be used to determine the net gas-exchange flux (F_g, ng/m^2 day) according to:

$$F_g = K_g\left(C_g - \frac{C_w H}{RT}\right) \tag{4.56}$$

where C_w, C_g, H, R, K_g, and T are the aqueous concentration (ng/m^3), atmospheric concentration (ng/m^3), Henry's Law constant (Pa/m^3 mol), the ideal gas constant (8.314 Pa m^3/mol K), the gas-phase overall mass transfer coefficient, and the absolute temperature at the air-water interface (K), respectively.

K_g is related to compound-specific mass transfer coefficients in gas (k_g) and water (k_w) film layers:

$$\frac{1}{K_g} = \frac{1}{k_g} + \frac{H}{RTk_w} \tag{4.57}$$

In a number of studies, liquid-film mass transfer coefficients of oxygen (O_2) and carbon dioxide (CO_2), and gas-film mass transfer coefficient of water vapor have been expressed as related with wind speed. Below equations can be used to determine k_g and k_w (cm/s) for organics, (Nightingale, Liss, & Schlosser, 2000; Schwarzenbach et al., 2003):

$$k_{g(compound)} = (0.2U_{10} + 0.3)\left[D_{g(compound)}/D_{g(H_2O)}\right]^{0.67} \tag{4.58}$$

$$k_{w(compound)} = [(0.24U_{10}^2 + 0.016U_{10})/3600]\left[D_{w(compound)}/D_{w_{(CO_2)}}\right]^{0.5} \tag{4.59}$$

where D_g, D_w, and U_{10} are the diffusion coefficient in air (cm^2/s), the diffusion coefficient in water (cm^2/s), and the wind speed at 10 m above the water surface (m/s), respectively.

The uncertainty of estimated fluxes were also evaluated by performing error propagation. Errors related to values of H', K_g, C_g and C_w were taken into account while errors for H', C_g and C_w employed as determined in the previous section. The uncertainty for K_g was evaluated according to errors in k_g and k_w. Unlike k_g, the relationship between k_w with wind speed is nonlinear. Averaging wind speeds over the experimental periods may cause underestimation on k_w and K_g. Additionally, H has a nonlinear relationship with temperature. In order to evaluate the effect of nonlinearity of temperature and wind speed on K_g, Odabasi and Adali (2016) conducted a sensitivity analysis using these meteorological parameters averaged over 1 min intervals. They reported a difference in K_g less than 3% compared to those determined according to long-term mean values. Therefore, the overall uncertainty for K_g was assumed as 40% based on previous studies and also the uncertainties associated with the k_g and k_w (Bamford et al., 2002; Cetin & Odabasi, 2007; Hoff et al., 1996; Nelson, McConnell, & Baker, 1998; Nightingale et al., 2000; Odabasi et al., 2008). Based on these assumptions, the estimated propagated errors in air-water exchange fluxes ranged between as 34±0.1% (TBOEP) and 57±15 (T2iPPP) (overall average: 42±8%).

Gas exchange fluxes of 11 OPEs ranged between -43,473 (volatilization-TnBP) and 14,629 (deposition-TCiPP1) ng/m^2 day (Table 4.17). Three OPEs (TCiPP1, TCiPP2 and TEHP) had prominently deposition fluxes while the other eight compounds primarily tend to evaporate from seawater. OPE concentrations in both atmospheric gas-phase (summer/winter=18.9±15.2) and also in seawater (summer/winter= 4.93±6.49) were relatively higher in summer. Thereby, fluxes were comparably higher in summer through both volatilization (according to absolute values) and deposition as illustrated in Figure 4.36. However, gas exchange directions of the most of samples did not vary with sampling site, except a few samples. For example, TEP has significantly higher atmospheric gas-phase concentration in sampling site Ind-10 resulting high deposition fluxes, while this compound was prone to volatilize in the remaining samples. Although TEP has the lowest H value of 0.021±0.003 Pa m^3/mol at 25°C, primarily showed volatilization tendency (except sampling site Ind-10) probably due to significantly increased

seawater concentrations (Section 4.2.5). Similarly, TCEP (with a *H* value of 0.162±0.023 Pa m^3/mol at 25°C) another compound that dominating summer seawater concentrations also demonstrated higher volatilization fluxes in summer. However, TCiPP1 and TCiPP2 also having lower *H* values tend to deposit into seawater since their atmospheric levels were comparably high. The effect of increased seawater concentrations may suppresses the effect of low *H* values, thus gas-phase levels may also be more effective than *H* values on air-seawater exchange fluxes. Wind speed is another parameter that directly affects air-seawater fluxes and it can be clearly pointed out that increased wind speeds yield higher mass transfer coefficients (K_g) promoting volatilization fluxes. The average wind speeds were measured slightly lower (5.2 m/s) in summer compared to winter (5.7 m/s), even though fluxes were higher in summer season. But, this seasonal wind speed difference can only accounts for ~1.08 times increase in K_g values. In related studies, Liu et al. (2015); Martinez, Awad, Herkert, and Hornbuckle (2019) reported averaged wind speeds as 4.2 and 5.1 m/s, respectively, and the effect of wind speed was more apparently revealed in these studies for PCB congeners. Because the difference between aqueous and atmospheric levels of PCBs covered in these studies was not as high as measured for OPEs in the present study. However, as mostly seen in the present study, Liu et al. (2015) also determined high deposition fluxes in particular sampling points arising from high atmospheric concentrations rather than wind speed and/or *H*. In the present study, air ($f_A=C_g$) and water fugacities ($f_W=C_WH'$) correlated significantly (r^2=0.41-0.88, p<0.01) indicating that air water exchange of OPEs was mainly driven by their air and aqueous concentrations and *H* values.

Table 4.17 Calculated air-water exchange fluxes (ng/m^2 day)

Samp. Point	TEP	TnBP	TCEP	TCiPP1	TCiPP2	TDCiPP	TBOEP	TPHP	EHDPP	TEHP	T2iPPP
						Winter					
U-1	-391	-9,478	-910	102	4.59	-197	-244	-32.9	-10.7	0.11	-0.00044
U-9	-444	-5,955	-160	142	23.1	-62.2	-125	-17.1	13.3	0.38	-0.0011
U-13	-704	-6,334	-296	96	14.6	-101	-198	-15.3	2.87	0.29	-0.0013
Ind-9	-461	-10,238	-551	110	0.22	-226	-758	-41.2	-10.9	0.18	-0.0036
Ind-10	412	-21,186	-1,505	721	220	-166	-922	-22.4	-3.00	1.68	0.0022
Ind-14	-652	-11,789	-324	59.8	-67.5	-173	-484	-24.1	-1.00	0.67	-0.0026
R-2	-294	-3,240	-159	68.0	12.2	-87.5	-138	-18.15	-0.66	0.10	0.0024
						Summer					
U-1	-540	-15,015	-10,110	2.263	749	-1,079	-1,526	-678	-89	5.42	-0.026
U-9	-126	-11,762	-8,057	329	70.2	-1,027	-822	-543	-59.7	7.7	-0.09
U-13	-144	-19,731	-7,666	1,683	514	-718	-1,083	-344	-26.7	5.53	-0.15
Ind-9	-653	-35,787	-19,149	1,545	303	-974	-9,124	-552	-121	14.5	0.029
Ind-10	13,906	-43,473	-17,167	14,629	4,494	-377	-7,679	-316	7.17	39.4	0.52
Ind-14	-511	-32,763	-14,138	281	-16.2	-1,126	-1,490	-593	-113	6.30	0.062
R-2	-309	-11,704	-6,610	242	45.6	-870	-537	-361	-71.7	1.44	-0.027

Values in blue (+) indicate deposition to water while values in red (-) indicate volatilization from water.

Although most researchers investigated air-water exchange behaviors of a number of organic compounds (i.e. PAHs, PCBs, BDEs, OCPs, and PCNs), there has been no previous studies focusing on air-water fluxes of OPEs. Therefore, the fluxes estimated in the present study were compared to those reported in the literature for other organic compounds. Ren, Wang, Wang, Gong, and Yao (2017) determined that deposition fluxes ranged from 2 ± 1 (benzo[a]pyrene) to 339 ± 604 ng/m^2 d (phenanthrene) for several PAHs while Tucca et al. (2020) reported a wider range from 327 to 22,917 ng/m^2 d for deposition fluxes of pyrene. Pyrene was dominated all the investigated PAH species in that study with high atmospheric (1.68–30.5 ng/m^3) concentrations which results in significantly high deposition fluxes. Gigliotti et al. (2002) reported up to 2,009 ng/m^2 day (deposition) fluxes for phenanthrene and 3,464 ng/m^2 day (volatilization) fluxes for pyrene in New York Harbor. Martinez et al. (2019) collected atmospheric and aqueous PCBs with PUF and LDPE passive samplers from a harbor and ship canal that heavily polluted due to industrial operations. They measured gas and aqueous phase ∑PCB concentrations with the medians of 4.0 ng/m^3 and 14 ng/L, respectively which resulted in volatilization fluxes with a median of 2,000 ng/m^2 day.

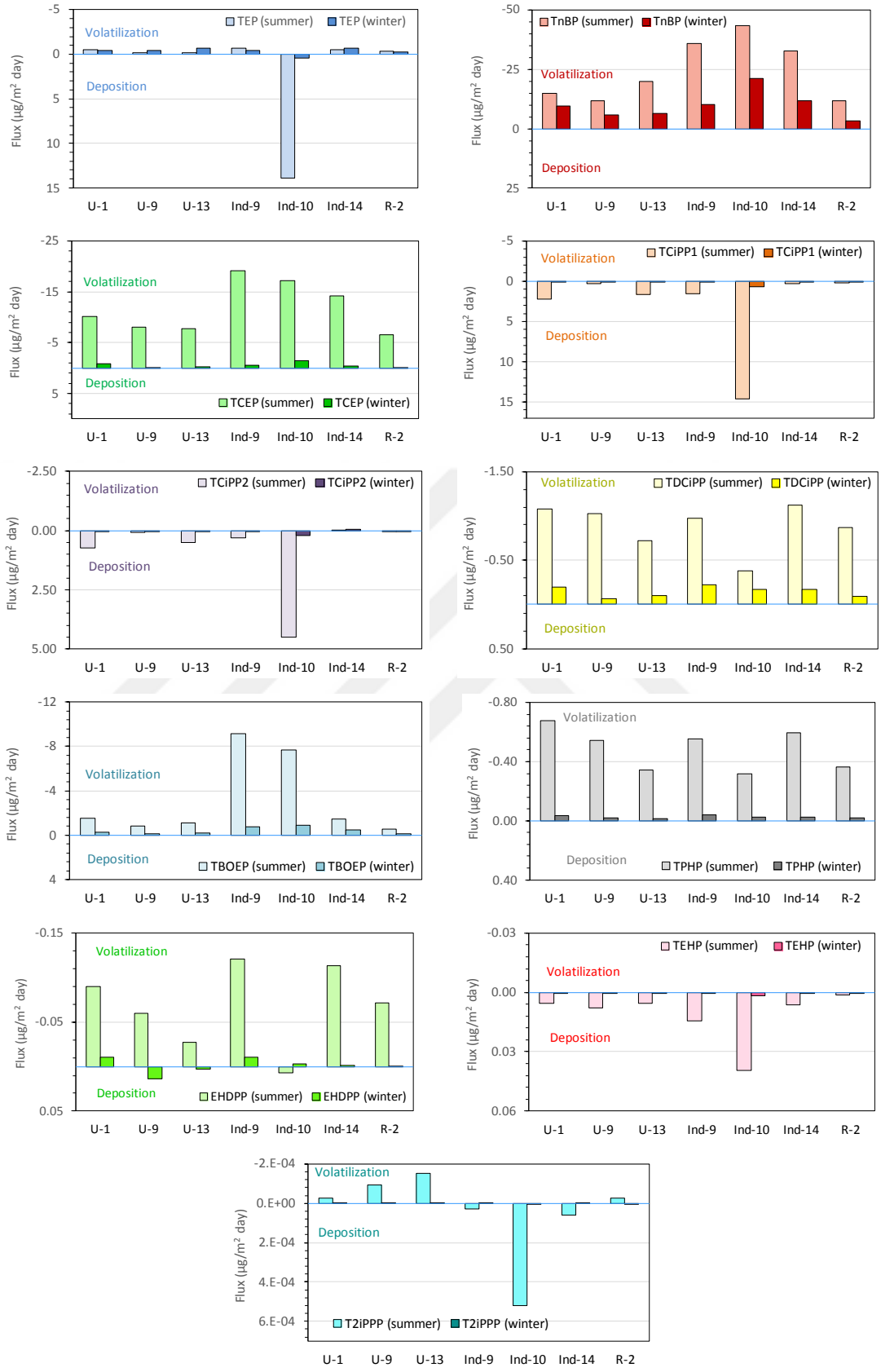


Figure 4.36 Air-water fugacity fluxes for individual OPEs

Further strong volatilization fluxes in intensively industrialized harbors were also reported (Martinez et al., 2017). McDonough et al. (2016) deployed pairs of polyethylene passive samplers to collect PBDEs in both lake water and ambient air. They also determined primarily deposition fluxes ranged from 0.964 to 0.030 ng/m^2 day.

There are a few studies that investigated air-water exchange of POPs in Izmir Bay in which the urban site samples of the present study were also collected. Air-water exchange fluxes for PAHs in Izmir Bay ranged between 5,659 and 16,686 ng/m^2 day (deposition) for phenanthrene and 0.2 and 0.3 ng/m^2 day (deposition) for benzo[*g,h,i*]perylene (Demircioglu et al., 2008). The reported net air-sea exchange fluxes for PCNs varied from -0.55 (volatilization, PCN-24/14) to 2.05 (deposition, PCN-23) ng/m^2 day (Odabasi and Adali (2016). For Izmir Bay, Mustafa Odabasi, Cetin, Demircioglu, & Sofuoglu, (2008) reported that calculated net gas-exchange PCB fluxes were mainly volatilization from the water, especially in summer, ranging from -0.2 (PCB-101) to -30.0 (PCB-31) ng/m^2 day while for OCPs, net fluxes ranged between -0.03 (volatilization, cis-nonachlor) to 1568 (deposition, endosulfan I) ng/m^2 day. In another study, reported net air-water exchange fluxes for PBDEs ranged from -0.9±1.0 (BDE-28) (volatilization) to 11.1±5.4 (BDE-209) ng/m^2 day (deposition) (Banu Cetin & Odabasi, 2007). In general, air-water exchange fluxes determined for 11 OPEs in the present study were generally higher than the fluxes reported for most organic compounds (PCBs, PCNs, OCPs, and PBDEs) in the literature and in Izmir Bay. However, fluxes were comparable to those reported for PAHs. The primary reason for the elevated fluxes of OPEs and PAHs was due to their relatively higher atmospheric and aqueous concentrations.

CHAPTER 5
CONCLUSIONS

Due to large production volumes and wide fields of usage during the manufacturing of consumer goods, OPEs have become an important group of additive compounds. In general, these additives are applied to improve certain characteristics of materials. Specifically, chlorinated OPEs are employed to reduce flammability of a product, while the non-chlorinated OPEs are mostly used as plasticizers and/or anti-foaming agents. Once OPEs applied to a material, they can be easily released into environmental compartments via volatilization, abrasion, or leaching. Since most of these compounds reported as neurotoxic, toxic, bioaccumulative and potentially carcinogenic, the number of studies aimed to monitor OPEs in the environment and investigate their distribution behavior/fate has increased. Studies on OPEs have mainly focused on their levels in environmental matrices (i.e., indoor or ambient air, water bodies, soil, sediment, and biota), human exposure and health effects, extraction and analytical techniques as well as physical and chemical properties. Although OPE containing goods are widely produced (or imported), and used or processed (i.e., as ferrous scrap) in Turkey, the studies are still inadequate. Physicochemical properties of OPEs are still poorly characterized and primarily depend on estimated values. As an important group of organic pollutants, effect of OPEs on the environment could be better understood by assessing their chemodynamics.

In order to assess chemodynamics of 11 OPEs in Izmir area, (i) five basic physicochemical properties (K_{OA}, P_L, H, K_{PEW}, $K_{PUF\text{-}Air}$) were experimentally determined for each individual OPE, (ii) ambient air, soil and seawater OPE concentrations were measured for summer and winter in 38 sampling sites under different levels of anthropogenic activities those located in urban, industrial, suburban and rural areas, (iii) environmental behaviors of these compounds were also investigated via gas-particle partitioning, air-soil and air-seawater exchange determined using data obtained within (i) and (ii).

As an essential parameter that controls the distribution of organic compounds in atmosphere, gas-particle partitioning coefficients, K_Ps for studied OPEs were determined experimentally as the first step of the study. OPEs showed a wide range of phase-distribution. Some OPEs were mainly in gas (TEP) or particle-phases (T2iPPP) while others were distributed between two-phases. Experimental K_P values were also compared to four widely used partitioning models. PUF-PAS measure total (gas+particle) concentrations. However, gas-phase OPE concentrations are required to determine air-soil and air-seawater exchange trends. Gas-phase concentrations were calculated according to K_{OA}-based model after some improvements (modified K_{OA} model).

K_{OA} and P_L values were measured following the GC retention time method. log K_{OA} of OPEs widely varied and ranged between 5.21 (TEP) and 11.78 (T2iPPP) while ΔU_{OA} values ranged from 65.0 (TEP) to 107.3 kJ/mol (T2iPPP). log P_L (Pa) of OPEs ranged between 1.59 (TEP) and -5.49 (T2iPPP) while ΔH_{vap} values ranged from 50.7 (TEP) to 117.2 kJ/mol (T2iPPP). The results were mostly agreed well with the literature values. In order to determine OPE concentrations collected with PUF samplers, $K_{PUF\text{-}Air}$ values were measured using a temperature-adjustable water jacketed glass column. log $K_{PUF\text{-}Air}$ values were measured between 5.04 (TEP) and 8.08 (TBOEP) while the range for $\Delta H_{PUF\text{-}air}$ was 60.3 (TCEP)-86.9 (TnBP) kJ/mol. OPEs had comparable values with the previous studies. A K_{OA} dependent equation was also derived using experimental values obtained within the present study. Henry's Law constants for OPEs were also measured following the gas-stripping technique. H values (at 25°C) were ranged between 12.012 ± 3.039 (TnBP) and 0.021 ± 0.003 Pa m^3/mol (TEP). Except TnBP, all the OPEs have H values <1 Pa m^3/mol. ΔH_H values ranged between 16.8 (TEP) and 125.7 (T2iPPP) kJ/mol in the present study. Comparison of experimental vs. estimated H values showed some scatter with the best agreement was for estimated from K_{OA} and K_{OW}. Since LDPE was used as seawater passive sampling medium throughout the study, K_{PEW}s were determined by absorption and desorption experiments. log K_{PEW} (L/kg) of OPEs widely varied and ranged between 0.83 (TEP) and 5.48 (T2iPPP). Experimental values correlated well with the estimations, however estimated values of nonvolatile

OPEs were substantially overestimated. Ratio of aqueous OPE concentrations calculated using predicted K_{PEW} values ($C_{SW\text{-}pred}$) and those derived using experimental K_{PEW} values ($C_{SW\text{-}exp}$) ($C_{SW\text{-}pred}/C_{SW\text{-}exp}$) ranged between 0.009 to 6.2. This indicated the importance of using experimental K_{PEW} values to accurately determine the aqueous OPE concentrations.

Atmospheric OPEs were measured during two seasons in 38 sites covering urban, industrial, suburban, and rural areas. Industrial emissions, along with elevated temperatures in summer was obviously critical factors increasing ambient air OPEs. Hence, the highest Σ_{11}OPE concentration (158 ng/m^3) was observed in an industrial sampling site in summer. Especially samplers deployed nearby iron-steel scrap processing facilities collected significantly higher levels of OPEs. Accordingly, the lowest Σ_{11}OPE concentrations were measured in rural samples in winter. The average ratio of summer/winter for 38 sampling sites was 4.20 (±6.58). In urban sampling sites, heavy traffic, extensive usage of household and office products containing OPEs, ventilation of indoor air also increased atmospheric OPE concentrations, especially during summer. Chlorinated OPEs dominated all the atmospheric samples, thus TCiPP1 and TCiPP2 had the highest concentrations followed by an aryl-OPE, EHDPP. Additionally, the most prominent alkyl-OPE, TEP, was relatively high in summer and in industrial sites.

Soil samples were collected from the same 38 sampling sites. Spatial distributions of Σ_{11}OPE concentrations were similar to atmospheric levels (industrial>urban> suburban>rural). However, seasonal variations of soil OPEs were different than atmospheric OPEs. In 23 of the 38 sampling points $\sum_{11}$OPE concentrations were higher in winter (summer/winter < 1). Hence, the mean of Σ_{11}OPE concentrations of 14 industrial sites had the highest value in winter as 766 ng/g. Accordingly, the 5 rural sites had the lowest averaged Σ_{11}OPE concentrations (22.4 ng/g) in summer. TCiPP1 and TCiPP2 also dominated soil samples in all four sampling areas and in both seasons. These two chlorinated-OPEs were contributed to total OPE concentrations not less than 45 and 15% in 76 soil samples, respectively. An aryl-OPE, EHDPP was observed as another prominent compound especially in winter. In

general, compound-specific compositions of soil samples were similar to atmospheric samples.

The transfer directions for the studied 11 OPEs between air and soil were investigated by determining their fugacity fractions. The compounds (TEP, TnBP, TCEP, TCiPP1, and TCiPP2) having lower molecular weights and low K_{OA} values tended to evaporate from the soil to the atmosphere both in summer and winter. The last five OPEs (TBOEP, TPHP, EHDPP, TEHP, and T2iPPP) with higher molecular weights and K_{OA}s were prone to deposit from air to soil in both seasons. Air-soil exchange trends did not showed a significant seasonality and had a limited temperature dependency. Exchange directions mostly controlled by OPE levels in soil and air.

Seawater OPE samples were also collected using LDPE passive samplers from 7 coastal sites (3 urban, 3 industrial, 1 rural). The average of $\sum_{11}$OPE concentrations in urban (n=3) and industrial sites (n=3) were 210 and 365 ng/L in winter, respectively. In summer samples, the average of $\sum_{11}$OPE concentrations were substantially higher, as 500 and 1,331 ng/L in urban and industrial sites, respectively. As it were in ambient air and soil samples, industrial site seawater samples also had considerably higher levels of OPEs compared to both urban and suburban sites. Although the reported values in the literature differ within a wide range, measured concentrations in the present study were mostly comparable with these values. OPE profiles of seawater samples were different than ambient air and soil. TEP and TCEP were the most prominent OPEs in seawater samples followed by TnBP. Although chlorinated OPEs were prominent in ambient air and soil samples, seawater samples mainly consisted of alkyl-OPEs (TEP, TnBP, TBOEP, and TEHP).

Air-seawater exchange directions of OPEs were evaluated using their fugacity fractions. TCiPP1, TCiPP2 and TEHP primarily deposited to seawater while for the remaining OPEs seawater acted as a source to the atmosphere. EHDPP and T2iPPP were near equilibrium between air and water, especially in winter. Gas exchange fluxes of 11 OPEs ranged between -43,473 (volatilization-TnBP) and 14,629

(deposition-TCiPP1) ng/m^2 day. Three OPEs (TCiPP1, TCiPP2 and TEHP) had prominently deposition fluxes while the other eight compounds primarily tend to evaporate from seawater. Air (f_A=C_g) and water fugacities (f_W=$C_W H$') correlated significantly (r^2=0.41-0.88, p<0.01) indicating that air water exchange of OPEs was mainly driven by their air and aqueous concentrations and H values.

This study was the first comprehensive work conducted in Turkey, focusing on seasonal and spatial OPE levels in different environmental compartments, as well as their several physicochemical properties. Although several organic pollutants were investigated in different parts of Turkey, OPEs have not been researched from a wide perspective as in the present study. OPEs are under consideration as new candidate POPs for inclusion in Stockhlom Convention POPs list. Thus, it is inarguably important to understand their environmental levels and chemodynamics. Considering the gaps present in the literature, obtained results will provide an insight for future studies. Nevertheless, these findings may possibly help regional decision-makers to take action on the production, usage, and disposal of OPE containing goods. On the other hand, it should be noted that results of the present study represent only the Izmir region. Studies covering larger areas and a higher number samples may provide a higher resolution for their spatiotemporal variations. Measuring OPEs in different matrices such as precipitation, aquatic organisms, sediments, plants, tap water, foods, and human blood may also fill the other gaps in the literature and thus thoroughly clarify the environmental paths of these compounds.

REFERENCES

Abdollahi, A., Eng, A., Jantunen, L. M., Ahrens, L., Shoeib, M., Parnis, M.J., & Harner, T. (2017). Characterization of polyurethane foam (PUF) and sorbent impregnated PUF (SIP) disk passive air samplers for measuring organophosphate flame retardants. *Chemosphere, 167,* 212-219.

Ahrens, L., Harner, T., Shoeib, M., Koblizkova, M., & Reiner, E. J. (2013). Characterization of two passive air samplers for per- and polyfluoroalkyl substances. *Environmental Science & Technology, 47*(24), 14024-14033.

Ali, N., Dirtu, A. C., Van den Eede, N., Goosey, E., Harrad, S., Neels, H., Mannetje, A., Coakley, J., Douwes, J., & Covaci, A. (2012). Occurrence of alternative flame retardants in indoor dust from New Zealand: Indoor sources and human exposure assessment. *Chemosphere, 88*(11), 1276-1282.

Alvarez, D. A., Petty, J. D., Huckins, J. N., Jones-Lepp, T. L., Getting, D. T., Goddard, J. P., & Manahan, S. E. (2004). Development of a passive, in situ, integrative sampler for hydrophilic organic contaminants in aquatic environments. *Environmental Toxicology and Chemistry, 23*(7), 1640-1648.

Alvarez, David A., Huckins, James N., Petty, Jimmie D., Jones-Lepp, Tammy, Stuer-Lauridsen, Frank, Getting, Dominic T., Goddard, Jon P., & Gravell, Anthony. (2007). Chapter 8 Tool for monitoring hydrophilic contaminants in water: polar organic chemical integrative sampler (POCIS). In G. M. R. Greenwood & B. Vrana (Eds.), *Comprehensive Analytical Chemistry* (Vol.48, 171-197) New York: Elsevier.

Andrae, N.J. (2007). *Durable and environmentally friendly flame retardants for synthetics.* M.Sc. Thesis, North Carolina University, Raleigh, North Carolina.

Andresen, J. A., Grundmann, A., & Bester, K. (2004). Organophosphorus flame retardants and plasticisers in surface waters. *Science of the Total Environment, 332*(1-3), 155-166.

Andresen, J. A., Muir, D., Ueno, D., Darling, C., Theobald, N., & Bester, K. (2007). Emerging pollutants in the north sea in comparison to Lake Ontario, Canada, data. *Environmental Toxicology and Chemistry, 26*(6), 1081-1089.

Arp, H. P. H., Schwarzenbach, R. P., & Goss, K. U. (2008). Ambient gas/particle partitioning. 2: The influence of particle source and temperature on sorption to dry terrestrial aerosols. *Environmental Science & Technology, 42*(16), 5951-5957.

Aston, L. S., Noda, J., Seiber, J. N., & Reece, C. A. (1996). Organophosphate flame retardants in needles of Pinus ponderosa in the Sierra Nevada foothills. *Bulletin of Environmental Contamination and Toxicology, 57*(6), 859-866.

Aydin, Y. M., Kara, M., Dumanoglu, Y., Odabasi, M., & Elbir, T. (2014). Source apportionment of polycyclic aromatic hydrocarbons (PAHs) and polychlorinated biphenyls (PCBs) in ambient air of an industrial region in Turkey. *Atmospheric Environment, 97*, 271-285.

Bacaloni, A., Cucci, F., Guarino, C., Nazzari, M., Samperi, R., & Lagana, A. (2008). Occurrence of organophosphorus flame retardant and plasticizers in three volcanic lakes of Central Italy. *Environmental Science & Technology, 42*(6), 1898-1903.

Bamford, H. A., Ko, F. C., & Baker, J. E. (2002). Seasonal and annual air-water exchange of polychlorinated biphenyls across Baltimore Harbor and the northern Chesapeake Bay. *Environmental Science & Technology, 36*(20), 4245-4252.

Bamford, H. A., Poster, D. L., & Baker, J. E. (2000). Henry's law constants of polychlorinated biphenyl congeners and their variation with temperature. *Journal of Chemical and Engineering Data, 45*(6), 1069-1074.

Bester, K. (2005). Comparison of TCPP concentrations in sludge and wastewater in a typical German sewage treatment plant - comparison of sewage sludge from 20 plants. *Journal of Environmental Monitoring, 7*(5), 509-513.

Bidleman, T. F., & Leone, A. D. (2004). Soil-air exchange of organochlorine pesticides in the Southern United States. *Environmental Pollution, 128*(1-2), 49-57.

Bidleman, T. F., Leone, A. D., & Falconers, R. L. (2003). Vapor pressures and enthalpies of vaporization for toxaphene congeners. *Journal of Chemical and Engineering Data, 48*(5), 1122-1127.

Bjorklund, J., Isetun, S., & Nilsson, U. (2004). Selective determination of organophosphate flame retardants and plasticizers in indoor air by gas chromatography, positive-ion chemical ionization and collision-induced dissociation mass spectrometry. *Rapid Communications in Mass Spectrometry, 18*(24), 3079-3083.

Bollmann, U. E., Moler, A., Xie, Z. Y., Ebinghaus, R., & Einax, J. W. (2012). Occurrence and fate of organophosphorus flame retardants and plasticizers in coastal and marine surface waters. *Water Research, 46*(2), 531-538.

Booij, K., Hofmans, H. E., Fischer, C. V., & Van Weerlee, E. M. (2003). Temperature-dependent uptake rates of nonpolar organic compounds by semipermeable membrane devices and low-density polyethylene membranes. *Environmental Science & Technology, 37*(2), 361-366.

Booij, K., Smedes, F., & Allan, I.J. (2017). Guidelines for determining polymer-water and polymer-polymer partition coefficients of organic compounds. *ICES Techniques in Marine Environmental Sciences*, *61*, 32.

Booij, K., Smedes, F., & van Weerlee, E. M. (2002). Spiking of performance reference compounds in low density polyethylene and silicone passive water samplers. *Chemosphere, 46*(8), 1157-1161.

Bopp, S., Weiss, H., & Schirmer, K. (2005). Time-integrated monitoring of polycyclic aromatic hydrocarbons (PAHs) in groundwater using the Ceramic Dosimeter passive sampling device. *Journal of Chromatography A, 1072*(1), 137-147.

Bozlaker, A., Muezzinoglu, A., & Odabasi, M. (2008a). Atmospheric concentrations, dry deposition and air-soil exchange of polycyclic aromatic hydrocarbons (PAHs) in an industrial region in Turkey. *Journal of Hazardous Materials, 153*(3), 1093-1102.

Bozlaker, A., Odabasi, M., & Muezzinoglu, A. (2008b). Dry deposition and soil-air gas exchange of polychlorinated biphenyls (PCBs) in an industrial area. *Environmental Pollution, 156*(3), 784-793.

Brommer, S., Jantunen, L. M., Bidleman, T. F., Harrad, S., & Diamond, M. L. (2014). Determination of vapor pressures for organophosphate esters. *Journal of Chemical and Engineering Data, 59*(5), 1441-1447.

Burgess, R.M., Driscoll, S.B.K., Burton, G.A., Gschwend, P.M., Ghosh, U., Reible, D., & Ahn, S. (2015). *Laboratory, field, and analytical procedures for using passive sampling in the evaluation of contaminated sediments: User's Manual*. U.S.A.: U.S. Environmental Protection Agency.

Campone, L., Piccinelli, A. L., Ostman, C., & Rastrelli, L. (2010). Determination of organophosphorous flame retardants in fish tissues by matrix solid-phase dispersion and gas chromatography. *Analytical and Bioanalytical Chemistry, 397*(2), 799-806.

Carlsson, H., Nilsson, U., Becker, G., & Ostman, C. (1997). Organophosphate ester flame retardants and plasticizers in the indoor environment: Analytical methodology and occurrence. *Environmental Science & Technology, 31*(10), 2931-2936.

Castro-Jimenez, J., Berrojalbiz, N., Pizarro, M., & Dachs, J. (2014). Organophosphate ester (OPE) flame retardants and plasticizers in the Open Mediterranean and Black Seas atmosphere. *Environmental Science & Technology, 48*(6), 3203-3209.

Cequier, E., Ionas, A. C., Covaci, A., Marce, R. M., Becher, G., & Thomsen, C. (2014). Occurrence of a broad range of legacy and emerging flame retardants in indoor environments in Norway. *Environmental Science & Technology, 48*(12), 6827-6835.

Cequier, E., Sakhi, A. K., Marce, R. M., Becher, G., & Thomsen, C. (2015). Human exposure pathways to organophosphate triesters - a biomonitoring study of mother-child pairs. *Environment International, 75*, 159-165.

Cetin, B. (2014). Soil concentrations and source apportionment of polybrominated diphenyl ethers (PBDEs) and trace elements around a heavily industrialized area in Kocaeli, Turkey. *Environmental Science and Pollution Research, 21*(13), 8284-8293.

Cetin, B., & Odabasi, M. (2005). Measurement of Henry's law constants of seven polybrominated diphenyl ether (PBDE) congeners as a function of temperature. *Atmospheric Environment, 39*(29), 5273-5280.

Cetin, B., & Odabasi, M. (2008). Atmospheric concentrations and phase partitioning of polybrominated diphenyl ethers (PBDEs) in Izmir, Turkey. *Chemosphere, 71*(6), 1067-1078.

Cetin, B., Ozer, S., Sofuoglu, A., & Odabasi, M. (2006). Determination of Henry's law constants of organochlorine pesticides in deionized and saline water as a function of temperature. *Atmospheric Environment, 40*(40), 8096-8096.

Cetin, B., Yatkin, S., Bayram, A., & Odabasi, M. (2007). Ambient concentrations and source apportionment of PCBs and trace elements around an industrial area in Izmir, Turkey. *Chemosphere, 69*(8), 1267-1277.

Cetin, Banu, & Odabasi, Mustafa. (2007). Air−water exchange and dry deposition of polybrominated diphenyl ethers at a coastal site in Izmir Bay, Turkey. *Environmental Science & Technology, 41*(3), 785-791.

ChemSpider. (2011). *Royal Society of Chemistry*. ChemSpider. Retrieved November 14, 2016, from http://www.chemspider.com/

Chen, D. H., Bi, X. H., Zhao, J. P., Chen, L. G., Tan, J. H., Mai, B. X., Sheng, G. Y., Fu, J. M., & Wong, M. H. (2009). Pollution characterization and diurnal variation of PBDEs in the atmosphere of an e-waste dismantling region. *Environmental Pollution, 157*(3), 1051-1057.

Chen, M. Q., Gan, Z. W., Qu, B., Chen, S. B., Dai, Y. Y., & Bao, X. M. (2019). Temporal and seasonal variation and ecological risk evaluation of flame retardants in seawater and sediments from Bohai Bay near Tianjin, China during 2014 to 2017. *Marine Pollution Bulletin, 146*, 874-883.

Chen, X. L., Hu, Y., & Song, L. (2008). Thermal behaviors of a novel UV cured flame retardant coatings containing phosphorus, nitrogen and silicon. *Polymer Engineering and Science, 48*(1), 116-123.

China Market Research Reports. (2016). *Global and China flame retardant Industry report, 2014−2016*. Research in China. Retrieved December 9, 2019, from https://www.reportlinker.com/p02232394/Global-and-China-Flame-Retardant-Industry-Report.html

Chung, H. W., & Ding, W. H. (2009). Determination of organophosphate flame retardants in sediments by microwave-assisted extraction and gas chromatography-mass spectrometry with electron impact and chemical ionization. *Analytical and Bioanalytical Chemistry, 395*(7), 2325-2334.

Civan, Y.M. (2016). Levels of halogenated persistent organic pollutants measured in indoor environment of a University (Üniversite iç ortaminda ölçülen halojenli kalici organik kirleticilerin seviyeleri). *Gazi University Science Journal: PART C: 'Design and Technology' 4 (4)*, 321-329.

Cristale, J., Dantas, R. F., De Luca, A., Sans, C., Esplugas, S., & Lacorte, S. (2017). Role of oxygen and DOM in sunlight induced photodegradation of organophosphorous flame retardants in river water. *Journal of Hazardous Materials, 323*, 242-249.

Cristale, J., Katsoyiannis, A., Chen, C. E., Jones, K. C., & Lacorte, S. (2013a). Assessment of flame retardants in river water using a ceramic dosimeter passive sampler. *Environmental Pollution, 172*, 163-169.

Cristale, J., Katsoyiannis, A., Sweetman, A. J., Jones, K. C., & Lacorte, S. (2013b). Occurrence and risk assessment of organophosphorus and brominated flame retardants in the River Aire (UK). *Environmental Pollution, 179*, 194-200.

Cristale, J., & Lacorte, S. (2013). Development and validation of a multiresidue method for the analysis of polybrominated diphenyl ethers, new brominated and organophosphorus flame retardants in sediment, sludge and dust. *Journal of Chromatography A, 1305*, 267-275.

Cristale, J., Vazquez, A. G., Barata, C., & Lacorte, S. (2013c). Priority and emerging flame retardants in rivers: Occurrence in water and sediment, Daphnia magna toxicity and risk assessment. *Environment International, 59*, 232-243.

Cui, K. Y., Wen, J. X., Zeng, F., Li, S. C., Zhou, X., & Zeng, Z. X. (2017). Occurrence and distribution of organophosphate esters in urban soils of the subtropical city, Guangzhou, China. *Chemosphere, 175*, 514-520.

Dachs, J., & Eisenreich, S. J. (2000). Adsorption onto aerosol soot carbon dominates gas-particle partitioning of polycyclic aromatic hydrocarbons. *Environmental Science & Technology*, *34*(17), 3690-3697.

Demircioglu, E., Sofuoglu, A., & Odabasi, M. (2008). Polisiklik aromatik hidrokarbonların (PAH'ların) İzmir Körfezi kıyısında hava-su arakesitindeki taşınımı. Paper presented at the *Hava Kirliliği ve Kontrolü Ulusal Sempozyumu-2008*, 220-235.

Dumanoglu, Y., Gaga, E. O., Gungormus, E., Sofuoglu, S. C., & Odabasi, M. (2017). Spatial and seasonal variations, sources, air-soil exchange, and carcinogenic risk assessment for PAHs and PCBs in air and soil of Kutahya, Turkey, the province of thermal power plants. *Science of the Total Environment, 580*, 920-935.

Dumanoglu, Y., Kara, M., Altiok, H., Odabasi, M., Elbir, T., & Bayram, A. (2014). Spatial and seasonal variation and source apportionment of volatile organic compounds (VOCs) in a heavily industrialized region. *Atmospheric Environment, 98*, 168-178.

EFRA. (2007). *Frequently asked questions.* European Flame Retardants Association. Retrieved July 10, 2018, from https://www.flameretardants-online.com/images/itempics/2/9/1/item_18192_pdf_1.pdf

EU, European Union (2008). *Risk assessment report tris(2-chloro-1-methylethyl) phosphate (TCPP).* Retrieved March 4, 2017, from https://echa.europa.eu/documents/10162/13630/trd_rar_ireland_tccp_en.pdf.

Falay, E. O., Tuna, G., Altiok, H., Kara, M., Dumanoglu, Y., Bayram, A., Tolunay, D., Elbir, T., & Odabasi, M. (2013). Spatial variation of polycyclic aromatic hydrocarbons (PAHs) in air, soil and tree components in Iskenderun industrial region, Turkey. *International Journal of Chemical, Environmental & Biological Sciences, 1*(2), 279-283.

Fisk, P.R., Girling, A.E., & Wildey, R.J. (2003). *Prioritisation of flame retardants for environmental risk assessment*. Retrieved March 4, 2017, from https://assets.publishing.service.gov.uk/government/uploads/system/uploads/attachment_data/file/291681/scho1008bote-e-e.pdf

Francisco, A. P., Harner, T., & Eng, A. (2017). Measurement of polyurethane foam-air partition coefficients for semivolatile organic compounds as a function of temperature: Application to passive air sampler monitoring. *Chemosphere, 174*, 638-642.

Fromme, H., Lahrz, T., Kraft, M., Fembacher, L., Mach, C., Dietrich, S., Burkardt, R., Volkel, W., & Goen, T. (2014). Organophosphate flame retardants and plasticizers in the air and dust in German daycare centers and human biomonitoring in visiting children (LUPE 3). *Environment International, 71*, 158-163.

Gigliotti, C. L., Brunciak, P. A., Dachs, J., Glenn, T. R., Nelson, E. D., Totten, L. A., & Eisenreich, S. J. (2002). Air-water exchange of polycyclic aromatic hydrocarbons in the New York-New Jersey, Usa, Harbor Estuary. *Environmental Toxicology and Chemistry, 21*(2), 235-244.

Greaves, A. K., Su, G. Y., & Letcher, R. J. (2016). Environmentally relevant organophosphate triesters in herring gulls: In vitro biotransformation and kinetics and diester metabolite formation using a hepatic microsomal assay. *Toxicology and Applied Pharmacology, 308*, 59-65.

Green, N. J. L., Schlabach, M., Bakke, T., Brevik, E., Dye, C., Herzke, D., Huber, S., Plosz, B., Remberger, M., Schøyen, M., Uggerud, H.T., & Vogelsang, C. (2008). *Screening of selected metals and new organic contaminants 2007. Phosphorus flame retardents, polyfluorinated organic compounds, nitro-PAHs, silver, platinum and sucralose in air, wastewater treatment falcilities, and freshwater and marine recipients.* Retrieved November 21, 2018 from https://niva.brage.unit.no/niva-xmlui/handle/11250/213998

Han, X., Hao, Y. F., Li, Y. M., Yang, R. Q., Wang, P., Zhang, G. X., Zhang, Q. H., & Jiang, G. B. (2020). Occurrence and distribution of organophosphate esters in the air and soils of Ny-Alesund and London Island, Svalbard, Arctic. *Environmental Pollution, 263,* 114495.

Harner, T., & Bidleman, T. F. (1996). Measurements of octanol-air partition coefficients for polychlorinated biphenyls. *Journal of Chemical and Engineering Data, 41*(4), 895-899.

Harner, T., & Bidleman, T. F. (1998a). Measurement of octanol-air partition coefficients for polycyclic aromatic hydrocarbons and polychlorinated naphthalenes. *Journal of Chemical and Engineering Data, 43*(1), 40-46.

Harner, T., & Bidleman, T. F. (1998b). Octanol-air partition coefficient for describing particle/gas partitioning of aromatic compounds in urban air. *Environmental Science & Technology, 32*(10), 1494-1502.

Harner, T., Farrar, N. J., Shoeib, M., Jones, K. C., & Gobas, F. A. P. C. (2003). Characterization of polymer-coated glass as a passive air sampler for persistent organic pollutants. *Environmental Science & Technology, 37*(11), 2486-2493.

Harner, T., Green, N. J. L., & Jones, K. C. (2000). Measurements of octanol-air partition coefficients for PCDD/Fs: A tool in assessing air-soil equilibrium status. *Environmental Science & Technology, 34*(15), 3109-3114.

Harner, T., & Mackay, D. (1995). Measurement of octanol - air partition-coefficients for chlorobenzenes, PCBs, and DDT. *Environmental Science & Technology, 29*(6), 1599-1606.

Harner, T., Mitrovic, M., Ahrens, L., & Schuster, J. (2014). Characterization of PUF disk passive air samplers for new priority chemicals: a review. *Organohalogen Compound*, 76(1), 11-29.

Harner, T., & Shoeib, M. (2002). Measurements of octanol-air partition coefficients (K-OA) for polybrominated diphenyl ethers (PBDEs): Predicting partitioning in the environment. *Journal of Chemical and Engineering Data, 47*(2), 228-232.

Harner, T., Su, K., Genualdi, S., Karpowicz, J., Ahrens, L., Mihele, C., Schuster, J., Charland, J. P., & Narayan, J. (2013). Calibration and application of PUF disk passive air samplers for tracking polycyclic aromatic compounds (PACs). *Atmospheric Environment, 75*, 123-128.

Hartmann, P. C., Burgi, D., & Giger, W. (2004). Organophosphate flame retardants and plasticizers in indoor air. *Chemosphere, 57*(8), 781-787.

He, J. H., Li, J. F., Ma, L. Y., Wu, N., Zhang, Y., & Niu, Z. G. (2019a). Large-scale distribution of organophosphate esters (flame retardants and plasticizers) in soil from residential area across China: Implications for current level. *Science of the Total Environment, 697*, 133997.

He, M. J., Lu, J. F., & Wei, S. Q. (2019b). Organophosphate esters in biota, water, and air from an agricultural area of Chongqing, western China: Concentrations, composition profiles, partition and human exposure. *Environmental Pollution, 244*, 388-397.

He, M. J., Yang, T., Yang, Z. H., Li, Q., & Wei, S. Q. (2017). Occurrence and distribution of organophosphate esters in surface soil and street dust from Chongqing, China: implications for human exposure. *Archives of Environmental Contamination and Toxicology*, *73*(3), 349-361.

Hippelein, M., & McLachlan, M. S. (1998). Soil/air partitioning of semivolatile organic compounds. 1. Method development and influence of physical-chemical properties. *Environmental Science & Technology, 32*(2), 310-316.

Hoff, R. M., Strachan, W. M. J., Sweet, C. W., Chan, C. H., Shackleton, M., Bidleman, T. F., Brice, K. A., Burniston, D. A., Cussion, S., Gatz, D. F., Harlin, K., & Schroeder, W. H. (1996). Atmospheric deposition of toxic chemicals to the Great Lakes: A review of data through 1994. *Atmospheric Environment, 30*(20), 3505-3527.

Hu, M. Y., Li, J., Zhang, B. B., Cui, Q. L., Wei, S., & Yu, H. X. (2014). Regional distribution of halogenated organophosphate flame retardants in seawater samples from three coastal cities in China. *Marine Pollution Bulletin, 86*(1-2), 569-574.

Ingerowski, G., Friedle, A., & Thumulla, J. (2001). Chlorinated ethyl and isopropyl phosphoric acid triesters in the indoor environment - An inter-laboratory exposure study. *Indoor Air-International Journal of Indoor Air Quality and Climate, 11*(3), 145-149.

Jonker, M. T. O., & Koelmans, A. A. (2002). Sorption of polycyclic aromatic hydrocarbons and polychlorinated biphenyls to soot and soot-like materials in the aqueous environment mechanistic considerations. *Environmental Science & Technology, 36*(17), 3725-3734.

Kara, M., Dumanoglu, Y., Altiok, H., Elbir, T., Odabasi, M., & Bayram, A. (2014). Seasonal and spatial variations of atmospheric trace elemental deposition in the Aliaga industrial region, Turkey. *Atmospheric Research, 149*, 204-216.

Karaca, G., & Tasdemir, Y. (2013). Effects of temperature and photocatalysts on removal of polycyclic aromatic hydrocarbons (PAHs) from automotive industry sludge. *Polycyclic Aromatic Compounds, 33*(4), 380-395.

Kaya, E., Dumanoglu, Y., Kara, M., Altiok, H., Bayram, A., Elbir, T., & Odabasi, M. (2012). Spatial and temporal variation and air-soil exchange of atmospheric PAHs and PCBs in an industrial region. *Atmospheric Pollution Research, 3*(4), 435-449.

Keller, A. S., Raju, N. P., Webster, T. F., & Stapleton, H. M. (2014). Flame Retardant Applications in Camping Tents and Potential Exposure. *Environmental Science & Technology Letters, 1*(2), 152-155.

Kemmlein, S., Hahn, O., & Jann, O. (2003). Emissions of organophosphate and brominated flame retardants from selected consumer products and building materials. *Atmospheric Environment, 37*(39-40), 5485-5493.

Khairy, M. A., & Lohmann, R. (2014). Field calibration of low density polyethylene passive samplers for gaseous POPs. *Environmental Science-Processes & Impacts, 16*(3), 414-421.

Khairy, M., Muir, D., Teixeira, C., & Lohmann, R. (2014). Spatial trends, sources, and air-water exchange of organochlorine pesticides in the Great Lakes Basin using low density polyethylene passive samplers. *Environmental Science & Technology, 48*(16), 9315-9324.

Kim, J. W., Isobe, T., Chang, K. H., Amano, A., Maneja, R. H., Zamora, P. B., Siringan, F. P., & Tanabe, S. (2011). Levels and distribution of organophosphorus flame retardants and plasticizers in fishes from Manila Bay, the Philippines. *Environmental Pollution, 159*(12), 3653-3659.

Kim, S. D., Cho, J., Kim, I. S., Vanderford, B. J., & Snyder, S. A. (2007). Occurrence and removal of pharmaceuticals and endocrine disruptors in South Korean surface, drinking, and waste waters. *Water Research, 41*(5), 1013-1021.

Kim, U. J., & Kannan, K. (2018). Occurrence and distribution of organophosphate flame retardants/plasticizers in surface waters, tap water, and rainwater: Implications for human exposure. *Environmental Science & Technology*, *52*(10), 5625-5633.

Komp, P., & McLachlan, M. S. (1997). Octanol/air partitioning of polychlorinated biphenyls. *Environmental Toxicology and Chemistry, 16*(12), 2433-2437.

Kurt-Karakus, P., Jantunen, L. M., Topcu, A., & Tepe, S. (2014). Selected organophosphate flame retardants in Turkish indoor dust. *Organohalogen Compounds, 76*(1), 649-652.

Kurt-Karakus, Perihan, Alegria, Henry, Birgul, Askin, Gungormus, Elif, & Jantunen, Liisa. (2018). Organophosphate ester (OPEs) flame retardants and plasticizers in air and soil from a highly industrialized city in Turkey. *Science of The Total Environment, 625*, 555-565.

Lai, N. L. S., Kwok, K. Y., Wang, X. H., Yamashita, N., Liu, G., Leung, K. M. Y., Lam, P. K. S., & Lam, J. C. W. (2019). Assessment of organophosphorus flame retardants and plasticizers in aquatic environments of China (Pearl River Delta, South China Sea, Yellow River Estuary) and Japan (Tokyo Bay). *Journal of Hazardous Materials, 371*, 288-294.

Lai, S. C., Xie, Z. Y., Song, T. L., Tang, J. H., Zhang, Y. Y., Mi, W. Y., Peng, J. H., Zhao, Y., Zou, S. C., & Ebinghaus, R. (2015). Occurrence and dry deposition of organophosphate esters in atmospheric particles over the northern South China Sea. *Chemosphere, 127*, 195-200.

Lei, Y. D., Chankalal, R., Chan, A., & Wania, F. (2002). Supercooled liquid vapor pressures of the polycyclic aromatic hydrocarbons. *Journal of Chemical and Engineering Data, 47*(4), 801-806.

Li, J., Xie, Z. Y., Mi, W. Y., Lai, S. C., Tian, C. G., Emeis, K. C., & Ebinghaus, R. (2017a). Organophosphate esters in air, snow, and seawater in the North Atlantic and the Arctic. *Environmental Science & Technology, 51*(12), 6887-6896.

Li, J., Yu, N. Y., Zhang, B. B., Jin, L., Li, M. Y., Hu, M. Y., Zhang, X. W., Wei, S., & Yu, H. X. (2014). Occurrence of organophosphate flame retardants in drinking water from China. *Water Research, 54*, 53-61.

Li, W. H., Shi, Y. L., Gao, L. H., Wu, C. D., Liu, J. M., & Cai, Y. Q. (2018). Occurrence, distribution and risk of organophosphate esters in urban road dust in Beijing, China. *Environmental Pollution, 241*, 566-575.

Li, W. H., Wang, Y., & Kannan, K. (2019). Occurrence, distribution and human exposure to 20 organophosphate esters in air, soil, pine needles, river water, and dust samples collected around an airport in New York state, United States. *Environment International, 131*, 105054.

Li, Y. F., Ma, W. L., & Yang, M. (2015). Prediction of gas/particle partitioning of polybrominated diphenyl ethers (PBDEs) in global air: A theoretical study. *Atmospheric Chemistry and Physics, 15*(4), 1669-1681.

Li, Y. F., Qiao, L. N., Ren, N. Q., Sverko, E., Mackay, D., & Macdonald, R. W. (2017b). Decabrominated piphenyl ethers (BDE-209) in Chinese and global air: Levels, gas/particle partitioning, and long-range transport: Is long-range transport of BDE-209 really governed by the movement of particles? *Environmental Science & Technology, 51*(2), 1035-1042.

Liang, K., & Liu, J. F. (2016). Understanding the distribution, degradation and fate of organophosphate esters in an advanced municipal sewage treatment plant based on mass flow and mass balance analysis. *Science of the Total Environment, 544*, 262-270.

Liu, L. Y., Salamova, A., He, K., & Hites, R. A. (2015). Analysis of polybrominated diphenyl ethers and emerging halogenated and organophosphate flame retardants in human hair and nails. *Journal of Chromatography A, 1406*, 251-257.

Liu, R. R., Lin, Y. F., Liu, R. Z., Hu, F. B., Ruan, T., & Jiang, G. B. (2016a). Evaluation of two passive samplers for the analysis of organophosphate esters in the ambient air. *Talanta, 147*, 69-75.

Liu, Y., Wang, S. Y., McDonough, C. A., Khairy, M., Muir, D. C. G., Helm, P. A., & Lohmann, R. (2016b). Gaseous and freely-dissolved PCBs in the lower Great Lakes based on passive sampling: Spatial trends and air-water exchange. *Environmental Science & Technology, 50*(10), 4932-4939.

Lohmann, R. (2012). Critical review of low-density polyethylene's partitioning and diffusion coefficients for trace organic contaminants and implications for its use as a passive sampler. *Environmental Science & Technology, 46*(2), 606-618.

Lu, J. X., Ji, W., Ma, S. T., Yu, Z. Q., Wang, Z., Li, H., Ren, G. F., & Fu, J. M. (2014). Analysis of organophosphate esters in dust, soil and sediment samples using gas chromatography coupled with mass spectrometry. *Chinese Journal of Analytical Chemistry, 42*(6), 859-865.

Lu, X. W., Wang, L. J., Lei, K., Huang, J., & Zhai, Y. X. (2009). Contamination assessment of copper, lead, zinc, manganese and nickel in street dust of Baoji, NW China. *Journal of Hazardous Materials, 161*(2-3), 1058-1062.

Luo, P., Bao, L. J., Guo, Y., Li, S. M., & Zeng, E. Y. (2016). Size-dependent atmospheric deposition and inhalation exposure of particle-bound organophosphate flame retardants. *Journal of Hazardous Materials, 301*, 504-511.

Luo, P., Bao, L. J., Wu, F. C., Li, S. M., & Zeng, E. Y. (2014). Health risk characterization for resident inhalation exposure to particle-bound halogenated flame retardants in a typical e-waste recycling zone. *Environmental Science & Technology, 48*(15), 8815-8822.

Ma, Y. G., Lei, Y. D., Xiao, H., Wania, F., & Wang, W. H. (2010). Critical review and recommended values for the physical-chemical property data of 15 polycyclic aromatic hydrocarbons at 25 degrees C. *Journal of Chemical and Engineering Data, 55*(2), 819-825.

Ma, Y. N., & Hites, R. A. (2013). Electron impact, electron capture negative ionization and positive chemical ionization mass spectra of organophosphorus flame retardants and plasticizers. *Journal of Mass Spectrometry, 48*(8), 931-936.

Makinen, M. S. E., Makinen, M. R. A., Koistinen, J. T. B., Pasanen, A. L., Pasanen, P. O., Kalliokoski, P. I., & Korpi, A. M. (2009). Respiratory and dermal exposure to organophosphorus flame retardants and tetrabromobisphenol A at five work environments. *Environmental Science & Technology, 43*(3), 941-947.

Marklund, A., Andersson, B., & Haglund, P. (2003). Screening of organophosphorus compounds and their distribution in various indoor environments. *Chemosphere, 53*(9), 1137-1146.

Marklund, A., Andersson, B., & Haglund, P. (2005a). Organophosphorus flame retardants and plasticizers in air from various indoor environments. *Journal of Environmental Monitoring, 7*(8), 814-819.

Marklund, A., Andersson, B., & Haglund, P. (2005b). Organophosphorus flame retardants and plasticizers in Swedish sewage treatment plants. *Environmental Science & Technology, 39*(19), 7423-7429.

Marklund, A., Andersson, B., & Haglund, P. (2005c). Traffic as a source of organophosphorus flame retardants and plasticizers in snow. *Environmental Science & Technology, 39*(10), 3555-3562.

Markovic, M. Z., Prokop, S., Staebler, R. M., Liggio, J., & Harner, T. (2015). Evaluation of the particle infiltration efficiency of three passive samplers and the PS-1 active air sampler. *Atmospheric Environment, 112*, 289-293.

Martinez, A., Awad, A. M., Herkert, N. J., & Hornbuckle, K. C. (2019). Determination of PCB fluxes from Indiana Harbor and Ship Canal using dual-deployed air and water passive samplers. *Environmental Pollution, 244*, 469-476.

Martinez, A., Hadnott, B. N., Awad, A. M., Herkert, N. J., Tomsho, K., Basra, K., Scammell, M. K., Heiger-Bernays, W., & Hornbuckle, K. C. (2017). Release of airborne polychlorinated biphenyls from New Bedford Harbor results in elevated concentrations in the surrounding air. *Environmental Science & Technology Letters, 4*(4), 127-131.

Matsukami, H., Suzuki, G., Someya, M., Uchida, N., Tue, N. M., Tuyen, L. H., Viet, P. H., Takahashi, S., Tanabe, S., & Takigami, H. (2017). Concentrations of polybrominated diphenyl ethers and alternative flame retardants in surface soils and river sediments from an electronic waste-processing area in northern Vietnam, 2012-2014. *Chemosphere, 167*, 291-299.

McDonough, C. A., Puggioni, G., Helm, P. A., Muir, D., & Lohmann, R. (2016). Spatial distribution and air-water exchange of organic flame retardants in the Lower Great Lakes. *Environmental Science & Technology*, *50*(17), 9133-9141.

Meijer, S. N., Harner, T., Helm, P. A., Halsall, C. J., Johnston, A. E., & Jones, K. C. (2001). Polychlorinated naphthalenes in UK soils: Time trends, markers of source, and equilibrium status. *Environmental Science & Technology, 35*(21), 4205-4213.

Meijer, S. N., Ockenden, W. A., Sweetman, A., Breivik, K., Grimalt, J. O., & Jones, K. C. (2003). Global distribution and budget of PCBs and HCB in background surface soils: Implications or sources and environmental processes. *Environmental Science & Technology, 37*(4), 667-672.

Mihajlovic, I., & Fries, E. (2012). Atmospheric deposition of chlorinated organophosphate flame retardants (OFR) onto soils. *Atmospheric Environment, 56*, 177-183.

Mihajlovic, I., Miloradov, M. V., & Fries, E. (2011). Application of Twisselmann Extraction, SPME, and GC-MS to assess input sources for organophosphate esters into soil. *Environmental Science & Technology, 45*(6), 2264-2269.

Moller, A., Sturm, R., Xie, Z. Y., Cai, M. H., He, J. F., & Ebinghaus, R. (2012). Organophosphorus flame retardants and plasticizers in airborne particles over the Northern Pacific and Indian Ocean toward the Polar Regions: Evidence for global occurrence. *Environmental Science & Technology, 46*(6), 3127-3134.

Moller, A., Xie, Z. Y., Caba, A., Sturm, R., & Ebinghaus, R. (2011). Organophosphorus flame retardants and plasticizers in the atmosphere of the North Sea. *Environmental Pollution, 159*(12), 3660-3665.

Muenhor, D., Harrad, S., Ali, N., & Covaci, A. (2010). Brominated flame retardants (BFRs) in air and dust from electronic waste storage facilities in Thailand. *Environment International, 36*(7), 690-698.

Nelson, E. D., McConnell, L. L., & Baker, J. E. (1998). Diffusive exchange of gaseous polycyclic aromatic hydrocarbons and polychlorinated biphenyls across the air-water interlace of the Chesapeake Bay. *Environmental Science & Technology, 32*(7), 912-919.

Ni, N., & Yalkowsky, S. H. (2003). Prediction of Setschenow constants. *International Journal of Pharmaceutics, 254*(2), 167-172.

Ni, Y., Kumagai, K., & Yanagisawa, Y. (2007). Measuring emissions of organophosphate flame retardants using a passive flux sampler. *Atmospheric Environment, 41*(15), 3235-3240.

Nightingale, P. D., Liss, P. S., & Schlosser, P. (2000). Measurements of air-sea gas transfer during an open ocean algal bloom. *Geophysical Research Letters, 27*(14), 2117-2120.

NIP. (2014). *National implementation plan for the Stockholm Convention on POPs*. Retrieved June 26, 2018, from http://chm.pops.int/Implementation/NationalImplementationPlans/NIPTransmission/tabid/253/Default.aspx

Niu, Z. G., Zhang, Z. Z., Li, J. F., He, J. H., & Zhang, Y. (2019). Threats of organophosphate esters (OPEs) in surface water to ecological system in Haihe River of China based on species sensitivity distribution model and assessment factor model. *Environmental Science and Pollution Research, 26*(11), 10854-10866.

Odabasi, M., & Adali, M. (2016). Determination of temperature dependent Henry's law constants of polychlorinated naphthalenes: Application to air-sea exchange in Izmir Bay, Turkey. *Atmospheric Environment, 147*, 200-208.

Odabasi, M., Bayram, A., Elbir, T., Seyfioglu, R., Dumanoglu, Y., Bozlaker, A., Demircioglu, H., Altiok, H., Yatkin, S., & Cetin, B. (2009). Electric arc furnaces for steel-making: Hot spots for persistent organic pollutants. *Environmental Science & Technology, 43*(14), 5205-5211.

Odabasi, M., & Cetin, B. (2012). Determination of octanol-air partition coefficients of organochlorine pesticides (OCPs) as a function of temperature: Application to air-soil exchange. *Journal of Environmental Management, 113*, 432-439.

Odabasi, M., Cetin, E., & Sofuoglu, A. (2006). Determination of octanol-air partition coefficients and supercooled liquid vapor pressures of PAHs as a function of temperature: Application to gas-particle partitioning in an urban atmosphere. *Atmospheric Environment, 40*(34), 6615-6625.

Odabasi, M., Dumanoglu, Y., Falay, E. O., Tuna, G., Altiok, H., Kara, M., Bayram, A., Tolunay, D., & Elbir, T. (2016). Investigation of spatial distributions and sources of persistent organic pollutants (POPs) in a heavily polluted industrial region using tree components. *Chemosphere, 160*, 114-125.

Odabasi, M., Falay, E. O., Tuna, G., Altiok, H., Kara, M., Dumanoglu, Y., Bayram, A., Tolunay, D., & Elbir, T. (2015). Biomonitoring the spatial and historical variations of persistent organic pollutants (POPs) in an industrial region. *Environmental Science & Technology, 49*(4), 2105-2114.

Odabasi, Mustafa, Cetin, Banu, Demircioglu, Eylem, & Sofuoglu, Aysun. (2008). Air–water exchange of polychlorinated biphenyls (PCBs) and organochlorine pesticides (OCPs) at a coastal site in Izmir Bay, Turkey. *Marine Chemistry, 109*(1), 115-129.

OECD. (1995). *Risk Reduction Monograph No.3: Selected brominated flame retardants background and national experience with reducing risk.* Retrieved June 26, 2018, from https://www.oecd.org/chemicalsafety/risk-management/seriesonriskmanagement-workonspecificchemicalexposuresofconcern.htm

OECD. (2011). OECD High Production Volume Chemicals Programme Phase 3.

Ohura, T., Amagai, T., Senga, Y., & Fusaya, M. (2006). Organic air pollutants inside and outside residences in Shimizu, Japan: Levels, sources and risks. *Science of the Total Environment, 366*(2-3), 485-499.

Okeme, J. O., Rodgers, F. M. Timothy, Jantunen, L., & Miriam, L. Diamond. (2018). Examining the gas-particle partitioning of organophosphate esters (OPEs): How reliable are air measurements? *Environmental Science & Technology* (52), 13834-13844.

Okeme, J. O., Rodgers, T. F. M., Parnis, J. M., Diamond, M. L., Bidleman, T. F., & Jantunen, L. M. (2020). Gas chromatographic estimation of vapor pressures and octanol-air partition coefficients of semivolatile organic compounds of emerging concern. *Journal of Chemical Engineering Data, 65*(5), 2467-2475.

Powell, R.M., & Puls, R.W. (1997). Ground water sampling: Turbidity effects on samples, hydrogeologic effects on samples and low-flow and passive purging and sampling. *Pollution Engineering, 29*(6), 50-54.

Pozo, K., Harner, T., Shoeib, M., Urrutia, R., Barra, R., Parra, O., & Focardi, S. (2004). Passive-sampler derived air concentrations of persistent organic pollutants on a north-south transect in Chile. *Environmental Science & Technology, 38*(24), 6529-6537.

Qiu, X. H., Zhu, T., & Hu, J. X. (2010). Polybrominated diphenyl ethers (PBDEs) and other flame retardants in the atmosphere and water from Taihu Lake, East China. *Chemosphere, 80*(10), 1207-1212.

Quednow, K., & Puttmann, W. (2009). Temporal concentration changes of DEET, TCEP, terbutryn, and nonylphenols in freshwater streams of Hesse, Germany: possible influence of mandatory regulations and voluntary environmental agreements. *Environmental Science and Pollution Research, 16*(6), 630-640.

Rauert, C., Harner, T., Schuster, J. K., Quinto, K., Fillmann, G., Castillo, L. E., Fentanes, O., Ibarra, M. V., Miglioranza, K. S. B., Rivadeneira, I. M., Pozo, K., Puerta, A. P., & Zuluagaj, B. H. A. (2016). Towards a regional passive air sampling network and strategy for new POPs in the GRULAC region: Perspectives from the GAPS Network and first results for organophosphorus flame retardants. *Science of the Total Environment, 573*, 1294-1302.

Reemtsma, T., Quintana, J. B., Rodil, R., Garcia-Lopez, M., & Rodriguez, I. (2008). Organophosphorus flame retardants and plasticizers in water and air I. Occurrence and fate. *Trac-Trends in Analytical Chemistry, 27*(9), 727-737.

Regnery, J., & Puttmann, W. (2009). Organophosphorus flame retardants and plasticizers in rain and snow from Middle Germany. *Clean-Soil Air Water, 37*(4-5), 334-342.

Regnery, J., & Puttmann, W. (2010a). Occurrence and fate of organophosphorus flame retardants and plasticizers in urban and remote surface waters in Germany. *Water Research, 44*(14), 4097-4104.

Regnery, J., & Puttmann, W. (2010b). Seasonal fluctuations of organophosphate concentrations in precipitation and storm water runoff. *Chemosphere, 78*(8), 958-964.

Regnery, J., Puttmann, W., Merz, C., & Berthold, G. (2011). Occurrence and distribution of organophosphorus flame retardants and plasticizers in anthropogenically affected groundwater. *Journal of Environmental Monitoring, 13*(2), 347-354.

Ren, G. F., Chu, X. D., Zhang, J., Zheng, K. W., Zhou, X. Y., Zeng, X. Y., & Yu, Z. Q. (2019). Organophosphate esters in the water, sediments, surface soils, and tree bark surrounding a manufacturing plant in north China. *Environmental Pollution, 246*, 374-380.

Ren, J., Wang, X. P., Wang, C. F., Gong, P., & Yao, T. D. (2017). Atmospheric processes of organic pollutants over a remote lake on the central Tibetan Plateau: implications for regional cycling. *Atmospheric Chemistry and Physics, 17*(2), 1401-1415.

Ribes, S., Van Drooge, B., Dachs, J., Gustafsson, O., & Grimalt, J. O. (2003). Influence of soot carbon on the soil-air partitioning of polycyclic aromatic hydrocarbons. *Environmental Science & Technology, 37*(12), 2675-2680.

Ricking, M., Schwarzbauer, J., & Franke, S. (2003). Molecular markers of anthropogenic activity in sediments of the Havel and Spree Rivers (Germany). *Water Research, 37*(11), 2607-2617.

Rodgers, T. F. M., Truong, J. W., Jantunen, L. M., Helm, P. A., & Diamond, M. L. (2018). Organophosphate ester transport, fate, and emissions in Toronto, Canada, estimated using an updated multimedia urban model. *Environmental Science & Technology, 52*(21), 12465-12474.

Rodriguez, I., Calvo, F., Quintana, J. B., Rubi, E., Rodil, R., & Cela, R. (2006). Suitability of solid-phase microextraction for the determination of organophosphate flame retardants and plasticizers in water samples. *Journal of Chromatography A, 1108*(2), 158-165.

Saini, A., Clarke, J., & Harner, T. (2019a). Direct measurements of polyurethane foam (PUF) – air partitioning coefficients for chemicals of emerging concern capable of equilibrating in PUF disk samplers. *Chemosphere, 234*, 925-930.

Saini, A., Clarke, J., Jariyasopit, N., Rauert, C., Schuster, J., Halappanavar, S., Evans, G. J., Su, Y., & Harner, T. (2019b). Flame retardants in urban air: A case study in Toronto targeting distinct source sectors. *Environmental Pollution, 247*, 89-97.

Saito, I., Onuki, A., & Seto, H. (2007). Indoor organophosphate and polybrominated flame retardants in Tokyo. *Indoor Air, 17*(1), 28-36.

Salamova, A., Hermanson, M. H., & Hites, R. A. (2014a). Organophosphate and halogenated flame retardants in atmospheric particles from a European arctic site. *Environmental Science & Technology, 48*(11), 6133-6140.

Salamova, A., Ma, Y. N., Venier, M., & Hites, R. A. (2014b). High levels of organophosphate flame retardants in the Great Lakes atmosphere. *Environmental Science & Technology Letters, 1*(1), 8-14.

Salamova, A., Peverly, A. A., Venier, M., & Hites, R. A. (2016). Spatial and temporal trends of particle phase organophosphate ester concentrations in the atmosphere of the Great Lakes. *Environmental Science & Technology, 50*(24), 13249-13255.

Schwarzenbach, R. P., Gschwend, P.M., & Imboden, D.M. (2003). *Environmental Organic Chemistry* (2nd ed.). New York: Wiley-Interscience.

Shi, Y. L., Gao, L. H., Li, W. H., Wang, Y., Liu, J. M., & Cai, Y. Q. (2016). Occurrence, distribution and seasonal variation of organophosphate flame retardants and plasticizers in urban surface water in Beijing, China. *Environmental Pollution, 209,* 1-10.

Shoeib, M., Ahrens, L., Jantunen, L., & Harner, T. (2014). Concentrations in air of organobromine, organochlorine and organophosphate flame retardants in Toronto, Canada. *Atmospheric Environment, 99,* 140-147.

Shoeib, M., & Harner, T. (2002a). Characterization and comparison of three passive air samplers for persistent organic pollutants. *Environmental Science & Technology, 36*(19), 4142-4151.

Shoeib, M., & Harner, T. (2002b). Using measured octanol-air partition coefficients to explain environmental partitioning of organochlorine pesticides. *Environmental Toxicology and Chemistry, 21*(5), 984-990.

Shoeib, T., Webster, G. M., Hassan, Y., Tepe, S., Yalcin, M., Turgut, C., Kurt-Karakus, P. B., & Jantunen, L. (2019). Organophosphate esters in house dust: A comparative study between Canada, Turkey and Egypt. *Science of the Total Environment, 650,* 193-201.

Sigma-Aldrich. (2016). Retrieved June 21, 2017 from http://www.sigmaaldrich.com/catalog/search?&interface=All&N=0+9634086&mode=partialmax&lang=en&region=TR&focus=product

Sjodin, A., Carlsson, H., Thuresson, K., Sjolin, S., Bergman, A., & Ostman, C. (2001). Flame retardants in indoor air at an electronics recycling plant and at other work environments. *Environmental Science & Technology, 35*(3), 448-454.

Smedes, F., Geertsma, R. W., van der Zande, T., & Booij, K. (2009). Polymer-water partition coefficients of hydrophobic compounds for passive sampling: Application of cosolvent models for validation. *Environmental Science & Technology, 43*(18), 7047-7054.

Stapleton, H. M., Klosterhaus, S., Eagle, S., Fuh, J., Meeker, J. D., Blum, A., & Webster, T. F. (2009). Detection of organophosphate flame retardants in furniture foam and us house dust. *Environmental Science & Technology, 43*(19), 7490-7495.

Su, G. Y., Letcher, R. J., & Yu, H. X. (2016). Organophosphate flame retardants and plasticizers in aqueous solution: pH-dependent hydrolysis, kinetics, and pathways. *Environmental Science & Technology, 50*(15), 8103-8111.

Suhring, R., Diamond, M. L., Scheringer, M., Wong, F., Pucko, M., Stern, G., Burt, A., Hung, H., Fellin, P., Li, H., & Jantunen, L. M. (2016a). Organophosphate esters in canadian arctic air: Occurrence, levels and trends. *Environmental Science & Technology, 50*(14), 7409-7415.

Suhring, R., Wolschke, H., Diamond, M. L., Jantunen, L. M., & Scheringer, M. (2016b). Distribution of organophosphate esters between the gas and particle phase-model predictions vs measured data. *Environmental Science & Technology, 50*(13), 6644-6651.

Sun, Y. L., & Zhu, H. K. (2021). A pilot study of organophosphate esters in surface soils collected from Jinan City, China: implications for risk assessments. *Environmental Science and Pollution Research*, 28, 3344–3353

Sundkvist, A. M., Olofsson, U., & Haglund, P. (2010). Organophosphorus flame retardants and plasticizers in marine and fresh water biota and in human milk. *Journal of Environmental Monitoring, 12*(4), 943-951.

Tajima, S., Araki, A., Kawai, T., Tsuboi, T., Bamai, Y. A., Yoshioka, E., Kanazawa, A., Cong, S., & Kishi, R. (2014). Detection and intake assessment of organophosphate flame retardants in house dust in Japanese dwellings. *Science of the Total Environment, 478*, 190-199.

Takeuchi, S., Kojima, H., Saito, I., Jin, K., Kobayashi, S., Tanaka-Kagawa, T., & Jinno, H. (2014). Detection of 34 plasticizers and 25 flame retardants in indoor air from houses in Sapporo, Japan. *Science of the Total Environment, 491*, 28-33.

Tao, F., Sellstrom, U., & de Wit, C. A. (2019). Organohalogenated flame retardants and organophosphate esters in office air and dust from Sweden. *Environmental Science & Technology*, *53*(4), 2124-2133.

Teo, T. L. L., McDonald, J. A., Coleman, H. M., & Khan, S. J. (2015). Analysis of organophosphate flame retardants and plasticisers in water by isotope dilution gas chromatography-electron ionisation tandem mass spectrometry. *Talanta, 143*, 114-120.

Tian, M., Chen, S. J., Wang, J., Zheng, X. B., Luo, X. J., & Mai, B. X. (2011). Brominated flame retardants in the atmosphere of e-waste and rural sites in southern china: seasonal variation, temperature dependence, and gas-particle partitioning. *Environmental Science & Technology*, *45*(20), 8819-8825.

TOXNET. (2016). *ChemIDplus: U.S. National Library of Medicine*. Retrieved March 2, 2017, from https://chem.nlm.nih.gov/chemidplus/

Tromp, P. C., Beeltje, H., Okeme, J. O., Vermeulen, R., Pronk, A., & Diamond, M. L. (2019). Calibration of polydimethylsiloxane and polyurethane foam passive air samplers for measuring semi volatile organic compounds using a novel exposure chamber design. *Chemosphere, 227*, 435-443.

Truong, J. W., Diamond, M. L., Helm, P. A., & Jantunen, L. M. (2017). Isomers of tris(chloropropyl) phosphate (TCPP) in technical mixtures and environmental samples. *Analytical and Bioanalytical Chemistry, 409*(30), 6989-6997.

Tucca, F., Luarte, T., Nimptsch, J., Woelfl, S., Pozo, K., Casas, G., Dachs, J., Barra, R., Chiang, G., & Galban-Malagon, C. (2020). Sources and diffusive air-water exchange of polycyclic aromatic hydrocarbons in an oligotrophic North-Patagonian lake. *Science of the Total Environment, 738*, 139838.

Ulrich, N., Endo, S., Brown, T.N., Watanabe, N., Bronner, G., Abraham, M.H., & Goss, K. U. (2017). *UFZ-LSER database v 3.2*. Retrieved May 18, 2019, from http://www.ufz.de/lserd

US-EPA. (2015). *Environmental profiles of chemical flame-retardant alternatives for low-density polyurethane foam*. Retrieved October, 10, 2016, from https://www.epa.gov/saferchoice/environmental-profiles-chemical-flame-retardant-alternatives-low-density-polyurethane

US-EPA. (2019). *EPI Suite - Estimation Program Interface (Version 4.11)*. Retrieved February, 24, 2016, from https://www.epa.gov/tsca-screening-tools/epi-suitetm-estimation-program-interface

van der Veen, I., & de Boer, J. (2012). Phosphorus flame retardants: Properties, production, environmental occurrence, toxicity and analysis. *Chemosphere, 88*(10), 1119-1153.

van Noort, P. C. M. (2003). A thermodynamics-based estimation model for adsorption of organic compounds by carbonaceous materials in environmental sorbents. *Environmental Toxicology and Chemistry, 22*(6), 1179-1188.

Venier, M., Dove, A., Romanak, K., Backus, S., & Hites, R. (2014). Flame retardants and legacy chemicals in Great Lakes' water. *Environmental Science & Technology, 48*(16), 9563-9572.

Vrana, B., Mills, G. A., Allan, I. J., Dominiak, E., Svensson, K., Knutsson, J., Morrison, G., & Greenwood, R. (2005). Passive sampling techniques for monitoring pollutants in water. *Trac-Trends in Analytical Chemistry, 24*(10), 845-868.

Wang, Q. Z., Zhao, H. X., Wang, Y., Xie, Q., Chen, J. W., & Quan, X. (2017a). Determination and prediction of octanol-air partition coefficients for organophosphate flame retardants. *Ecotoxicology and Environmental Safety, 145*, 283-288.

Wang, Q. Z., Zhao, H. X., Wang, Y., Xie, Q., Chen, J. W., & Quan, X. (2017b). Determination and prediction for vapor pressures of organophosphate flame retardants by gas chromatography. *Chinese Journal of Chromatography, 35*(9), 1008-1013.

Wang, R. M., Tang, J. H., Xie, Z. Y., Mi, W. Y., Chen, Y. J., Wolschke, H., Tian, C. G., Pan, X. H., Luo, Y. M., & Ebinghaus, R. (2015). Occurrence and spatial distribution of organophosphate ester flame retardants and plasticizers in 40 rivers draining into the Bohai Sea, north China. *Environmental Pollution, 198*, 172-178.

Wang, Y., Li, Z. Y., Tan, F., Xu, Y., Zhao, H. X., & Chen, J. W. (2020). Occurrence and air-soil exchange of organophosphate flame retardants in the air and soil of Dalian, China. *Environmental Pollution, 265*, 114850.

Wang, Y., Yao, Y. M., Li, W. H., Zhu, H. K., Wang, L., Sun, H. W., & Kannan, K. (2019). A nationwide survey of 19 organophosphate esters in soils from China: Spatial distribution and hazard assessment. *Science of the Total Environment, 671*, 528-535.

Wania, I. R., Lei, Y. D., & Harner, T. (2002). Estimating octanol-air partition coefficients of nonpolar semivolatile organic compounds from gas chromatographic retention times. *Analytical Chemistry, 74*(14), 3476-3483.

Wei, G. L., Li, D. Q., Zhuo, M. N., Liao, Y. S., Xie, Z. Y., Guo, T. L., Li, J. J., Zhang, S. Y., & Liang, Z. Q. (2015). Organophosphorus flame retardants and plasticizers: Sources, occurrence, toxicity and human exposure. *Environmental Pollution, 196*, 29-46.

WHO. (1991a). Environmental Health Criteria 111 *International Program on Chemical Safety*. Geneva, Switzerland: World Health Organization.

WHO. (1991b). Environmental Health Criteria 112 *International Program on Chemical Safety*. Geneva, Switzerland: World Health Organization.

WHO. (1997). Environmental Health Criteria 192 *International Program on Chemical Safety*. Geneva, Switzerland: World Health Organization.

WHO. (1998). Environmental Health Criteria 209 *International Program on Chemical Safety*. Geneva, Switzerland: World Health Organisation.

WHO. (2000). Environmental Health Criteria 218 *International Program on Chemical Safety*. Geneva, Switzerland: World Health Organization.

Wolschke, H., Suhring, R., Mi, W. Y., Moller, A., Xie, Z. Y., & Ebinghaus, R. (2016). Atmospheric occurrence and fate of organophosphorus flame retardants and plasticizer at the German coast. *Atmospheric Environment, 137*, 1-5.

Wolschke, H., Suhring, R., Xie, Z. Y., & Ebinghaus, R. (2015). Organophosphorus flame retardants and plasticizers in the aquatic environment: A case study of the Elbe River, Germany. *Environmental Pollution, 206*, 488-493.

Wong, A., Lei, Y. D., Alaee, M., & Wania, F. (2001). Vapor pressures of the polybrominated diphenyl ethers. *Journal of Chemical and Engineering Data, 46*(2), 239-242.

Wong, F., de Wit, C. A., & Newton, S. R. (2018). Concentrations and variability of organophosphate esters, halogenated flame retardants, and polybrominated diphenyl ethers in indoor and outdoor air in Stockholm, Sweden. *Environmental Pollution, 240*, 514-522.

Wu, M., Yu, G., Cao, Z. G., Wu, D. K., Liu, K., Deng, S. B., Huang, J., Wang, B., & Wang, Y. J. (2016). Characterization and human exposure assessment of organophosphate flame retardants in indoor dust from several microenvironments of Beijing, China. *Chemosphere, 150*, 465-471.

Wu, Y., Venier, M., & Salamova, A. (2020). Spatioseasonal variations and partitioning behavior of organophosphate esters in the Great Lakes atmosphere. *Environmental Science & Technology, 54*(9), 5400-5408.

Yadav, I. C., & Devi, N. L. (2019). Data relating to fate and transport of organophosphate ester flame retardants in indoor air and dust from Nepal. *Data in Brief, 25*, 104287.

Yadav, I. C., Devi, N. L., Li, J., & Zhang, G. (2018). Organophosphate ester flame retardants in Nepalese soil: Spatial distribution, source apportionment and air-soil exchange assessment. *Chemosphere, 190*, 114-123.

Yaman, B., Dumanoglu, Y., & Odabasi, M. (2020). Measurement and modeling the phase partitioning of organophosphate esters using their temperature-dependent octanol-air partition coefficients and vapor pressures. *Environmental Science & Technology, 54*(13), 8133-8143.

Yang, Cunman, Li, Ying, Zha, Daoping, Lu, Guanghua, Sun, Qin, & Wu, Donghai. (2017). A passive sampling method for assessing the occurrence and risk of organophosphate flame retardants in aquatic environments. *Chemosphere, 167*, 1-9.

Yang, F. X., Ding, J. J., Huang, W., Xie, W., & Liu, W. P. (2014). Particle size-specific distributions and preliminary exposure assessments of organophosphate flame retardants in office air particulate matter. *Environmental Science & Technology, 48*(1), 63-70.

Yazdani, A., Dillner, A. M., & Takahama, S. (2020). Estimating mean molecular weight, carbon number, and OM/OC with mid-infrared spectroscopy in organic particulate matter samples from a monitoring network. *Atmospheric Measurement Techniques Discussion, 2020*, 1-32.

Zhang, W. W., Wang, P., Li, Y. M., Wang, D., Matsiko, J., Yang, R. Q., Sun, H. Z., Hao, Y. F., Zhang, Q., & Jiang, G. B. (2019a). Spatial and temporal distribution of organophosphate esters in the atmosphere of the Beijing-Tianjin-Hebei region, China. *Environmental Pollution, 244*, 182-189.

Zhang, Z. Y., Shao, H. Y., Wu, M. H., Zhang, J. Y., Li, D. Y., Li, J. S., Wang, H. Y., Shi, W. Y., & Xu, G. (2019b). Occurrence, distribution, and potential sources of organophosphate esters in urban and rural surface water in Shanghai, China. *Archives of Environmental Contamination and Toxicology*, *77*(1), 115-126.

Zheng, C. L., Feng, S. S., Liu, P. P., Fries, E., Wang, Q. R., Shen, Z. X., Liu, H. X., & Zhang, T. C. (2016). Sorption of organophosphate flame retardants on pahokee peat soil. *Clean-Soil Air Water*, *44*(9), 1163-1173.

Zhong, M. Y., Tang, J. H., Mi, L. J., Li, F., Wang, R. M., Huang, G. P., & Wu, H. F. (2017). Occurrence and spatial distribution of organophosphorus flame retardants and plasticizers in the Bohai and Yellow Seas, China. *Marine Pollution Bulletin, 121*(1-2), 331-338.

Zhou, L. L., Hiltscher, M., Gruber, D., & Puttmann, W. (2017). Organophosphate flame retardants (OPFRs) in indoor and outdoor air in the Rhine/Main area, Germany: comparison of concentrations and distribution profiles in different microenvironments. *Environmental Science and Pollution Research, 24*(12), 10992-11005.